TABLE OF CONTENTS

LIST OF FIGURES

LIST OF FIGURES (contd…)

CHAPTER 1

INTRODUCTION

"I am careful not to confuse excellence with perfection.
Excellence, I can reach for;
Perfection is God's business."
Michael J. Fox

1.1 TUBERCULOSIS

Infectious diseases are the world's leading cause of premature deaths, killing almost 50,000 people per day. In recent years, drug resistance exhibited by human pathogenic organisms has been commonly reported all over the world [Protopopova, M., *et al.*, 2007; Davis, J., 1994; Robin, E. H., *et al.*, 1998]. Despite continued control efforts, tuberculosis (abbreviated as TB for Tubercle Bacillus) remains the leading cause of worldwide death among the infectious diseases [Zumla, A., *et al.*, 1998] and is responsible for the greatest morbidity and mortality. [Zignol, M., *et al.*, 2006; Dye, C., *et al.*, 1999]

In 1993, the World Health Organization (WHO) declared tuberculosis (TB) to be a global emergency, the first infectious disease to be recognized as such [Raviglione *et al.*, 1995; Ang, D., *et al.*, 2006]. TB still remains one of the foremost among infectious diseases in the world, despite the availability of the BCG vaccine and antibiotic treatment, which causes maximum death from a single microorganism [Frieden, T. R., *et al.*, 2003]. Approximately one third of the world's population has been infected with the causative organism *Mycobacterium tuberculosis* (MTB), a facultative intracellular organism discovered by Robert Koch in 1882, eight million become sick with TB every year, and globally it accounts for almost 3 million deaths annually [Ginsburg, A. S., *et al.*, 2003; Collins, H. L., *et al.*, 2001]. It is estimated that nearly 1 billion people will become newly infected, over 150 million will become sick, and 36 million will die worldwide between now and 2020 -if control is not further strengthened. Each year there are more than 9 million cases and close to 2 million deaths attributed to TB. Co-infection with Human Immunodeficiency Virus (HIV) is driving the increase in incidence [Williams, B. G., *et al.*, 2003], and the cause of death in

31% of Acquired Immuno Deficiency Syndrome (AIDS) cases can be attributed to TB in the African region [Corbett, E. L., *et al.,* 2003]. When coupled with the emergence of multidrug-resistant strains of *Mycobacterium tuberculosis* (MDR-TB) [Zignol, M., *et al.,* 2006]

One fifth of all deaths of adults in developing countries results are due to TB, which is a re-emergent problem particularly in many industrialized countries. In 1990s, nearly 90 million new cases were predicted, and in 1991 it was estimated that 1,700 million people are infected with MTB [Ellner, J. J., *et al.,* 1993]. It was reported that around 19 – 43 % of the world's population might get infected with MTB between 2000 and 2020 if control measures are not strengthened further [Raviglione *et al.,* 1995]. Not only is there a global increase in the disease itself, there is a worrying rise in the number of cases resistant to the two principal antituberculosis drugs, isoniazid (INH) and rifampicin (RIF) [Zumla, A., *et al.,* 2001]. The situation is worsened by the HIV pandemic, since the risk of death in HIV infected patients with TB is twice as that of HIV infected patients without TB [Barnes, P. F., *et al.,* 2002]. Further, immunodeficiencies occurring under conditions of malnutrition, deterioration of general health or after the HIV infection have become responsible for an increase in the incidence of central nervous system (CNS) TB [Gupta, R. K., *et al.,* 1996; Schutte, C. M., *et al.,* 1996].

Pulmonary TB, the most common type of the disease, is usually acquired by inhalation of aerosols carrying the bacilli from an infectious patient. The organism is capable of affecting almost all parts of the body [Koch, R., 1882] except hair and nail. TB is known since antiquity and evidence of spinal tuberculosis in the form of fossil bones around 8000 BC [Ayyazian, L. F., 1993; Basel, H. H., 1998] has been unearthed.

It is important to understand that there is a difference between being infected with TB and having TB disease. Even if someone becomes infected with TB, that does not mean they will get the disease. Most people who get infected do not develop TB disease because their body's defense mechanisms protect them. Most active cases of TB disease result from activating old infection in people with impaired immune systems [WHO, 2006]

Tuberculosis poses a major threat to the health of people living in South East Asia, especially India. At least one in three people living in this part of the world are infected with MTB, and every year 1 million people die from TB. India has been particularly hit by the dual threat of HIV and TB [Sharma, S. K., *et al.*, 2005].

The re-emergence of TB is mainly due to the compromise of immune mechanisms, and particularly in HIV-infected individuals the risk is more. The HIV infection and the evidence of an association between TB and HIV infection has caused marked increase in the incidence of TB in many countries [Sharma, S. K., *et al.*, 2005; Gallant, J. E., *et al.*, 1994]. Around 30 % of the AIDS related deaths are due to TB [Grange, J. M., *et al.*, 2002]. Not only do many developed countries face the gloomy scenario of increasing TB incidence, but also the problem of MDR-TB that has emerged in several major urban centers of countries worldwide **[**Lane, H. C., *et al.*, 1994; Bastian, I., *et al.*, 2003; Frieden, T. R., *et al.*, 2003; Cohen, T., *et al.*, 2003; Caminero, J. A., 2005]. It could be stated that TB is currently a global disaster on an unprecedented scale. Things are getting worse due to the lack of proper TB control programs, co-existence of HIV infection, population growth and poverty. TB has resurged as an opportunistic infection in immuno-compromised patients, and new drugs are needed to control this global epidemic. The alarming statistics reveal the need for urgent action by both basic scientists and pharmaceutical companies to prevent a global catastrophe [Kaufmann, S. H., 2000].

1.1.1 Incidence of Tuberculosis

Tuberculosis has probably killed 100 million people over the past 100 years [Iseman, M. D., 2000], and is the world's second commonest cause of death from infectious disease, after HIV/AIDS. There were an estimated 8 - 9 million new cases of tuberculosis in 2000, fewer than half of which were reported; 3 - 4 million cases were sputum - smear positive, the most infectious form of the disease [Corbett, E. L., *et al.*, 2003]. Most cases (5 - 6 million) are in people aged 15 - 49 years. Sub - Saharan Africa has the highest incidence rate (290 per 100,000 populations), but the most populous countries of Asia have the largest numbers of cases: India, China, Indonesia, Bangladesh, and Pakistan together account for more than half

the global burden. 80% of new cases occur in 22 high-burden countries [WHO Report, 2003].

Every minute of every day 15 people in the world develop, and six people die from, TB; this translates into 8 million new cases each year from which 2 - 2.5 million will die [Collins, H. L., *et al.*, 2001]. As if these figures were not alarming enough, it is estimated that only 45 % of actual TB cases are detected and reported [WHO Report, 2001]. As with the other two top infectious disease killers, AIDS and malaria, the biggest burden of morbidity and mortality is in developing countries; however, industrialized nations across Europe and in the USA, the incidence of TB is on the increase. There have been striking increases in countries of the former Soviet Union and in sub - Saharan Africa [Dye, C., *et al.*, 1999].

TB remains a serious public - health problem in India accounting for nearly one-third of the global burden, and it has been estimated that 3.5 million of the population are infected with TB [Granich, R., *et al.*, 2003; Sharma, D. C., 2003]. Despite the introduction of the National Tuberculosis Control Programme in 1962, India has about 2 million new cases every year, of which nearly 1 million are infectious smear - positive pulmonary cases [Dye, C., *et al.*, 1999]. One person dies from TB in India every minute – more than 1000 every day and 4.50,000 every year [Khatri, G. R., *et al.*, 2000]. India's TB problem is further compounded by an estimated 3.97 million people infected with HIV [Cock, K. M., *et al.*, 2000], TB being the most common opportunistic disease amongst HIV - infected people.

1.1.2 Drug Resistance and Development of Modern Anti-Tuberculosis Chemotherapy

The 'golden age' of TB chemotherapy began with the discovery of the aminoglycoside streptomycin (SM) by Waksman and colleagues in 1944. Two years later, the potent anti-tubercular activity of *p*-aminosalicylic acid (PAS) was discovered. In 1952, the investigation of nicotinamide activity on MTB *in vivo* led to the simultaneous discovery of INH by three drug discovery teams and pyrazinamide (PZA). Four years later, further development of the same lead gave rise to ethionamide (ETH) and prothionamide (PTH). In 1961, investigation

of the anti-TB activity of polyamines and diamines prompted the production of a series of diamine analogues that gave rise to ethambutol (EMB). Several other anti-TB agents have been discovered from the screening of compounds produced by soil organisms including cycloserine, kanamycin, viomycin, capreomycin, rifamycin and its derivative RIF. Using this array of agents, modern TB therapy was developed with the only significant introduction to the anti-TB arsenal since the 1960s being the introduction of the broad range quinolones to TB therapy in the late 1980s.

Currently, the recommended standard chemotherapeutic regime for TB treatment is prescribed under DOTS (directly observed treatment, short-course). Initially, the acronym described the chemotherapy regime but has later become the term used to describe a broader public health strategy with five principal elements: political commitment; case detection by sputum smear microscopy; standard short-course chemotherapy with supportive patient management, including DOT (directly observed treatment); a system to ensure regular drug supplies; and a standard recording and reporting system, including the evaluation of treatment outcomes [Bhowruth, V., *et al.,* 2007]. The chemotherapeutic regimen consists of an initial 2-month phase of treatment with INH, RIF, PZA and EMB followed by a continuation phase of treatment lasting 4 months with INH and RIF [Bass, J. B., *et al.*, 1994; Bhowruth, V., *et al.,* 2007]. The need for a long therapeutic regimen involving four drugs stems from several contributing factors: bacterial dormancy and phenotypic resistance to antimicrobials are certainly important, as is the issue of exposure to drugs, the structure and pathology of necrotic tuberculous lesions vary and the intracellular location of many of the bacteria might limit exposure. Variations in TB lesions effectively define the metabolic status of the bacteria *in vivo* and give rise to at least four sub-populations: active growers, that can be killed by INH; those with sporadic metabolic bursts that can be killed by RIF; a population with low metabolic activity that also experience acidic surroundings killed by PZA; and finally dormant bacilli that are not killed by any current agents [Bhowruth, V., *et al.,* 2007].

Poor patient compliance can promote the emergence of drug resistance and this is particularly true in TB chemotherapy [Bhowruth, V., *et al.,* 2007]. Strains of MTB resistant to INH were noted soon after the introduction of the drug, and MDR-TB strains have since

emerged, which further necessitated the inclusion of ethambutol in the WHO-recommended treatment regimens [Frieden, T. R., *et al.*, 2003].

1.1.3 MDR-TB and Mechanism of Resistance

Currently TB is treated with an initial intensive 2-month regime comprising multiple antibiotics - RIF, INH, PZA, and EMB or SM - to ensure that mutants resistant to a single drug do not emerge. In the next four months, only RIF and INH are administered to eliminate any persisting tubercle bacilli. INH and RIF, the two most potent antituberculous drugs, kill more than 99 % of tubercle bacilli within 2 months of initiation of therapy. Along with these two drugs, PZA, with a high sterilizing effect, appears to act on semi-dormant bacilli not affected by any other antitubercular drugs. Using these drugs in conjunction with each other reduces antitubercular therapy from 18 months to 6 months. Therefore, the emergence of strains resistant to either of these drugs causes major concern, as it leaves only drugs that are far less effective, have more toxic side effects, and result in higher death rates, especially among HIV-infected persons.

The phrase “MDR state” in mycobacteriology refers to simultaneous resistance to at least RIF and INH (with or without resistance to other drugs). Genetic and molecular analysis of drug resistance in MTB suggests that resistance is usually acquired by the bacilli either by alteration of the drug target through mutation or by titration of the drug through overproduction of the target. MDR-TB results primarily from accumulation of mutations in individual drug target genes. The probability of resistance is very high for less effective antitubercular drugs such as thiacetazone, ethionamide, capreomycin, cycloserine, and viomycin (10^{-3}); intermediate for drugs such as INH, SM, EMB, kanamycin, and PAS (10^{-6}); and lowest for RIF (10^{-8}). Consequently, the probability of a mutation is directly proportional to the bacterial load. A bacillary load of 10^{9} will contain several mutants resistant to any one antitubercular drug. Because the mutations conferring drug resistance are chromosomal, the likelihood of a mutant being simultaneously resistant to two or more drugs is the product of individual probabilities; thus the probability of MDR is multiplicative. Resistance to a drug does not confer any selective advantage to the bacterium unless it is exposed to that drug.

Under such circumstances, the sensitive strains are killed and the drug-resistant mutants flourish. When the patient is exposed to a second course of drug therapy with yet another drug, mutants resistant to the new drug are selected, and the patient may eventually have bacilli resistant to two or more drugs. Serial selection of drug resistance, thus, is the predominant mechanism for the development of MDR strains; the patients with MDR strains constitute a pool of chronic infections, which propagate primary MDR resistance. In addition to accumulation of mutations in the individual drug target genes, the permeability barrier imposed by the MTB cell wall can also contribute to the development of low-level drug resistance. Studies addressing resistance to SM have found evidence of such a two-step mechanism for the development of drug resistance [Rattan, A., *et al.,* 1998].

1.1.4 TB Drug Development Pipeline [Bhowruth, V., *et al.,* 2007; Spigelman, M. K., *et al.,* 2007]

Several promising anti-TB agents are currently at various stages of development. The following are the agents under development:

a. FLUOROQUINOLONES (MOXIFLOXACIN AND GATIFLOXACIN)

The fluoroquinolones gatifloxacin (GAT) and moxifloxacin (MXFX) are both currently being studied in phase 2 and/or 3 trials for the shortening of the treatment duration for active, drug-susceptible pulmonary TB. Both compounds are being tested in combination regimens in which they replace EMB during the initial 2-month phase of intensive therapy, whereas moxifloxacin is also being studied in a combination regimen replacing INH. GAT is active against MTB, with MIC 0.03 - 0.12 μg/mL. Four week treatment of MTB infected mice with GAT at 300 mg/kg is more effective than therapy with INH at 25 mg/kg, but at lower doses GAT was less effective in this timeframe. MXFX is effective against MTB *in vitro,* with MIC range of 0.06 - 0.5 μg/mL MXFX at 100 mg/kg was almost as effective as INH at 25 mg/kg: after 4 weeks of treatment.

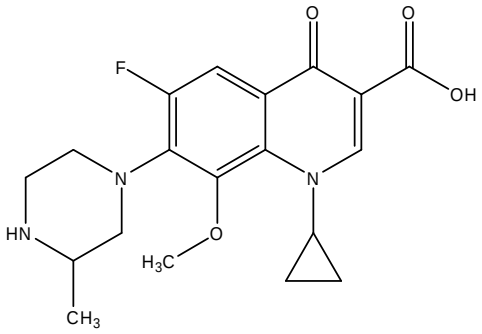

Gatifloxacin

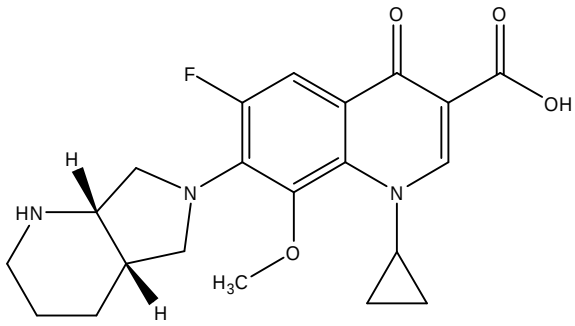

Moxifloxacin

b. DIARYLQUINOLINE (JOHNSON & JOHNSON)

TMC207910 inhibits both drug-sensitive and drug-resistant MTB *in vitro* with MIC of 0.06 μg/mL. In mice, it exceeded the bactericidal activities of INH and RIF by at least 1 log unit. Drug targets the proton pump of adenosine triphosphate (ATP) synthase.

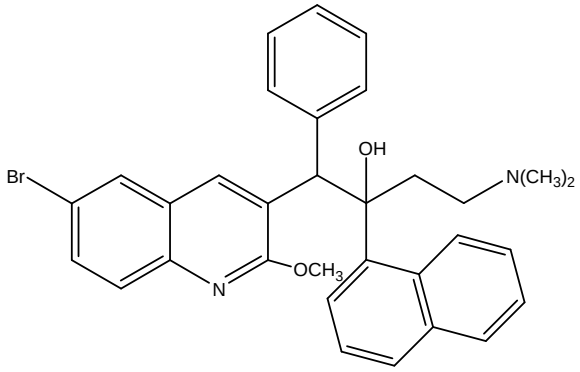

TMC207910

c. NITROIMIDAZOLES (Otsuka Pharmaceutical, Tokushima, Japan)

OPC-67683, a Nitro-dihydro-imidazooxazole derivative. It is active against TB, including MDR-TB, as shown by its exceptionally low minimum inhibitory concentration (MIC) range of 0.006 - 0.024 μg/ml *in vitro* and highly effective therapeutic activity at low doses *in vivo*. The effective plasma concentration was 0.100 mg/mL, which was achieved with an oral dose of 0.625 mg/kg, confirming the remarkable *in vivo* potency of the compound.

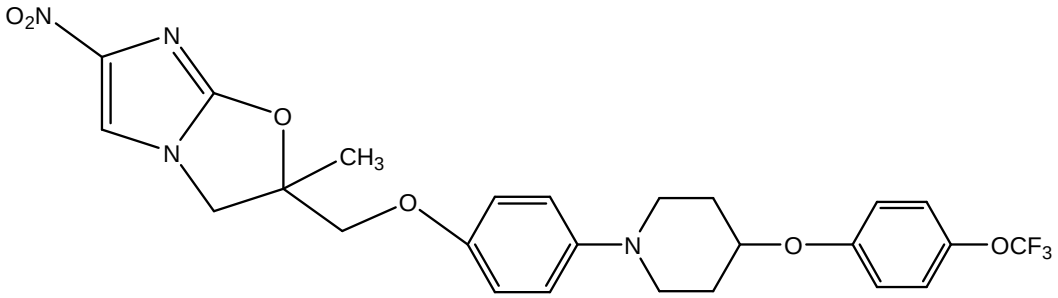

OPC-67683

d. PA-824 (PATHOGENESIS/CHIRON AND GATB)

PA-824 exhibits activity against both drug-susceptible and drug-resistant strains of MTB, with MIC ranging from 0.015 - 0.25 μg/ml. Notably, it has bactericidal activity against both replicating bacteria and non-replicating bacilli *in vitro.* PA-824 has a novel mechanism of action and inhibits both protein production and cell wall lipid biosynthesis. PA-824 is a prodrug that requires bacterial activation by reducing its nitro group: activation likely involves a F420-dependent mechanism. PA-824 lacks experimental animal model mutagenicity commonly associated with nitroimidazoles.

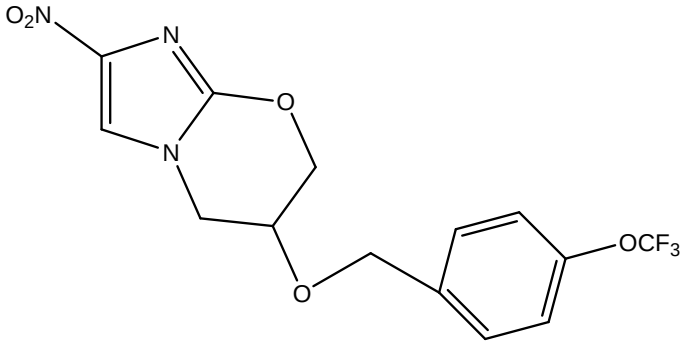

PA-824

e. DIAMINE (SEQUELLA AND NIH)

SQ109 has high specificity for *Mycobacteria* with MIC range (0.16 - 0.63 μg/ml) against MTB that are drug sensitive, MDR, and XDR. It has synergistic interactions *in vitro* and *in vivo* with two of the most important TB drugs in use today, RIF and INH. In the studies

using INH + RIF + SQ109 + PZA, no bacteria were cultured from lungs of mice treated for 2 months.

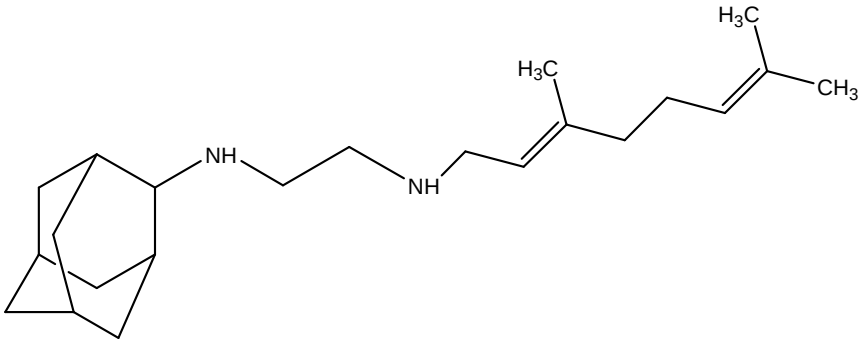

SQ109

f. SUDOTERB (LUPIN LTD)

LL 3858 demonstrated an MIC range of 0.125 - 0.25 μg/ml against drug-susceptible and drug resistant *M. tuberculosis*. *In vivo* efficacy of LL 3858 was evaluated at 12.5 mg/kg and 25 mg/kg. Mice were infected with a sub lethal dose of *M. tuberculosis* and treated with LL 3858 for 4, 8 and 12 weeks. As mono therapy, LL 3858 was more effective than INH.

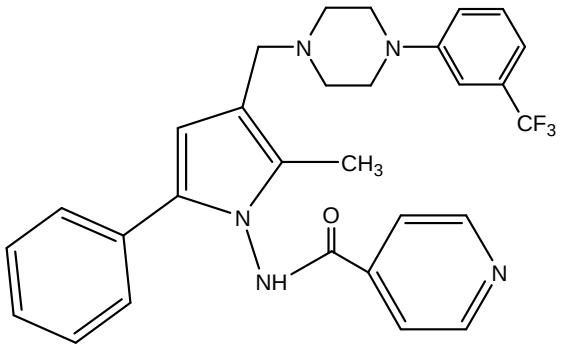

LL 3858

1.1.5 Quinolones and Tuberculosis

A great deal of interest has been generated in the quinolone antibiotics following the publication of recent clinical and pre-clinical data confirming their potential for use in treatment of TB. Data from a study of ofloxacin-containing regimens suggests that this drug (or a more potent quinolone) may be used to shorten the duration of chemotherapy. Patients treated with daily INH, RIF, PZA and ofloxacin (OFLO) for three months, followed by one or two months of twice-weekly INH and RIF had cure rates of 92 – 98 % and relatively low relapse rates (2 – 4 %). New generation quinolones possess significantly greater *in vitro* activity against MTB than OFLO and therefore offer the greatest potential benefit to patients. GAT and MXFX are particularly active, having MIC_{90} (minimum inhibitory concentration) values of 0.031 mg/mL and 0.125 mg/mL, respectively, compared with 1 mg/mL for levofloxacin (LVFX). The sterilising activity of various quinolones was investigated in a controversial *in vitro* model of persistence. GAT and MXFX were found to kill RIF-tolerant bacteria much more effectively than LVFX or OFLO suggesting they may possess greater sterilising activity in the clinic [Duncan, K., *et al.,* 2004].

It remains to be seen whether resistance will limit the use of fluoroquinolones. High level phenotypic resistance in MTB clinical isolates from patients in Hong Kong who had not received prior drug treatment was found predominantly to be associated with point mutations in DNA gyrase. In a recent study in South Korea, 26 % of patients with primary treatment failures showed resistance to ofloxacin suggesting that widespread use of fluoroquinolones for other infections may be contributing to the rapid loss of this class of molecule to the TB armory [Duncan, K., *et al.,* 2004].

CHAPTER 2

LITERATURE REVIEW

2.1 HISTORY AND OVERVIEW OF QUINOLONES

The quinolone anti-infective agents are of wholly synthetic origin and are not modeled knowingly after any natural antibiotic. Several ring systems are or have been involved. The numbering system is illustrated as follows:

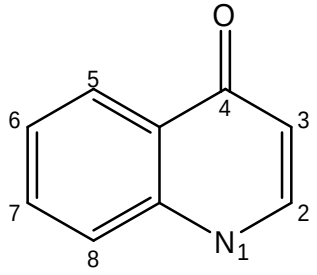

4-Oxo-1,4-dihydro-quinolone

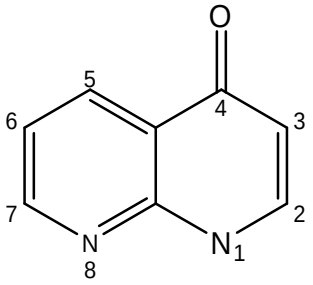

4-Oxo-1,4-dihydro-[1,8]-naphthyridine

Of all the totally synthetic antimicrobial agents, the (fluoro)quinolones have proven to be the most successful economically and clinically. They are orally and parenterally active, have a broad antimicrobial spectrum that includes many frequently encountered pathogens, are bactericidal in clinically achievable doses, generate comparatively tolerable resistance levels, possess a fascinating molecular mode of action, are comparatively easily synthesized, and with a few notable exceptions are safe. That is not to say that they are perfect drugs and cannot be improved but rather that they are important weapons in the ongoing struggle against morbidity and mortality caused by microbial pathogens.

The first antimicrobial quinolone was discovered about 50 years ago, in 1960s, as an impurity in the chemical manufacture of a batch of the antimalarial agent chloroquine.

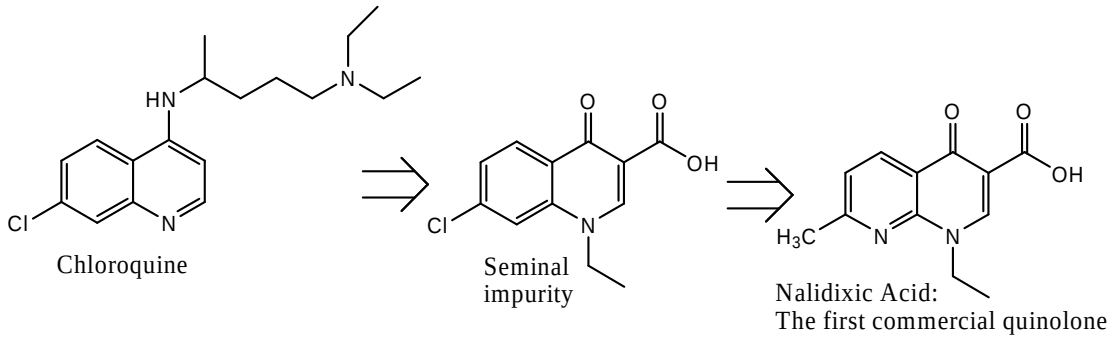

It demonstrated anti Gram-negative antibacterial activity, but its potency and antimicrobial spectrum were not significant enough to be useful in therapy. Building on this lead, however, subsequently nalidixic acid was commercialized. Nalidixic acid remains on the market today and represents the so-called **first generation quinolones**. Its antibacterial properties appeared immediately to be very interesting [Sissi, C., *et al.*, 2003]. Despite its convenient oral activity, bactericidal action, and ease of synthesis, its limited antimicrobial spectrum (primarily activity against *Escherichia coli*) and poor pharmacokinetic characteristics limit its use primarily to treatment of sensitive community-acquired urinary tract infections.

The first of the **second-generation family of quinolones**, norfloxacin (NOR), had dramatically enhanced and broader spectrum anti Gram-negative activity and possessed significant anti Gram-positive activity as well. The potency of NOR was in the same range as that of many fermentation-derived antibiotics, and its comparative structural simplicity and synthetic accessibility lead to a very significant effort to find even more improved analogues.

Shortly thereafter, ciprofloxacin (CIP) and OFLO, as well as its optically active form LVFX, were introduced. The second-generation agents have significant broad-spectrum antimicrobial activity including important Gram-positive pathogens. This is coupled with gratifying safety and pharmacokinetic characteristics.

A wide variety of clinical indications have been approved for quinolones including many infections commonly encountered in community practice including upper and lower respiratory infections, gynecologic infections, sexually transmitted diseases, prostatitis, and some skin, bone and soft tissue infections.

Recently introduced members of the fluoroquinolone family belong to the **third generation**. These include GAT and MXFX, which possess further enhanced activity against Gram-positive infections, and anti-anaerobic coverage is now present although at present only trovafloxacin is approved for this indication. (Table 2.1). [Mitscher, A. L., 2005]

2.1.1 Development of Quinolones

Quinolones were derived from quinine [Andersson, M. I., *et al.,* 2003]. A most successful achievement was the preparation of fluoroquinolones. In fact, the introduction of a fluorine atom at the C_6 position increased several folds the activity of the drug and led to compounds active against a broader spectrum of bacteria [Sissi, C., *et al.,* 2003; Andersson, M. I., *et al.,* 2003]. The first fluoroquinolone clinically used was NOR. Its poor tissue distribution limited its applications to the treatment of urinary tract infections. Modification of the substituent at N_1 position produced CIP. This drug presents an excellent systemic activity upon oral administration and has become indeed one of the most frequently prescribed antibiotics. Fluoroquinolones have been further optimized to improve both pharmacokinetic and pharmacodynamic properties like favorable bioavailability allowing oral administration, good tolerability, high tissue concentrations as well as superior bactericidal activity against a broad spectrum of clinically relevant pathogens. Thus, new generations of fluoroquinolones are now available. They preserve excellent potency against Gram-negative bacteria and, at the same time, they show an increased activity towards Gram-positive bacteria compared to CIP. At the moment, the main interest for these compounds is related to the treatment of respiratory diseases [Sissi, C., *et al.,* 2003]. Two major groups have been developed from the basic structure: quinolones and naphthyridones. The presence of nitrogen at position 8 identifies the naphthyridones, a carbon and associated group at position 8 identifies the quinolones [Andersson, M. I., *et al.,* 2003] (Figure 2.1).

Table 2.1: The various generations of the family of quinolones.

Structure	Name
First-generation compounds (often all included as 4-quinolones)	
1,8 naphthyridine	Nalidixic acid
(carboxylic acid)	Piromidic acid
7-methyl, 7-pyrrole	
1,2-cinnoline (carboxylic acid)	Cinoxacin
4-quinolone (carboxylic acid)	Oxolinic acid
7-piperazine (pyrido-pyrimidine)	Pipemidic acid
6,7,8 side chain substituents	**Name**
Second-generation compounds (IIA)	
A. Fluoroquinolones with enhanced but predominantly Gram-negative activity	
6-Fluoro	Flumequine
6-Fluoro-7-piperazinyl	Ciprofloxacin, Pefloxacin, Norfloxacin
	Ofloxacin, Levofloxacin, Rufloxacin
6,8-difluoro-7-piperazinyl	Lomefloxacin, Fleroxacin
Second-generation compounds (IIB)	
B. Fluoroquinolones with balanced broad spectrum activity	
6-fluoro-7-piperazinyl	Temafloxacin
6,8-difluoro-7-dimethylpiperazinyl	Grepafloxacin
6-fluoro-8-chloro-7-pyrrolodinyl	Sparfloxacin
6-fluoro-7-pyrrolodinyl naphthyridone	Clinafloxacin, Sitafloxacin, Tosufloxacin
Third-generation compounds	
Fluoroquinolones with enhanced Gram-positive activity	
6-fluoro-7-azabicyclo naphthyridone	Trovafloxacin
6-fluoro-8-methoxy-7-azabicyclo	Moxifloxacin
6-fluoro-8-methoxy-7-piperazinyl	Gatifloxacin
6-fluoro-7-methoxyiminonaphthyridone	Gemifloxacin

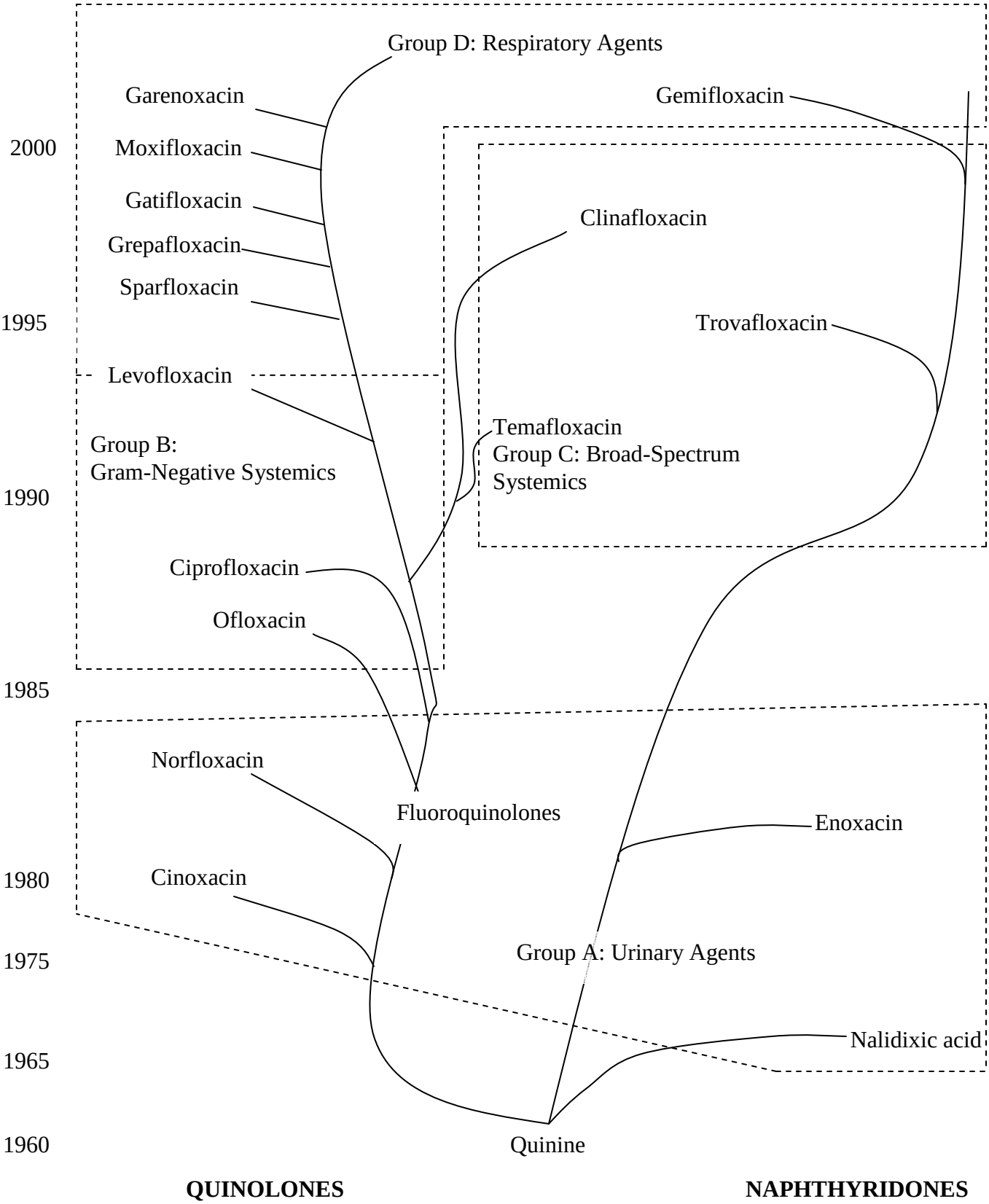

Figure 2.1: Development of quinolones.

Fluoroquinolones exhibit potent *in vitro* and *in vivo* antimycobacterial activity [Shandil, R. K., *et al.,* 2007]. The quinolones would appear to fulfill most of the criteria for an ideal class of antimycobacterial drugs. The *in vitro* activity of quinolones against mycobacteria and the efficacy of these drugs in murine models of mycobacterial infection have been documented in various studies and reviews [Sato, K., *et al.,* 2003; Aubry, A., *et al.,* 2004; Alangaden, G. J., *et al.,* 1997]. Quinolones have shown excellent bactericidal activity against several mycobacteria. Most strains of MTB, *M. leprae, M. bovis, M. kansasii, M. marinum and M. xenopi* were inhibited *in vitro* by CIP or OFLO at concentrations ranging between 0.5 mg/L and 2.0 mg/L [Sato, K., *et al.,* 2003; Aubry, A., *et al.,* 2004].

Quinolones can be administered orally with good absorption, and favorable pharmacokinetics which permit once- or twice-daily administration [Hooper. D. C., *et al.,* 1985]. Quinolones have excellent oral bioavailability and penetrate extremely well into tissues and into host cells, such as macrophages, in which mycobacteria often reside [von Rosenstiel, N., *et al.,* 1994; Takemura, M., *et al.,* 2001]. The incidence and severity of side effects of the quinolone are generally low [von Rosenstiel, N., *et al.,* 1994]. The incidence of mycobacterial resistance to quinolone is relatively low at the present time [Frieden, T. R., *et al.,* 1993], and there is no cross-resistance [Cambau, E., *et al.,* 1994] or antagonism with other classes of antimycobacterial agents [Grange, J. M., *et al.,* 1994], so they may be used for long-term therapy in combination with other antimycobacterial agents and with the diverse array of drugs that patients with HIV infection may be receiving.

Although quinolones have several advantages, pre-marketing trials showed the fluoroquinolone agents to have a favorable side-effect profile, with treatment - related adverse events comprising gastrointestinal, central nervous system and dermatologic effects that were generally mild and reversible on cessation of treatment. However, post-marketing surveillance studies have identified severe adverse events, including severe anaphylaxis, QTc-interval prolongation by SPFX and grepafloxacin [Andersson, M. I., *et al.,* 2003], and potential cardiotoxicity, associated with 3 quinolone agents that either

resulted in the removal of the agent from the market (temafloxacin and grepafloxacin) or significantly restricted its use due to substantial mortality and morbidity associated with liver toxicity (trovafloxacin). To date, there have been no such significant adverse events associated with the older fluoroquinolone agents, including CIP, OFLO, NOR, and LXFX [Bertino, J. Jr., *et al.,* 2000; Stratton, C. W., 1998]. Lomefloxacin, fluoroquinolone containing fluorine group at C_8 position, shows phototoxicity towards (Ultraviolet) UV radiation [Man, I., et al., 1999]. NOR, CIP and enoxacin are very photohemolytic, but sparfloxacin (SPFX) was not, indicating that the *in vivo* phototoxic potencies of fluoroquinolones might not be predictable by the photohemolysis study. GAT is a non-phototoxic quinolone [Yamamoto, T., *et al.,* 2001]. Quinolones are shown to produce convulsions when administered orally or intracerebrally in mice along with non-steroidal anti-inflammatory drugs like fenbufen. [Hirai, S., *et al.,* 1989; Furuhama, K., *et al.,* 1997]. Other effects include a haemolytic uraemic-like syndrome with temafloxacin, a metallic taste with grepafloxacin, hepatitis with trovafloxacin, unexpected hypoglycaemia with CNFX and temafloxacin, a number of immunologically mediated adverse events with tosufloxacin, and an immune-mediated rash in young women with gemifloxacin. To date there are little toxicological data on garenoxacin [Andersson, M. I., *et al.,* 2003].

2.1.2 Mode of Action

Forty years of research in the quinolone field has allowed to elucidating some key aspects of their mechanism of action. Their main biological targets are the DNA gyrase and topoisomerase IV, two enzymes belonging to the type II topoisomerase family. These enzymes are present in all bacteria and are expressed in prokaryotic organisms only, features that make them ideal antibacterial drug targets. Indeed, the prominent selectivity of quinolones in poisoning the bacterial type II topoisomerases, as the corresponding mammalian enzymes represents the rational basis for their safe use in antibacterial chemotherapy [Sissi, C., *et al.,* 2003; Maxwell., 1997].

Quinolone antibacterials, by inhibiting bacterial topoisomerase II (DNA gyrase) and topoisomerase IV [Maxwell., 1997] in Gram-positive species, inhibit tertiary negative

supercoiling of bacterial DNA. This effect, probably associated with binding of quinolones to a DNA gyrase complex, is rapidly bactericidal. The minimum bactericidal concentration is usually only two- to four folds the MIC, and a prolonged post-antibiotic effect is produced at concentrations exceeding the MIC. Fluoroquinolones only rarely demonstrate synergy or antagonism with other agents. [Andriole, V. T., 2000]

The target for quinolone action in Gram-negative bacteria is the A subunit of DNA gyrase. DNA gyrase is a bacterial type II topoisomerase. It is made up of a tetramer of two parts, A2 and B2. This protein converts relaxed DNA into supercoiled DNA. The A subunit is responsible for breakage and resealing of chromosomal DNA. The B subunit is responsible for energy transduction from ATP hydrolysis [Bonomo, R. A., 1998]. The mechanism of action responsible for the bactericidal activity of quinolone antimycobacterial appears to be an inhibition of bacterial DNA gyrase. Quinolones interfere with the action of DNA gyrase, preventing closure of the double stranded nicks produced by the A subunits [Doughety, T. J., *et al.,* 1985] by forming a quinolone-gyrase-DNA ternary complex [Bonomo, R. A., 1998]. Failure to close these nicks inhibits supercoiling and results in the degradation of chromosomal DNA into fragments by exonucleases [Fairweather, N. F., *et al.,* 1980], leading to termination of chromosomal replication and interference with cell division and gene expression [Fairweather, N. F., *et al.,* 1980], penetration through macrophages and phagosome walls especially for lomefloxacin [Mozhokina, G. N., *et al.,* 1998]. Topoisomerase IV is responsible for the separation of daughter DNA strands during bacterial cell division in Gram-positive bacteria. Topoisomerase IV is likely to be the primary target for quinolone action in Gram-positive bacteria. In addition to attacking DNA gyrase and topoisomerase IV, quinolones are bactericidal by other mechanisms. Three mechanisms A, B, and C have been proposed. Mechanism A requires RNA and protein synthesis as well as cell division for bactericidal action. Mechanism B is the ability to kill non-dividing cells without concomitant protein or RNA synthesis. Mechanism C is the bactericidal activity that occurs in the absence of multiplication, yet in the presence of protein and RNA synthesis. The action of these mechanisms is organism specific [Bonomo, R. A., 1998].

2.1.3 Quinolones and Immune Function

Quinolone antibiotics diffuse into human polymorphonuclear leukocytes (PMNs) and monocytes in concentrations one to five times greater than into the extracellular compartment. Intracellular quinolones may be bactericidal and may exert effects against *Staphylococcus aureus*, *Serratia marcescens*, *Mycobacterium fortuitum*, and *Salmonella typhimurium*. Although there is no effect on chemotaxis of PMNs, low concentrations have been reported to enhance phagocytosis [Bonomo, R. A., 1998].

2.1.3.1 Resistance Mechanism

Resistance to quinolone antibiotics is generally mediated by alterations in the chromosomal DNA of bacteria. In the main, most bacteria accumulate several mutations that affect both DNA gyrase and permeability.

Mutations in the regulatory genes that govern permeability channels or porins and efflux pumps are common. The expression of *marA***,** a transcriptional activator involved in multiple antibiotic resistance, results in diminished entry of quinolones into cells. Mutations that lead to a decrease porin expression of the bacterial outer membrane of Gram-negative bacteria also limit entry. Efflux pumps responsible for quinolone resistance have been characterized in both Gram-positive and Gram-negative bacteria. The physical properties of the quinolone determine whether it is pumped out.

Point mutations in residues 67 to 106 of the A subunit of DNA gyrase, the quinolone-resistance determining region (QRDR), also result in resistance. Mutations in this region are associated with increased resistance to all quinolones.

Resistance to quinolone agents may emerge during therapy e.g., CIP-resistant *pseudomonas aeruginosa*, *S. aureus* and *S. epidermidis*. In addition, strains of ciprofloxacin-resistant *Neisseria gonorrhoeae* have been reported from Southeast Asia, Australia, Africa, and the United Kingdom and from Ohio, California, Hawaii, and

Washington. In one sexually transmitted disease clinic in Ohio, 145 gonococcal isolates had reduced susceptibility to ciprofloxacin. Treatment failures have been reported with single dose regimens if the MIC of CIP for a strain of *N. gonorrhoeae* was ≥ 1µg/mL [Bonomo, R. A., 1998].

2.1.4 BACTERIAL RESISTANCE TO QUINOLONES

Fluoroquinolone resistance may result from chromosomal mutations coding for modifications in target subunits (primarily *gyr A*, but also *gyr B*) of bacterial topoisomerase II, alterations in expression of outer membrane proteins — most importantly OmpF— and, in Gram-positive species, by variations in the uptake/efflux processes and mutations in topoisomerase IV. Thus, resistance in the pneumococci requires mutations in both par C and *gyr A* configurations. Plasmid-mediated resistance has not been confirmed to occur. [Andriole, V. T., 2000]

1. **Chromosomal mutations** in the genes encoding DNA gyrase and Topo IV
    - Changes the target region where the drug binds to the enzyme
    - The drug exhibits reduced affinity for the target site, now ineffective
2. **Porin mutations**
    - Alteration of the outer membrane porin proteins of Gram-negative organisms lead to decreased permeability of the drug through the outer membrane so less drug reaches the target enzyme
3. **Efflux mutations**
    - Enhance the organism's efflux capability, increasing the amount of drug pumped out of the cell.

2.1.5 STRUCTURE - ACTIVITY RELATIONSHIP (SAR): Quinolone molecule

Recently, understanding of how molecular modifications of the core quinolone structure affect(s) antimicrobial agent activity has progressed rapidly. Three positions (2, 3, and 4) cannot be changed without a significant loss of biological activity. Furthermore, it appears that a cyclopropyl group is optimal at position 1. Substituents at positions 5 and 8

affect planar configuration, and either a methyl or methoxy appear optimal at these sites. Hydrogen and amino groups have been investigated as useful substituents at position 6, replacing the fluorine of the fluoroquinolones. Interestingly, *in vitro* activity Enhancement observed with alterations at positions 5 and 6 is not always accompanied by improved *in vivo* action. For all these modifications, the substituents at positions 7 and 8 are critical for potent antimicrobial activity. Optimizing overall molecular configuration enhances the number of intracellular targets for antimicrobial action (R-8) and impedes the efficiency of efflux proteins (R-7) that diminish intracellular penetration. [Peterson, L. R., 2001]

- Position 6 fluorine results in more than 10-fold increase in gyrase inhibition
- C_7 substituents - associated with increased potency against Gram-positive bacteria
    - Cyclic amino groups…
        - Piperazine rings = increase potency against Gram-bacteria
        - Pyrrolidine rings = increased potency against Gram-positive bacteria, yet lower water solubility
        - Methyl groups shown to help
- C_8 position - alkylation increases activity against Gram-positive bacteria and tissue penetration

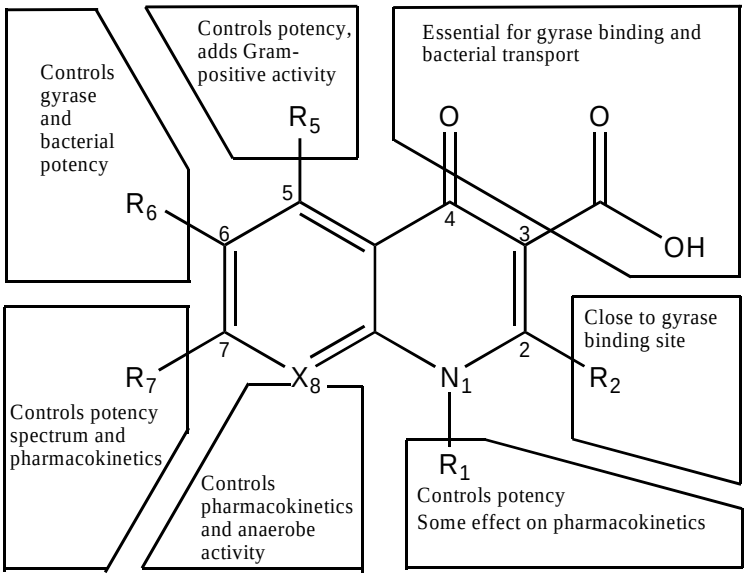

Figure 2.2: Overview of SAR of quinolone and napthyridone molecule. In molecules where X is a carbon atom, the molecule is a quinolone (cinoxacin, NOR, OFLO, CIP, temafloxacin, SPFX, grepafloxacin, LVFX, CLFX, MXFX, GAT). Where X is a nitrogen atom the molecule is a naphthyridone (nalidixic acid, enoxacin, tosufloxacin, trovafloxacin, gemifloxacin). [Andersson, M. I., *et al.*, 2003]

2.2 ANTITUBERCULAR QUINOLONES

CIP, OFLO and NOR were ineffective at clinically relevant concentrations against the *Mycobacterium avium* complex (MAC) *in vitro* as measured by radiometric respirometry, when administered alone. But good antimycobacterial activity was obtained when any of the quinolones was combined with ethambutol. The synergistic effect was most pronounced for the combination of EMB and CIP. This suggests that the synergism is based on an enhanced penetration of the quinolones by EMB [Hoffner, S. E., *et al.*, 1989]. SPFX was also tested against 30 strains of *Mycobacterium avium* complex (MAC) isolated from patients with acquired immune deficiency syndrome, alone and in combination with various antitubercular drugs. [Yajko, D. M., *et al.*, 1990]

In 1991, Rastogi, N., and Goh, K. S., determined the MICs of the new fluoroquinolone drugs, OFLO, CIP, and SPFX (AT-4140) for 10 strains of MTB by using both a BACTEC radiometric method and testing on solid 7H11 agar medium. Radiometric MICs by 7H12 broth testing ranged from 0.5 to 1.0, 0.25 to 0.5, and 0.1 to 0.2 µg/ml for OFLO, CIP, and SPFX respectively, whereas MICs in solid medium ranged from 0.5 to 1.0, 0.5 to 1.0, and 0.2 to 0.5 µg/ml, respectively. The bactericidal action of the quinolones compared with their reported peak concentrations in human serum showed that SPFX is the most bactericidal, followed by CIP and OFLO. The results suggested the potential of the new difluorinated quinolone SPFX for use against the tubercle bacillus and its antimycobacterial spectrum. [Rastogi, N., *et al.*, 1991]

In 1992, Tomioka, H., *et al.*, showed that the compounds with morpholine substitution at 7^{th} position are equipotent to that of ofloxacin [Tomioka, H., *et al.*, 1992]. Tomioka, H., *et al.*, in 1993, measured *in vitro* antimicrobial activities of OFLO, CIP, SPFX, fleroxacin, Y-26611, OPC-17116 against *Mycobacterium avium* and *M. intracellulare* by the two-fold dilution methods using two types of media, 7H11 agar medium and 1 % Ogawa egg medium. [Tomioka, H., *et al.*, 1993]

Ji, B., *et al.*, reported *in vitro* and *in vivo* activities of LVFX against MTB. In tests with 18 drug-susceptible strains of MTB, the MIC at which 50 % of the strains are inhibited by LVFX was one dilution less than that at which 50 % of the strains are inhibited by OFLO, but the MICs at which 90 % of the strains are inhibited were similar. The *in vivo* activity of LVFX against MTB was compared with the activities of INH, OFLO, and SPFX. Mice were inoculated intravenously with 1.74×10^6 CFU of H37Rv, and treatments began the next day and were carried out six times weekly for 4 weeks. The severity of infection and effectiveness of treatment were assessed by survival rate, spleen weights, gross lung lesions, and enumeration of CFU in the spleen. In terms of CFU counts, the ranking of the anti- MTB activities of the treatments used ran in the following order: LVFX (300 mg/kg of body weight) = SPFX (100 mg/kg) > INH (50 mg/kg) > SPFX (50 mg/kg) > OFLO (300 mg/kg) = LVFX (150 mg/kg) > OFLO (150 mg/kg) = LVFX (50 mg/kg). It seems, therefore, that the *in vivo* activity of LVFX is comparable to that produced by a two fold - greater dosage of OFLO. It is assumed that the maximal clinically tolerated dosage of LVFX is similar to that of OFLO, i.e., 800 mg daily, which is equivalent to 300 mg of LVFX per kg in mice. Because LVFX displayed powerful bactericidal activity, promising effects against human tuberculosis may be achieved if patients are treated with the maximal clinically tolerated dosage of LVFX. [Ji, B., *et al.*, 1995]

The fluoroquinolones have been shown to be highly active *in vitro* against many mycobacterial species, including most strains of MTB and *M. fortuitum*, and some strains of *M. kansasii*, *M. avium*-intracellulare (MAI) complex and *M. leprae*. CIP, OFLO and SPFX are the best studied of this class of drugs to date, and they are among the most active of these against MTB and other mycobacteria. The use of ofloxacin in the treatment of patients with multidrug-resistant pulmonary tuberculosis has resulted in the selection of quinolone - resistant mutants in a few patients [Jacobs, M. R., 1995]. The dramatic increase in drug resistant MTB has caused resurgence in research targeted toward these organisms. As part of a systematic study to optimize the quinolone antibacterials against mycobacteria, Renau, T. E., *et al.*, have prepared a series of N-l-phenyl-substituted derivatives to explore the effect of increasing lipophilicity on potency

at this position. The compounds, synthesized by the modification of a literature procedure, were evaluated for *Mycobacterium fortuitum* and activity against Gram-negative and Gram-positive bacteria, *Mycobacterium smegmatis* (MC^2), and the results correlated with log *P*, pKa, and other attributes. The activity of the compounds against the rapidly growing, less hazardous organism *M. fortuitum* was used as a measure of MTB activity. The results demonstrate that increasing lipophilic character by itself does not correlate with increased potency against mycobacteria. Rather, intrinsic activity against Gram-negative and/or Gram-positive bacteria is the governing factor for corresponding activity against mycobacteria. [Renau, T. E., *et al.*, 1995]

As part of a study to optimize the quinolone antibacterials against MTB, Renau, T. E., *et al.*, have prepared a series of N_1– and C_7– substituted quinolones to examine specific structure - activity relationships between modifications of the quinolone at these two positions and activity against mycobacteria. The compounds were evaluated for activity against *Mycobacterium fortuitum* and MC^2as well as Gram - negative and Gram - positive bacteria. The activity of the compounds against *M. fortuitum* was used as a barometer of MTB activity. The results demonstrated that (i) the activity against mycobacteria was related more to antibacterial activity than to changes in the lipophilicity of the compounds, (ii) the antimycobacterial activity imparted by the N_1 substituent was in the order *tert* – butyl > cyclopropyl > 2,4 - difluorophenyl > ethyl ≈ cyclobutyl > isopropyl, and (iii) substitution with either piperazine or pyrrolidine heterocycles at C_7 afforded similar activity against mycobacteria. [Renau, T. E., *et al.*, 1996a]

Renau, T. E., *et al.*, reported a series of quinolones with substitutions at the 8^{th} position to examine the relationship between structural modifications at this position and activity against mycobacteria. The compounds were prepared by procedures described in the literature and were evaluated for their activities against *Mycobacterium fortuitum* and MC^2. The activities of the compounds against these two organisms were used as a measure of MTB activity. The results demonstrate that the contribution of the 8^{th} position to antimycobacterial activity was dependent on the substituent at N_1 and was in the order

(i) COMe ≈ CBr > CCI > CH ≈ CF ≈ COEt > N > CCF_3 when N_1 was cyclopropyl; (ii) N ≈ CH > CF > COMe when N_1 was 2,4-difluorophenyl; (iii) N > or = CH when N_1 was *tert*-butyl; and (iv) N > CH when N_1 was ethyl. In general, derivatives with piperazine substitutions at C_7 were slightly less active against mycobacteria than the analogs with pyrrolidine substitutions, regardless of the pattern of substitution at the 8 position. Several of the best compounds were evaluated for their potential side effects as well as their activities against *Mycobacterium aurum, Mycobacterium avium, M. intracellulare*, and MTB. These agents exhibited biological profiles similar to or better than those of the positive controls CIP and SPFX. [Renau, T. E., *et al.,* 1996b]

In 1996, Klopman, G., *et al.,* showed the importance of *tert*-butyl group at N_1 position and said that *tert*-butyl substituents at least as good as cyclopropyl in rendering high levels of antimycobacterial activity. The 63 synthesized molecules were tested against *Mycobacterium avium, Mycobacterium intracellulare* complex. [Klopman, G., *et al.,* 1996]

Sbarbaro, J. A., *et al.,* reported that clinically achievable level of PZA enhances the antimycobacterial effect of low, non-bactericidal levels of OFLO and does not impede the bactericidal effect of a higher clinically effective level of OFLO. Unlike the combination of PZA and rifampin, these interactive effects are not affected by the sequence of drug administration. Findings support the use of these agents as a potentially effective preventive therapy combination for individuals exposed to multi-drug resistant tuberculous organisms. [Sbarbaro, J. A., *et al.,* 1996]

Ji, B., *et al.,* On 10 % oleic acid – albumin – dextrose – catalase - enriched 7H11 agar medium, the MIC at which 90 % of the isolates are inhibited for 20 strains of MTB was 0.5 µg of SPFX or MXFX per ml and 1.0 µg of clinafloxacin (CNFX) per ml, indicating that the *in vitro* activities of SPFX and MXFX were virtually identical and were slightly greater than that of CNFX. However, the *in vivo* activities of these drugs in a murine tuberculosis model differed considerably. Female Swiss mice were infected intravenously with 6.2 x 10^6 CFU of the H37Rv strain and treated for 4 weeks, beginning the next day

after infection, with INH serving as the positive control. By the criteria of 30 - day survival rate, spleen weight, gross lung lesion, and mean number of CFU in the spleen, treatment with CNFX at up to 100 mg/kg of body weight six times weekly displayed no measurable effect against MTB, whereas both SPFX and MXFX were effective; administration six times weekly of either of the latter two drugs demonstrated dosage-dependent bactericidal effects, as measured by enumeration of CFU in the spleens, and MXFX appeared more bactericidal than the same dosage of SPFX. Of the three fluoroquinolones, only MXFX at 100 mg/kg six times weekly appeared as bactericidal as INH at 25 mg/kg six times weekly. Thus, MXFX may be an important component of the newer combined regimens for treatment of tuberculosis. [Ji, B., *et al.,* 1998]

In 1999, Vacher, S., *et al.,* compared the antimycobacterial activities of fluoroquinolones *viz.,* ofloxacin, ciprofloxacin and grepafloxacin against three complex strains of *Mycobacterium avium*, *Mycobacterium kansasii*, *Mycobacterium marinum* and *Mycobacterium tuberculosis*. [Vacher, S., *et al.,* 1999]

Bermudez, L. E., *et al.,* evaluated MXFX activity against MAC *in vitro* against 25 strains. The results showed that MXFX, EMB, and azithromycin were active as single agents in liver, spleen, and blood. Rifabutin showed inhibitory activity only in the blood. Two-drug combinations containing azithromycin were no more active than azithromycin alone. Similarly, the three-drug combination was not more active than azithromycin alone in the spleen. Rifabutin did not add to the activity of any other single agent or two - drug combination. MXFX at both the concentrations in combination with ethambutol was significantly more active than each drug alone. [Bermudez, L. E., *et al.,* 2001]

The *in vitro* inhibitory activities of quinolones against supercoiling activity of MTB DNA gyrase were measured by Onodera, Y., *et al*. The various quinolones studied were sitafloxacin (DU-6859a), SPFX, CIP and LVFX. Two altered proteins of *GyrA* containing Ala-90Val, or Ala-90Val and Asp-94Gly were also purified and the inhibitory activities were studied and were found to be weaker than those against the wild - type

enzyme. These results suggested that mutations in the corresponding genes confer quinolone resistance. [Onodera, Y., *et al.*, 2001]

Savini, L., *et al.*, reported the synthesis of a series of 4-quinolylhydrazones and tested against MTB H37Rv. For the most of derivatives interesting antitubercular properties were showed; two compounds (**1** and **2**), identified as the most active, were tested also against *Mycobacterium avium*. Both compounds (**1** and **2**), with a high SI value (11.68 and 10.24 respectively), were then tested for efficacy *in vitro* in a TB-infected macrophage model, showing good values of EC_{90} and EC_{99}. Furthermore, these compounds were evaluated for their inhibitory activity against a single strain of *M. avium*, an opportunistic pathogen which has been associated with tuberculosis in patients infected by HIV. As for compounds **1** and **2**, which showed a SI of 23.32 and 20.45 respectively. It is important to point out the low toxicity particularly shown by quinolylhydrazones **1** and **2** active against MTB H37Rv and *M. avium*. [Savini, L., *et al.*, 2002]

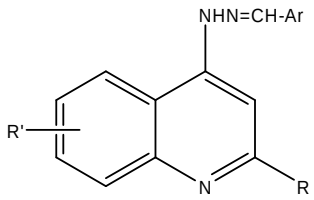

Compd	R	R’	Ar
1	H	7-OCH_3	2-OCH_3-Naphthyl
2	CH_3	6-Cyclopropyl	C_6H_5

Rodríguez, J. C., *et al.*, in 2002 evaluated the *in vitro* activity of MXFX, GAT, LVFX and linezolid against 234 strains of MTB isolated in the Southeast of Spain. All drugs tested showed good activity, with an MIC_{90} of less than 1 mg/l, and were active against INH and RIF resistant strains. [Rodríguez, J. C., *et al.*, 2002]

Alvirez-Freites, E. J., *et al.*, evaluated GAT and MXFX *in vitro* and *in vivo* to determine their activities against MTB. GAT was subsequently compared in a dose range study to INH in a murine tuberculosis model. They found that GAT was somewhat less active

than INH. GAT and MXFX were found to have similar activities. GAT was studied alone and in combination with EMB, ETH, and PZA and compared to INH and RIF. [Alvirez-Freites, E. J., *et al.,* 2002]

Foroumadi, A., *et al.,* reported a series of N-[2-oxo-2-(4-substitutedphenyl)ethyl]piperazinyl quinolones and N-[2-hydroxyimino-2-(4-substitutedphenyl)ethyl]piperazinyl quinolones for antituberculosis activity against MTB H37R. Active compounds were also screened by serial dilution to assess toxicity to a Vero cell line. Nine compounds were efficient antimycobacterial agents showing MIC values ranging from 0.78 to 6.25 µg/ml. Generally, CIP derivatives were more active than NOR and enoxacin derivatives and the oxime analogues were less active than corresponding ketones [Foroumadi, A., *et al.,* 2002a]. Various CIP derivatives containing 2-(2-furyl)-2-oxoethyl group [Foroumadi, A., *et al.,* 2002b], 2-phenyl-2-axoethyl and 2-(4-fluorophenyl)-2-axoethyl groups [Foroumadi, A., *et al.,* 2003a] at N_4 position of piperazine ring was tested for efficacy *in vitro* in TB - infected macrophage model.

Jain, R., *et al.,* reported the synthesis and antituberculosis activities of a series of novel ring-substituted quinolines. The most effective compound of the series **3** (MIC = 6.25 mg/mL, MTB H37Rv strain) was synthesized in one step; thus is an attractive lead molecule for antituberculosis drug development. The results of this study represent the discovery of ring-substituted 4-methylquinolines as new class of potential antituberculosis agents. [Jain, R., *et al.,* 2003]

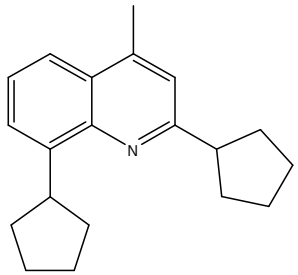

3

Ciccone, R., *et al.,* reported the antimycobacterial activity of NCX 976 (**4**), a new molecule obtained adding a NO moiety to the fluoroquinolone CIP, on MTB H37Rv

strain, both in a cell-free model and in infected human macrophages. Unlike unaltered ciprofloxacin, **4** displayed a marked activity also at low-nanomolar concentrations. [Ciccone, R., *et al.,* 2003]

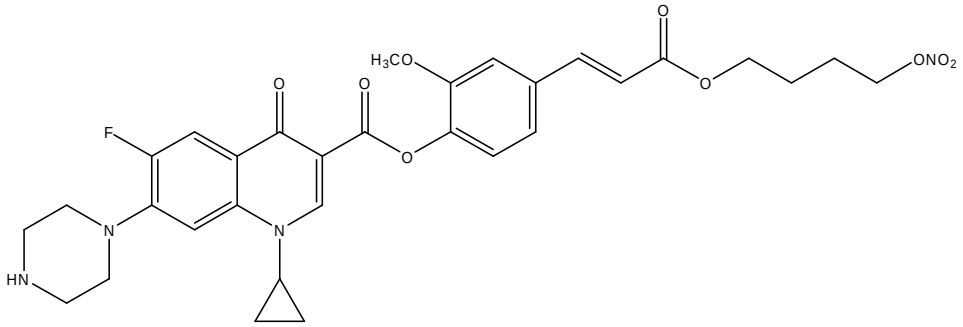

4

Foroumadi, A., *et al.,* reported a series of N-[2-(2-furyl)-2-oxoethyl], N-[2-(2-furyl)-2-oxyiminoethyl], N-[2-oxo-2-(2-thienyl)ethyl] and N-[2-oxyimino-2-(2-thienyl)ethyl] piperazinyl quinolones and evaluated for antituberculosis activity against MTB H37Rv using the BACTEC 460 radiometric system and BACTEC 12B medium. CIP derivatives were more active than NOR derivatives and the oxime analogues were less active than the corresponding ketones. [Foroumadi, A., *et al.,* 2003b]

Sbardella, G., *et al.,* synthesized novel 1,7-disubstituted-6-nitroquinolones which were tested against MTB and MAC as well as against both Gram-positive and Gram-negative bacteria. *In vitro* assays showed some derivatives were endowed with good inhibiting activities against tested mycobacteria. Some derivatives were also found more potent than CIP and OFLO against Gram-positive bacteria. [Sbardella, G., *et al.,* 2004]

Vaitilingam, B., *et al.,* synthesized four new series of ring-substituted quinolinecarboxylic acids/esters constituting 45 analogues from the structural optimization of recently discovered new chemical entity, 2,8-dicyclopentyl-4-methylquinoline (MIC= 6.25 µg/mL, MTB H37Rv). All new derivatives were evaluated for *in vitro* antimycobacterial activities against MTB H37Rv. Certain ring-substituted-2-quinolinecarboxylic acid ester and ring-substituted-2-quinoline acetic acid ester analogues described showed moderate to good inhibitory activity. In particular, three analogues methyl 4,5-dicyclopentyl-2-quinolinecarboxylate (**5**), methyl 4,8-

dicyclopentyl-2-quinolinecarboxylate and ethyl 2-(2,8-dicyclopentyl-4-quinolyl)acetate exhibited excellent MIC values of 1.00, 2.00 and 4.00 µg/mL, respectively. Results obtained indicated that substitution of the quinoline ring with dicyclopentyl substituent presumably enhances the antimycobacterial activities in the quinoline analogues described herein. [Vaitilingam, B., *et al.*, 2004]

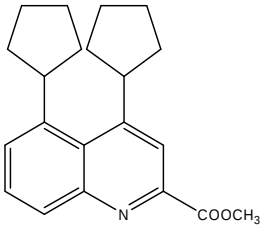

5

Vangapandu, S., *et al.*, report *in vitro* antimycobacterial properties of ring substituted quinolines constituting 56 analogues against drug-sensitive and drug-resistant MTB H37Rv strains. The most effective compounds **6** and **7** have exhibited an MIC value of 1 µg/mL against drug-sensitive MTB H37Rv strain that is comparable to first line anti-tuberculosis drug, INH. Selected analogues (with MIC: 6.25 µg/mL) upon further evaluation against single-drug-resistant (SDR) strains of MTB H37Rv have produced potent efficacy in the range between 6.25 and 50 µg/mL. [Vangapandu, S., *et al.*, 2004]

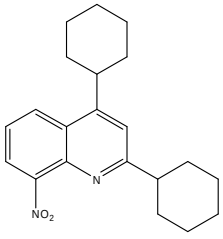

6

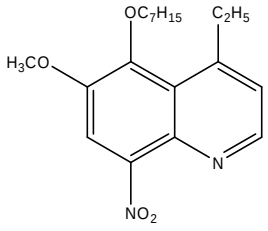

7

Monga, V., *et al.*, performed additional structural modifications of the new chemical entity, 2,8-dicyclopentyl-4-methylquinoline (MIC = 6.25 µg/mL, *M. tuberculosis* H37Rv) resulted in the synthesis of four new series of the ring-substituted quinolinecarbohydrazides constituting 22 analogues. All new derivatives were evaluated for *in vitro* antimycobacterial activities against drug-sensitive MTB H37Rv strain. Certain ring substituted 2-quinolinecarbohydrazide analogues described herein showed good inhibitory activity. In particular, analogues 4-(1-adamantyl)-2-quinolinecarbohydrazide, 4,5-dicyclopentyl-2-quinoline-carbohydrazide, 4,8-

dicyclopentyl-2-quinolinecarbohydrazide and 4,5-dicyclohexyl-2-quinolinecarbohydrazide have exhibited the MIC value of 6.25 µg/mL. Further investigation of the most suitable lead prototype, 4-(1-adamantyl)-2-quinolinecarbohydrazide led to the synthesis of N_2-alkyl/N_2, N_2-dialkyl/N_2-aryl-4-(1-adamantyl)-2-quinolinecarboxamides consisting of 13 analogues. Some of the synthesized carboxamides **8** and **9** reported herein have exhibited excellent antimycobacterial activities in the range of 6.25 - 3.125 µg/mL against drug-sensitive and drug-resistant MTB H37Rv strains. [Monga, V., *et al.,* 2004]

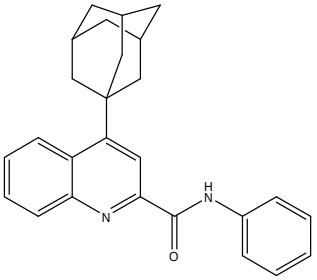

8

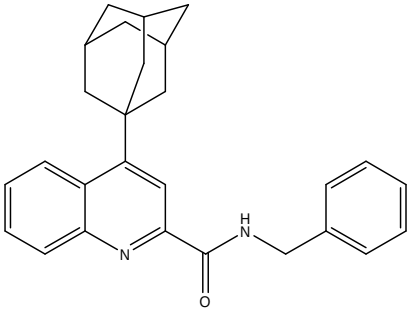

9

Various nitroheterocycles like nitrofuranylamides [Tangallapally, R. P., *et al.,* 2004; Tangallapally, R. P., *et al.,* 2005], 6-nitro-2,3-dihydroimidazo[2,1-*b*]oxazoles [Sasaki, H., *et al.,* 2006], nitroimidazopyran [Lenaerts, A. J., *et al.,* 2005], 5-nitro-2,3-dihydroimidazo-oxazole [Ashtekar, D. R., *et al.,* 1993] and nitroimidazole [Barry, C. E., *et al.,* 2004] inhibited MTB H37Rv (MTB) *in vitro* and *in vivo*. Till date few 6-nitroquinolones were studied [Artico, M., *et al.,* 1999; Sbardella, G., *et al.,* 2004], and were mostly bearing identical substituents at positions 1 and 7 of the quinolone moiety.

Zhao, Y. L., *et al.,* reported synthesis and antimycobacterial activity of a number of fluoroquinolone derivatives. Preliminary results were (1) for 1-aryl fluoroquinolones, 1-(4-nitrophenyl) derivatives were inactive while their 1-(2-fluoro-4-nitrophenyl) counterparts were active anti-TB agents (**10** vs **12**; **9** vs **11**) indicated the fluoro substituent at C_2 position is important. For the 1-(2-fluoro-4-nitrophenyl)quinolones, 7-piperidinyl derivative **12** and 7-(3,5-dimethylpiperazinyl) derivative **16**, which exhibited 97 % and 98 % inhibition, respectively, were more active than their 7-morpholinyl, 7-(4-methylpiperazinyl) and 7-piperazinyl congeners, **13**, **14** and **15**, respectively. In addition,

7-[4-(8-hydroxyquinolin-2-ylmethyl)piperazin-1-yl] derivative **20** exhibited 44 % inhibition on the growth of MTB while its 7-(4-methylpiperazin-1-yl) counterpart was inactive implied the metal-chelating 8-hydroxyquinoline moiety was capable of enhancing the anti-TB activity, (2) for the bifunctional fluoroquinolone-hydroxyquinoline complexes, CIP and OFLO derivatives, which exhibited the same anti-TB activity (98 % inhibition), are more potent than norfloxacin counterpart, which in turn is more potent than 1-aryl congeners (**18**, **19** > **17** > **20**, **21**). [Zhao, Y. L., *et al.*, 2005]

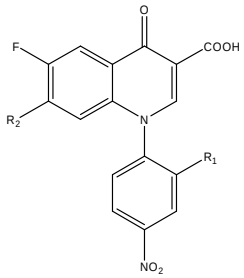

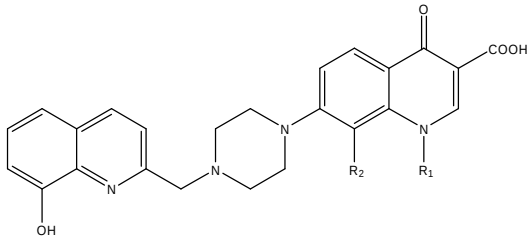

Comp	R_1	R_2
10	H	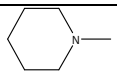
11	H	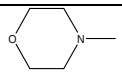
12	F	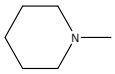
13	F	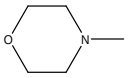
14	F	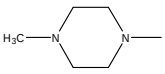
15	F	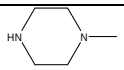
16	F	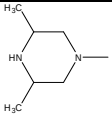

Comp	R_1	R_2
17	-CH2CH3	H
18	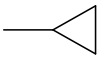	H
19	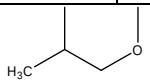	
20	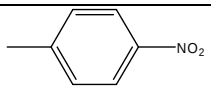	H
21	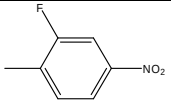	H

Shindikar, A. V., *et al.*, reported that novel 6,8-difluoro-1-alkyl-5-amino-1,4-dihydro-4-oxo-7-{4-substituted piperazin-1-yl}-quinoline-3-carboxylic acids, with the substituents at 4th position of piperazine being -[2(pyridine-4-carbonyl) hydrazono]propyl and -2 [(pyrazine-2-carbonyl) amino] ethyl, were synthesized and evaluated *in vivo* against

MTB H37Rv in Swiss albino mice. Test compounds exhibited activity comparable to that of SPFX (survival rate, reduction of splenomegaly and reduced tubercular lesions) at a dose of 200 mg/kg. Compound **22** with 100 % survival rate, absence of lung lesions, and 75 % inhibition of CFUs emerged as the most potent compound. [Shindikar, A. V., *et al.*, 2005]

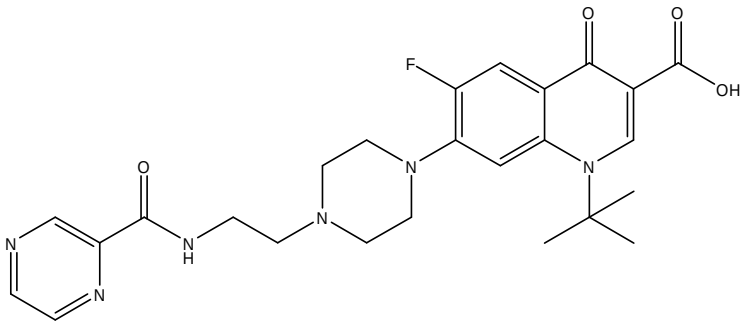

22

Sriram, D., *et al.,* synthesized various 7-substituted CIP derivatives and evaluated for antimycobacterial activity *in vitro* and *in vivo* against MTB and for inhibition of the supercoiling activity of DNA gyrase from MC^2. Preliminary results indicated that most of the compounds demonstrated better *in vitro* antimycobacterial activity against MTB than CIP. Compound 1-cyclopropyl-6-fluoro-1,4-dihydro-4-oxo-7-[[N4-[1'-(5-methylisatinyl-beta-semicarbazo)]methyl]N1-piperazinyl]-3-quinoline carboxylic acid (**23**) decreased the bacterial load in spleen tissue with 0.76-log10 protections and was considered to be moderately active in reducing bacterial count in spleen. The results demonstrated the potential and importance of developing new quinolone derivatives against mycobacterial infections. [Sriram, D., *et al.,* 2005]

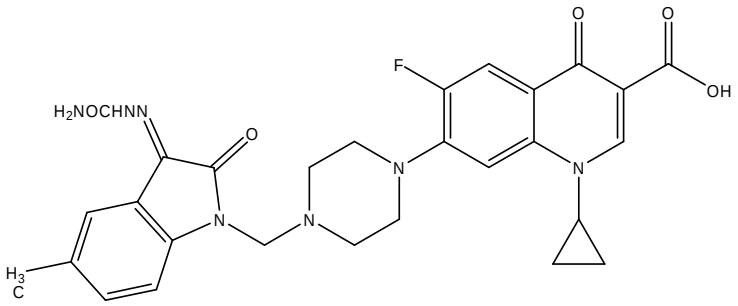

23

Zhao, G., *et al.,* described the syntheses and anti-tuberculosis activity of quinolone-cephalosporin conjugates (**24** and **25**). Both showed broad-spectrum antibacterial activity

and significant anti-TB activity. The carbamate-linked quinolone-cephem **25** showed better antimycobacterial activity, including anti - TB activity, than the direct amine - linked quinolone - cephem **24**, while quinolone - cephem **25** was slightly more effective against some Gram-negative bacterial strains. [Zhao, G., *et al.*, 2006]

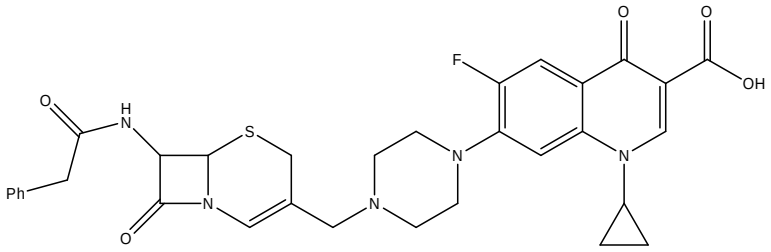

24

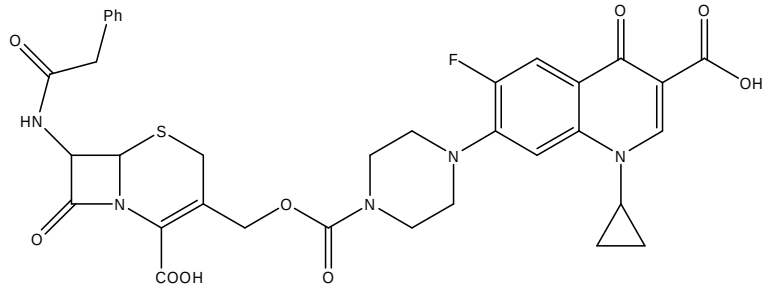

25

Schwartz, Y. S., *et al.*, prepared the MXFX - conjugated dansylated carboxymethylglucan (M-DCMG) conjugate by chemically linking dansylcadaverine (D) and MXFX to carboxymethylglucan (CMG), a known ligand of macrophage scavenger receptors. The targeted delivery to macrophages and the antituberculosis activity of the conjugate MXFX-DCMG were studied *in vitro* and *in vivo*. Using fluorescence microscopy, fluorimetry, and the J774 macrophage cell line, MXFX-DCMG was shown to accumulate in macrophages through scavenger receptors in a dose-dependent (1 to 50 µg/ml) manner. After intravenous administration of MXFX-DCMG into C57BL/6 mice, the fluorescent conjugate was concentrated in the macrophages of the lungs and spleen. Analyses of the pharmacokinetics of the conjugate demonstrated that MXFX-DCMG was more rapidly accumulated and more persistent in tissues than free MXFX. Importantly, therapeutic studies of mycobacterial growth in C57BL/6 mice showed that the MXFX-DCMG conjugate was significantly more potent than free MXFX. [Schwartz, Y. S., *et al.*, 2006]

Foroumadi, A., *et al.,* synthesized a number of N-substituted piperazinylquinolone derivatives and evaluated for antibacterial activity against Gram - positive and Gram - negative bacteria. Preliminary results indicated that most compounds tested in this study demonstrated comparable or better activity against *Staphylococcus aureus* and *Staphylococcus epidermidis* than their parent piperazinylquinolones as reference drugs. Among these derivatives, CIP derivative **26**, containing N-[2-[5-(methylthio)thiophen-2-yl]-2-oxoethyl] residue, showed significant improvement of potency against staphylococci, maintaining Gram-negative coverage. [Foroumadi, A., *et al.*, 2006]

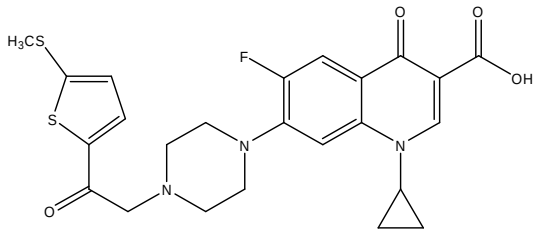

26

Nayyar, A., *et al.,* have previously identified ring substituted quinolines as a new structural class of antituberculosis agents. In this article, efforts at structural optimization of this class, four series of ring-substituted-2/4-quinolinecarbaldehyde derivatives were synthesized. All twenty four compounds were synthesized using short and convenient one to two high yielding steps. The newly synthesized compounds were tested *in vitro* against drug - sensitive MTB H37Hv strain. Several derivatives were found to be promising inhibitors of MTB displaying > 90 % inhibition at 6.25 µg/mL in the primary assay. The most active compounds, N-(2-fluorophenyl)-N-quinolin-2-ylm-ethylene-hydrazine (**27**), N-(2-adamantan-1-yl-quinolin-4-ylmethylene)-N-(4-fluorophenyl)hydrazine (**28**), and N-(2-cyclohexyl-quinolin-4-ylmethylene)-N-(2-fluorophenyl)hydrazine (**29**), exhibited 99 % inhibition at the lowest tested concentration of 3.125 µg/mL against drug-sensitive MTB H37Rv strain. The similarity index based on steric and electrostatic features of the molecules was used, in conjunction with principal component analysis and linear discriminant analysis, successively to classify the molecules based on their activity into two classes. This classification method gives confidence in predicting the activity class of any new unsynthesized molecule belonging to these series. [Nayyar, A., *et al.*, 2006]

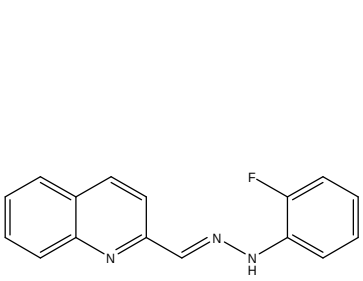

27

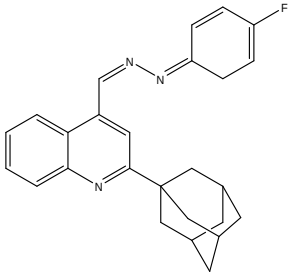

28

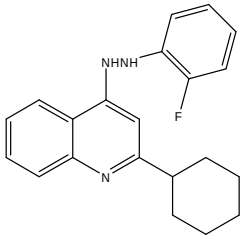

29

Anquetin, G., *et al.,* reports on the rational design of a series of new 6-fluoroquinolones by QSAR analysis against *Toxoplasma gondii*, their synthesis, their biological evaluation against *T. gondii* and *Plasmodium* spp., and their effect on MTB DNA gyrase and growth inhibition. Of the 12 computer-designed 8-ethyl(or methoxy)- and 5-ethyl-8-methoxy-6-fluoroquinolones predicted to be active against *T. gondii*, they synthesized four 6-fluoro-8-methoxyquinolones. The four 6-fluoro-8-methoxy-quinolones were active on *T. gondii* but only one is as active as predicted. One of these four compounds appears to be an antiparasitical drug of great potential with inhibitory activities comparable to or higher than that of trovafloxacin, GAT, and MXFX. They also inhibit DNA supercoiling by MTB gyrase with an efficiency comparable to that of the most active quinolones but were poor inhibitors of MTB growth. Compounds **30** and **31** inhibited DNA supercoiling by MTB gyrase with IC_{50} of < 6 µg/ml. [Anquetin, G., *et al.,* 2006]

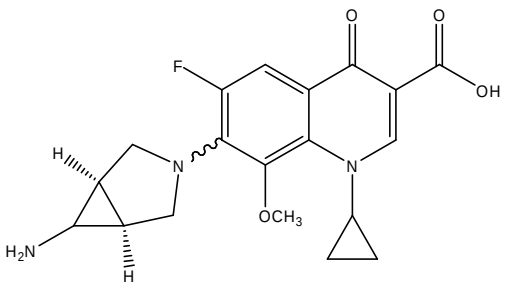

30

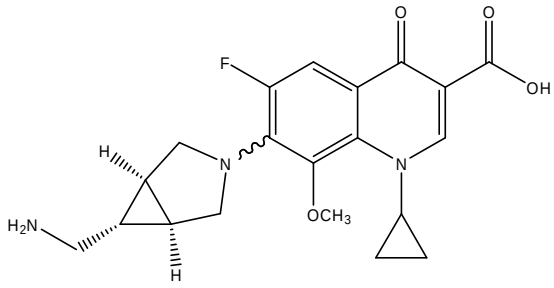

31

Sriram, D., *et al.,* synthesized sixteen 7-substituted GAT derivatives and evaluated for antimycobacterial activity *in vitro* and *in vivo* against MTB H37Rv and multi-drug resistant *M. tuberculosis* (MDR-TB), and also tested for the ability to inhibit the supercoiling activity of DNA gyrase from MTB. Among the synthesized compounds, 1-cyclopropyl-6-fluoro-8-methoxy-7-[[[N^4-[1'-(5-isatinyl-β-semicarbazo)]methyl]-3-methyl]N^1-piperazinyl]-4-oxo-1,4-dihydro-3-quinoline carboxylic acid (**32**) was found to

be the most active compound *in vitro* with an MIC of 0.0125 µg/mL against MTB and MDR-TB. In the *in vivo* animal model **32** decreased the bacterial load in lung and spleen tissues with 3.62- and 3.76-log10 protections, respectively. Compound **32** was also found to be equally active as gatifloxacin in the inhibition of the supercoiling activity of wild-type MTB DNA gyrase with an IC_{50} of 3.0 µg/mL. The results demonstrate the potential and importance of developing new quinolone derivatives against mycobacterial infections. [Sriram, D., *et al.,* 2006a]

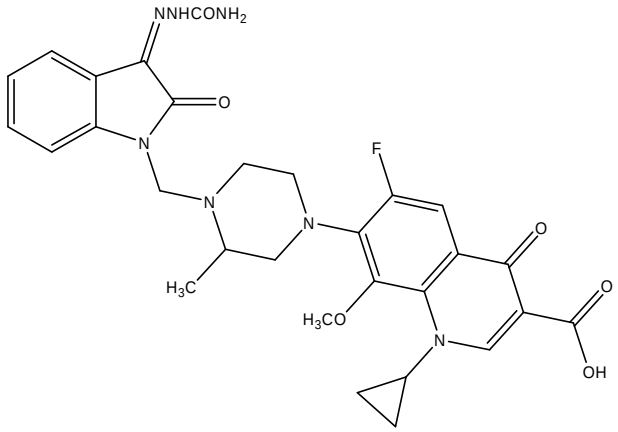

32

Sriram, D., *et al.,* tested the antimycobacterial activity (both *in vitro* and *in vivo*) and DNA gyrase inhibition of newly synthesized fluoroquinolone derivatives against MTB H37Rv and MC^2, respectively. Among the synthesized compounds, compound **33** was found to exhibit the most potent *in vitro* antimycobacterial activity with a MIC value of 0.78 µg/ml, and a selectivity index of more than 80 while not being cytotoxic to the Vero cell line up to 62.5 µg/ml. When evaluated for *in vivo* antimycobacterial activity, compound **33** demonstrated a paramount decrease of bacterial load in lung and spleen tissues compared to the control and better than the standard drug CIP. [Sriram, D., *et al.*, 2006b]

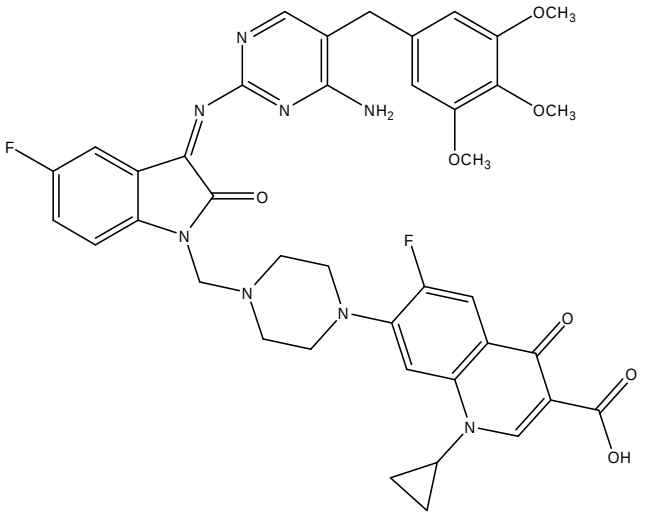

33

Sriram, D., *et al.*, designed an isatinimino lead compound as a novel non-nucleoside reverse transcriptase inhibitor with antimycobacterial properties for the effective treatment of AIDS and AIDS-related tuberculosis. Among the compounds synthesized, 1-cyclopropyl-6-fluoro-8-methoxy-1,4-dihydro-4-oxo-7[[N^4-[3'-[(4,6-dimethylpyrimidin-2-yl)benzenesulfonamido-4-yl]imino-1'-(5-fluoroisatinyl)]methyl]-3-methyl N^1-piperazinyl]-3-quinoline carboxylic acid (**34**) emerged as the most potent broad-spectrum chemotherapeutic agent active against HIV (EC_{50}: 12.1 µg/ml), and MTB (MIC: 1.22 µg/ml). [Sriram, D., *et al.*, 2006c]

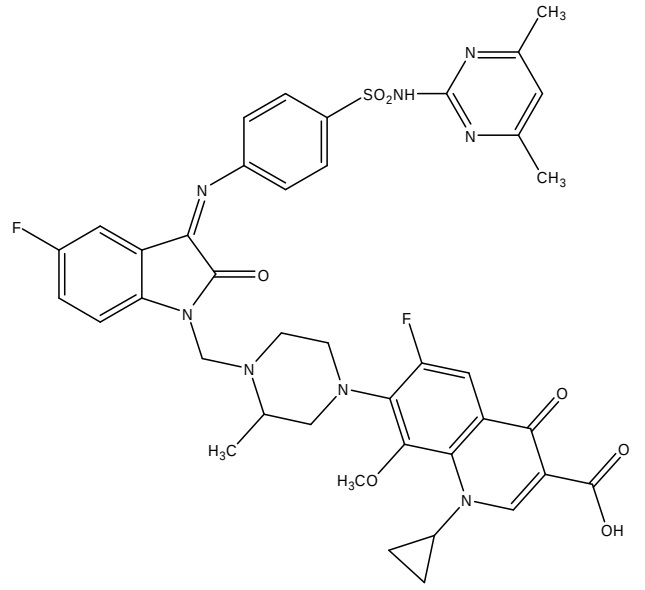

34

Sriram, D., *et al.*, synthesized a series of PZA mannich bases by reacting PAZ, formaldehyde, and various substituted piperazines using microwave irradiation with the yield ranging from 46 % to 86 %. The synthesized compounds were evaluated for antimycobacterial activity *in vitro* and *in vivo* against MTB H37Rv (MTB). Among the synthesized compounds, 1-cyclopropyl-6-fluoro-1,4-dihydro-8-methoxy-7-(3-methyl-4-((pyrazine-2-carboxamido)methyl)piperazin-1-yl)-4-oxoquin-
oline-3-carboxylic acid (**35**) was found to be the most active compound *in vitro* with MIC of 0.39 and 0.2 µg/mL against MTB and MDR-TB, respectively. In the *in vivo* animal model **35** decreased the bacterial load in lung and spleen tissues with 1.86 and 1.66-log10 protections, respectively. [Sriram, D., *et al.*, 2006d]

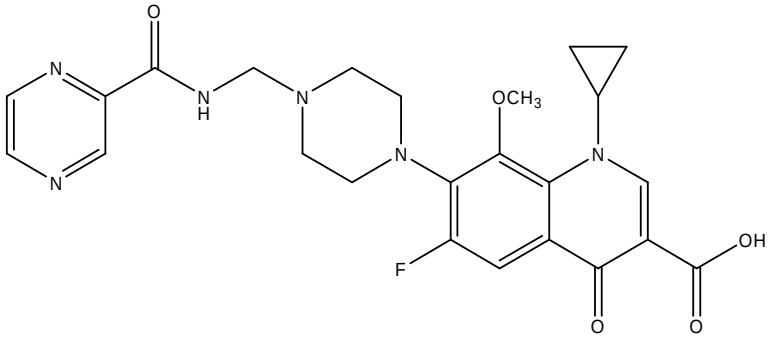

35

de Almeida, M. V., *et al.*, reported the synthesis and biological evaluation of 12 lipophilic MXFX or GAT derivatives, by reaction of 1-cyclopropyl-6,7-difluoro-1,4-dihydro-8-methoxy-4-oxoquinoline-3-carboxylic acid with several N-monoalkyl 1,2-ethanediamine or 1,3-propanediamine. Compound **36** inhibited growth at 0.31 µg/ml. The author states that the antitubercular activity depends on the alkyl chains, size or ramification. Ideal chain contains 10 carbon atoms. [de Almeida, M. V., *et al.*, 2007]

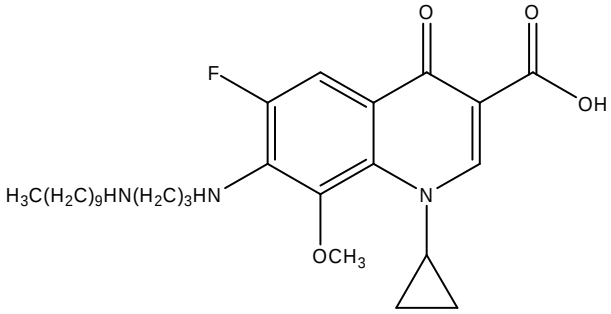

36

Nayyar, A., *et al.*, based on there previously identified molecule, designed two series of 4-(adamantan-1-yl)-2-substituted quinolines. All new derivatives were evaluated *in vitro* for antimycobacterial activities against drug-sensitive MTB H37Rv strain. Several 4-adamantan-1-yl-quinoline-2-carboxylic acid *N'*-alkylhydrazides (AQCH) described showed promising inhibitory activity. In particular, few analogs displayed MIC of 3.125 µg/mL. Further investigation of AQCH by its reaction with various aliphatic, aromatic, and heteroaromatic aldehydes led to the synthesis of 4-adamantan-1-yl-quinoline-2-carboxylic acid alkylidene hydrazides which have produced promising antimycobacterial activities (99 % inhibition) at 3.125 µg/mL against drug-sensitive MTB H37Rv strain. The most potent analog **37** of the series produced 99 % inhibition at 1.00 µg/mL against drug-sensitive strain, and MIC of 3.125 µg/mL against isoniazid-resistant TB strain. To understand the relationship between structure and activity, a 3D-QSAR analysis has been carried out by three methods –comparative molecular field analysis (CoMFA), CoMFA with inclusion of a hydropathy field (HINT), and comparative molecular similarity indices analysis (CoMSIA). Several statistically significant CoMFA, CoMFA with HINT, and CoMSIA models were generated. Prediction of the activity of a test set of molecules was the best for the CoMFA model generated with database alignment. Based on the CoMFA contours, the authors have tried to explain the structure – activity relationships of the compounds reported. [Nayyar, A., *et al.*, 2007]

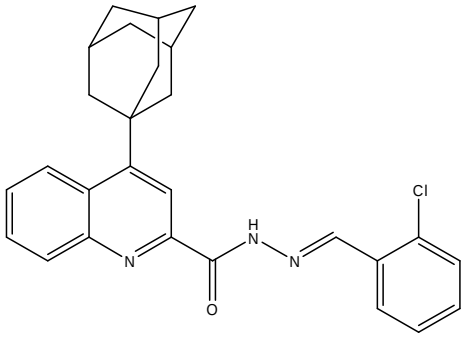

37

2.3 ANTIMICROBIAL QUINOLONES

Lesher, G. Y., *et al.,* prepared a series of l-alkyl-l,8-naphthyridin-4-one-3-carboxylic acid derivatives. Several members of the series were found to be highly effective antibacterial agents both *in vitro* and *in vivo.* [Lesher, G. Y., *et al.,* 1962]

Santilli, A. A., *et al.,* reported the synthesis of a series of 1,2,3,4-tetrahydro-4-oxo-1,8-naphthyridine-3-carboxylic acid esters, carbonitriles, and carboxamides and evaluated (dose range 50 - 400 mg/kg) in mice infected with *Escherichia coli.* Only two derivatives, the ethyl and butyl esters of l-ethyl-1,2-dihydro-4-hydroxy-7-methyl-l,8-naphthyridine-3-caboxylic acid, protected the animals against *E. coli* and several other Gram-negative bacterial pathogenic infections. A pro-drug type of mechanism was suggested to be operable. [Santilli, A. A., *et al.,* 1975]

Mitscher, L. A., *et al.,* developed a flexible reaction sequence starting with anthranilic acids or isatoic anhydrides and leads regiospecifically to 1-alkyl-1,4-dihydro-4-oxo-3-quinolinecarboxylic acids after reaction with 1,3-dicarbonyl compounds. A number of new and known antimicrobial agents were prepared and tested in vitro, demonstrating, inter alia, that substitution of the H at C_2 abolished antibacterial activity. [Mitscher, L. A., *et al.,* 1978]

Curran, D. P., *et al.,* gave a novel method for synthesis of quinolones by employment of polyphosphoric acid as the dehydrating reagent as one method for cyclization of the ring. [Curran, D. P., *et al.,* 1984]

Chu, D. T. W., *et al.,* prepared a series of novel arylfluoroquinolones having a fluorine atom at the 6^{th} position, substituted amino groups at the 7-position, and substituted phenyl groups at the 1^{st} position. SAR studies indicate that the *in vitro* antibacterial potency is greatest when the 1-substituent is either p-fluorophenyl or p-hydroxyphenyl and the 7-substituent is either 1-piperazinyl, 4-methyl-1-piperazinyl, or 3-amino-1-pyrrolidinyl. The electronic and spatial properties of the 1-substituent, as well as the steric bulk, play

important roles in the antimicrobial potency in this class of antibacterials. [Chu, D. T. W., *et al.,* 1985]

Miyamoto, H., *et al.,* prepared a series of substituted 4-oxoquinoline-3-carboxylic acids having a methyl group at the 8th position and tested for their antibacterial activity. 7-(*trans*-3-Amino-4-methyl-1-pyrrolidinyl)-1-cyclopropyl-1,4-dihydro-6-fluoro-8-methyl-4-oxoquinoline-3-carboxylic acid (**38**) exhibited highly potent antibacterial activity against both Gram-positive and Gram-negative bacteria, including *Pseudomonas aeruginosa*. [Miyamoto, H., *et al.,* 1990]

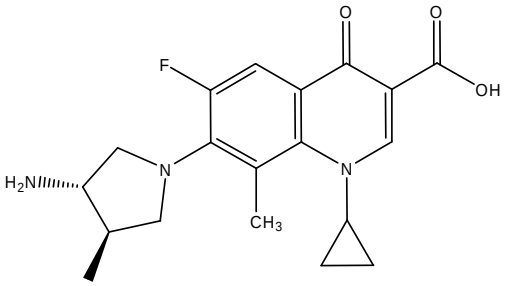

38

Xin, T., *et al.,* synthesized twenty four 1-amino-6-fluoro-1,4-dihydro-4-oxo-7-(substituted) piperazinyl-3-quinoline carboxylic acids and evaluated for there *in vitro* antibacterial activity. [Xin, T., *et al.,* 1993]

The 6-aminoquinolone had previously been identified as a new class of quinolone antibacterial agents. To continue SAR study in this series, Cecchetti, V., *et al.*, synthesized novel 6-amino-8-methylquinolone derivatives and evaluated for *in vitro* antibacterial activity. The coupled presence of a methyl group at the C_8 position with an amino group at C_6 is effective for enhancing antibacterial activity, particularly against Gram-positive bacteria. [Cecchetti, V., *et al.,* 1996a]

In a furtherance of SAR study on the C_6 position of quinolone antibacterials, a series of 6-desfluoro-8-methylquinolones were synthesized by Cecchetti, V., *et al.,* and evaluated for their *in vitro* antimicrobial activity. As a result of this study, compounds with strong activity against Gram-positive bacteria, including ciprofloxacin-resistant and methicillin-resistant *Staphylococcus aureus*, were identified. The best Gram-positive antibacterial

activity was exhibited by piperidinyl derivative **39**, which was 17 times more potent than CIP and displayed extremely high activity against *Streptococcus pneumoniae* with an MIC value of < 0.016 µg/mL. Thus, it was shown that substituent combinations in the quinolone ring, excluding the C_6 fluorine atom, might produce powerful antibacterial agents. [Cecchetti, V., *et al.*, 1996b]

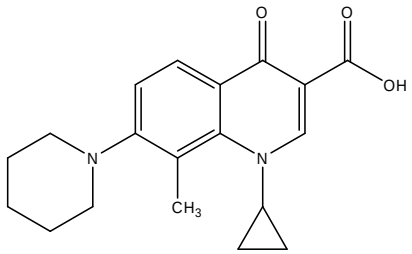

39

New pyrrolidine derivatives, which bear an alkyloxime substituent in the 4-position and an aminomethyl substituent in the 3-position of the pyrrolidine ring, have been synthesized by Hong, C. Y., *et al.*, and coupled with various quinolone carboxylic acids to produce a series of new fluoroquinolone antibacterials. These fluoroquinolones were found to possess potent antimicrobial activity against both Gram-negative and Gram-positive organisms, including methicillin-resistant *Staphylococcus aureus* (MRSA). Variations at the C_8 position of the quinolone nucleus included fluorine, chlorine, nitrogen, methoxy, and hydrogen atom substitution. The activity imparted to the substituted quinolone nucleus by the C_8 substituent was in the order F (C_5-NH_2) > F (C_5-H) > naphthyridine > Cl = OMe = H against Gram-positive organisms. In the case of Gram-negative strains, activity was in the order F (C_5-NH_2) > naphthyridine = F (C_5-H) > H > Cl > OMe. [Hong, C. Y., *et al.*, 1997]

Topoisomerase IV is the primary cellular target for most quinolones in Gram-positive bacteria; however, its interaction with these agents is poorly understood. Therefore, the effects of four clinically relevant antibacterial quinolones (CIP, and three new generation quinolones: trovafloxacin, LVFX, and SPFX) on the DNA cleavage / religation reaction of *Staphylococcus aureus* topoisomerase IV were characterized by Anderson, V. E., *et al.* These quinolones stimulated enzyme - mediated DNA scission to a similar extent, but their potencies varied significantly. Drug order in the absence of ATP was trovafloxacin

> CIP > LVFX > SPFX. The most striking correlation, however, was between quinolone potency and Inhibition of enzyme – mediated DNA religation: the greater the potency, the stronger the inhibition. [Anderson, V. E., *et al.,* 2000]

Fang, K. C., *et al.,* report herein the synthesis and biological evaluation of two series of 7-substituted norfloxacin derivatives. Most compounds tested in this study demonstrated better activity against MRSA than NOR. Preliminary *in vitro* evaluation indicated that the 7-[4-(2-hydroxyiminoethyl)piperazin-1-yl] derivatives possess distinct cytotoxicity profiles as compared with their alpha-methylene-gamma-butyrolactone counterparts, i.e., excellent activities against the renal cancer subpanel. Among them, 1-ethyl-6-fluoro-7-{4-[2-(4-chlorophenyl)-2-hydroxyiminoethyl]-1-piperazinyl}-4-oxo-1,4-dihydro-3-quinolinecarboxylic acid (**40**) demonstrated the most significant activities against renal cancer cell lines, with log GI_{50} values of -6.40 against CAK-1, -6.14 against RXF 393, and -7.54 against UO-31, compared with a mean log GI_{50} value of -5.03. [Fang, K. C., *et al.,* 2000]

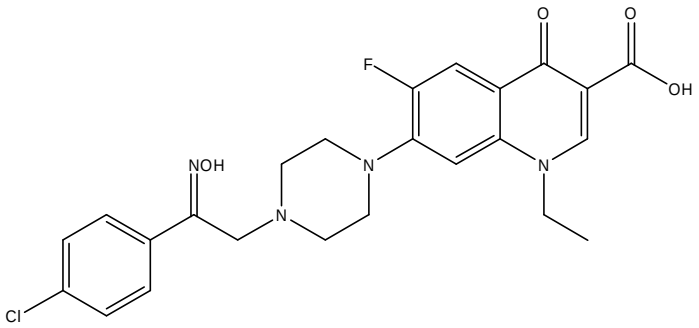

40

Kawakami, K., et al., synthesized a series of 8-methoxyquinolones bearing 3-amino-4-methylpyrrolidines or 3-amino-4-fluoromethylpyrrolidines at the C_7 position and evaluated for their physicochemical and biological properties. All of the compounds synthesized showed more potent activity than LVFX against both Gram-positive and negative bacteria. Increases in lipophilicity of these compounds had desirable effects on their potency of single intravenous toxicity and pharmacokinetic profiles in animals. Among the compounds synthesized, 1-fluorocyclopropyl derivatives, and 7-(*cis*-3-amino-4-fluoromethylpyrrolidinyl) derivative showed negative responses in the micronucleus test in mice while 1-cyclopropyl-7-(3-aminopyrrolidinyl) derivative showed a positive

response. These results suggested that the introduction of a fluorine atom into the 3-aminopyrrolidinyl substituent resulted in favorable influence on genetic toxicity as well as into the N_1 cyclopropyl substituent. [Kawakami, K., *et al.*, 2000]

Chen, Y. L., *et al.*, reported the synthesis of a number of 7-substituted quinolone derivatives and evaluated for antibacterial and cytotoxic activities. Preliminary results indicated that most compounds tested in this study demonstrated better activity against MRSA than NOR. Among them, 1-(4-amino-2-fluorophenyl)-6-fluoro-1,4-dihydro-7-[4-[2-(4-methoxyphenyl)-2-hydroxyiminoethyl]-1-piperazinyl]-4-oxo-3-quinolinecarboxylic acid (**41**) and its ketone precursor exhibited significant activities against *Klebsiella pneumoniae*, MRSA, erythromycin- and ampicillin-resistant *Streptococcus pneumoniae*, and vancomycin-resistant *Enterococcus faecalis*. Due to strong cytotoxicities of **41** (a mean log GI_{50} of -5.40), with good antibacterial activities and low cytotoxicities (a mean log GI_{50} of -4.67), is a more potential drug candidate. [Chen, Y. L., *et al.*, 2001]

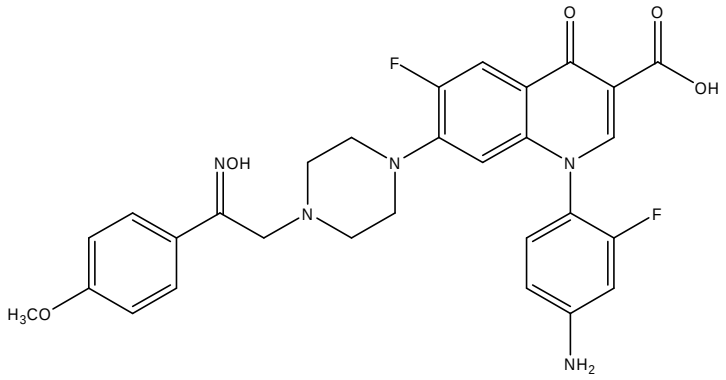

41

Herczegh, P., *et al.*, reported that bisphosphonates conjugated to fluoroquinolone (**42**) antibacterials through an intermediate carbon had better activity than conjugates lacking the carbon. Virtually all molar-based activity of these esterified bisphosphonate derivatives was identical to that of its parent. De-esterified free-acid forms retained good activity against most Gram-negative bacteria, but not against Gram-positives. A free-acid derivative remained bound to washed bone and completely inhibited *Staphylococcus aureus* growth. The more potent parent CIP, failed to bind significantly, resulting in the occurrence of bacterial growth. [Herczegh, P., *et al.*, 2002]

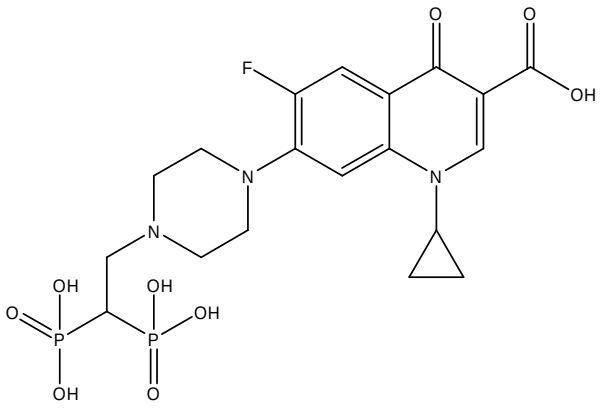

42

Miolo, G., *et al.*, investigated a representative set of potent antibacterial 6-desfluoro-8-methylquinolones, in which the C_6 fluorine atom is replaced by -NH_2 or -H, and their 6-fluoro counterparts, to evaluate their phototoxic potential and to explore the mechanism behind their phototoxicity. The capacity to photosensitize biological substrates (lipids, proteins, DNA) has been analyzed, as well as their photocytotoxicity on red blood cells and 3T3 murine fibroblasts. The results obtained show that a major correlation with phototoxicity lies in the structure of the individual antibacterials and their hydrophobicity; in particular, 6-amino derivatives are less phototoxic than corresponding unsubstituted and fluorinated compounds. Cellular phototoxicity was inhibited by the addition of free radical and hydroxyl radical scavengers (BHA, GSH and DMTU), suggesting the involvement of a radical mechanism in their cytotoxicity. A good correlation was observed between lipid peroxidation and phototoxicity, indicating that the test compounds exert their toxic effects mainly in the cellular membrane. [Miolo, G., *et al.*, 2002]

Hu, X. E., *et al.*, designed novel quinolone antibacterial agents bearing (3*S*)-amino-(4*R*)-ethylpiperidines by using low energy conformation analysis and synthesized by applying a conventional coupling reaction of the quinolone nuclei with new piperidine side chains. These compounds were tested in MIC assays and found to be highly potent against Gram-positive and Gram-negative organisms. In particular, the new compounds exhibited high activity against the resistant pathogens *Staphylococcus aureus* (MRSA) and *Streptococcus pneumoniae* (penicillin resistant). Importantly, when the (3*S*)-amino-(4*R*)-ethylpiperidinyl quinolones (**43**) were compared with marketed quinolones sharing the

same quinolone nuclei but different side chains at the C_7 position, the new quinolones showed superior activity against Gram-positive organisms, including resistant pathogens. [Hu, X. E., *et al.*, 2003]

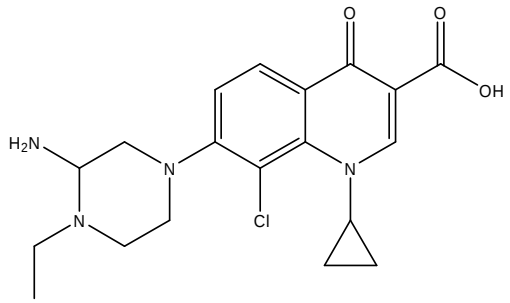

43

Inagaki, H., *et al.*, synthesized a series of novel 5-amino-6-fluoro-1-[(1R,2S)-2-fluorocyclopropan-1-yl]-8-methylquinolones bearing fluorinated (3R)-3-(1-aminocyclopropan-1-yl)pyrrolidin-1-yl substituents at the C_7 position to obtain potent drugs for infections caused by Gram-positive pathogens, which include resistant strains such as MRSA, penicillin - resistant *Streptococcus pneumoniae* (PRSP), and vancomycin-resistant enterococci (VRE). These fluorinated compounds exhibited potent antibacterial activity comparable with that of a compound bearing a non-fluorinated (3*R*)-3-(1-aminocyclopropan-1-yl)pyrrolidine moiety at the C_7 position (**44**) and had at least 4 times more potent activity against representative Gram-positive bacteria than CIP, GAT, or MXFX. Among them, the 7-[(3S,4R)-4-(1-aminocyclopropan-1-yl)-3-fluoropyrrolidin-1-yl] derivative (**45**), which showed favorable profiles in preliminary toxicological and nonclinical pharmacokinetic studies, exhibited potent antibacterial activity against clinically isolated resistant Gram-positive pathogens. [Inagaki, H., *et al.*, 2003]

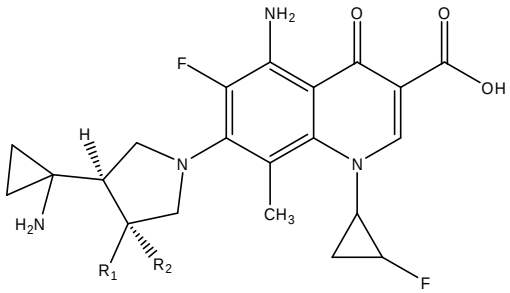

44 $R_1 = R_2 = H$

45 $R_1 = F$; $R_2 = H$

Kuramoto, Y., *et al.*, designed *m*-aminophenyl groups as novel N_1 substituents of naphthyridones and quinolones. Among newly synthesized compounds, 7-(3-aminoazetidin-1-yl)-1-(5-amino-2,4-difluorophenyl)-8-chloro-6-fluoro-4-oxo-1,4-dihydroquinoline-3-carboxylic acid (**46**) has extremely potent antibacterial activities against Gram-positive as well as Gram-negative bacteria. This compound is significantly more potent than trovafloxacin against clinical isolates: 30 times against *Streptococcus pneumoniae* and 128 times against MRSA. The SAR study revealed that a limited combination of 1-(5-amino-2,4-difluorophenyl) group, 7-(azetidin-1-yl) group, and 8-Cl atom (or Br atom or Me group) gave potent antibacterial activity. An X-ray crystallographic study of a 7-(3-ethylaminoazetidin-1-yl)-8-chloro derivative demonstrated that the N_1 aromatic group was remarkably distorted out of the core quinolone plane by steric repulsion between the C_8 chlorine atom and the N_1 substituent. Furthermore, a molecular modeling study of **46** and its analogues demonstrated that a highly distorted orientation was induced by a steric hindrance of the C_8 substituent, such as chlorine, bromine, or a methyl group. Thus, their highly strained conformation should be a key factor for the potent antibacterial activity. [Kuramoto, Y., *et al.*, 2003]

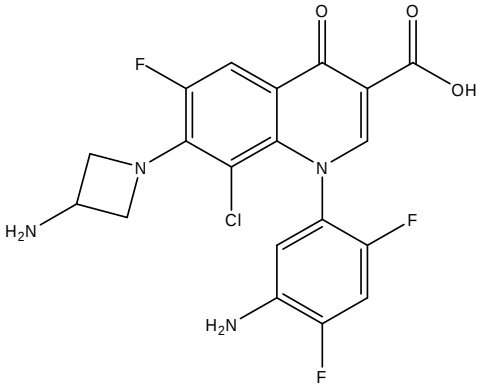

46

A series of N-[5-(5-nitro-2-thienyl)-1,3,4-thiadiazole-2-yl]piperazinyl quinolones were synthesized by Foroumadi, A., *et al.*, and evaluated for *in vitro* antibacterial activity against some Gram-positive and Gram-negative bacteria. Compound **47** (ciprofloxacin analogue) was the most active compound against Gram-positive bacteria (MIC = 0.008 - 0.015 µg mL^{-1}). [Foroumadi, A., *et al.*, 2003c]

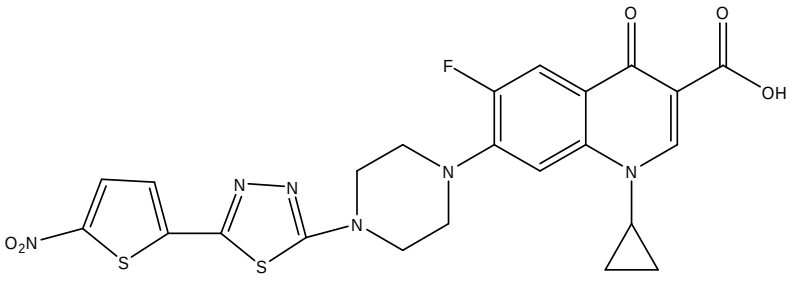

47

Baker, W. R., *et al.,* prepared a fluoroquinolone prodrug, PA2808 (**49**), and shown to convert to the highly active parent drug PA2789 (**48**). *In vitro* and *in vivo* activation of **49** by alkaline phosphatase was demonstrated using disk diffusion and rat lung infection models. The water solubility of **49** showed a marked increase compared to **48** over a pH range suitable for aerosol drug delivery. A total of forty eight analogues based on **48** were prepared and screened against a panel of Gram-positive and Gram-negative pathogens. Incorporating a cyclopropane-fused pyrrolidine (amine) at C_7 resulted in some of the most active analogues. [Baker, W. R., *et al.,* 2004]

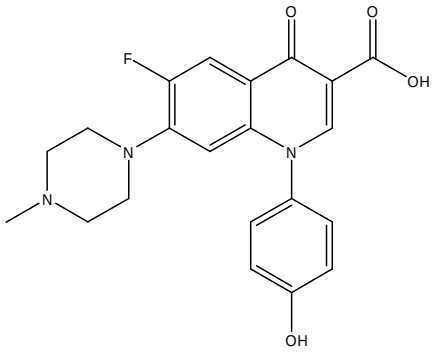

48: PA2789

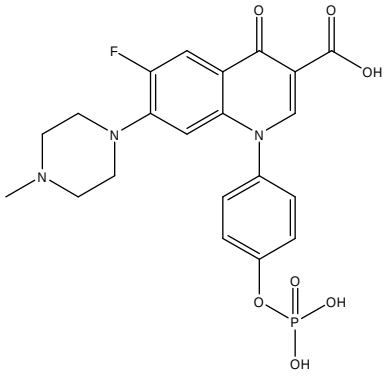

49: PA2808

Asahina, Y., *et al.,* synthesized novel 1-trifluoromethyl-4-quinolone derivative and evaluated the antibacterial activity of each. An oxidative desulfurization – fluorination reaction was employed to introduce a trifluoromethyl group at the N_1 position as a key step. Among the derivatives, **50** was found to exhibit antibacterial activity comparable to that of NOR against *Staphylococcus aureus*, *Streptococcus pneumoniae* IID1210, and *Escherichia coli* NIHJ JC-2. [Asahina, Y., *et al.,* 2005a]

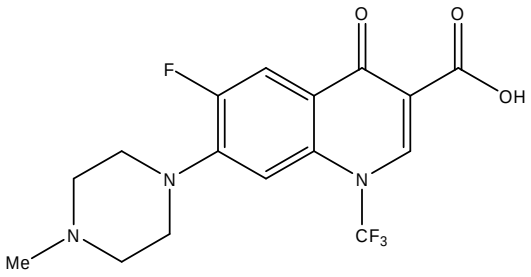

50

Asahina, Y., *et al.,* synthesized novel 1-(2-fluorovinyl)-4-quinolone-3-carboxylic acid derivatives, conformationally restricted analogues of fleroxacin and evaluated their *in vitro* antibacterial activity. A dehydrosulfenylation of a 2-fluoro-2-[(4-methoxyphenyl)sulfinyl]ethyl group was employed as a key step for the construction of a 2-fluorovinyl group at the N_1 position. It appeared evident that the *Z*-isomers exhibited 2- to 32- fold more potent *in vitro* antibacterial activity than the corresponding *E*- isomers. Furthermore, since **51** showed *in vitro* antibacterial activity and DNA gyrase inhibition comparable to that of fleroxacin, it was hypothesized that the conformation of **51** would be equivalent to the active conformer of fleroxacin. The results revealed that the antibacterial *Z*-1-(2-fluorovinyl)quinolone derivatives carry the novel N_1 substituent of the fluoroquinolones. [Asahina, Y., *et al.*, 2005b]

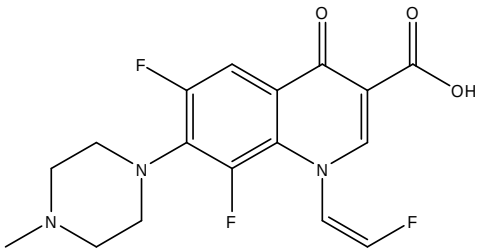

51

Dizman, B., *et al.,* synthesized a novel methacrylate monomer containing a quinolone moiety and homopolymerized in N,N-dimethylformamide (DMF) by using azobisisobutyronitrile (AIBN) as an initiator. The new monomer was copolymerized with poly(ethylene glycol) methyl ether methacrylate (MPEGMA) in DMF using the same initiator. The monomer, homopolymer, and copolymer were characterized by elemental analysis, thermo gravimetric analysis (TGA), differential scanning calorimetry (DSC), size exclusion chromatography (SEC), FTIR, ^{13}C NMR, and ^{1}H NMR. The antibacterial activities of the monomer as well as polymers were investigated against *Staphylococcus*

aureus and *Escherichia coli*, which are representative of Gram-positive and Gram-negative bacteria, respectively. All compounds showed excellent antibacterial activities against these two types of bacteria. The antibacterial activities were determined using the shaking flask method, where 25 mg/mL concentrations of each compound were tested against 10^5 CFU/mL bacteria solutions. The number of viable bacteria was calculated by using the spread plate method, where 100 µL of the incubated antibacterial agent in bacteria solutions were spread on agar plates and the number of viable bacteria was counted after 24 h of incubation period at 37 °C. philic polymer. The monomer and polymers showed excellent antimicrobial activities against *S. aureus* and *E. coli*. These results indicate that the new monomer and polymers have potential as potent antimicrobial agents although mode of activity is not clear. Since these agents are relatively stable to high temperatures, they can be used for medical and biomaterial applications requiring thermal sterilization. [Dizman, B., *et al.,* 2005]

Hansen, T. M., *et al.,* prepared a series of 5-methoxy- and 5-hydroxy-6-fluoro-1,8-naphthyridone-3-carboxylic acid derivatives and evaluated for cell - free bacterial protein synthesis inhibition and whole cell antibacterial activity. When compared to the analogous 5-hydrogen compounds, the presence of the 5-hydroxyl group negatively affects biochemical potency. [Hansen, T. M., *et al.,* 2005]

Nieto, M. J., *et al.,* studied the SAR of new antibacterial benzenesulfonamidefluoroquinolones (BSFQs, **52**), from derivatization of N^4-piperazinyl of CIP. The behavior of the new BSFQ series was similar to the NOR analogs, making possible a Quantitative Structure - Activity Relationships (QSAR) analysis of the complete set of BSFQs. The presence of the benzenesulfonylamido (BS) groups shifted the activity of classic antimicrobial fluoroquinolones from being more active against Gram-negative to Gram-positive strains. QSAR studies through Hansch analysis showed a linear correlation of the activity with electronic and steric parameters. Small electron - donor groups would increase the *in vitro* activity against Gram-positive bacteria. Hydrophobic properties played a minor role when activity is measured as MIC. [Nieto, M. J., *et al.,* 2005]

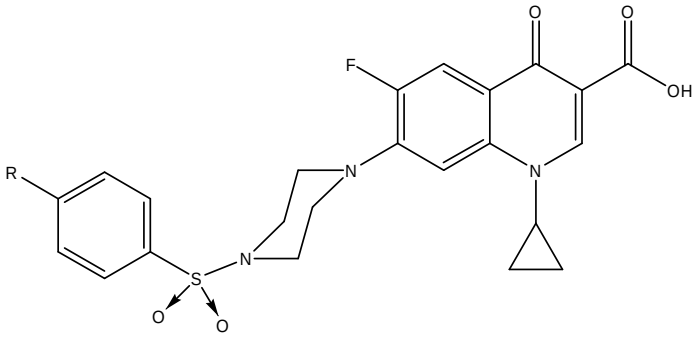

52

Zhi, C., *et al.*, reported novel Gram-positive antibacterial compounds consisting of a DNA polymerase IIIC (pol IIIC) inhibitor covalently connected to a topoisomerase/gyrase inhibitor. Specifically, 3-substituted 6-(3-ethyl-4-methylanilino)uracils (EMAUs) in which the 3-substituent is a fluoroquinolone moiety (FQ) connected by various linkers were synthesized. The resulting "AU-FQ" hybrid (**53**) compounds were significantly more potent than the parent EMAU compounds as inhibitors of pol IIIC and were up to 64 - fold more potent as antibacterials *in vitro* against Gram-positive bacteria. The hybrids inhibited the FQ targets, topoisomerase IV and gyrase, with potencies similar to NOR but 10 - fold lower than newer agents, for example, CIP and SPFX. Representative hybrids protected mice from lethal *Staphylococcus aureus* infection after intravenous dosing, and one compound showed protective effect against several antibiotic-sensitive and -resistant Gram-positive infections in mice. The AU - FQ hybrids are a promising new family of antibacterials for treatment of antibiotic-resistant Gram-positive infections. [Zhi, C., *et al.*, 2006]

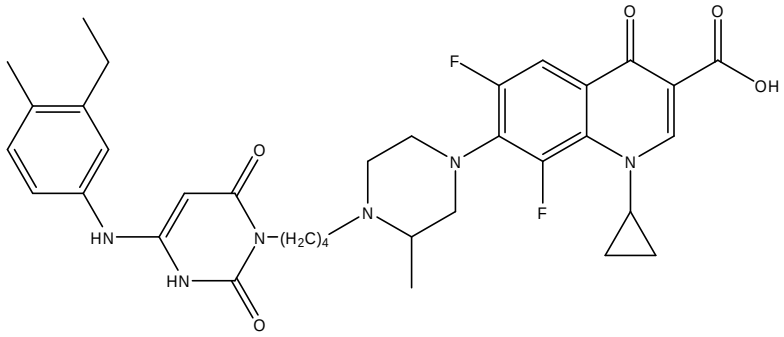

53

CHAPTER 3

OBJECTIVES AND PLAN OF WORK

After reviewing the literature, to develop the pharmacophore for antimycobacterial quinolone, the following modifications may be considered important,

a) the antimycobacterial activity imparted by the N_1 substituents was in the order of *tert*-butyl > cyclopropyl > 2,4-difluorophenyl > ethyl ≈ cyclobutyl > isopropyl;
b) introduction of nitro group or electron withdrawing groups at C_6 position; and
c) highly lipophilic substituents at C_7 position of quinolone nucleus.

3.1 OBJECTIVES

The research work was aimed

- To synthesize novel quinolone derivatives with structural changes at N_1, C_5, C_6, C_7 and C_8 positions.
- To conduct *in vitro* and *in vivo* antimycobacterial screening of the synthesized compounds against *Mycobacterium tuberculosis*; multi-drug resistant *Mycobacterium tuberculosis*; and *Mycobacterium smegmatis.*
- To evaluate cytotoxicity of the synthesized compounds.
- To perform DNA gyrase enzyme inhibition studies for the synthesized compounds.
- To study the phototoxicity effect of the synthesized compounds.
- To perform quantum mechanical modeling studies for the synthesized compounds.
- To propose a pharmacophore model for the antitubercular drugs using the synthesized quinolones.

3.2 PLAN OF WORK

The plan of work was classified into the following categories:

3.2.1 Synthesis

3.2.1.1 Synthesis of fluoroquinolone (**FQ**) derivatives.

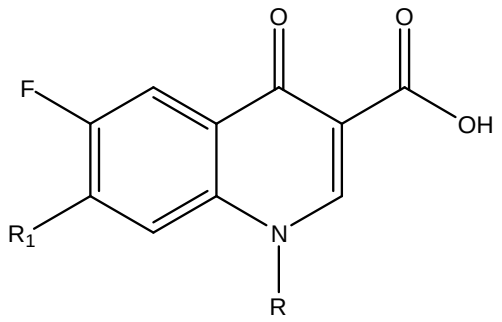

R = Cyclopropyl; 2,4-Difluorophenyl; *t*-Butyl

R_1 = Various substituted piperazines, (thio) morpholines, substituted piperidines and fused piperazines & piperidines

FQ 7-9 a-q

3.2.1.2 Synthesis of nitroquinolone (**NQ**) derivatives.

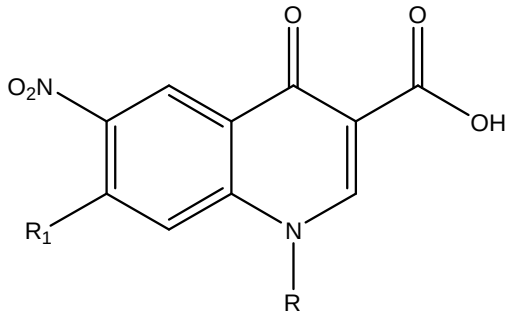

R = Cyclopropyl; 4-Fluorophenyl; *t*-Butyl

R_1 = Various substituted piperazines, (thio) morpholines, substituted piperidines and fused piperazines & piperidines

NQ 8-10 a-p

3.2.1.3 Synthesis of 8-methoxyquinolone (**MQ**) derivatives.

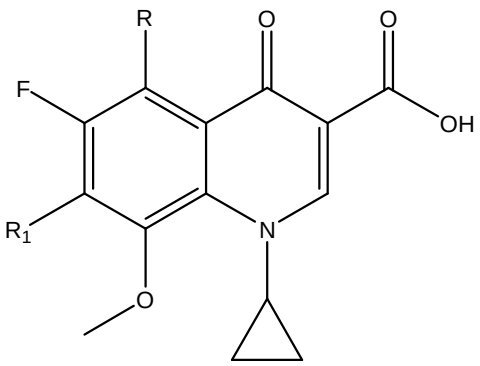

R = H; NO_2

R_1 = Various substituted piperazines, (thio) morpholines, substituted piperidines and fused piperazines & piperidines

MQ 12-13 a-p

3.2.1.4 Synthesis of nitro naphthyridone (**NN**) derivatives.

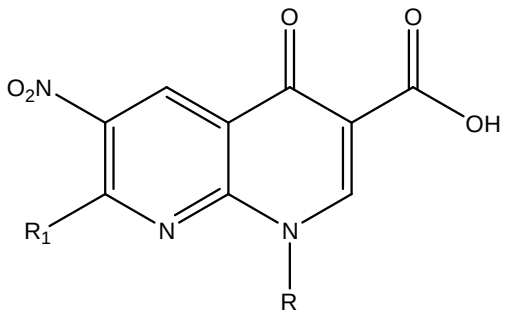

R = Cyclopropyl; 4-Fluorophenyl; *t*-Butyl

R_1 = Various substituted piperazines, (thio) morpholines, substituted piperidines and fused piperazines & piperidines

NN 8-10 a-q

3.2.2 *In vitro* antimycobacterial and cytotoxicity

3.2.2.1 *In vitro* study against *Mycobacterium tuberculosis*,

3.2.2.2 *In vitro* study against multi-drug resistant *Mycobacterium tuberculosis* and

3.2.2.3 *In vitro* study against *Mycobacterium smegmatis*

3.2.2.4 Cytotoxicity study

3.2.3 *In vivo* antimycobacterial study

3.2.4 DNA gyrase supercoiling assay

3.2.5 Phototoxicity evaluation

3.2.6 Quantum mechanical modeling

3.2.7 Pharmacophore modeling

CHAPTER 4

MATERIALS AND METHODS

Melting points were determined on an electrothermal melting point apparatus (Buchi BM530) in open capillary tubes and are uncorrected. Infra Red (IR) spectra (KBr disc) were run on Jasco IR Report 100 spectrometer and are reported in reciprocal centimeters (cm^{-1}). Proton Nuclear Magnetic Resonance (^{1}H-NMR) spectra were scanned on JEOL Fx 300 MHz NMR spectrometer using DMSO-d_6 as solvent. Chemical shifts are expressed in δ (ppm) relative to tetramethylsilane (TMS) as an internal reference standard. Elemental analyses (C, H, and N) were performed on Perkin Elmer model 240C analyzer. The progress of the reactions and homogeneity of the compounds were monitored by ascending Thin-Layer Chromatography (TLC) on silica gel G (pre-coated silica gel plate 60 F_{254}, Merck) and visualized by using UV radiation/iodine. Some of the reactions were carried out using microwave oven from Catalyst Microwave Systems, India. The clog P values were determined using ChemDraw 8.0 software. All the animal studies were carried out with Institutional Animal Ethical Committee approval (Protocol No. IAEC/RES/7/2)

4.1 SYNTHETIC SCHEME

4.1.1 Fluoroquinolone (FQ) Derivatives

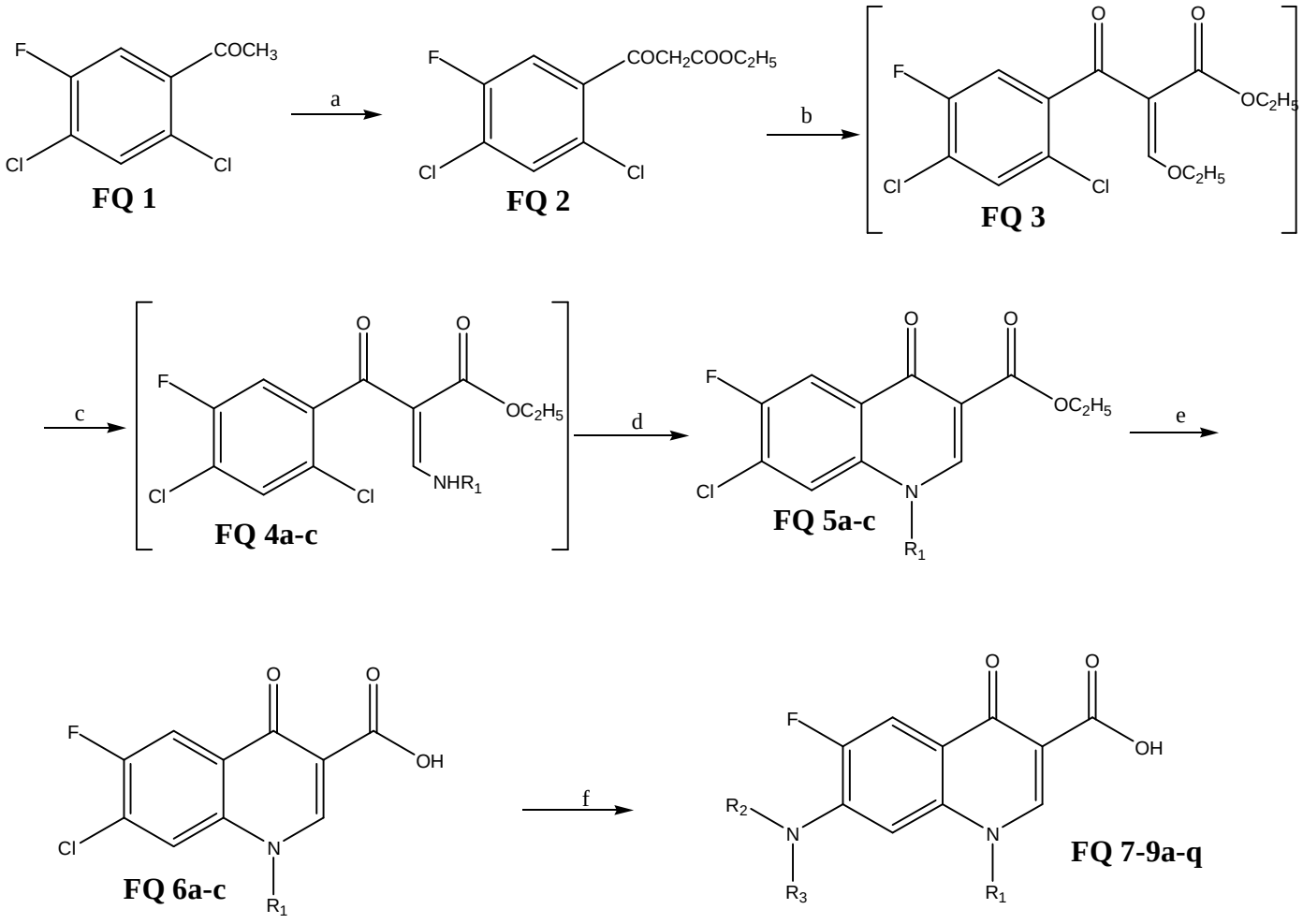

a. $(C_2H_5O)_2CO$, NaH; b. $CH(OC_2H_5)_3$, $(CH_3CO)_2O$; c. Cyclopropylamine/2,4-difluoroaniline/t-butylamine; d. K_2CO_3, DMSO; e. 6N HCl; f. Sec. amines, K_2CO_3, MWI

Figure 4.1: Synthetic protocol for fluoroquinolone (**FQ**) Derivatives

4.1.2 Nitroquinolone (NQ) Derivatives

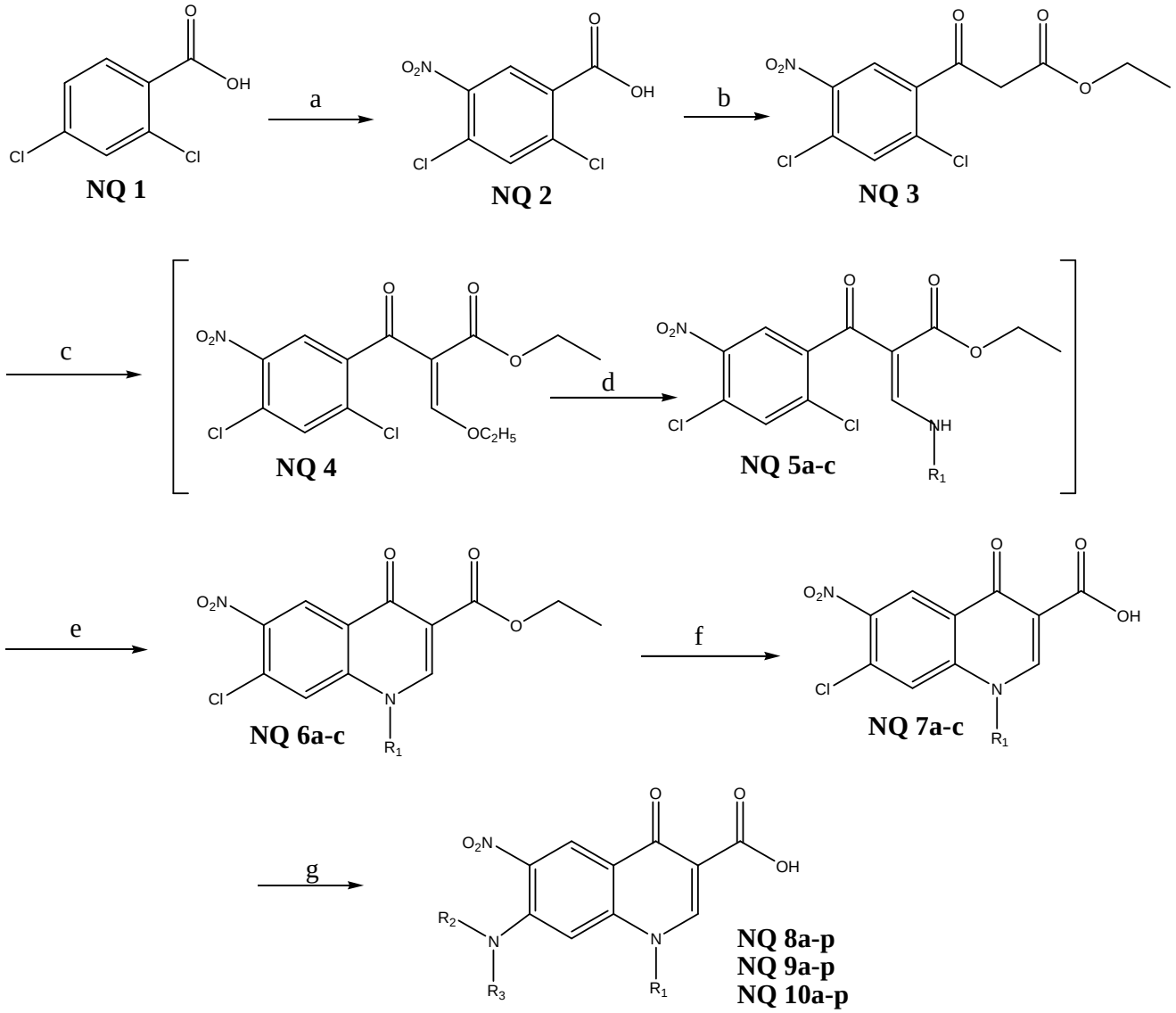

(a) HNO_3 , H_2SO_4; (b) CDI, $C_2H_5OOCCH_2COOK$, $MgCl_2$, $(C_2H_5)_3N$; (c) $(C_2H_5O)_3CH$, $(CH_3CO)_2O$; (d) R_1NH_2; (e) K_2CO_3; (f) HCl; (g) sec. amines , K_2CO_3, MWI

Figure 4.2: Synthetic protocol for nitroquinolone (**NQ**) Derivatives

4.1.3 8-Methoxyquinolone (MQ) Derivatives

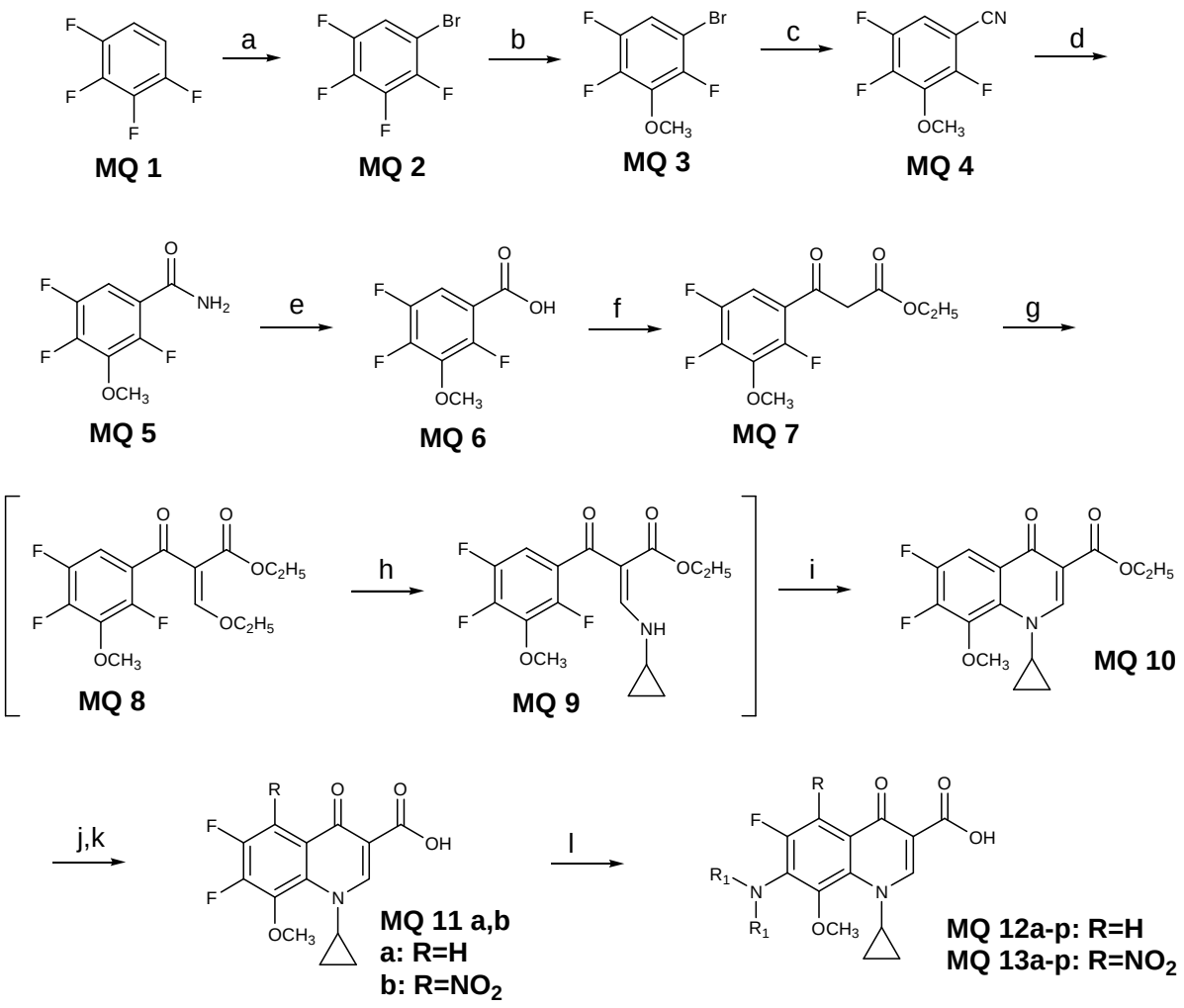

a. Br_2, $AlBr_3$, oleum; b. MeONa, MeOH; c. CuCN, NMP, $FeCl_3.6H_2O$, HCl; d. H_2SO_4, H_2O; e. 18N H_2SO_4; f. CDI, $EtOCOCH_2CO_2K$, $MgCl_2$, Et_3N; g. $(EtO)_3CH$, AC_2O; h. cyclopropanolamine, EtOH:Et_2O(50:50); i. DMSO, K_2CO_3; j. H_2SO_4, KNO_3; k. HCl; l. Var. Sec. amines, DMSO, MWI

Figure 4.3: Synthetic protocol for 8-methoxyquinolone (**MQ**) Derivatives

4.1.4 Nitro Naphthyridone (NN) Derivatives

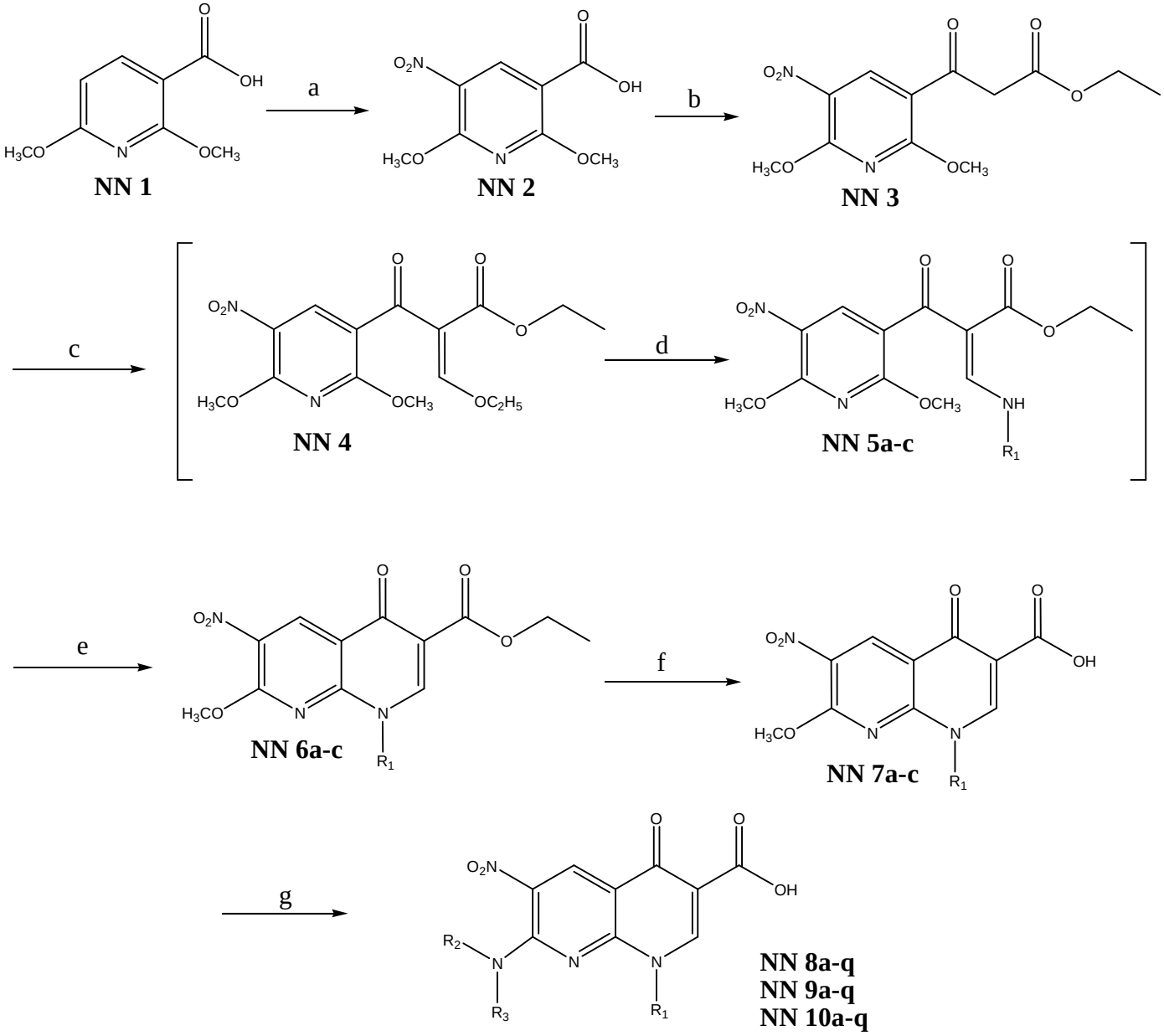

(a) HNO_3 , $(CH_3CO)O$; (b) CDI, $C_2H_5OOCCH_2COOK$, $MgCl_2$, $(C_2H_5)_3N$; (c) $(C_2H_5O)_3CH$, $(CH_3CO)_2O$; (d) R_1NH_2; (e) K_2CO_3; (f) HCl; (g) sec. amines , K_2CO_3, MWI

Figure 4.4: Synthetic protocol for nitro naphthyridone (**NN**) Derivatives

4.2 *IN VITRO* ANTIMYCOBACTERIAL STUDY [NCCL Standards, 1995]

4.2.1 *Mycobacterium tuberculosis* (MTB) and Multi Drug Resistant *Mycobacterium tuberculosis* (MDR-TB)

- **Micro-organisms:** *Mycobacterium tuberculosis* $H_{37}Rv$ ATCC 27294 and multi-drug resistant *Mycobacterium tuberculosis* (resistant to isoniazid, rifampicin, ethambutol and ofloxacin) obtained from Tuberculosis Research Center, Chennai, India

- **Culture Media:** Middlebrook 7H11 agar with OADC (Oleic acid Albumin Dextrose Catalase) Growth Supplement

Composition:

Middlebrook 7H9 Broth Base	-	0.47 g
Distilled Water	-	90 mL
Glycerol	-	0.4 mL
Tween 80	-	0.2 mL

ADC Growth Supplement:

Bovine Albumin Fraction V	-	0.5 g
Oleic acid	-	0.02 mL
Dextrose	-	0.2 g
Sodium Chloride	-	0.085 g
Distilled Water	-	10 mL

- **Method (Agar Dilution Method):**

1. 10 fold serial dilutions of each test compound/drug (in DMSO/Water mixture) were incorporated into Middlebrook 7H11 agar medium with OADC growth supplement.
2. Inoculum of *M. tuberculosis* $H_{37}Rv$ were prepared from fresh Middlebrook 7H11 agar slants with OADC growth supplement adjusted to 1 mg/mL (wet weight) in Tween 80 (0.05%) saline diluted to 10^{-2} to give a concentration of approximately 10^7 cfu/mL.
3. A 5 µL amount of bacterial suspension was spotted into 7H11 agar tubes containing 10-fold serial dilutions of drugs per mL.
4. The tubes were incubated at 37 °C, and final readings were recorded after 30 days.
5. The minimum inhibitory concentration (MIC) is defined as the minimum concentration of compound required to give complete inhibition of bacterial growth.

4.2.2 *Mycobacterium smegmatis* (MC^2)

- **Micro-organism:** *Mycobacterium smegmatis* ATCC 14468 (MC^2) obtained from IMTECH, Chandigarh.

- **Culture Media:** Luria Bertani Media with Glycerol and Tween 80 (LBGT)

Composition:

Casein Enzyme Hydrolysate	-	1.0 %
Yeast Extract	-	0.5 %
Sodium Chloride	-	1.0 %
Glycerol	-	0.5 %
Tween 80	-	0.2 %
Distilled Water	-	q. s.

- **Method:**

1. 5 fold serial dilutions of each test compound/drug (in DMSO/Water mixture) were incorporated into LBGT broth medium.
2. Inoculum of *M. smegmatis* were prepared from the exponential culture of the organism (OD~1.0) diluted to OD~0.1 to give a concentration of approximately 10^7 cfu/ml.
3. A 10 µl amount of suspension was inoculated into LBGT media containing 5 fold serial dilutions of drugs per mL.
4. The tubes were incubated at 37 °C, and final readings were recorded after 3 days.
5. The minimum inhibitory concentration (MIC) is defined as the minimum concentration of compound required to give complete inhibition of bacterial growth.

4.3 CYTOTOXICITY

Selected compounds were examined for toxicity (IC_{50}) in a mammalian Vero cell line till the concentration of 62.5 µg/mL [Gundersen, L. L., *et al.*, 2002] by serial dilution method. After 72 h of exposure, viability was assessed on the basis of cellular conversion of MTT into a formazan product using the Promega Cell Titer 96 non-radioactive cell proliferation assay.

4.4 *IN VIVO* ANTIMYCOBACTERIAL STUDY

Prior to animal screening the maximum tolerated dose (MTD) was performed for all the compounds, to be screened, using C57BL/6 female mice by administration of a one-time dose/animal of an escalating dose of drug (100 and 300 mg/kg). The nine mice (3 mice/dose) in each study were observed for a total of 1 week. Surviving mice were sacrificed and the organs examined for signs of over toxicity.

The compounds were tested for efficacy against MTB at a dose of 50 mg/kg in six-week-old Female CD-1 mice six per group. In this model [Sriram, D., *et al.,* 2005], the mice were infected intravenously through caudal vein with approximately 10^7 viable MTB ATCC 35801. Drug treatment by intra-peritoneal route began after 10 days of inoculation of the animal with microorganism and continued for 10 days. After 35 days post infection the spleen and right lung were aseptically removed and ground in a tissue homogenizer, the number of viable organisms was determined by serial 10-fold dilutions and subsequent inoculation onto 7H10 agar plates. Cultures were incubated at 37 °C in ambient air for 4 weeks prior to counting. Bacterial counts were measured, and compared with the counts from negative controls (vehicle treated) in lung and in spleen.

4.5 DNA GYRASE SUPERCOILING ASSAY

In order to carry out gyrase inhibition assays, DNA gyrase purified from MC^2 was used. The enzyme was prepared and stored by standardized procedures [Manjunatha, U. H., *et al.,* 2002]. The compounds tested were dissolved in 5 % DMSO and pre-incubated with gyrase. Supercoiling assays were carried out as described previously [Manjunatha, U. H., *et al.,* 2002], by incubating 400 ng of relaxed pUC18 at 37 °C in supercoiling buffer [35 mM Tris-HCl pH 7.5, 5 mM $MgCl_2$, 25 mM potassium glutamate, 2 mM spermidine, 2 mM ATP, 50 µg/ml bovine serum albumin, and 90 µg/ml yeast t-RNA in 5 % v/v glycerol] for 1 hour. Moxifloxacin at 5 µg/ml and ciprofloxacin at 10 µg/ml final concentration were used as positive controls and a control reaction having 5 % DMSO in absence of compounds was also performed. The reaction samples were heat inactivated and applied on to 1 % agarose gel electrophoresis in Tris - acetate - EDTA buffer for 12 hours. The gels were stained with ethidium bromide and recorded by gel documentation.

4.6 PHOTOTOXICITY EVALUATION

Female swiss albino mice, approximately 2 months old and weighing 20-25 g, were used in this study. Before oral dosing, they were fasted overnight for at least 18 h. Food was returned at the end of the 4 h photo-irradiation period. Eighteen mice were randomly

distributed into three dosing groups. First group received a single dose of screened compound at 140 mg/kg by oral gavage. The second group received a single dose of 140 mg/kg of lomefloxacin HCl. This lomefloxacin dose is one that, in preliminary experiments in this test system, produced a consistent erythema and ear thickening response. The final group served as a vehicle control, and received 10 mL/kg of the 0.5 % sodium carboxymethylcellulose vehicle only. Test animals were exposed to UVA light in a manner adapted from that described previously [Mayne, T. N., *et al.*, 1997]. Animals were irradiated for 4 h, equal to a total UV light irradiation of approximately 18 J/cm^2. Before dosing, at the end of the irradiation period and at approximately 24, 48, 72 and 96 h after dosing, both ears of each mouse were evaluated for changes indicative of a positive response: erythema, edema or a measurable increase in ear thickness. The drug and time factors were analyzed by separate univariate methods. Orthogonal contrasts were used to test for both linear and quadratic trends over time in each group by Student's *t*-test to test whether the change from baseline ear thickness was significantly different from zero.

4.7 QUANTUM MECHANICAL MODELING

The quantum mechanical (QM) calculations were carried out using Hyperchem 7.5 and Argus Lab version 4.0.1. The three-dimensional structures of the compounds were geometry optimized using Hamiltonian PM3 (Parameterized Method 3) semi-empirical QM method. For the estimation of HOMO and LUMO surfaces, the single-point energy calculation using RHF-SCF (Restricted Hartree-Fock-Single consistent Field) method (Basis set STO-6G) [Zerner, M. C., 1991] was employed. The HOMO surfaces were visualized using a contour value of 0.05 in opaque mode using green/orange and yellow for positive and negative phase of the orbital in space.

CHAPTER 5

FLUOROQUINOLONE (FQ) DERIVATIVES

5.1 SYNTHESIS

Various 1-(cyclopropyl/2,4-difluorophenyl/*t*-butyl)-1,4-dihydro-6-fluoro-7-(sub secondary amino)-4-oxoquinoline-3-carboxylic acids were synthesized from 2,4-dichloro-5-fluoroacetophenone by the following steps of reaction:

STEP 1: Synthesis of ethyl 3-(2,4-dichloro-5-fluorophenyl)-3-oxopropanoate (FQ 2)

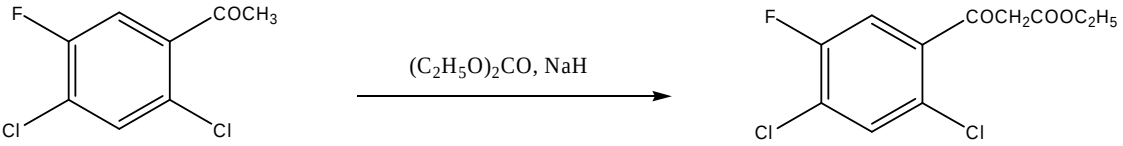

2,4-Dichloro-5-fluoroacetophenone
FQ 1

Ethyl 3-(2,4-dichloro-5-fluorophenyl)-3-oxopropanoate
FQ 2

A 60 % sodium hydride-in-oil suspension (2 equiv.) was added slowly at room temperature to a cold solution of 2,4-dichloro-5-fluoroacetophenone (**FQ 1)** (1 equiv.) in diethyl carbonate (300 mL). The mixture was then heated at 80 °C for 1.5 h. It was poured into ice - cold water (700 mL) solution containing acetic acid (25 mL). The mixture was extracted with three portions of ether (400 mL). The organic phase was dried and evaporated, and the residual oil was distilled at 111 °C (0.7 mmHg) to give **FQ 2**.

Yield: 80 %; B.P.: 109-111 °C (111 °C); IR (KBr) cm^{-1}: 2900, 1726, 1705, 582; ^1H NMR (DMSO-d_6) δ ppm: 1.17 (t, 3H, ethyl CH_3), 1.27 (t, 3H, ethyl CH_3), 4.07 (s, 2H, CH_2), 4.17 (q, 2H, ethyl CH_2), 4.27 (q, 2H, ethyl CH_2), 5.65 (s, 1H, vinyl H), 7.47 (m, two sets of 2H, Ar-H), 12.48 (s, 1H, enol OH); Anal ($C_{11}H_9Cl_2FO_3$) C, H, N.

STEP 2: Synthesis of ethyl 1-(cyclopropyl/2,4-difluorophenyl/*t*-butyl)-7-chloro-6-fluoro-4-oxo-1,4-dihydro-quinoline-3-carboxylates (FQ 5a-c)

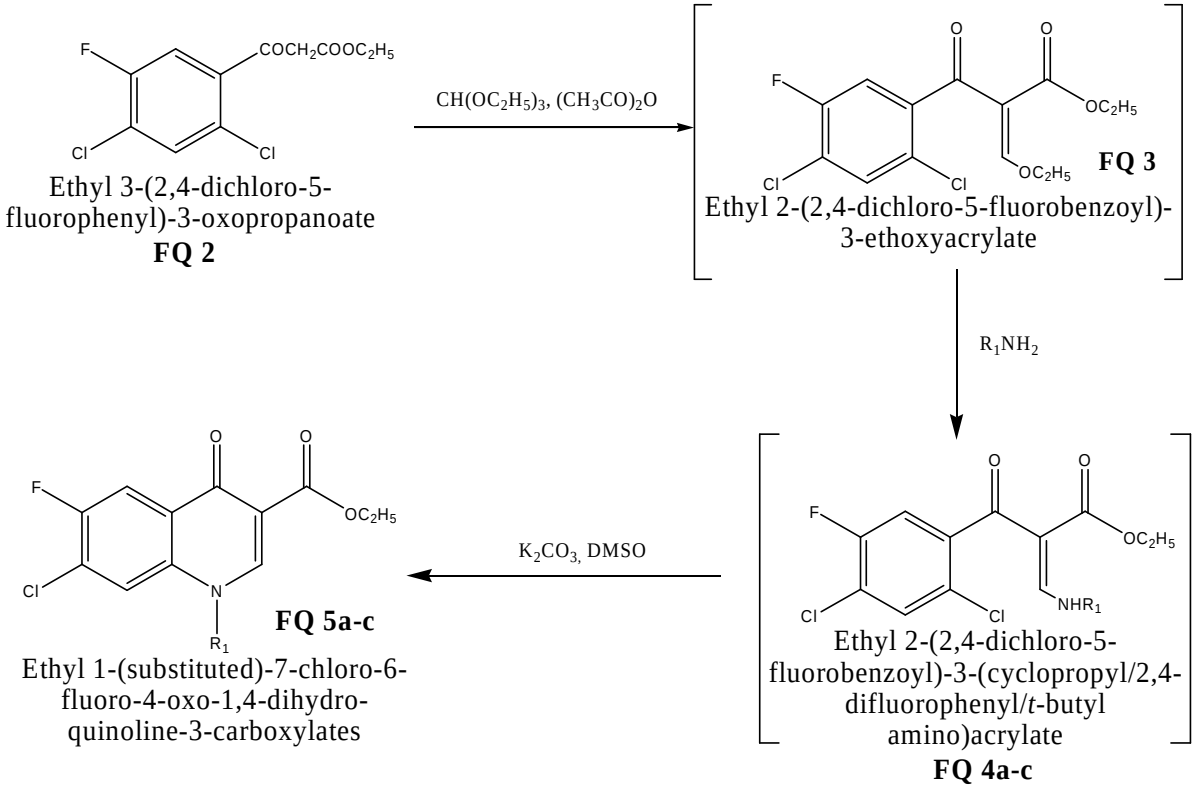

A mixture of **FQ 2** (1.00 equiv.), triethylorthoformate (1.5 equiv.) and acetic anhydride (2.5 equiv.) were refluxed at 140 ºC for 1 h. The ethyl acetate produced as a by product was distilled simultaneously under atmospheric pressure. After completion of reaction the reaction mixture was concentrated under reduced pressure to yield intermediate ethyl 2-(2,4-dichloro-5-fluorobenzoyl)-3-ethoxyacrylate (**FQ 3**) as an oil. The above residue was dissolved in a mixture of ether (20 ml) and ethanol (20 ml). Added corresponding primary amine (1.10 equiv.) at 0 ºC and stirred for 30 minutes under nitrogen atmosphere, followed by distillation yielded ethyl 2-(2,4-dichloro-5-fluorobenzoyl)-3-(cyclopropyl/2,4-difluorophenyl/*t*-butyl amino)acrylate (**FQ 4a-c**). The above crude solid (1.00 equiv.) was dissolved in DMSO (30 ml) and added anhydrous potassium carbonate (1.60 equiv.) and refluxed at 60 ºC for 3 h. After completion of reaction, the mixture was diluted with ice cold water and neutralized with 20 % HCl to a pH of 5-6. The precipitate thus formed was filtered and washed with water followed by 30 % ethyl acetate : hexane mixture to yield ethyl 1-(substituted)-7-chloro-6-fluoro-4-oxo-1,4-dihydro-quinoline-3-carboxylates (**FQ 5a-c**).

Ethyl 1-cyclopropyl-7-chloro-1,4-dihydro-6-fluoro-4-oxoquinoline-3-carboxylates (FQ 5a): Yield: 75 %; M.P.: > 250 ºC; IR (KBr) cm^{-1}: 2900, 1726, 1705, 1616; ^1H NMR (DMSO - d_6) δ ppm: 0.28 - 0.44 (m, 4H, cyclopropyl), 1.36 (m, 1H, cyclopropyl), 1.45 (t, 3H, $-CH_2CH_3$), 4.2 (m, 2H, $-CH_2CH_3$), 8.3 (s, 1H, C_8 - H), 9.34 (s, 1H, C_5 - H), 9.52 (s, 1H, C_2 - H); Anal ($C_{13}H_9ClFNO_3$) C, H, N.

Ethyl 1-(2,4-difluorophenyl)-1,4-dihydro-6-fluoro-7-methoxy-4-oxoquinoline-3-carboxylates (FQ 5b): Yield: 82 %; M.P.: > 250 ºC; IR (KBr) cm^{-1}: 2900, 1726, 1705, 1616; ^1H NMR (DMSO - d_6) δ ppm: 1.45 (t, 3H, $-CH_2CH_3$), 4.2 (m, 2H, $-CH_2CH_3$), 6.48 - 6.68 (m, 3H, Ar - H), 8.3 (s, 1H, C_8 - H), 9.34 (s, 1H, C_5 - H), 9.52 (s, 1H, C_2 - H); Anal ($C_{13}H_8ClF_3NO_3$) C, H, N.

Ethyl 1-*t*-butyl-7-methoxy-1,4-dihydro-6-fluoro-4-oxoquinoline-3-carboxylates (FQ 5c): Yield: 86 %; M.P.: 232 - 234 ºC; IR (KBr) cm^{-1}: 2900, 1726, 1705, 1616; ^1H NMR (DMSO - d_6) δ ppm: 1.45 (t, 3H, $-CH_2CH_3$), 1.6 (s, 9H, *t*-butyl), 4.2 (m, 2H, $-CH_2CH_3$), 8.3 (s, 1H, C_8 - H), 9.34 (s, 1H, C_5 - H), 9.52 (s, 1H, C_2 - H); Anal ($C_{13}H_9ClFNO_3$) C, H, N.

STEP 3: Synthesis of 1-(cyclopropyl/2,4-difluorophenyl/*t*-butyl)-1,4-dihydro-7-chloro-6-fluoro-4-oxoquinoline-3-carboxylic acid (FQ 6a-c)

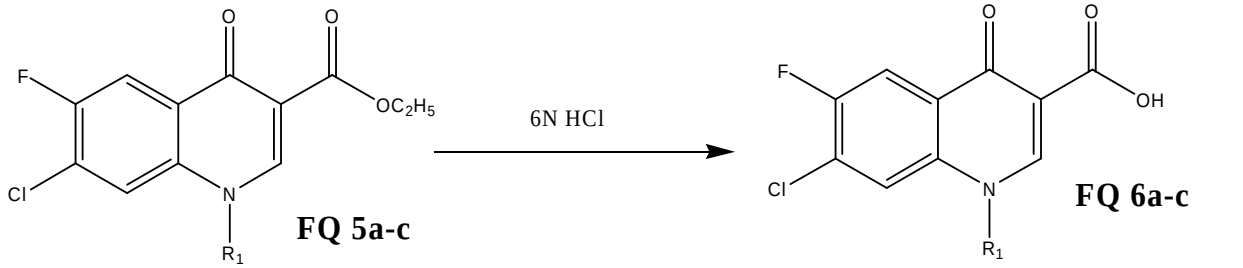

Ethyl 1-(substituted)-7-chloro-6-fluoro-4-oxo-1,4-dihydro-quinoline-3-carboxylates

1-(Cyclopropyl/2,4-difluorophenyl/*t*-butyl)-1,4-dihydro-7-chloro-6-fluoro-4-oxoquinoline-3-carboxylic acid

Compound **FQ 5a-c** (1.00 equiv.) was suspended in 6N HCl (5 ml) and refluxed for 6 h and then cooled to 0 ºC. The precipitate obtained was filtered, washed with water followed by 20% ethyl acetate yielded **FQ 6a-c**.

7-Chloro-1-cyclopropyl-1,4-dihydro-6-fluoro-4-oxoquinoline-3-carboxylic acid (FQ 6a): Yield: 72 %; M.P.: 229 - 231 ºC; IR (KBr) cm^{-1}: 2900, 1726, 1705, 1616; ^1H NMR (DMSO - d_6) δ ppm: 0.28 - 0.44 (m, 4H, cyclopropyl), 1.36 (m, 1H, cyclopropyl), 8.3 (s, 1H,

C_8 - H), 9.34 (s, 1H, C_5 - H), 9.52 (s, 1H, C_2 - H), 14.60 (s, 1H, COOH); Anal ($C_{13}H_9ClFNO_3$) C, H, N.

7-Chloro-1-(2,4-difluorophenyl)-1,4-dihydro-6-fluoro-4-oxoquinoline-3-carboxylic acid (FQ 6b): Yield: 76 %; M.P.: > 250 ºC; IR (KBr) cm^{-1}: 2900, 1728, 1710, 1620; ^1H NMR (DMSO - d_6) δ ppm: 6.48 - 6.68 (m, 3H, Ar - H), 8.3 (s, 1H, C_8 - H), 9.34 (s, 1H, C_5 - H), 9.54 (s, 1H, C_2 - H), 14.68 (s, 1H, COOH); Anal ($C_{16}H_7ClF_3NO_3$) C, H, N.

1-*t*-Butyl-7-chloro-1,4-dihydro-6-fluoro-4-oxoquinoline-3-carboxylic acid (FQ 6c): Yield: 75 %; M.P.: 225 - 227 ºC; IR (KBr) cm^{-1}: 2900, 1726, 1705, 1620; ^1H NMR (DMSO - d_6) δ ppm: 1.6 (s, 9H, *t*-butyl), 8.3 (s, 1H, C_8 - H), 9.34 (s, 1H, C_5 - H), 9.56 (s, 1H, C_2 - H), 14.6 (s, 1H, COOH); Anal ($C_{14}H_{13}ClFNO_3$) C, H, N.

STEP 4: Synthesis of 1-(cyclopropyl/2,4-difluorophenyl/*t*-butyl)-1,4-dihydro-6-fluoro-7-(substituted secondary amines)-4-oxoquinoline-3-carboxylic acid (FQ 7-9a-q)

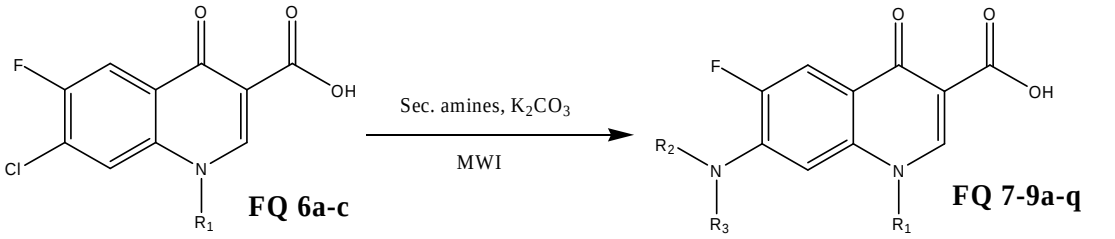

1-(Cyclopropyl/2,4-difluorophenyl/*t*-butyl)-1,4-dihydro-7-chloro-6-fluoro-4-oxo-quinoline-3-carboxylic acid

1-(Cyclopropyl/2,4-difluorophenyl/*t*-butyl)-1,4-dihydro-6-nitro-7-(substituted secondary amines)-4-oxoquinoline-3-carboxylic acid

Compound **FQ 6a-c** (1.0 equiv.) in dimethyl sulphoxide (2.5 ml) and appropriate secondary amines (1.1 equiv.) were irradiated in a microwave oven at an intensity of 80 % (560 watts) with 30 sec/cycle. The number of cycles in turn depended on the completion of the reaction, which was checked by TLC. The reaction timing varied from 1.5 - 3 min. After completion of the reaction, the mixture was poured into ice cold water and washed with water and isopropanol to give the titled products.

Physical constants of the synthesized compounds are presented in table 5.1

Spectral and elemental analysis data of representative fluoroquinolones (**FQ**) are presented in table 5.2.

5.2 *IN VITRO* ANTIMYCOBACTERIAL AND CYTOTOXICITY

The synthesized compounds were tested for antimycobacterial activities against *Mycobacterium tuberculosis*, multi-drug resistant *Mycobacterium tuberculosis* and *Mycobacterium smegmatis* by agar dilution method and the results are tabulated in table 5.3. The compounds were also tested for there cytotoxicity in mammalian vero cell lines and the results are tabulated in table 5.3.

5.3 *IN VIVO* ANTIMYCOBACTERIAL STUDY

One compound **FQ 7l** was tested in *in vivo* model against *M. tuberculosis* and the results are tabulated in table 5.4

5.4 DNA GYRASE SUPERCOILING ASSAY

Six compounds were tested for DNA gyrase enzyme supercoiling assay and the results are tabulated in table 5.5. The gel picture of the enzyme inhibition study is shown in figure 5.1.

Table 5.1: Physical constants of fluoroquinolones (FQ 7-9 a-q)

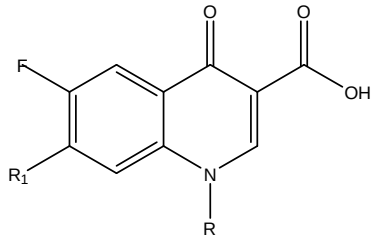

Compd	R	R_1	Yield (%)	M.P. (°C)	Molecular Formula	Molecular Weight	cLog P
FQ 7a	Cyclopropyl	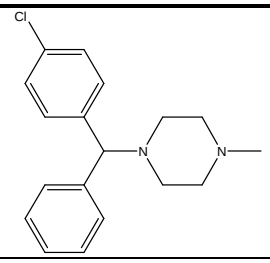	70	184-186	$C_{30}H_{27}ClFN_3O_3$	532.01	5.70
FQ 8a	2,4-F_2-Phenyl	- do -	75	155-157	$C_{33}H_{25}ClF_3N_3O_3$	604.02	7.14
FQ 9a	*t*-Butyl	- do -	71	170-172	$C_{31}H_{31}ClFN_3O_3$	548.05	6.28
FQ 7b	Cyclopropyl	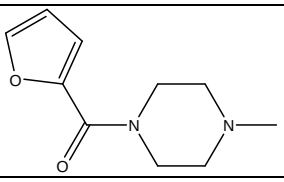	77	203-205	$C_{22}H_{20}FN_3O_5$	425.41	1.48
FQ 8b	2,4-F_2-Phenyl	- do -	76	150-152	$C_{25}H_{18}F_3N_3O_5$	497.42	2.92
FQ 9b	*t*-Butyl	- do -	70	223225	$C_{23}H_{24}FN_3O_5$	441.45	2.05
FQ 7c	Cyclopropyl	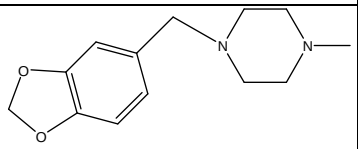	73	199-201	$C_{25}H_{24}FN_3O_5$	465.47	1.05
FQ 8c	2,4-F_2-Phenyl	- do -	72	178-180	$C_{28}H_{22}F_3N_3O_5$	537.49	2.73
FQ 9c	*t*-Butyl	- do -	75	183-185	$C_{26}H_{28}FN_3O_5$	481.52	1.94
FQ 7d	Cyclopropyl	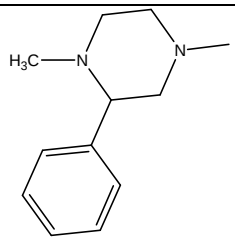	75	203-205	$C_{24}H_{24}FN_3O_3$	421.46	0.86
FQ 8d	2,4-F_2-Phenyl	- do -	73	201-203	$C_{27}H_{22}F_3N_3O_3$	493.48	2.53
FQ 9d	*t*-Butyl	- do -	74	172-174	$C_{25}H_{28}FN_3O_3$	437.51	1.74
FQ 7e	Cyclopropyl	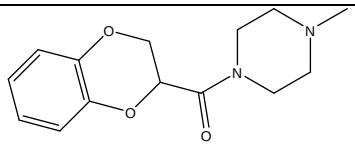	77	206-208	$C_{26}H_{24}FN_3O_6$	493.48	2.44
FQ 8e	2,4-F_2-Phenyl	- do -	75	180-182	$C_{29}H_{22}F_3N_3O_6$	565.50	4.11
FQ 9e	*t*-Butyl	- do -	73	>250	$C_{27}H_{28}FN_3O_6$	509.53	3.32

Table 5.1: Physical constants of fluoroquinolones (FQ 7-9 a-q) (contd…)

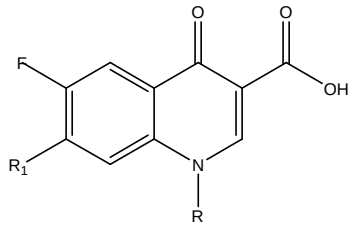

Compd	R	R_1	Yield (%)	M.P. (°C)	Molecular Formula	Molecular Weight	cLog P
FQ 7f	Cyclopropyl	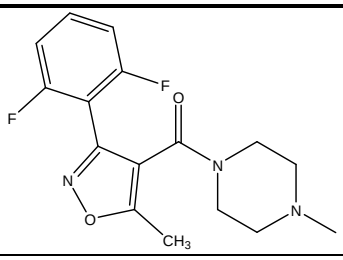	70	241-243	$C_{28}H_{23}F_3N_4O_5$	552.50	3.14
FQ 8f	2,4-F_2-Phenyl	- do -	84	223-225	$C_{31}H_{21}F_5N_4O_5$	624.51	4.82
FQ 9f	*t*-Butyl	- do -	81	>250	$C_{29}H_{27}F_3N_4O_5$	568.54	4.03
FQ 7g	Cyclopropyl	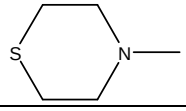	77	208-210	$C_{17}H_{17}FN_2O_3S$	348.39	2.99
FQ 8g	2,4-F_2-Phenyl	- do -	81	114-116	$C_{20}H_{15}F_3N_2O_3S$	420.40	4.67
FQ 9g	*t*-Butyl	- do -	71	>250	$C_{18}H_{21}FN_2O_3S$	364.43	3.88
FQ 7h	Cyclopropyl	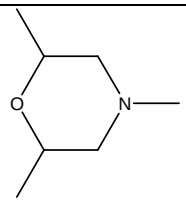	73	172-174	$C_{19}H_{21}FN_2O_4$	360.38	3.04
FQ 8h	2,4-F_2-Phenyl	- do -	84	103-105	$C_{22}H_{19}F_3N_2O_4$	432.39	4.72
FQ 9h	*t*-Butyl	- do -	74	108-110	$C_{20}H_{25}FN_2O_4$	376.42	3.93
FQ 7i	Cyclopropyl	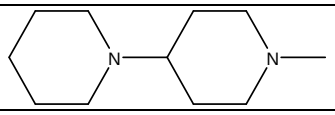	74	173-175	$C_{23}H_{28}FN_3O_3$	413.49	1.24
FQ 8i	2,4-F_2-Phenyl	- do -	81	108-110	$C_{26}H_{26}F_3N_3O_3$	485.50	2.91
FQ 9i	*t*-Butyl	- do -	78	156-158	$C_{24}H_{32}FN_3O_3$	429.53	2.12
FQ 7j	Cyclopropyl	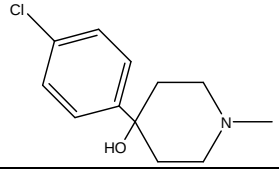	70	197-199	$C_{24}H_{22}ClFN_2O_4$	456.89	4.03
FQ 8j	2,4-F_2-Phenyl	- do -	76	145-147	$C_{27}H_{20}ClF_3N_2O_4$	528.91	5.69
FQ 9j	*t*-Butyl	- do -	75	127-129	$C_{25}H_{26}ClFN_2O_4$	472.94	4.91
FQ 7k	Cyclopropyl	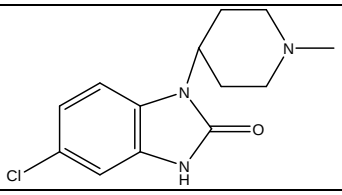	67	209-210	$C_{25}H_{22}ClFN_4O_4$	496.92	4.76
FQ 8k	2,4-F_2-Phenyl	- do -	78	181-183	$C_{28}H_{20}ClF_3N_4O_4$	560.93	6.43
FQ 9k	*t*-Butyl	- do -	69	>250	$C_{26}H_{26}ClFN_4O_4$	512.96	5.64

Table 5.1: Physical constants of fluoroquinolones (FQ 7-9 a-q) (contd…)

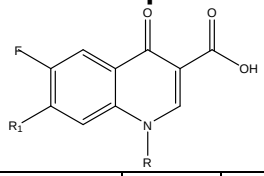

Compd	R	R_1	Yield (%)	M.P. (°C)	Molecular Formula	Molecular Weight	cLog P
FQ 7l	Cyclopropyl	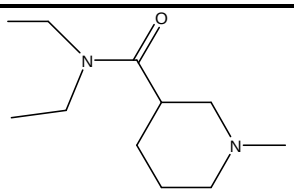	72	174-176	$C_{23}H_{28}FN_3O_4$	429.48	3.47
FQ 8l	2,4-F_2-Phenyl	- do -	73	75-77	$C_{26}H_{26}F_3N_3O_4$	501.50	5.14
FQ 9l	*t*-Butyl	- do -	70	152-154	$C_{24}H_{32}FN_3O_4$	445.53	4.35
FQ 7m	Cyclopropyl	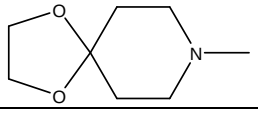	64	182-184	$C_{20}H_{21}FN_2O_5$	388.39	2.08
FQ 8m	2,4-F_2-Phenyl	- do -	69	110-112	$C_{23}H_{19}F_3N_2O_5$	460.40	3.75
FQ 9m	*t*-Butyl	- do -	71	136-138	$C_{21}H_{25}FN_2O_5$	404.43	2.96
FQ 7n	Cyclopropyl	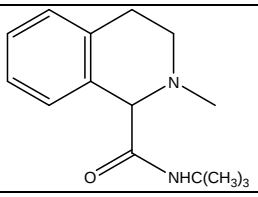	75	206-208	$C_{27}H_{28}FN_3O_4$	477.53	4.54
FQ 8n	2,4-F_2-Phenyl	- do -	82	112-114	$C_{30}H_{26}F_3N_3O_4$	549.54	6.21
FQ 9n	*t*-Butyl	- do -	72	135-137	$C_{28}H_{32}FN_3O_4$	493.57	5.42
FQ 7o	Cyclopropyl	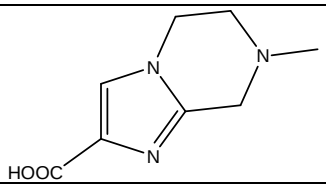	78	210-212	$C_{20}H_{17}FN_4O_5$	412.37	2.54
FQ 8o	2,4-F_2-Phenyl	- do -	84	179-181	$C_{23}H_{15}F_3N_4O_5$	484.38	4.21
FQ 9o	*t*-Butyl	- do -	72	>250	$C_{21}H_{21}FN_4O_5$	428.41	3.42
FQ 7p	Cyclopropyl	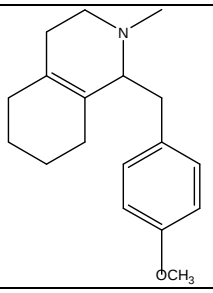	71	208-210	$C_{30}H_{31}FN_2O_4$	502.58	6.69
FQ 8p	2,4-F_2-Phenyl	- do -	76	114-116	$C_{33}H_{29}F_3N_2O_4$	574.59	8.37
FQ 9p	*t*-Butyl	- do -	73	69-71	$C_{31}H_{35}FN_2O_4$	518.62	7.58
FQ 7q	Cyclopropyl	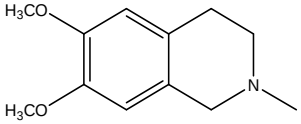	74	191-193			
FQ 8q	2,4-F_2-Phenyl	- do -	76	184-186	$C_{27}H_{21}F_3N_2O_5$	510.46	5.73
FQ 9q	*t*-Butyl	- do -	70	196-198	$C_{25}H_{27}FN_2O_5$	454.49	4.94

Table 5.2: Spectral data and elemental analysis data of representative fluoroquinolone (FQ) derivatives

Compd	IR Spectroscopy (cm^{-1}; KBr)	^1H NMR (δ ppm, DMSO – d_6)	Elemental Analyses (Calculated/Found)		
			C	H	N
FQ 7a	2900, 1724, 1708, 1620	0.28 – 0.48 (m, 4H, cyclopropyl), 1.35 (m, 1H, cyclopropyl), 2.59 – 3.12 (m, 8H, 4 CH_2 of piperazine), 4.2 (s, 1H, CH of diphenylmethyl), 7.0 – 7.18 (m, 9H, Ar-H), 8.32 (s, 1H, C_8 – H), 9.34 (s, 1H, C_5 – H), 9.56 (s, 1H, C_2 – H), 14.6 (s, 1H, COOH)	67.73 67.19	5.12 5.15	7.90 7.96
FQ 8b	2890, 1724, 1710, 1624	3.16 – 3.3 (m, 8H, 4 CH_2 of piperazine), 6.5 – 7.68 (m, 6H, Ar – H), 8.34 (s, 1H, C_8 – H), 9.32 (s, 1H, C_5 – H), 9.56 (s, 1H, C_2 – H), 14.6 (s, 1H, COOH)	60.36 60.00	3.65 3.69	8.45 8.44
FQ 9c	3250, 2890, 1724, 1710, 1624	1.76 (s, 9H, *t*-butyl), 2.82 – 3.12 (m, 8H, 4 CH_2 of piperazine), 3.6 (s, 2H, CH_2 of piperanoyl), 5.86 (s, 2H, -OCH_2O-), 6.42 – 6.62 (m, 3H, Ar – H), 8.34 (s, 1H, C_8 – H), 9.34 (s, 1H, C_5 – H), 9.56 (s, 1H, C_2 – H), 14.6 (s, 1H, COOH)	64.85 64.41	5.86 5.86	8.73 8.76
FQ 7d	2890, 1724, 1710, 1620	0.28 – 0.52 (m, 4H, cyclopropyl), 1.38 (m, 1H, cyclopropyl), 2.2 (s, 3H, CH_3), 2.6 (t, 2H, 5-CH_2 of piperazine), 3.15 (t, 2H, 6-CH_2 of piperazine), 3.4 (d, 2H, 2-CH_2 of piperazine), 4.12 (t, 1H, 3-CH of piperazine), 7.0 – 7.2 (m, 5H, Ar – H), 8.34 (s, 1H, C_8 – H), 9.32 (s, 1H, C_5 – H), 9.56 (s, 1H, C_2 – H), 14.4 (s, 1H, COOH)	68.39 68.35	5.74 5.76	9.97 9.92
FQ 8e	2890, 1724, 1710, 1624	3.26 – 3.4 (m, 8H, 4 CH_2 of piperazine), 4.6 (d, 2H, 3-CH_2 of dihydrobenzodioxinyl), 5.14 (t, 1H, 2-CH of dihydrobenzodioxinyl), 6.5 – 6.98 (m, 7H, Ar – H), 8.34 (s, 1H, C_8 – H), 9.3 (s, 1H, C_5 – H), 9.56 (s, 1H, C_2 – H), 14.6 (s, 1H, COOH)	61.59 61.44	3.92 3.99	7.43 7.45
FQ 9f	2890, 1724, 1710, 1624, 1208	1.74 (s, 9H, *t*-butyl), 2.3 (s, 3H, 5-CH_3 of isoxazolyl), 3.12 – 3.28 (m, 8H, 4 CH_2 of piperazine), 6.82 – 7.08 (m, 3H, Ar – H), 8.34 (s, 1H, C_8 – H), 9.32 (s, 1H, C_5 – H), 9.54 (s, 1H, C_2 – H), 14.6 (s, 1H, COOH)	61.26 61.36	4.79 4.75	9.85 9.83
FQ 7g	2890, 1724, 1710, 1620	0.28 – 0.54 (m, 4H, cyclopropyl), 1.36 (m, 1H, cyclopropyl), 2.64 – 3.4 (m, 8H, 4 CH_2 of thiomorpholine), 8.34 (s, 1H, C_8 – H), 9.32 (s, 1H, C_5 – H), 9.56 (s, 1H, C_2 – H), 14.4 (s, 1H, COOH)	58.61 58.36	4.92 4.98	8.04 8.03
FQ 8h	2892, 1724, 1710, 1628	1.2 (d, 6H, 2,6 CH_3 of morpholino), 3.0 (d, 4H, 2 CH_2 of morpholine), 3.9 (m, 2H, 2 CH of morpholine), 6.4 – 6,7 (m, 3H, Ar – H), 8.34 (s, 1H, C_8 – H), 9.3 (s, 1H, C_5 – H), 9.56 (s, 1H, C_2 – H), 14.6 (s, 1H, COOH)	61.11 61.19	4.43 4.41	6.48 6.42

Table 5.2: Spectral data and elemental analysis data of representative fluoroquinolone (FQ) derivatives (contd…)

Compd	IR Spectroscopy (cm^{-1}; KBr)	^1H NMR (δ ppm, DMSO-d_6)	Elemental Analyses (Calculated/Found)		
			C	H	N
FQ 9i	2890, 1724, 1710, 1624	1.5 – 1.6 (m, 10H, 5 CH_2), 1.78 (s, 9H, *t*-butyl), 2.2 (t, 4H, 2 CH_2), 2.7 (m, 1H, CH), 2.8 (t, 4H, 2 CH_2), 8.34 (s, 1H, C_8 – H), 9.32 (s, 1H, C_5 – H), 9.54 (s, 1H, C_2 – H), 14.6 (s, 1H, COOH)	67.11 67.22	7.51 7.55	9.78 9.78
FQ 7j	2900, 1724, 1708, 1620	0.28 – 0.46 (m, 4H, cyclopropyl), 1.32 (m, 1H, cyclopropyl), 2.0 – 2.7 (m, 8H, 4 CH_2 of piperidine), 7.1 – 7.18 (m, 4H, Ar – H), 8.34 (s, 1H, C_8 – H), 9.30 (s, 1H, C_5 – H), 9.56 (s, 1H, C_2 – H), 10.0 (bs, 1H, OH), 14.6 (s, 1H, COOH)	63.09 63.01	4.85 4.87	6.13 6.19
FQ 8k	3110, 2896, 1728, 1712, 1710, 1624	1.6 – 2.4 (m, 8H, 4 CH_2 of piperidine), 4.1 (bm, 1H, CH of piperidine), 6.4 – 6.9 (m, 6H, Ar – H), 8.34 (s, 1H, C_8 – H), 9.26 (s, 1H, C_5 – H), 9.56 (s, 1H, C_2 – H), 10.8 (s, 1H, NH), 14.6 (s, 1H, COOH)	59.11 59.10	3.54 3.56	9.85 9.84
FQ 9l	2890, 1724, 1710, 1624, 1208	1.2 (t, 6H, 2 CH_3 of ethyl), 1.7 (s, 9H, *t*-butyl), 1.78 – 2.7 (m, 9H, H of piperidine), 3.24 (q, 4H, 2 CH_2 of ethyl), 8.32 (s, 1H, C_8 – H), 9.28 (s, 1H, C_5 – H), 9.54 (s, 1H, C_2 – H), 14.6 (s, 1H, COOH)	64.70 64.30	7.24 7.29	9.43 9.40
FQ 7m	2890, 1724, 1712, 1618	0.28 – 0.52 (m, 4H, cyclopropyl), 1.38 (m, 1H, cyclopropyl), 1.78 – 2.4 (m, 8H, 4 CH_2 of azaspirodecane), 3.96 (m, 4H, 2 CH_2 of azaspirodecane), 8.32 (s, 1H, C_8 – H), 9.30 (s, 1H, C_5 – H), 9.56 (s, 1H, C_2 – H), 14.4 (s, 1H, COOH)	61.85 61.80	5.45 5.44	7.21 7.19
FQ 8n	2890, 1724, 1712, 1626	1.3 (s, 9H, 3 CH_3), 2.66 – 2.9 (m, 4H, 2 CH_2 of isoquinoline), 4.85 (s, 1H, CH of isoquinoline), 6.7 – 7.1 (m, 7H, Ar – H), 8.32 (s, 1H, C_8 – H), 9.28 (s, 1H, C_5 – H), 9.56 (s, 1H, C_2 – H), 10.2 (s, 1H, NH), 14.6 (s, 1H, COOH)	65.57 65.80	4.77 4.75	7.65 7.69
FQ 9º	3200, 2890, 1724, 1710, 1624, 1208	1.74 (s, 9H, *t*-butyl), 3.1 – 3.8 (m, 6H, 3 CH_2), 7.6 (s, 1H, CH), 8.32 (s, 1H, C_8 – H), 9.32 (s, 1H, C_5 – H), 9.54 (s, 1H, C_2 – H), 12.12 (s, 1H, 2-COOH), 14.6 (s, 1H, 3-COOH)	58.87 58.60	4.94 4.93	13.08 13.10
FQ 7p	3210, 2890, 1724, 1710, 1620	0.28 – 0.54 (m, 4H, cyclopropyl), 1.36 (m, 1H, cyclopropyl), 1.6 – 1.95 (m, 8H, 4 CH_2 of isoquinolinyl), 2.2 – 3.4 (m, 7H, 2 CH_2 and 1 CH of isoquinolinyl, and CH_2), 3.73 (s, 3H, -OCH_3), 6.8 – 7.1 (m, 4H, Ar – H), 8.34 (s, 1H, C_8 – H), 9.32 (s, 1H, C_5 – H), 9.56 (s, 1H, C_2 – H), 14.4 (s, 1H, COOH)	71.69 71.65	6.22 6.18	5.57 5.60

Table 5.3: *In vitro* antimycobacterial and cytotoxicity data of fluoroquinolones (FQ 7-9 a-q)

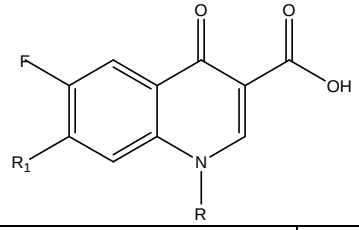

Compd	R	R_1	CC_{50} (μM)	MIC (μM)		
				MTB	MDR-TB	MC^2
FQ 7a	Cyclopropyl	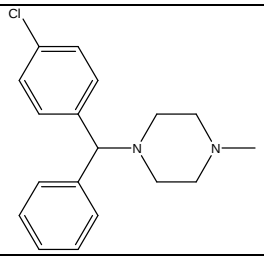	>117.5	0.17	0.17	1.47
FQ 8a	2,4-F_2-Phenyl	- do -	NT	10.35	NT	41.39
FQ 9a	*t*-Butyl	- do -	NT	1.42	NT	11.42
FQ 7b	Cyclopropyl	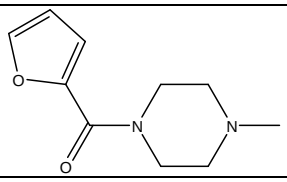	NT	3.68	NT	58.77
FQ 8b	2,4-F_2-Phenyl	- do -	NT	6.29	NT	25.13
FQ 9b	*t*-Butyl	- do -	NT	7.09	NT	28.32
FQ 7c	Cyclopropyl	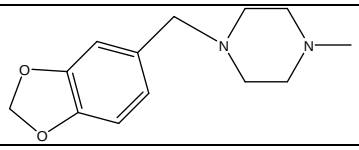	>134.3	0.19	0.41	1.68
FQ 8c	2,4-F_2-Phenyl	- do -	NT	5.82	NT	23.26
FQ 9c	*t*-Butyl	- do -	129.8	0.81	1.62	25.96
FQ 7d	Cyclopropyl	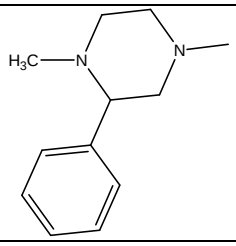	>148.3	0.93	0.93	7.43
FQ 8d	2,4-F_2-Phenyl	- do -	NT	6.34	NT	25.33
FQ 9d	*t*-Butyl	- do -	142.9	1.78	1.78	28.57
FQ 7e	Cyclopropyl	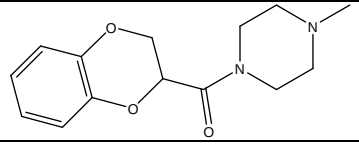	NT	3.17	NT	50.66
FQ 8e	2,4-F_2-Phenyl	- do -	NT	5.53	NT	2.76
FQ 9e	*t*-Butyl	- do -	NT	3.06	3.06	49.06

Table 5.3: *In vitro* antimycobacterial and cytotoxicity data of fluoroquinolones (FQ 7-9 a-q) (contd…)

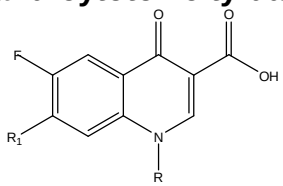

Compd	R	R_1	CC_{50} (µM)	MIC (µM)		
				MTB	MDR-TB	MC^2
FQ 7f	Cyclopropyl	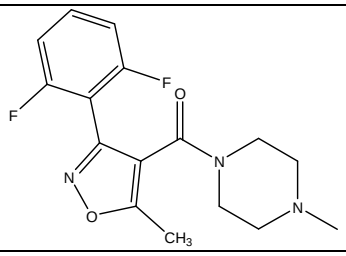	NT	5.67	NT	45.25
FQ 8f	2,4-F_2-Phenyl	- do -	NT	10.01	NT	5.01
FQ 9f	*t*-Butyl	- do -	NT	5.51	NT	43.97
FQ 7g	Cyclopropyl	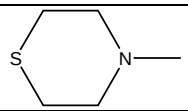	NT	8.98	NT	35.88
FQ 8g	2,4-F_2-Phenyl	- do -	NT	14.87	NT	14.87
FQ 9g	*t*-Butyl	- do -	NT	8.59	NT	68.60
FQ 7h	Cyclopropyl	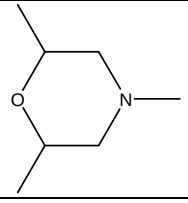	NT	1.08	2.16	4.33
FQ 8h	2,4-F_2-Phenyl	- do -	NT	7.24	7.24	3.61
FQ 9h	*t*-Butyl	- do -	NT	16.60	NT	66.42
FQ 7i	Cyclopropyl	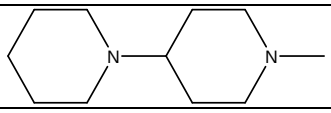	>151.1	0.94	0.94	1.89
FQ 8i	2,4-F_2-Phenyl	- do -	NT	6.45	NT	25.75
FQ 9i	*t*-Butyl	- do -	NT	1.82	1.82	29.10
FQ 7j	Cyclopropyl	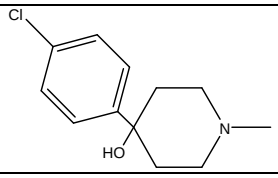	>136.79	0.42	0.85	1.71
FQ 8j	2,4-F_2-Phenyl	- do -	NT	5.92	NT	23.63
FQ 9j	*t*-Butyl	- do -	NT	3.29	0.82	52.86
FQ 7k	Cyclopropyl	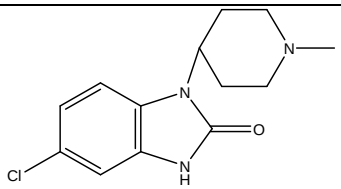	NT	3.14	NT	25.16
FQ 8k	2,4-F_2-Phenyl	- do -	NT	5.50	NT	21.97
FQ 9k	*t*-Butyl	- do -	NT	1.52	0.37	48.74

Table 5.3: *In vitro* antimycobacterial and cytotoxicity data of fluoroquinolones (FQ 7-9 a-q) (contd…)

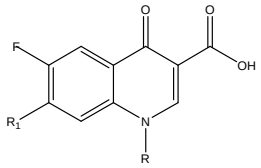

Compd	R	R_1	CC_{50} (μM)	MIC (μM)		
				MTB	MDR-TB	MC^2
FQ 7l	Cyclopropyl	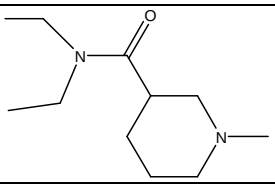	>145.52	0.09	0.09	1.82
FQ 8l	2,4-F_2-Phenyl	- do -	62.38	1.56	NT	12.46
FQ 9l	*t*-Butyl	- do -	140.28	0.43	0.09	56.11
FQ 7m	Cyclopropyl	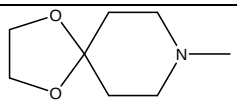	NT	2.01	2.01	4.02
FQ 8m	2,4-F_2-Phenyl	- do -	NT	6.79	NT	27.15
FQ 9m	*t*-Butyl	- do -	NT	3.86	7.74	61.82
FQ 7n	Cyclopropyl	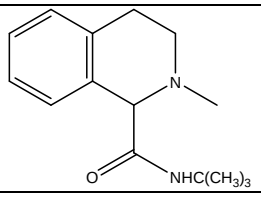	NT	3.27	6.55	13.09
FQ 8n	2,4-F_2-Phenyl	- do -	NT	11.37	NT	22.75
FQ 9n	*t*-Butyl	- do -	NT	6.34	NT	25.33
FQ 7o	Cyclopropyl	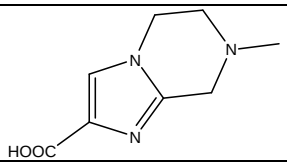	NT	3.78	7.59	30.31
FQ 8o	2,4-F_2-Phenyl	- do -	NT	12.90	NT	25.81
FQ 9o	*t*-Butyl	- do -	145.9	0.44	0.44	29.18
FQ 7p	Cyclopropyl	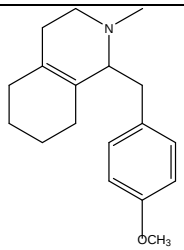	NT	6.22	NT	24.87
FQ 8p	2,4-F_2-Phenyl	- do -	NT	5.45	5.45	2.72
FQ 9p	*t*-Butyl	- do -	NT	6.04	NT	48.20
FQ 7q	Cyclopropyl	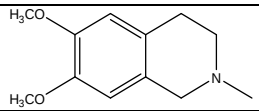	>142.5	0.19	0.38	13.75
FQ 8q	2,4-F_2-Phenyl	- do -	NT	6.13	NT	24.49
FQ 9q	*t*-Butyl	- do -	NT	0.86	0.42	55.01
Gatifloxacin	-	-	>155.3	1.04	8.34	2.08
INH	-	-	>455.8	0.36	45.57	45.57

Table 5.4: *In vivo* activity data of FQ 7l, gatifloxacin and isoniazid against *M. tuberculosis* ATCC 35801 in mice.

Compound	Lungs (log CFU ± SEM)	Spleen (log CFU ± SEM)
Control	7.99 ± 0.16	9.02 ± 0.21
Gatifloxacin (50 mg/kg)	6.02 ± 0.23	6.92 ± 0.07
Isoniazid (25 mg/kg)	5.86 ± 0.23	4.71 ± 0.10
FQ 7l (50 mg/kg)	5.46 ± 0.14	4.22 ± 0.13

Table 5.5: IC_{50} values for DNA gyrase inhibition of fluoroquinolones (FQ)

Compounds	IC_{50} (μM)
FQ 7a	187.97
FQ 8e	70.73
FQ 7h	277.48
FQ 8h	92.51
FQ 7l	232.84
FQ 7m	102.99
Ciprofloxacin	15.09
Moxifloxacin	12.46

5.5 PHOTOTOXICITY EVALUATION

Two compounds were evaluated for potential phototoxicity in a standardized *in vivo* test system and the results are tabulated in table 5.6.

7.6 QUANTUM MECHANICAL MODELING

In the present study the HOMO and LUMO surfaces were visualized for the titled compounds for comparison (Figure 5.2)

Table 5.6: Phototoxicity evaluation of fluoroquinolones (FQ)

Group	Ear thickness (mm)[a]						Erythema[b]					
	Time (approximately) after start of irradiation (h)[c]											
	0	4	24	48	72	96	0	4	24	48	72	96
Control[d]	0.29 ± 0.02	0.29 ± 0.01	0.32 ± 0.02	0.31 ± 0.01	0.34 ± 0.03	0.34 ± 0.03	0	0	0	0	0	0
FQ 7a	0.25 ± 0.02	0.27 ± 0.01	0.28 ± 0.01	0.29 ± 0.01	0.29 ± 0.02	0.28 ± 0.01	0	2	0	0	0	0
FQ 7m	0.25 ± 0.02	0.27 ± 0.02	0.29 ± 0.02	0.29 ± 0.01	0.31 ± 0.01[#]	0.31 ± 0.02[#]	0	3	0	0	0	0
Lomefloxacin	0.31 ± 0.01	0.40 ± 0.02[*#]	0.48 ± 0.02[*#]	0.53 ± 0.02[*#]	0.64 ± 0.04[*#]	0.60 ± 0.06[*#]	0	6	6	6	6	6

[a] Mean Ear Thickness ± SEM; left and right ears were averaged
[b] Number of mice with erythema
[c] Time zero = pre-dose (mice exposed to UVA light immediately after dosing); 4 h = end of irradiation period.
[d] Control = 0.5% aqueous solution of sodium carboxymethylcellulose (4 Ns/m^2) dosed at 10 mL/kg.
[*] Mean Ear Thickness ± SEM; significant difference from control at $P < 0.05$.
[#] Mean Ear Thickness ± SEM; significant difference from 0 h at $P < 0.05$.

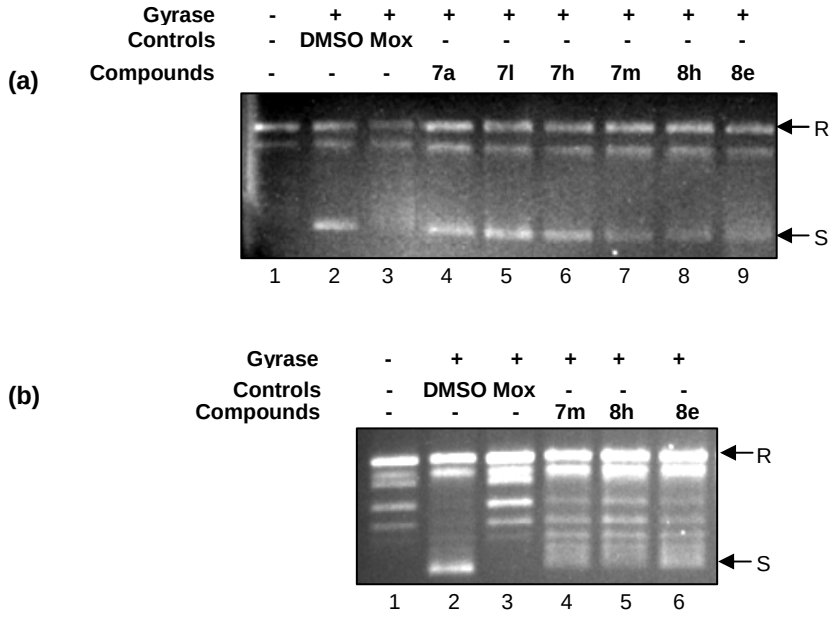

Figure 5.1: Gel picture for DNA gyrase supercoiling assay of fluoroquinolones (**FQ**).
The assays were performed as described in experimental section. DNA gyrase was incubated with indicated concentrations of the compounds before the addition of rest of the components.
(a) Lane 1: relaxed DNA, lane 2: supercoiling reaction in presence of 5 % DMSO, Lane 3: moxifloxacin at concentration of 5 μg/ml was used as the positive control for inhibition of enzyme. Lanes 4 to 9: supercoiling reaction in presence of 50 μg/ml of compounds **FQ 7a**, **FQ 7l**, **FQ 7h**, **FQ 7m**, **FQ 8h**, **FQ 8e** respectively.
(b) Lane 1: relaxed DNA, lane 2: supercoiling reaction in presence of 5 % DMSO, Lane 3: moxifloxacin at concentration of 5 μg/ml was used as the positive control for inhibition of enzyme. Lanes 4 to 6: supercoiling reaction in presence of 40 μg/ml of compounds **FQ 7m**, **FQ 8h** and **FQ 8e** respectively. R and S stand for relaxed and supercoiled DNA respectively.

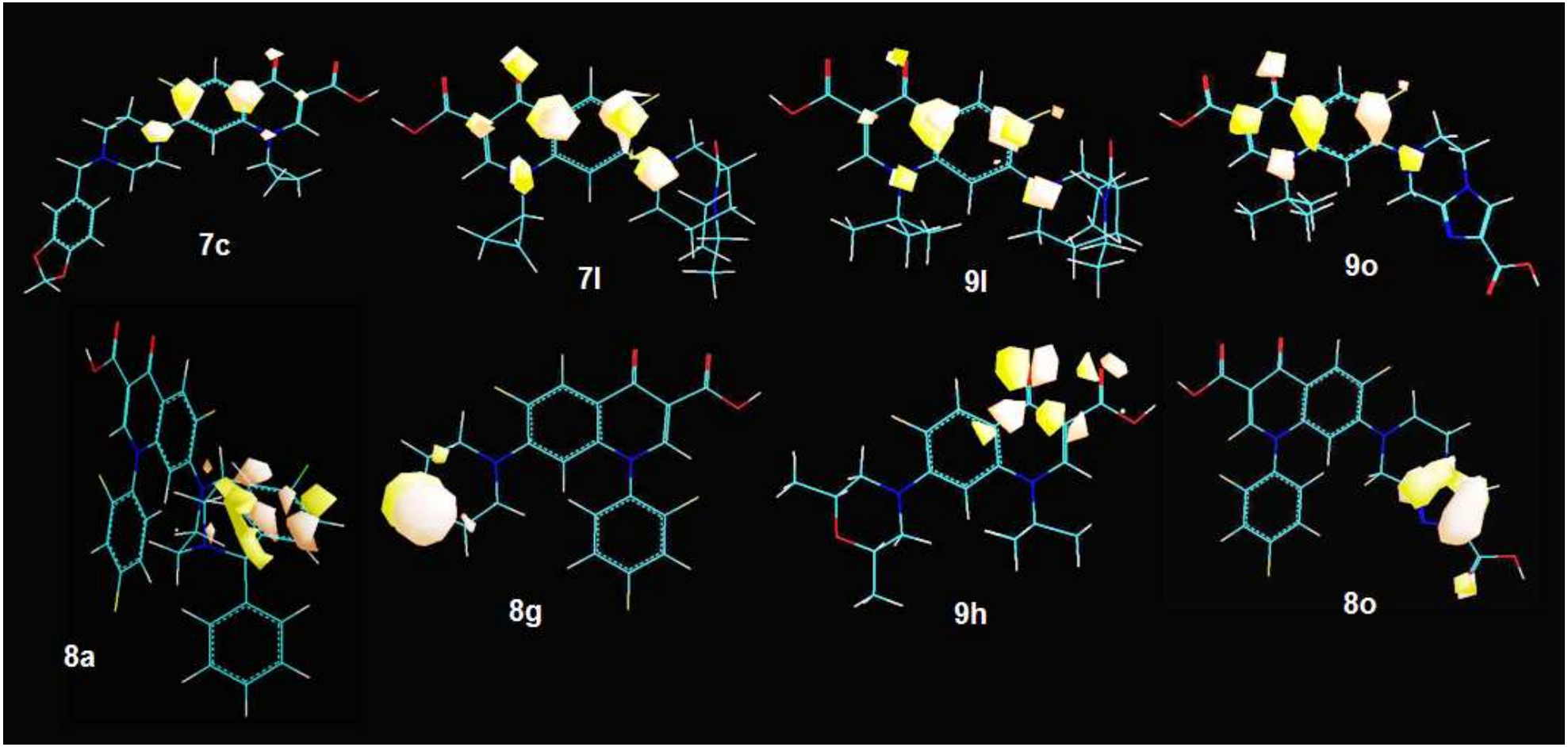

Figure 5.2: HOMO surface visualization (Contour value = 0.05) of some representative of fluoroquinolones (**FQ**) in opaque mode. The colors indicate the phase of the orbital in space (orange for positive and yellow for negative).

5.7 DISCUSSION

Fifty one novel 1-(cyclopropyl/2,4-difluorophenyl/*t*-butyl)-1,4-dihydro-6-fluoro-7-(sub secondary amino)-4-oxoquinoline-3-carboxylic acids (**FQ 7-9 a-q**) were synthesized from 2,4-dichloro-5-fluoroacetophenone by a six step synthesis (Figure. 4.1) according to the literature procedure [Chu, D. T. W., *et al.,* 1985]. Briefly, condensation of 2,4-dichloro-5-fluoroacetophenone (**FQ 1**) with diethyl carbonate in the presence of sodium hydride yielded ethyl 3-(2,4-dichloro-5-fluorophenyl)-3-oxopropanoate (**FQ 2**). Ethyl 1-(cyclopropyl/2,4-difluorophenyl/*t*-butyl)-1,4-dihydro-6-fluoro-7-chloro-4-oxoquinoline-3-carboxylates (**FQ 5a-c**) were prepared by a three-step one-pot reaction. First treatment of the keto ester **FQ 2** with triethyl orthoformate in acetic anhydride gave the one-carbon homologue enol ether intermediate ethyl 2-(2,4-dichloro-5-fluorobenzoyl)-3-ethoxyacrylate (**FQ 3**), which upon evaporation to dryness was allowed to react with slight excess of appropriate amines under nitrogen atmosphere in a mixture of ether and ethanol at 0 °C gave the enamino ester ethyl 3-(substituted aminomethylene)-2-(2,4-dichloro-5-fluorobenzoyl)acrylate (**FQ 4a-c**), and base catalyzed cyclization of **FQ 4a-c** with potassium carbonate in DMSO yielded quinolones **FQ 5a-c**. Ethyl esters were finally hydrolyzed in acidic condition to yield 1-(cyclopropyl/2,4-difluorophenyl/*t*-butyl)-7-chloro-6-fluoro-1,4-dihydro-4-oxoquinoline-3-carboxylic acid (**FQ 6a-c**). The titled compounds **FQ 7-9 a-q** were prepared by treating **FQ 6a-c** with appropriate secondary amines in presence of potassium carbonate under microwave irradiation in DMSO. When compared to conventional method [Chu, D. T. W., *et al.,* 1985] of 2 - 3 hours process, microwave assisted synthesis was performed with short reaction times (2 - 3 minutes), with ease and was environment friendly. The over all yield of the synthesized compounds were in the range of 64 - 84 %. The purity of the synthesized compounds was monitored by TLC and elemental analyses and the structures were identified by spectral data.

In general, IR spectra showed C=O stretching peak of carboxylic acid at 1720 - 1730 cm^{-1}; C=O stretching peak of pyridine carbonyl at 1620 - 1630 cm^{-1}. In the ^{1}H NMR spectra the

signals of the respective protons of the prepared derivatives were verified on the basis of their chemical shifts, multiplicities and coupling constants. The spectra showed a broad singlet at δ 14.6 ppm corresponding to COOH proton; singlet at δ 9.52 ppm corresponding to C_2 proton; singlet at δ 9.34 ppm corresponding to C_5 proton; N_1 cyclopropyl protons showed multiplets at δ 1.42 (1H) and 0.28 - 0.48 (4H) ppm; N_1 *t*-butyl protons showed singlet at δ 1.62 (9H) ppm; and N_1 2,4-difluorophenyl protons showed multiplet at δ 6.50 - 6.72 (3H) ppm. The elemental analysis results were within ± 0.4% of the theoretical values.

Most of the compounds were found to be more lipophilic indicated by their calculated log of partition coefficient value greater than 2 [log P > 2]. No correlation has been established between the calculated log P and antimycobacterial activity of the compounds, as compounds with low log P were found to be more active than compounds with high log P.

In the first phase of screening against MTB, all the compounds showed excellent *in vitro* activity against MTB with MIC ranging from 0.08 - 16.6 μM. Eleven compounds (**FQ 7a**, **FQ 7c, FQ 9c, FQ 7d, FQ 7i, FQ 7j, FQ 7l, FQ 9l, FQ 9o, FQ 7q** and **FQ 9q**) inhibited MTB with MIC of less than 1 μM and were more potent than standard fluoroquinolone gatifloxacin (MIC: 1.04 μM). When compared to isoniazid (MIC: 0.36 μM), four compounds (**FQ 7a, FQ 7c, FQ 7l** and **FQ 7q**) were found to be more active against MTB.

Compound 7-(3-(diethylcarbamoyl)piperidin-1-yl)-1-cyclopropyl-6-fluoro-1,4-dihydro-4-oxoquinoline-3-carboxylic acid (**FQ 7l**) was found to be the most active compound *in vitro* with MIC of 0.09 μM against MTB and was 4 & 11.5 times more potent than INH & GAT respectively.

With respect to structure-MTB activity relationship, we have studied with various substituted piperazines (**FQ 7-9a-f**), (thio) morpholines (**FQ 7-9g-h**), substituted piperidines (**FQ 7-9i-l**), and fused piperazines & piperidines (**FQ 7-9m-q**) at C_7 position. The results demonstrated that the contribution of the C_7 position to antimycobacterial activity was dependent on the substituent at N_1 and was in the order of substituted piperidines > substituted piperazines > fused piperazines & piperidines > (thio) morpholines when N_1 was cyclopropyl and *t*-butyl

and substituted piperidines > substituted piperazines ≥ fused piperazines & piperidines ≥ (thio) morpholines when N_1 was 2,4-difluorophenyl. Overall, a comparison of the substitution pattern at C_7 demonstrated that the order of activity was substituted piperidines > substituted piperazines > fused piperazines & piperidines > (thio) morpholines.

The results demonstrated that the antimycobacterial activity imparted by the N_1 substituent was in the order of cyclopropyl > *tert*-butyl > 2,4-difluorophenyl. This result correlates well with the previous report on the importance of cyclopropyl and *tert*-butyl group as antimycobacterial pharmacophore [Renau, T. E., *et al.*, 1996]. Overall, it appears that the *tert*-butyl group is at least as good as the cyclopropyl group as a substituent at the N_1 position of the quinolone. This discovery casts some doubts on at least two hypotheses made to explain the previous belief that the cyclopropyl substituent at the N_1 position conveys unusually high activity to the quinolones that contain this feature. One hypothesis is based on the belief that the antibacterial activity of quinolones is related to the amount of un-ionized drug that is able to penetrate the cell membranes. This in turn was associated with a highly acidic carboxyl group and a less basic C_7 amino substituent [Nikaido, H., *et al.*, 1993]. The carboxyl group is more acidic if the N_1 substituent is electron - donating. The greater activity of cyclopropyl substituted quinolones was therefore associated with the electron - donating effect of this moiety. However, the *tert*-butyl substituent is also an electron - releasing substituent. Therefore, the suggestion that cyclopropyl is better than other alkyl substituents because of its ability to activate the carboxylic acid at C_3, do not appear to be valid. On the other hand, the fact that the *tert*-butyl group is a better electron-donating group and possesses higher hydrophobicity than the cyclopropyl group provides support for the co-operative binding model for the inhibition of DNA gyrase proposed by Shen, in which two quinolone molecules self associate by π-π ring stacking and tail-to-tail hydrophobic interactions between the N_1 substituents [Shen, L. L., 1994].

Subsequently some of the compounds were evaluated against MDR-TB, and the compounds inhibited MDR-TB with MIC ranging from 0.09 - 14.45 μM and among the twenty four compounds screened; all the compounds were found to be more active than INH (MIC: 45.57

μM), and GAT (MIC: 8.34 μM). Twelve compounds (**FQ 7a**, **FQ 7c, FQ 7d, FQ 7i, FQ 7j, FQ 9j, FQ 9k, FQ 7l, FQ 9l, FQ 9o, FQ 7q** and **FQ 9q**) inhibited MDR-TB with MIC less than 1 μM.

Compounds **FQ 7l** and 1-*tert*-butyl-7-(3-(diethylcarbamoyl)piperidin-1-yl)-6-fluoro-1,4-dihydro-4-oxoquinoline-3-carboxylic acid (**FQ 9l**) were found to be the most active compounds *in vitro* with MIC of 0.09 μM against MDR-TB and was 92 and 506 times more potent than GAT and INH respectively.

In MDR-TB, the results demonstrated that the antimycobacterial activity imparted by N_1 substituents was in the order cyclopropyl > *tert*-butyl > 2,4-difluorophenyl. By introducing bulky lipophilic secondary amines at C_7, enhanced the antimycobacterial activity which might be due to more penetration of these compounds into mycobacterial cells.

The compounds were also evaluated against MC^2 in which all the compounds inhibited MC^2 with MIC ranging from 1.47 - 68.98 μM and thirty nine compounds were found to be more active than isoniazid (MIC: 45.57 μM).

In MC^2, the results demonstrated that the antimycobacterial activity imparted by N_1 substituents was in the order cyclopropyl > 2,4-difluorophenyl > *tert*-butyl.

Twelve compounds when tested for cytotoxicity showed CC_{50} values ranging from 62.38 - > 151.15 μM. A comparison of the substitution pattern at N_1 demonstrated that 2,4-difluorophenyl substituted analogs were more cytotoxic than the cyclopropyl analogs. These results are important as the 2,4-difluorophenyl substituted compounds with their increased cytoliability, are much less attractive in the development of a quinolone for the treatment of TB. This is primarily due to the fact that the eradication of TB requires a lengthy course of treatment, and the need for an agent with a high margin of safety becomes a primary concern. The compound **FQ 7l** was found to be non-toxic up to 145.5 μM and showed selectivity index (CC_{50}/ MIC) of more than 1616.

Compound **FQ 7l** was tested for *in vivo* efficacy against MTB at a dose of 50 mg/kg (Table 5.4) in CD-1 mice. Compound **FQ 7l** showed no effect or adverse reactions/toxicity at the maximum dose tested (300 mg/kg). Compound **FQ 7l** decreased the bacterial load in lung and spleen tissues with 2.53 and 4.88-log10 protections respectively and was considered to be promising in reducing bacterial count in lung and spleen tissues. When compared to gatifloxacin, at the same dose level, **FQ 7l** decreased the bacterial load with 0.56 and 2.7-log10 protections in lung and spleen tissues respectively.

The 6-fluoroquinolone-3-carboxylic acid derivatives synthesized were tested for their ability to inhibit supercoiling activity of DNA gyrase. Quinolones target two Type II topoisomerases in bacteria *viz.* DNA gyrase and topoisomerase IV. Both the enzymes act by a transient double - stranded DNA break, followed by strand passage and religation reactions to facilitate DNA transaction processes [Levine, C. H., *et al.,* 1998]. DNA gyrase is the only enzyme known so far having the ability to introduce negative supercoils in DNA. In all the species of mycobacteria including MTB, DNA gyrase is the sole type II topoisomerase carrying out the reactions of both gyrase and topoisomerase IV. Since the DNA gyrase from MTB and MC^2 are highly similar at functional as well as protein sequence level and antigenic properties [Manjunatha, U. H., *et al.,* 2000], we have used MC^2 DNA gyrase for carrying out the supercoiling assays. The results of gyrase inhibition with various compounds are presented in figure 5.1 (1a and 1b). The IC_{50} values were calculated after performing the reactions with various concentrations of the compounds and the concentration at which the enzyme was 50 % inhibited was taken as IC_{50}. Table 5.5 shows the IC_{50} of different compounds tested. Compounds **FQ 7a**, **FQ 7l** and **FQ 7h** has IC_{50} values of approx. 200 μM and compounds **FQ 7m**, **FQ 8h** and **FQ 8e** has IC_{50} values of 102.99, 92.51, 70.73 μM respectively. The IC_{50} values of compounds **FQ 7a**, **FQ 7l** and **FQ 7h** are much higher compared to the positive control ciprofloxacin and moxifloxacin. However, in cell based assays these three compounds *i.e.*, **FQ 7a**, **FQ 7l** and **FQ 7h** showed higher potency than other compounds. The reason for this difference between *in vitro* and *in vivo* efficacy is not very clear at this stage and needs to be investigated.

Fluoroquinolones in general have favorable safety profiles; phototoxicity has become a significant factor in the clinical use of some [Ferguson, J., *et al.,* 1989]. Indeed, the first quinolone, nalidixic acid, caused light-induced dermal effects. This type of response has now been demonstrated for almost all fluoroquinolones [Domagala, J. M., 1994], although the relative phototoxic potential varies greatly among compounds. Phototoxicity is considered to be an acute, light-induced irritation response characterized by dermal inflammation, with erythema and edema as primary clinical endpoints. Phototoxicity with the quinolones is generally thought to result from the absorption of light by the parent compound or a metabolite in tissue [Takayama, S., *et al.,* 1995]. This photosensitized chromophore may then transfer its absorbed photo energy to oxygen molecules, creating an environment for the production of reactive oxygen species such as singlet oxygen. These reactive species are then thought to attack cellular lipid membranes, initiating the inflammatory process.

Two (**FQ 7a** and **FQ 7m**) compounds were evaluated for potential phototoxicity in a standardized *in vivo* test system that has been used previously to assess quinolone antibiotics [Mayne, T. N., *et al.,* 1997]. The test compounds (140 mg/kg) and the positive control lomefloxacin hydrochloride (140 mg/kg) were evaluated for phototoxicity and both ears of each mouse were evaluated for changes indicative of a positive response: erythema, edema or a measurable increase in ear thickness. Change from baseline was calculated separately for each animal and time point and analyzed for statistical significance and presented in Table 5.6. The results indicated that lomefloxacin showed significant increase in ear thickness from 4 - 96 h when compared within time points and with the control. No significant difference in ear thickness was observed with the test compounds at various time-points when compared with the pre-drug reading (0 h) but were less or non toxic when compared with the negative (vehicle - treated) and positive controls (lomefloxacin). No significant erythema occurred in mice dosed with 140 mg/kg of **FQ 7a** and **FQ 7m** throughout the 96 h study.

In theory, quantum mechanical (QM) methods enable completely accurate predictions of any property; there are some important classes of property (notably reactivity, electronic, magnetic, and optical behavior) that can only be modeled using QM methods, because they are determined by electronic behavior that cannot be approximated well using other methods. In the present study the titled compounds were geometry optimized by semi-empirical PM3 QM method and subjected to single-point energy calculation to determine their HOMO (Highest occupied molecular orbital) and LUMO (Lowest unoccupied molecular orbital) surfaces. Electron-rich and electron-poor species tend to reveal the localization or delocalization of the partial or full charge by the shape of the HOMO or LUMO. Molecular orbitals, when viewed in a qualitative graphical representation, can provide insight into the nature of reactivity, and some of the structural and physical properties of molecules.

In the present study the HOMO and LUMO surfaces were visualized for the synthesized compounds for comparison and the following observations were made. The N_1, N_7 and the 4-oxo functions were found to play a crucial role in the antitubercular activity of fluoroquinolones. This hypothesis was confirmed with the HOMO surface analysis (Figure 5.2), in which the most of the active compounds with lower MICs showed HOMO surfaces on the N_1, N_7 and the 4-oxo functions. The compounds with bulkier substituents (phenyl, fused aryl system) at the N_7 end showed electron cloud over the aryl function and hence the N_7 becomes electron deficient. The compounds with cyclopropyl and *t*-butyl substitution at N_1 position were able to retain the electron cloud compared to 2,4-difluorophenyl substitution as seen with compounds **FQ 9o and FQ 8o**. In the compounds, like **FQ 8g** and **FQ 9h** having morpholine and thio morpholine substituents at C_7 position, the normal pattern of electron distribution was not seen and the compounds were not found to be active. The less active compounds were devoid of electron cloud around N_1, N_7, and the oxo function at C_4. This observation was observed with all the less active compounds as seen with compounds **FQ 8a, FQ 8g, FQ 9h** and **FQ 8o** in figure 5.2. With respect to N_1 substituent cyclopropyl was more preferable over 2,4-difluorophenyl and *t*-butyl in retaining the electron-rich cloud over the N_1 nitrogen as seen in the Figure 5.2 with compounds **FQ 7c and FQ 7l**. There was no significant difference observed in the LUMO orbital surfaces.

5.8 STRUCTURE - ACTIVITY RELATIONSHIP

The extensive studies on the activity profile against mycobacterium shows the following relationship between activity and the structure.

1. With respect to the substituents at N_1 position, the order of activity is cyclopropyl > *tert*-butyl > 2,4-difluorophenyl.
2. With respect to the substituents at C_7 position, the order of activity is substituted piperidines > substituted piperazines > fused piperazines and piperidines > (thio) morpholines.
3. The N_1, N_7 and the 4-oxo functions were found to play a crucial role in the antitubercular activity of fluoroquinolones.
4. 2,4-Difluorophenyl substituted compounds were found to be cytotoxic when compared with cyclopropyl or *t*-butyl compounds.

MOST POTENT FLUOROQUINOLONE (FQ) DERIVATIVE

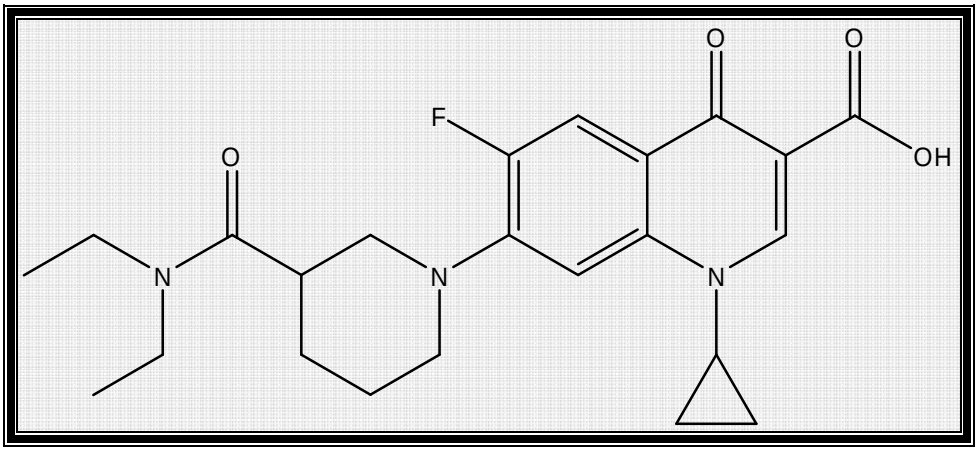

FQ 7l

1-Cyclopropyl-7-(3-(diethylcarbamoyl)piperidine-1-yl)- 6-fluoro-1,4-dihydro-4-oxoquinoline-3-carboxylic acid

- ***In vitro***:
  - **Against MTB**: 11.5 and 4 times more potent than GAT and INH respectively.
  - **Against MDR-TB:** 92 and 506 times more potent than GAT and INH respectively.
  - **Against MC^2:** 1.14 and 25.04 times more active than GAT and INH respectively.
- ***Cytotoxicity***: Non - toxic up to 145.5 µM and showed selectivity index (CC_{50} / MIC) of more than 1616.
- ***In vivo***: Compared to GAT at the same dose level **FQ 7l** decreased the bacterial load with 0.56 and 2.7-log10 protections in lung and spleen tissues respectively.

CHAPTER 6

NITROQUINOLONE (NQ) DERIVATIVES

6.1 SYNTHESIS

Various 1-(cyclopropyl/4-fluorophenyl/*t*-butyl)-1,4-dihydro-6-nitro-4-oxo-7-(sub secondary amino)quinoline-3-carboxylic acids were synthesized from 2,4-dichloro benzoic acid by the following steps of reaction:

STEP 1: Synthesis of 2,4-dichloro-5-nitrobenzoic acid (NQ 2)

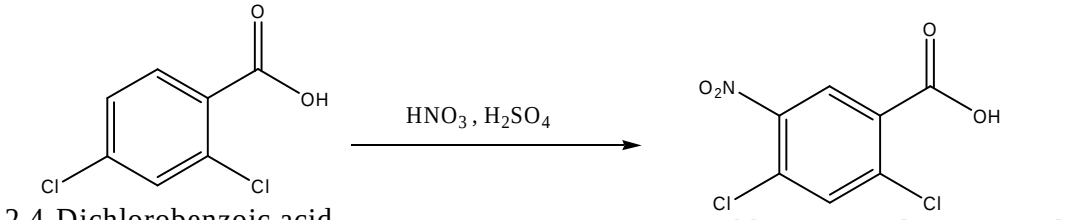

2,4-Dichlorobenzoic acid
NQ 1

2,4-Dichloro-5-nitrobenzoic acid
NQ 2

To a solution of 2,4-dichlorobenzoic acid (**NQ 1**) (1.00 equiv.) in 96 % sulfuric acid (40 ml), 65 % nitric acid (1.50 equiv.) was added slowly at 0 - 5 ºC and the resulting mixture was then stirred at room temperature for 1 hour. The mixture is then poured into ice-cold water and extracted with ethyl acetate (3 x 50 ml). The combined extracts were dried over magnesium sulphate and evaporated under reduced pressure to yield **NQ 2**.

Yield: 98 %; M.P.: 138 – 141 ºC; IR (KBr) cm^{-1}: 2900, 1726, 1470 - 1370; ^1H NMR (DMSO - d_6) δ ppm: 7.80 (s, 1H, ArH), 8.84 (s, 1H, ArH), 14.60 (s, 1H, COOH); Anal ($C_7H_3Cl_2NO_4$) C, H, N.

STEP 2: Synthesis of ethyl 3-(2,4-dichloro-5-nitrophenyl)-3-oxopropanoate (NQ 3)

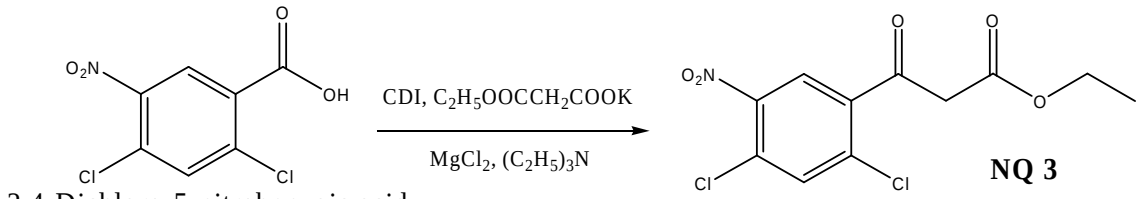

2,4-Dichloro-5-nitrobenzoic acid
NQ 2

NQ 3
Ethyl 3-(2,4-dichloro-5-nitrophenyl)-3-oxopropanoate

To a solution of **NQ 2** (1.00 equiv.) in tetrahydrofuran, CDI (1.20 equiv.) was added for 30 minutes at a temperature of 70 ºC. The resulting crude imidazolide was used without further purification in the next step. To a solution of potassium salt of ethyl malonate (1.30 equiv.) in acetonitrile was added drop wise magnesium chloride (2.00 equiv.) and triethyl amine (4.0 equiv.) at 0 ºC and stirred at room temperature for 2.5 h. To this solution, the imidazolide prepared above was added and the reaction mixture was refluxed at 70 ºC for 2.5 h. After completion of reaction, the solvent was distilled off and poured into ice water and acidified to pH 5-6 with 20 % HCl, then extracted with ethyl acetate (3 x 25 ml) and dried over magnesium sulphate and distilled the solvent to give **NQ 3**.

Yield: 82 %; M.P.: 141 – 143 ºC; IR (KBr) cm^{-1}: 2900, 1726, 1705, 1470 - 1370; ^1H NMR (DMSO - d_6) δ ppm: 1.45 (t, 3H, $-CH_2CH_3$), 3.40 (s, 2H, CH_2), 4.2 (m, 2H, $-CH_2CH_3$), 7.66 (s, 1H, ArH), 8.64 (s, 1H, ArH); Anal ($C_{11}H_9Cl_2NO_5$) C, H, N.

STEP 3: Synthesis of ethyl 1-(cyclopropyl/4-fluorophenyl/*t*-butyl)-7-chloro-1,4-dihydro-6-nitro-4-oxoquinoline-3-carboxylates (NQ 6a-c)

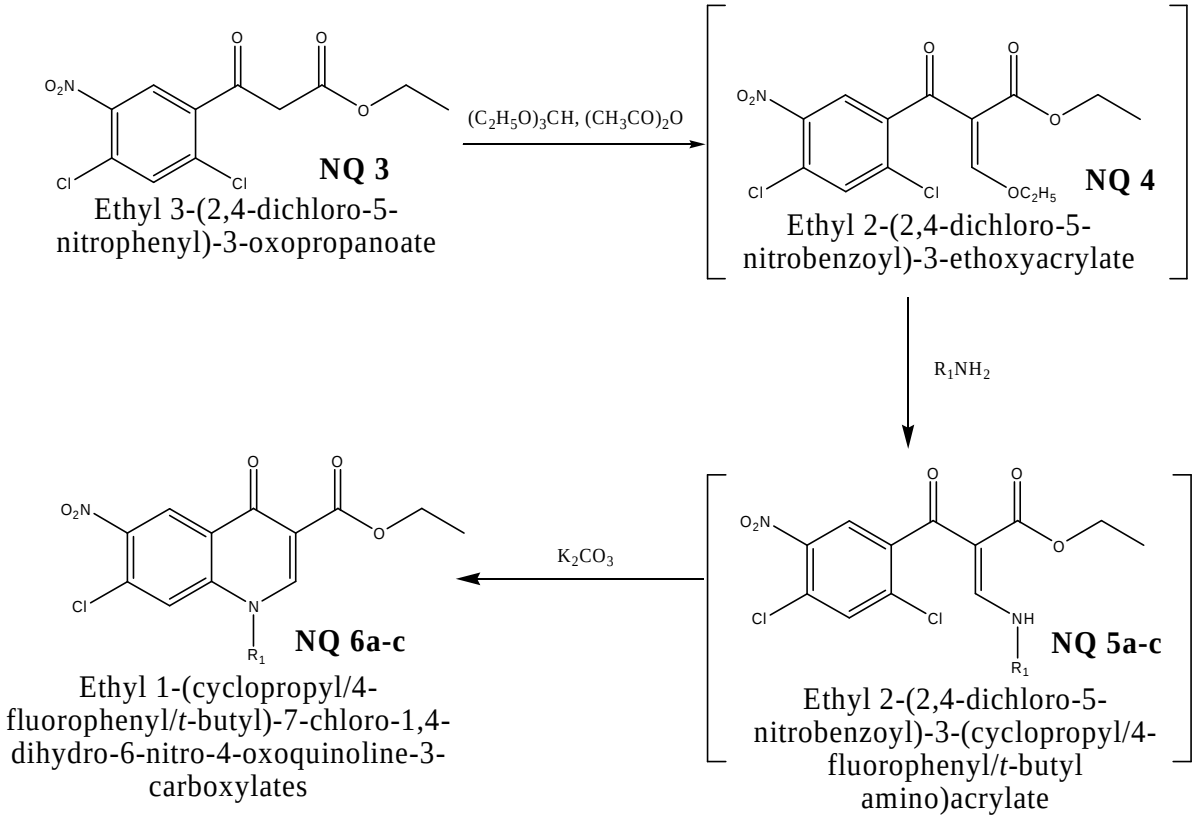

A mixture of **NQ 3** (1.00 equiv.), triethylorthoformate (1.50 equiv.) and acetic anhydride (2.50 equiv.) were refluxed at 140 ºC for 1 h. The ethyl acetate produced as a by product was distilled simultaneously under atmospheric pressure. After completion of reaction the reaction mixture was concentrated under reduced pressure to yield ethyl 2-(2,4-dichloro-5-nitrobenzoyl)-3-ethoxyacrylate (**NQ 4**). The above residue was dissolved in a mixture of ether (20 ml) and ethanol (20 ml). Added corresponding primary amine (1.10 equiv.) at 0 ºC and stirred for 30 minutes under nitrogen atmosphere, followed by distillation yielded ethyl 2-(2,4-dichloro-5-nitrobenzoyl)-3-(cyclopropyl/4-fluorophenyl/*t*-butyl amino)acrylate (**NQ 5a-c**). The above crude solid (1.00 equiv.) was dissolved in DMSO (30 ml) and added anhydrous potassium carbonate (1.60 equiv.) and refluxed at 60 ºC for 3 h. After completion of reaction, the mixture was diluted with ice cold water and neutralized with 20 % HCl to a pH of 5-6. The precipitate thus formed was filtered and washed with water followed by 30 % ethyl acetate : hexane mixture to yield ethyl 1-(substituted)-7-chloro-1,4-dihydro-6-nitro-4-oxoquinoline-3-carboxylates (**NQ 6a-c**).

Ethyl 1-cyclopropyl-7-chloro-1,4-dihydro-6-nitro-4-oxoquinoline-3-carboxylates (NQ 6a): Yield: 90 %; M.P.: > 280 ºC; IR (KBr) cm^{-1}: 2900, 1726, 1705, 1616, 1470 - 1370; ^1H NMR (DMSO - d_6) δ ppm: 0.28 - 0.44 (m, 4H, cyclopropyl), 1.36 (m, 1H, cyclopropyl), 1.45 (t, 3H, $-CH_2CH_3$), 4.2 (m, 2H, $-CH_2CH_3$), 8.3 (s, 1H, C_8 - H), 9.34 (s, 1H, C_5 - H), 9.52 (s, 1H, C_2 - H); Anal ($C_{13}H_9ClN_2O_5$) C, H, N.

Ethyl 1-(4-fluorophenyl)-7-methoxy-1,4-dihydro-6-nitro-4-oxoquinoline-3-carboxylates (NQ 6b): Yield: 92 %; M.P.: > 280 ºC; IR (KBr) cm^{-1}: 2900, 1726, 1705, 1616, 1470 - 1370; ^1H NMR (DMSO - d_6) δ ppm: 1.45 (t, 3H, $-CH_2CH_3$), 4.2 (m, 2H, $-CH_2CH_3$), 6.48 - 6.68 (m, 4H, Ar - H), 8.3 (s, 1H, C_8 - H), 9.34 (s, 1H, C_5 - H), 9.52 (s, 1H, C_2 - H); Anal ($C_{13}H_9ClN_2O_5$) C, H, N.

Ethyl 1-*t*-butyl-7-methoxy-1,4-dihydro-6-nitro-4-oxoquinoline-3-carboxylates (NQ 6c): Yield: 86 %; M.P.: 276 – 278 ºC; IR (KBr) cm^{-1}: 2900, 1726, 1705, 1616, 1470 - 1370; ^1H NMR (DMSO - d_6) δ ppm: 1.45 (t, 3H, $-CH_2CH_3$), 1.6 (s, 9H, *t*-butyl), 4.2 (m, 2H, $-CH_2CH_3$), 8.3 (s, 1H, C_8 - H), 9.34 (s, 1H, C_5 - H), 9.52 (s, 1H, C_2 - H); Anal ($C_{13}H_9ClN_2O_5$) C, H, N.

STEP 4: Synthesis of 1-(cyclopropyl/4-fluorophenyl/*t*-butyl)-7-chloro-1,4-dihydro-6-nitro-4-oxoquinoline-3-carboxylic acid (NQ 7a-c)

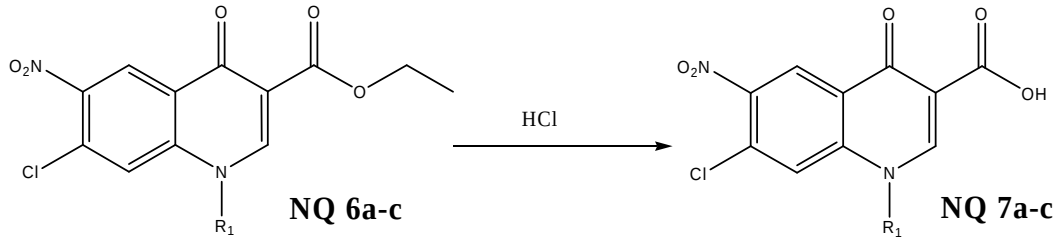

Ethyl 1-(cyclopropyl/4-fluorophenyl/*t*-butyl)-7-chloro-1,4-dihydro-6-nitro-4-oxoquinoline-3-carboxylates

1-(Cyclopropyl/4-fluorophenyl/*t*-butyl)-7-chloro-1,4-dihydro-6-nitro-4-oxoquinoline-3-carboxylic acid

Compound **NQ 6a-c** (1.00 equiv.) was suspended in 6N HCl (5 ml) and refluxed for 6 h and then cooled to 0 ºC. The precipitate obtained was filtered, washed with water followed by 20% ethyl acetate yielded **NQ 7a-c**.

7-Chloro-1-cyclopropyl-1,4-dihydro-6-nitro-4-oxoquinoline-3-carboxylic acid (NQ 7a): Yield: 82 %; M.P.: 249 – 251 ºC; IR (KBr) cm^{-1}: 2900, 1726, 1705, 1616, 1470 - 1370; ^1H NMR (DMSO - d_6) δ ppm: 0.28-0.44 (m, 4H, cyclopropyl), 1.36 (m, 1H,

cyclopropyl), 8.3 (s, 1H, C_8 - H), 9.34 (s, 1H, C_5 - H), 9.52 (s, 1H, C_2 - H), 14.60 (s, 1H, COOH); Anal ($C_{13}H_9ClN_2O_5$) C, H, N.

7-Chloro-1-(4-fluorophenyl)-1,4-dihydro-6-nitro-4-oxoquinoline-3-carboxylic acid (NQ 7b): Yield: 86 %; M.P.: > 280 ºC; IR (KBr) cm^{-1}: 2900, 1728, 1710, 1620, 1460 - 1370; ^1H NMR (DMSO - d_6) δ ppm: 6.48 - 6.68 (m, 4H, Ar - H), 8.3 (s, 1H, C_8 - H), 9.34 (s, 1H, C_5 - H), 9.54 (s, 1H, C_2 - H), 14.68 (s, 1H, COOH); Anal ($C_{16}H_8ClFN_2O_5$) C, H, N.

1-*t*-Butyl-7-chloro-1,4-dihydro-6-nitro-4-oxoquinoline-3-carboxylic acid (NQ 7c): Yield: 85 %; M.P.: 245 – 247 ºC; IR (KBr) cm^{-1}: 2900, 1726, 1705, 1620, 1470 - 1370; ^1H NMR (DMSO - d_6) δ ppm: 1.6 (s, 9H, *t*-butyl), 8.3 (s, 1H, C_8 - H), 9.34 (s, 1H, C_5 - H), 9.56 (s, 1H, C_2 - H), 14.6 (s, 1H, COOH); Anal ($C_{14}H_{13}ClN_2O_5$) C, H, N.

STEP 5: Synthesis of 1-(cyclopropyl/4-fluorophenyl/*t*-butyl)-1,4-dihydro-6-nitro-7-(substituted secondary amines)-4-oxoquinoline-3-carboxylic acid (NQ 8-10 a-p)

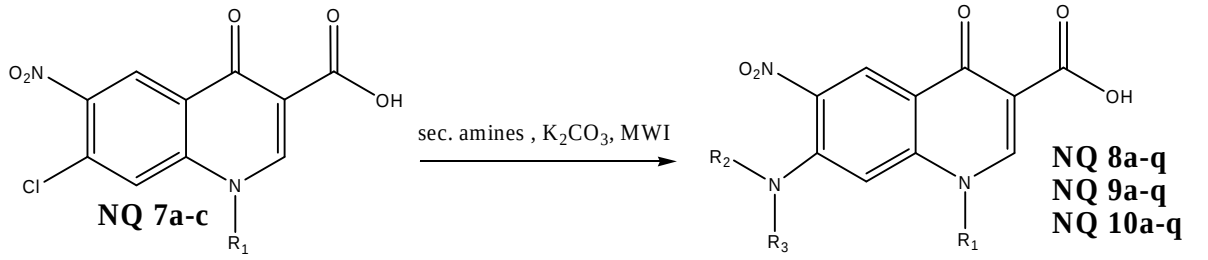

1-(Cyclopropyl/4-fluorophenyl/*t*-butyl)-1,4-dihydro-7-chloro-6-nitro-4-oxoquinoline-3-carboxylic acid

1-(Cyclopropyl/4-fluorophenyl/*t*-butyl)-1,4-dihydro-6-nitro-7-(substituted secondary amines)-4-oxoquinoline-3-carboxylic acid

Compound **NQ 7a-c** (1.0 equiv.) in dimethyl sulfoxide (2.5 ml) and appropriate secondary amines (1.1 equiv.) were irradiated in a microwave oven at an intensity of 80 % (560 watts) with 30 sec/cycle. The number of cycle in turn depended on the completion of the reaction, which was checked by TLC. The reaction timing varied from 1.5 - 3 min. After completion of the reaction, the mixture was poured into ice cold water and washed with water and isopropanol to give titled products.

Physical constants of the synthesized compounds are presented in table 6.1

Spectral and elemental analysis data of representative nitroquinolones (**NQ**) are presented in table 6.2.

6.2 *IN VITRO* ANTIMYCOBACTERIAL AND CYTOTOXICITY

The synthesized compounds were tested for antimycobacterial activities against *Mycobacterium tuberculosis*, multi-drug resistant *Mycobacterium tuberculosis* and *Mycobacterium smegmatis* by agar dilution method and the results are tabulated in table 6.3. The compounds were also tested for there cytotoxicity in mammalian vero cell lines and the results are tabulated in table 6.3.

6.3 *IN VIVO* ANTIMYCOBACTERIAL STUDY

One compound **NQ 8c** was tested in *in vivo* model against *M. tuberculosis* and the results are tabulated in table 6.4

6.4 DNA GYRASE SUPERCOILING ASSAY

Nine compounds were tested for DNA gyrase enzyme supercoiling assay and the results are tabulated in table 6.5. The gel picture of the enzyme inhibition study is shown in figure 6.1.

Table 6.1: Physical constants of nitroquinolones (NQ 8-10 a-p)

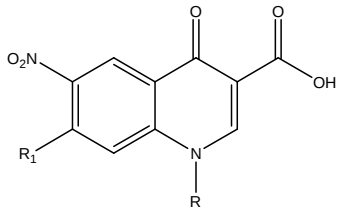

Compd	R	R_1	Yield (%)	M.P. (°C)	Molecular Formula	Molecular Weight	cLog P
NQ 8a	Cyclopropyl	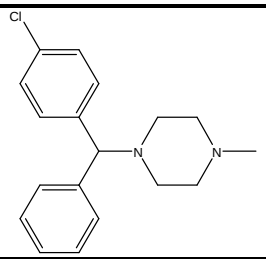	68	192-194	$C_{30}H_{27}ClN_4O_5$	559.01	2.91
NQ 9a	4-F-Phenyl	- do -	62	134-136	$C_{33}H_{26}ClFN_4O_5$	613.03	4.43
NQ 10a	*t*-Butyl	- do -	71	128-130	$C_{31}H_{31}ClN_4O_5$	575.05	3.79
NQ 8b	Cyclopropyl	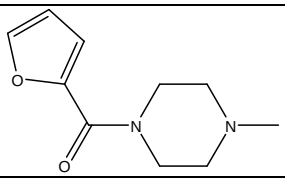	73	237-239	$C_{22}H_{20}N_4O_7$	562.03	0.93
NQ 9b	4-F-Phenyl	- do -	66	127-129	$C_{25}H_{19}FN_4O_7$	506.44	2.45
NQ 10b	*t*-Butyl	- do -	68	222-224	$C_{23}H_{24}N_4O_7$	468.46	1.81
NQ 8c	Cyclopropyl	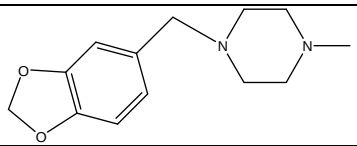	73	148-150	$C_{25}H_{24}N_4O_7$	492.48	0.81
NQ 9c	4-F-Phenyl	- do -	80	108-110	$C_{28}H_{23}FN_4O_7$	546.50	2.34
NQ 10c	*t*-Butyl	- do -	71	182-184	$C_{26}H_{28}N_4O_7$	508.52	1.69
NQ 8d	Cyclopropyl	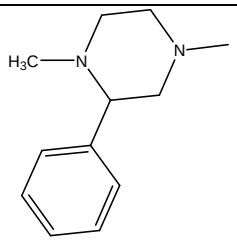	69	198-200	$C_{24}H_{24}N_4O_5$	448.47	0.62
NQ 9d	4-F-Phenyl	- do -	80	126-128	$C_{27}H_{23}FN_4O_5$	502.49	2.14
NQ 10d	*t*-Butyl	- do -	67	147-149	$C_{19}H_{24}N_4O_5$	388.42	-0.06
NQ 8e	Cyclopropyl	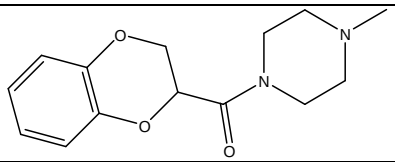	70	134-136	$C_{26}H_{24}N_4O_8$	520.49	2.19
NQ 9e	4-F-Phenyl	- do -	83	70-72	$C_{29}H_{23}FN_4O_8$	574.51	3.72
NQ 10e	*t*-Butyl	- do -	71	231-233	$C_{27}H_{28}N_4O_8$	536.53	3.08

Table 6.1: Physical constants of nitroquinolones (NQ 8-10 a-p) (contd…)

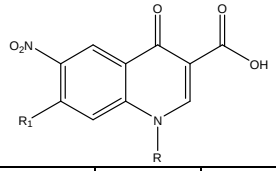

Compd	R	R_1	Yield (%)	M.P. (°C)	Molecular Formula	Molecular Weight	cLog P
NQ 8f	Cyclopropyl	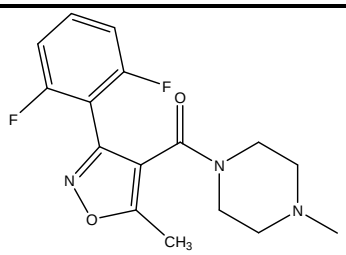	70	241-243	$C_{28}H_{23}F_2N_5O_7$	579.51	2.91
NQ 9f	4-F-Phenyl	- do -	84	223-225	$C_{31}H_{22}F_3N_5O_7$	633.53	4.43
NQ 10f	*t*-Butyl	- do -	81	> 250	$C_{29}H_{27}F_2N_5O_7$	595.55	3.79
NQ 8g	Cyclopropyl	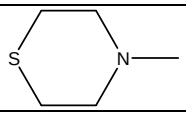	77	208-210	$C_{17}H_{17}N_3O_5S$	375.4	2.76
NQ 9g	4-F-Phenyl	- do -	81	114-116	$C_{20}H_{16}FN_3O_5S$	429.42	4.28
NQ 10g	*t*-Butyl	- do -	71	> 250	$C_{18}H_{21}N_3O_5S$	391.44	3.64
NQ 8h	Cyclopropyl	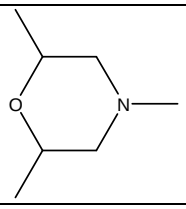	73	172-174	$C_{19}H_{21}N_3O_6$	387.39	2.80
NQ 9h	4-F-Phenyl	- do -	84	103-105	$C_{22}H_{20}FN_3O_6$	441.41	4.33
NQ 10h	*t*-Butyl	- do -	74	108-110	$C_{20}H_{25}N_3O_6$	403.43	3.69
NQ 8i	Cyclopropyl	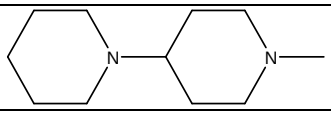	74	173-175	$C_{23}H_{28}N_4O_5$	440.49	1.002
NQ 9i	4-F-Phenyl	- do -	81	106-108	$C_{26}H_{27}FN_4O_5$	494.51	2.53
NQ 10i	*t*-Butyl	- do -	78	156-158	$C_{24}H_{32}N_4O_5$	456.03	1.89
NQ 8j	Cyclopropyl	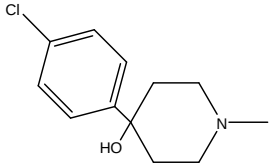	70	197-199	$C_{24}H_{22}ClN_3O_6$	483.9	3.79
NQ 9j	4-F-Phenyl	- do -	76	145-147	$C_{27}H_{21}ClFN_3O_6$	537.92	5.31
NQ 10j	*t*-Butyl	- do -	75	127-129	$C_{25}H_{26}ClN_3O_6$	499.94	4.67
NQ 8k	Cyclopropyl	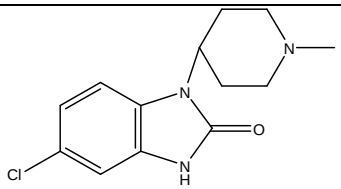	67	209-210	$C_{24}H_{21}ClN_6O_6$	524.91	3.68
NQ 9k	4-F-Phenyl	- do -	78	181-183	$C_{28}H_{21}ClFN_5O_6$	577.95	6.04
NQ 10k	*t*-Butyl	- do -	69	>250	$C_{25}H_{25}ClN_6O_6$	540.96	4.56

Table 6.1: Physical constants of nitroquinolones (NQ 8-10 a-p) (contd…)

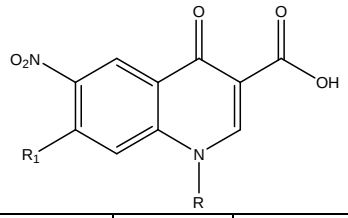

Compd	R	R_1	Yield (%)	M.P. (°C)	Molecular Formula	Molecular Weight	cLog P
NQ 8l	Cyclopropyl	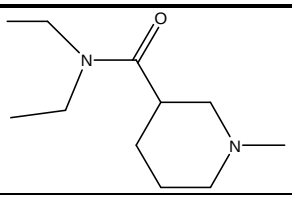	72	174-176	$C_{23}H_{28}N_4O_6$	456.49	3.23
NQ 9l	4-F-Phenyl	- do -	73	75-77	$C_{26}H_{27}FN_4O_6$	510.51	4.75
NQ 10l	*t*-Butyl	- do -	70	152-154	$C_{24}H_{32}N_4O_6$	472.53	4.11
NQ 8m	Cyclopropyl	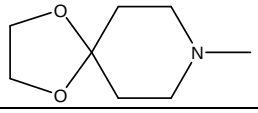	64	182-184	$C_{20}H_{21}N_3O_7$	415.4	1.84
NQ 9m	4-F-Phenyl	- do -	69	110-112	$C_{23}H_{20}FN_3O_7$	469.42	3.37
NQ 10m	*t*-Butyl	- do -	71	136-138	$C_{20}H_{21}N_3O_7$	431.44	2.73
NQ 8n	Cyclopropyl	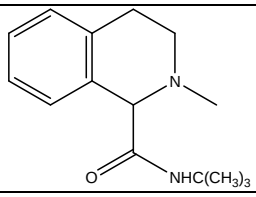	75	206-208	$C_{27}H_{28}N_4O_6$	504.53	3.99
NQ 9n	4-F-Phenyl	- do -	82	112-114	$C_{30}H_{27}FN_4O_6$	558.56	5.51
NQ 10n	*t*-Butyl	- do -	72	135-137	$C_{28}H_{32}N_4O_6$	520.58	4.87
NQ 8o	Cyclopropyl	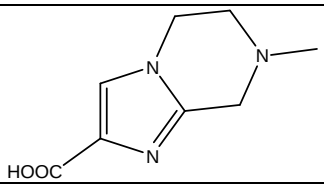	78	210-212	$C_{20}H_{17}N_5O_7$	439.38	2.29
NQ 9o	4-F-Phenyl	- do -	84	179-181	$C_{23}H_{16}N_5O_7$	493.4	3.82
NQ 10o	*t*-Butyl	- do -	72	> 250	$C_{21}H_{21}N_5O_7$	455.42	3.18
NQ 8p	Cyclopropyl	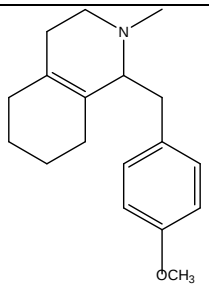	71	208-210	$C_{30}H_{31}N_3O_5$	513.58	7.04
NQ 9p	4-F-Phenyl	- do -	76	114-116	$C_{33}H_{30}FN_3O_6$	583.61	7.98
NQ 10p	*t*-Butyl	- do -	73	69-71	$C_{31}H_{35}N_3O_6$	545.63	7.34

Table 6.2: Spectral data and elemental analysis data of representative nitroquinolone (NQ) derivatives

Compd	IR Spectroscopy (cm^{-1}; KBr)	^1H NMR (δ ppm, DMSO - d_6)	Elemental Analyses (Calculated/Found)		
			C	H	N
NQ 8a	2900, 1724, 1708, 1620, 1460 - 1370	0.28 - 0.48 (m, 4H, cyclopropyl), 1.35 (m, 1H, cyclopropyl), 2.59 - 3.12 (m, 8H, 4 CH_2 of piperazine), 4.2 (s, 1H, CH of diphenylmethyl), 7.0 - 7.18 (m, 9H, Ar-H), 8.32 (s, 1H, C_8 - H), 9.34 (s, 1H, C_5 - H), 9.56 (s, 1H, C_2 - H), 14.6 (s, 1H, COOH)	64.46 64.19	4.87 4.85	10.02 10.06
NQ 9b	2890, 1724, 1710, 1624, 1460 - 1360	3.16 - 3.3 (m, 8H, 4 CH_2 of piperazine), 6.5 - 7.68 (m, 7H, Ar - H), 8.34 (s, 1H, C_8 - H), 9.32 (s, 1H, C_5 - H), 9.56 (s, 1H, C_2 - H), 14.6 (s, 1H, COOH)	59.29 59.00	3.78 3.79	11.06 11.00
NQ 10c	3250, 2890, 1724, 1710, 1624, 1464 - 1360	1.76 (s, 9H, *t*-butyl), 2.82 - 3.12 (m, 8H, 4 CH_2 of piperazine), 3.6 (s, 2H, CH_2 of piperanoyl), 5.86 (s, 2H, -OCH_2O-), 6.42 - 6.62 (m, 3H, Ar - H), 8.34 (s, 1H, C_8 - H), 9.34 (s, 1H, C_5 - H), 9.56 (s, 1H, C_2 - H), 14.6 (s, 1H, COOH)	61.41 61.01	5.55 5.56	11.02 11.06
NQ 8d	2890, 1724, 1710, 1620, 1460 - 1368	0.28 - 0.52 (m, 4H, cyclopropyl), 1.38 (m, 1H, cyclopropyl), 2.2 (s, 3H, CH_3), 2.6 (t, 2H, 5-CH_2 of piperazine), 3.15 (t, 2H, 6-CH_2 of piperazine), 3.4 (d, 2H, 2 CH_2 of piperazine), 4.12 (t, 1H, 3-CH of piperazine), 7.0 - 7.2 (m, 5H, Ar - H), 8.34 (s, 1H, C_8 - H), 9.32 (s, 1H, C_5 - H), 9.56 (s, 1H, C_2 - H), 14.4 (s, 1H, COOH)	64.28 64.55	5.39 5.36	12.49 12.40
NQ 9e	2890, 1724, 1710, 1624, 1460 - 1360	3.26 - 3.4 (m, 8H, 4 CH_2 of piperazine), 4.6 (d, 2H, 3-CH_2 of dihydrobenzodioxinyl), 5.14 (t, 1H, 2-CH of dihydrobenzodioxinyl), 6.5 - 6.98 (m, 8H, Ar - H), 8.34 (s, 1H, C_8 - H), 9.3 (s, 1H, C_5 - H), 9.56 (s, 1H, C_2 - H), 14.6 (s, 1H, COOH)	60.63 60.44	4.04 3.99	9.75 9.70
NQ 10f	2890, 1724, 1710, 1624, 1464 - 1360, 1208	1.74 (s, 9H, *t*-butyl), 2.3 (s, 3H, 5-CH_3 of isoxazolyl), 3.12 - 3.28 (m, 8H, 4 CH_2 of piperazine), 6.82 - 7.08 (m, 3H, Ar - H), 8.34 (s, 1H, C_8 - H), 9.32 (s, 1H, C_5 - H), 9.54 (s, 1H, C_2 - H), 14.6 (s, 1H, COOH)	58.49 58.36	4.57 4.55	11.76 11.73
NQ 8g	2890, 1724, 1710, 1620, 1460 - 1368	0.28 - 0.54 (m, 4H, cyclopropyl), 1.36 (m, 1H, cyclopropyl), 2.64 - 3.4 (m, 8H, 4 CH_2 of thiomorpholine), 8.34 (s, 1H, C_8 - H), 9.32 (s, 1H, C_5 - H), 9.56 (s, 1H, C_2 - H), 14.4 (s, 1H, COOH)	54.39 54.36	4.56 4.58	11.19 11.13
NQ 9h	2892, 1724, 1710, 1628, 1460 - 1360	1.2 (d, 6H, 2 CH_3 of morpholino), 3.0 (d, 4H, 2 CH_2 of morpholine), 3.9 (m, 2H, 2 CH of morpholine), 6.4 - 6,7 (m, 4H, Ar - H), 8.34 (s, 1H, C_8 - H), 9.3 (s, 1H, C_5 - H), 9.56 (s, 1H, C_2 - H), 14.6 (s, 1H, COOH)	59.86 59.99	4.57 4.51	9.52 9.52

Table 6.2: Spectral data and elemental analysis data of representative nitroquinolone (NQ) derivatives (contd…)

Compd	IR Spectroscopy (cm^{-1}; KBr)	^{1}H NMR (δ ppm, DMSO-d_6)	Elemental Analyses (Calculated/Found)		
			C	H	N
NQ 10i	2890, 1724, 1710, 1624, 1464 - 1360	1.5 - 1.6 (m, 10H, 5 CH_2), 1.78 (s, 9H, *t*-butyl), 2.2 (t, 4H, 2 CH_2), 2.7 (m, 1H, CH), 2.8 (t, 4H, 2 CH_2), 8.34 (s, 1H, C_8 - H), 9.32 (s, 1H, C_5 - H), 9.54 (s, 1H, C_2 - H), 14.6 (s, 1H, COOH)	63.14 63.22	7.06 7.05	12.27 12.28
NQ 8j	2900, 1724, 1708, 1620, 1460 - 1370	0.28 - 0.46 (m, 4H, cyclopropyl), 1.32 (m, 1H, cyclopropyl), 2.0 - 2.7 (m, 8H, 4 CH_2 of piperidine), 7.1 - 7.18 (m, 4H, Ar - H), 8.34 (s, 1H, C_8 - H), 9.30 (s, 1H, C_5 - H), 9.56 (s, 1H, C_2 - H), 10.0 (bs, 1H, OH), 14.6 (s, 1H, COOH)	59.57 59.01	4.58 4.57	8.68 8.69
NQ 9k	3110, 2896, 1728, 1712, 1710, 1624, 1460 - 1360	1.6 - 2.4 (m, 8H, 4 CH_2 of piperidine), 4.1 (bm, 1H, CH of piperidine), 6.4 - 6.9 (m, 7H, Ar - H), 8.34 (s, 1H, C_8 - H), 9.26 (s, 1H, C_5 - H), 9.56 (s, 1H, C_2 - H), 10.8 (s, 1H, NH), 14.6 (s, 1H, COOH)	58.19 58.10	3.66 3.66	12.12 12.14
NQ 10l	2890, 1724, 1710, 1624, 1464 - 1360, 1208	1.2 (t, 6H, 2 CH_3 of ethyl), 1.7 (s, 9H, *t*-butyl), 1.78 - 2.7 (m, 9H, H of piperidine), 3.24 (q, 4H, 2 CH_2 of ethyl), 8.32 (s, 1H, C_8 - H), 9.28 (s, 1H, C_5 - H), 9.54 (s, 1H, C_2 - H), 14.6 (s, 1H, COOH)	61.00 61.30	6.83 6.89	11.86 11.80
NQ 8m	2890, 1724, 1712, 1618, 1466 - 1368	0.28 - 0.52 (m, 4H, cyclopropyl), 1.38 (m, 1H, cyclopropyl), 1.78 - 2.4 (m, 8H, 4 CH_2 of azaspirodecane), 3.96 (m, 4H, 2 CH_2 of azaspirodecane), 8.32 (s, 1H, C_8 - H), 9.30 (s, 1H, C_5 - H), 9.56 (s, 1H, C_2 - H), 14.4 (s, 1H, COOH)	57.83 57.80	5.10 5.14	10.12 10.16
NQ 9n	2890, 1724, 1712, 1626, 1468 - 1360	1.3 (s, 9H, 3 CH_3), 2.66 - 2.9 (m, 4H, 2 CH_2 of isoquinoline), 4.85 (s, 1H, CH of isoquinoline), 6.7 - 7.1 (m, 8H, Ar - H), 8.32 (s, 1H, C_8 - H), 9.28 (s, 1H, C_5 - H), 9.56 (s, 1H, C_2 - H), 10.2 (s, 1H, NH), 14.6 (s, 1H, COOH)	64.51 64.20	4.87 4.89	10.03 10.07
NQ 10o	3200, 2890, 1724, 1710, 1624, 1464 - 1360, 1208	1.74 (s, 9H, *t*-butyl), 3.1 - 3.8 (m, 6H, 3 CH_2), 7.6 (s, 1H, CH), 8.32 (s, 1H, C_8 - H), 9.32 (s, 1H, C_5 - H), 9.54 (s, 1H, C_2 - H), 12.12 (s, 1H, 2-COOH), 14.6 (s, 1H, 3-COOH)	55.38 55.60	4.65 4.63	15.38 15.40
NQ 8p	3210, 2890, 1724, 1710, 1620, 1460 - 1368	0.28 - 0.54 (m, 4H, cyclopropyl), 1.36 (m, 1H, cyclopropyl), 1.6 - 1.95 (m, 8H, 4 CH_2 of isoquinolinyl), 2.2-3.4 (m, 7H, 2 CH_2 and 1 CH of isoquinolinyl, and CH_2), 3.73 (s, 3H, -OCH_3), 6.8 - 7.1 (m, 4H, Ar - H), 8.34 (s, 1H, C_8 - H), 9.32 (s, 1H, C_5 - H), 9.56 (s, 1H, C_2 - H), 14.4 (s, 1H, COOH)	68.04 68.65	5.90 5.98	7.93 7.90

Table 6.3: *In vitro* antimycobacterial and cytotoxicity data of nitroquinolones (NQ 8-10 a-p)

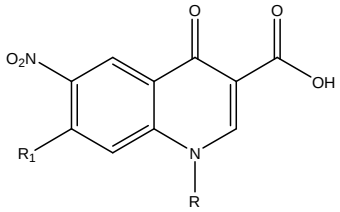

Compd	R	R_1	CC_{50} (μM)	MIC (μM)		
				MTB	MDR-TB	MC^2
NQ 8a	Cyclopropyl	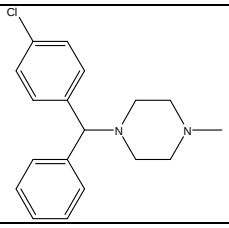	NT	5.59	NT	5.59
NQ 9a	4-F-Phenyl	- do -	NT	10.19	NT	40.78
NQ 10a	*t*-Butyl	- do -	NT	5.44	NT	10.87
NQ 8b	Cyclopropyl	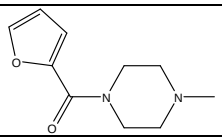	111.2	0.69	0.34	1.39
NQ 9b	4-F-Phenyl	- do -	NT	6.18	NT	24.68
NQ 10b	*t*-Butyl	- do -	NT	6.68	NT	13.34
NQ 8c	Cyclopropyl	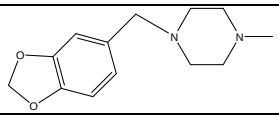	126.9	0.08	0.16	0.79
NQ 9c	4-F-Phenyl	- do -	NT	2.85	0.71	22.87
NQ 10c	*t*-Butyl	- do -	NT	3.07	1.53	24.58
NQ 8d	Cyclopropyl	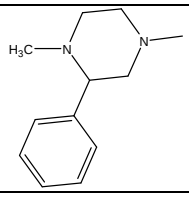	136.36	0.20	0.20	0.87
NQ 9d	4-F-Phenyl	- do -	NT	6.23	NT	24.88
NQ 10d	*t*-Butyl	- do -	NT	16.09	NT	64.36
NQ 8e	Cyclopropyl	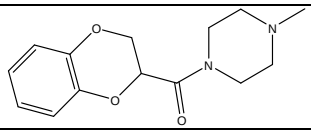	NT	2.99	6.01	12.01
NQ 9e	4-F-Phenyl	- do -	54.39	2.72	0.68	10.88
NQ 10e	*t*-Butyl	- do -	NT	5.83	NT	23.29
NQ 8f	Cyclopropyl	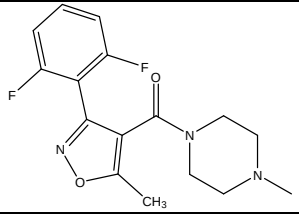	NT	2.69	2.69	10.79
NQ 9f	4-F-Phenyl	- do -	NT	4.94	NT	19.73
NQ 10f	*t*-Butyl	- do -	104.9	2.62	0.65	10.49

Table 6.3: *In vitro* antimycobacterial and cytotoxicity data of nitroquinolones (NQ 8-10 a-p) (contd...)

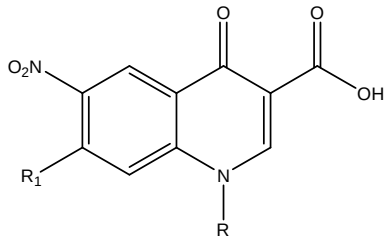

Compd	R	R_1	CC_{50} (μM)	MIC (μM)		
				MTB	MDR-TB	MC^2
NQ 8g	Cyclopropyl	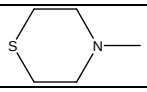	NT	4.17	NT	33.29
NQ 9g	4-F-Phenyl	- do -	NT	14.55	NT	29.11
NQ 10g	*t*-Butyl	- do -	NT	7.99	NT	31.93
NQ 8h	Cyclopropyl	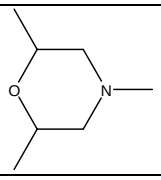	NT	2.01	4.03	8.08
NQ 9h	4-F-Phenyl	- do -	70.79	3.53	1.77	14.16
NQ 10h	*t*-Butyl	- do -	NT	7.76	NT	30.98
NQ 8i	Cyclopropyl	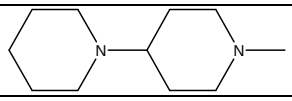	141.9	0.43	0.43	1.77
NQ 9i	4-F-Phenyl	- do -	NT	6.33	NT	25.28
NQ 10i	*t*-Butyl	- do -	NT	6.86	NT	27.41
NQ 8j	Cyclopropyl	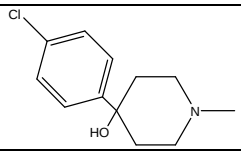	129.2	0.81	0.39	3.22
NQ 9j	4-F-Phenyl	- do -	NT	5.82	NT	23.24
NQ 10j	*t*-Butyl	- do -	NT	6.26	NT	25.00
NQ 8k	Cyclopropyl	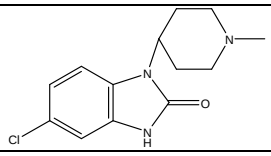	NT	1.49	2.97	2.97
NQ 9k	4-F-Phenyl	- do -	NT	5.42	NT	43.26
NQ 10k	*t*-Butyl	- do -	NT	5.79	NT	23.11
NQ 8l	Cyclopropyl	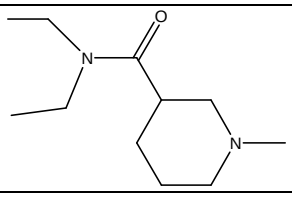	NT	3.42	3.42	6.86
NQ 9l	4-F-Phenyl	- do -	NT	6.13	NT	24.49
NQ 10l	*t*-Butyl	- do -	NT	6.62	NT	26.45

Table 6.3: *In vitro* antimycobacterial and cytotoxicity data of nitroquinolones (NQ 8-10 a-p) (contd...)

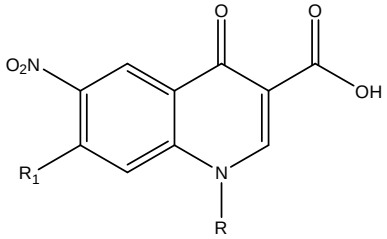

Compd	R	R_1	CC_{50} (µM)	MIC (µM)		
				MTB	MDR-TB	MC^2
NQ 8m	Cyclopropyl	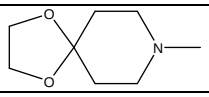	NT	3.76	1.88	15.05
NQ 9m	4-F-Phenyl	- do -	NT	6.67	NT	26.63
NQ 10m	*t*-Butyl	- do -	NT	7.45	NT	28.97
NQ 8n	Cyclopropyl	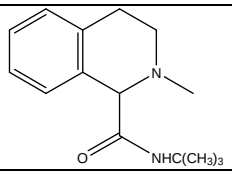	NT	1.55	1.55	3.09
NQ 9n	4-F-Phenyl	- do -	NT	5.60	NT	22.38
NQ 10n	*t*-Butyl	- do -	NT	12.01	NT	24.01
NQ 8o	Cyclopropyl	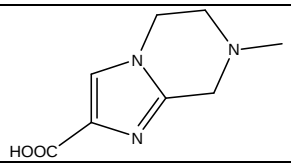	142.2	1.78	0.43	7.12
NQ 9o	4-F-Phenyl	- do -	NT	12.67	NT	50.67
NQ 10o	*t*-Butyl	- do -	NT	6.87	NT	54.89
NQ 8p	Cyclopropyl	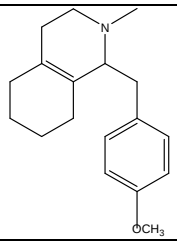	NT	3.04	NT	24.34
NQ 9p	4-F-Phenyl	- do -	NT	5.36	NT	21.42
NQ 10p	*t*-Butyl	- do -	NT	5.74	NT	22.91
Gatifloxacin	-	-	>155.3	1.04	8.34	2.08
INH	-	-	>455.8	0.36	45.57	45.57

Table 6.4: *In vivo* activity data of NQ 8c, gatifloxacin and isoniazid against *M. tuberculosis* ATCC 35801 in mice.

Compound	Lungs (log CFU ± SEM)	Spleen (log CFU ± SEM)
Control	7.99 ± 0.16	9.02 ± 0.21
Gatifloxacin (50 mg/kg)	6.02 ± 0.23	6.92 ± 0.07
Isoniazid (25 mg/kg)	5.86 ± 0.23	4.71 ± 0.10
NQ 8c (50 mg/kg)	5.21 ± 0.17	4.87 ± 0.13

Table 6.5: IC_{50} values for DNA gyrase inhibition of nitroquinolones (NQ)

Compounds	IC_{50} (μM)
NQ 8b	53.38
NQ 8c	60.92
NQ 8d	66.89
NQ 8i	68.11
NQ 8j	61.99
NQ 8k	57.15
NQ 8n	59.46
NQ 9e	34.81
NQ 9h	45.31
NQ 10a	8.69
NQ 10b	42.69
NQ 10f	50.37
Ciprofloxacin	15.09
Moxifloxacin	12.46

6.5 PHOTOTOXICITY EVALUATION

Three compounds were evaluated for potential phototoxicity in a standardized *in vivo* test system and the results are tabulated in table 6.6.

6.6 QUANTUM MECHANICAL MODELING

In the present study the HOMO and LUMO surfaces were visualized for the titled compounds for comparison (Figure 6.2)

Table 6.6: Phototoxicity evaluation of nitroquinolones (NQ)

Group	Ear thickness (mm)[a]						Erythema[b]					
	Time (approximately) after start of irradiation (h)[c]											
	0	4	24	48	72	96	0	4	24	48	72	96
Control[d]	0.37 ± 0.03	0.36 ± 0.02	0.38 ± 0.03	0.37 ± 0.03	0.37 ± 0.03	0.38 ± 0.03	0	0	0	0	0	0
NQ 8c	0.25 ± 0.01	0.27 ± 0.01	0.28 ± 0.003	0.28 ± 0.01	0.31 ± 0.01[#]	0.29 ± 0.02	0	0	0	0	0	0
NQ 8d	0.30 ± 0.02	0.31 ± 0.02	0.30 ± 0.01	0.32 ± 0.02	0.32 ± 0.01	0.34 ± 0.02	0	0	2[e]	0	0	0
NQ 8i	0.24 ± 0.01	0.26 ± 0.02	0.26 ± 0.01	0.26 ± 0.01	0.29 ± 0.01[#]	0.28 ± 0.01[#]	0	0	0	0	3	0
Lomefloxacin	0.31 ± 0.01	0.40 ± 0.02[*#]	0.48 ± 0.02[*#]	0.53 ± 0.02[*#]	0.64 ± 0.04[*#]	0.60 ± 0.06[*#]	0	6	6	6	6	6

[a] Mean Ear Thickness ± SEM; left and right ears were averaged
[b] Number of mice with erythema
[c] Time zero = pre-dose (mice exposed to UVA light immediately after dosing); 4 h = end of irradiation period.
[d] Control = 0.5% aqueous solution of sodium carboxymethylcellulose (4 Ns/m^2) dosed at 10 mL/kg.
[e] Very slight erythema, not considered to be drug-related.
[*] Mean Ear Thickness ± SEM; significant difference from control at $P < 0.05$.
[#] Mean Ear Thickness ± SEM; significant difference from 0 h at $P < 0.05$.

2 a.

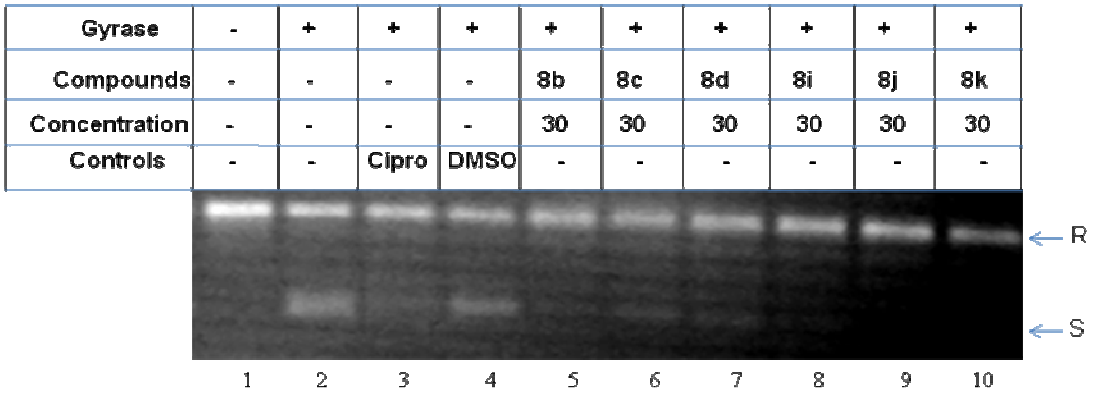

2 b.

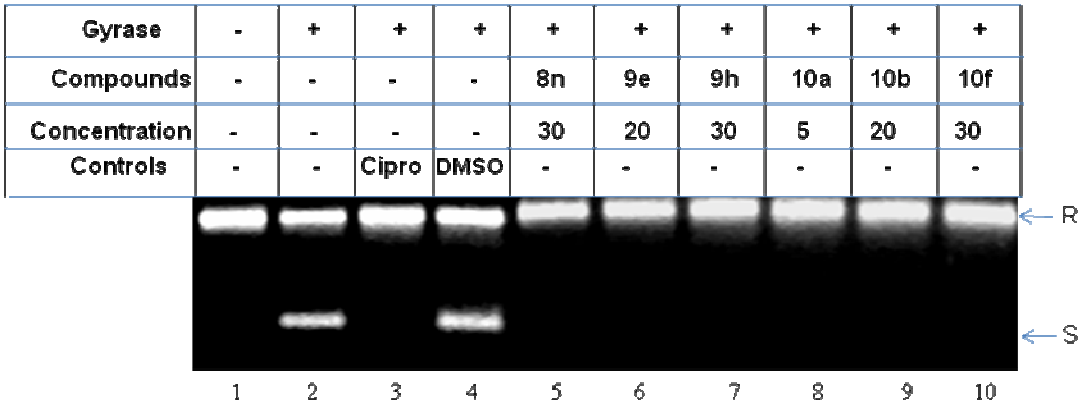

Figure 6.1: Gel picture for DNA gyrase supercoiling assay of nitroquinolones (**NQ**). The assays were performed as described in experimental section. DNA gyrase was incubated with indicated concentrations of the compounds before the addition of rest of the components.
(a) Lane 1: relaxed DNA, lane 2: supercoiling reaction, lane 3: supercoiling reaction in presence of 5 % DMSO. Ciprofloxacin at concentration of 10 µg/ml (lane 4) was used as the positive control for inhibition of enzyme. Lanes 5 to 10 have 30 µg/ml concentrations of compounds **NQ 8b, NQ 8c, NQ 8d, NQ 8i, NQ 8j, NQ 8k** respectively.
(b) Lane 1: relaxed DNA, lane 2: supercoiling reaction, lane 3: supercoiling reaction in presence of 5 % DMSO. Ciprofloxacin at concentration of 10 µg/ml (lane 4) was used as the positive control for inhibition of enzyme. Lane 5: 30 µg/ml **NQ 8n**, lane 6: 20 µg/ml **NQ 9e**, lane7: 30 µg/ml **NQ 9h**, lane 8: 5 µg/ml **NQ 10a**, lane 9: 20 µg/ml **NQ 10b** and lane 10: 30 µg/ml **NQ 10f**. R and S indicate relaxed and supercoiled pUC18 DNA respectively.

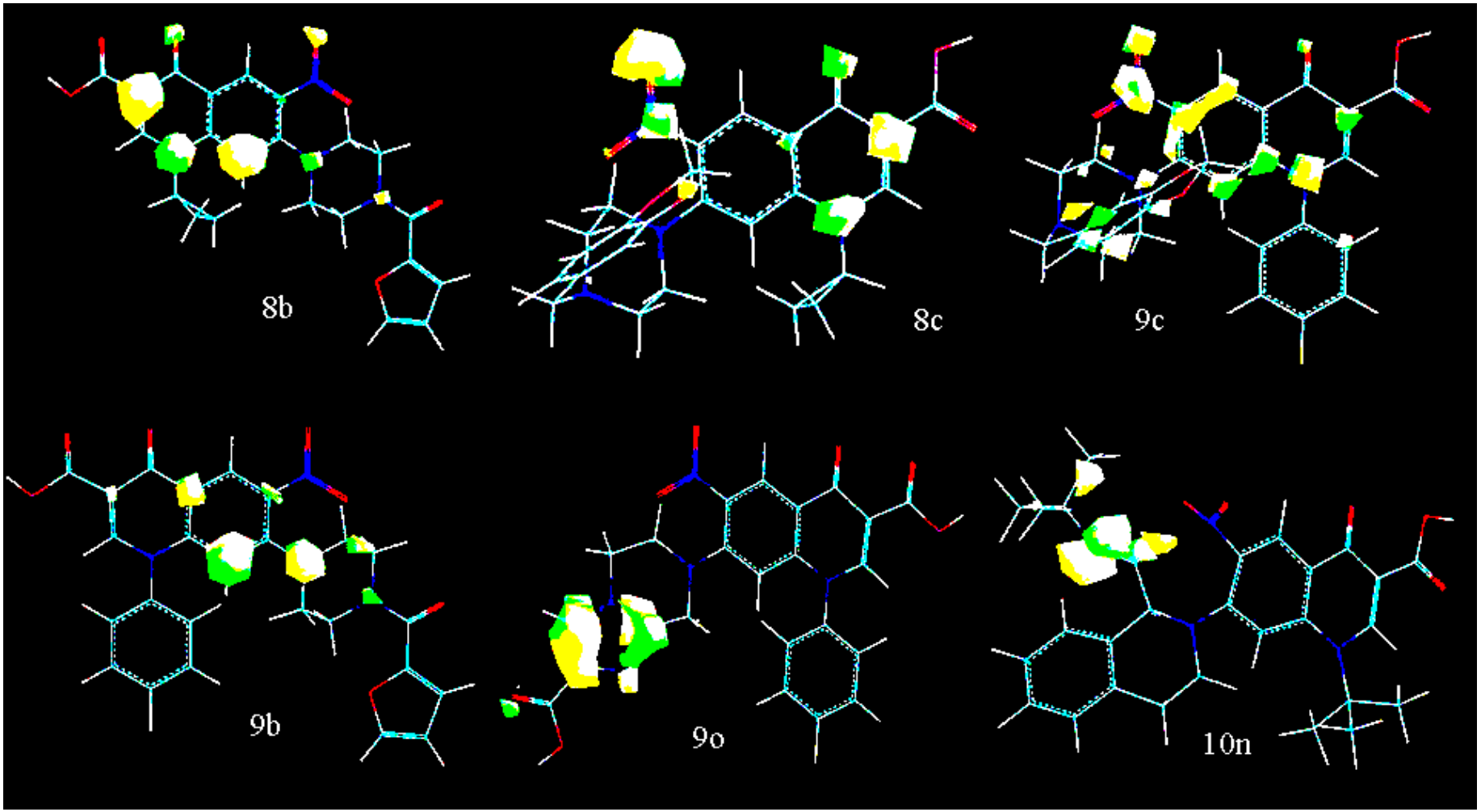

Figure 6.2: HOMO surface visualization (Contour value = 0.05) of some representative of nitroquinolones (**NQ**) in opaque mode. The colors indicate the phase of the orbital in space (green for positive and yellow for negative).

6.7 DISCUSSION

The synthesis of forty eight 6-nitroquinolone (**NQ 8-10a-p)** is outlined in figure 4.2. The 2,4-dichlorobenzoic acid (**NQ 1**) was converted to 2,4-dichloro-5-nitrobenzoic acid (**NQ 2**) by treatment with nitric acid in presence of sulphuric acid at 0-5 ºC. Compound **NQ 2** on reaction with 1,1'-carbonyldiimidazole (CDI) in tetrahydrofuran afforded the corresponding imidazolide, which, in-situ was treated with neutral magnesium salt of ethyl potassium malonate in presence of tri-ethyl amine to yield ethyl 3-(2,4-dichloro-5-nitrophenyl)-3-oxopropanoate (**NQ 3**). Ethyl 1-(cyclopropyl/4-fluorophenyl/*t*-butyl)-7-chloro-1,4-dihydro-6-nitro-4-oxoquinoline-3-carboxylates (**NQ 6a-c**) were prepared by a three-step one-pot reaction. First treatment of the keto ester **NQ 3** with triethyl orthoformate in acetic anhydride gave the one-carbon homologue enol ether intermediate ethyl 2-(2,4-dichloro-5-nitrobenzoyl)-3-ethoxyacrylate (**NQ 4**), which upon evaporation to dryness was allowed to react with slight excess of appropriate amines under nitrogen atmosphere in a mixture of ether and ethanol at 0 °C gave the enamino ester ethyl 2-(2,4-dichloro-5-nitrobenzoyl)-3-(cyclopropyl/4-fluorophenyl/*t*-butyl amino)acrylate (**NQ 5a-c**), and base catalyzed cyclization of **NQ 5a-c** with potassium carbonate in DMSO yielded quinolones **NQ 6a-c**. Ethyl esters were finally hydrolyzed in acidic condition to yield 1-(cyclopropyl/4-fluorophenyl/*t*-butyl)-7-chloro-1,4-dihydro-6-nitro-4-oxoquinoline-3-carboxylic acid (**NQ 7a-c**). The titled compounds **NQ 8-10a-p** was prepared by treating **NQ 7a-c** with appropriate secondary amines under microwave irradiation in DMSO. When compared to conventional method [Chu, D. T. W., *et al.*, 1985] of 24 hours process, microwave assisted synthesis was performed with short reaction times (2 - 3 minutes), with ease and was environment friendly. The over all yield of the synthesized compounds were in the range of 62 - 84 %. The purity of the synthesized compounds was monitored by TLC and elemental analyses and the structures were identified by spectral data.

In general, IR spectra showed C=O stretching peak of carboxylic acid at 1720 - 1730 cm^{-1}; C=O stretching peak of pyridine carbonyl at 1620 - 1630 cm^{-1} and absorption of aryl nitro group at 1470 - 1370 cm^{-1}. In the ^{1}H NMR spectra the signals of the respective protons of the prepared derivatives were verified on the basis of their chemical shifts, multiplicities and

coupling constants. The spectra showed a broad singlet at δ 14.6 ppm corresponding to COOH proton; singlet at δ 9.52 ppm corresponding to C_2 proton; singlet at δ 9.34 ppm corresponding to C_5 proton; N_1 cyclopropyl protons showed multiplets at δ 1.42 (1H) and 0.28-0.48 (4H) ppm; N_1 *t*-butyl protons showed singlet at δ 1.62 (9H) ppm; and N_1 4-fluorophenyl protons showed multiplet at δ 6.50 - 6.72 (4H) ppm. The elemental analysis results were within ± 0.4% of the theoretical values.

Most of the compounds were found to be more lipophilic indicated by their calculated log of partition coefficient value greater than 2 [log P > 2]. No correlation has been established between the calculated log P and antimycobacterial activity of the compounds, as compounds with low log P were found to be more active than compounds with high log P.

In the first phase of screening against MTB, all the compounds showed excellent *in vitro* activity against MTB with MIC less than 15 μM. Five compounds (**NQ 8b, NQ 8c, NQ 8d, NQ 8i** and **NQ 8j**) inhibited MTB with MIC of less than 1 μM and were relatively more potent than standard fluoroquinolone GAT (MIC: 1.04 μM). When compared to INH (MIC: 0.36 μM), two compounds (**NQ 8c** and **NQ 8d**) were found to be more active against MTB. Compound 7-(4-((benzo[d][1,3]dioxol-5-yl)methyl)piperazin-1-yl)-1-cyclopropyl-1,4-dihydro-6-nitro-4-oxoquinoline-3-carboxylic acid (**NQ 8c**) was found to be the most active compound *in vitro* with MIC of 0.08 μM against MTB and was 4.50 and 13 times more potent than INH and GAT respectively.

With respect to structure-MTB activity relationship, we have studied with various substituted piperazines (**NQ 8-10a-f**), (thio) morpholines (**NQ 8-10g-h**), substituted piperidines (**NQ 8-10i-l**), fused piperazines & piperidines (**NQ 8-10m-p**) at C_7 position. The results demonstrated that the contribution of the C_7 position to antimycobacterial activity was dependent on the substituent at N_1 and was in the order of substituted piperazines > substituted piperidines > fused piperazines & piperidines > (thio) morpholines when N_1 was cyclopropyl; substituted piperazines ≥ substituted piperidines and (thio) morpholines > fused piperazines and piperidines when N_1 was 4-fluorophenyl; substituted piperazines ≥ substituted piperidines, fused piperazines & piperidines and (thio) morpholines when N_1 was *tert*-butyl. Overall, a comparison of the substitution pattern at C_7 demonstrated that the order

of activity was substituted piperazines > substituted piperidines > fused piperazines & piperidines ≥ (thio) morpholines.

The results demonstrated that the antimycobacterial activity imparted by N_1 substituent was in the order of cyclopropyl > 4-fluorophenyl > *tert*-butyl. This result correlated with the other antibacterial fluoroquinolones, wherein cyclopropyl group was the favorable substituent. This result also correlated well with the previous report on the importance of cyclopropyl group as antimycobacterial pharmacophore [Renau, T. E., *et al.*, 1996]. The enhanced activity of the cyclopropyl group could be supported by a hypothesis based on the belief that the antibacterial activity of quinolones is related to the amount of un-ionized drug that is able to penetrate the cell membranes. This in turn associated with a highly acidic carboxyl group and a less basic C_7 amino substituent [Hooper, D. C., 1999]. The carboxyl group becomes more acidic if the N_1 substituent is electron donating in nature. The greater activity of cyclopropyl substituted quinolones was therefore associated with the electron-donating effect of this moiety.

Subsequently some of the compounds were evaluated against MDR-TB, and among the eighteen compounds screened, all the compounds inhibited MDR-TB with MIC ranging from 0.16 - 6.01 μM and were found to be more active than INH (MIC: 45.57 μM), and GAT (MIC: 8.34 μM). Eight compounds (**NQ 8b**, **NQ 8c, NQ 8d, NQ 9e, NQ 10f, NQ 8i, NQ 8j** and **NQ 8o**) inhibited MDR-TB with MIC less than 1 μM.

Compound **NQ 8c** was found to be the most active compound *in vitro* with MIC of 0.16 μM against MDR-TB and was 52 and 284 times more potent than GAT and INH respectively.

In MDR-TB, the results demonstrated that the antimycobacterial activity imparted by N_1 substituents was in the order cyclopropyl > 4-fluorophenyl > *tert*-butyl. By introducing bulky lipophilic secondary amines at C_7, enhanced the antimycobacterial activity which might be due to more penetration of these compounds into mycobacterial cells.

The compounds were also evaluated against MC^2 strain in which all the compounds inhibited the bacteria with MIC ranging from 0.79 - 64.36 μM and forty five compounds were found to be more active than INH (MIC: 45.57 μM).

In MC^2, the results demonstrated that the antimycobacterial activity imparted by N_1 substituents was in the order cyclopropyl > *tert*-butyl, 4-fluorophenyl.

Nine compounds when tested for cytotoxicity showed IC_{50} values ranging from 54.39 - 142.30 μM. A comparison of the substitution pattern at N_1 demonstrated that 4-fluorophenyl group was more cytotoxic than the cyclopropyl group. These results are important as the N_1 phenyl substituted compounds with their increased cytoliability, are much less attractive in the development of a quinolone for the treatment of TB. This is primarily due to the fact that the eradication of TB requires a lengthy course of treatment, and the need for an agent with a high margin of safety becomes a primary concern. Compound **NQ 8c** was found to be non-toxic upto 126.90 μM and showed selectivity index (CC_{50}/ MIC) of more than 1586.

Compound **NQ 8c** showed no effect or adverse reactions/toxicity at the maximum dose tested (300 mg/kg). Compound **NQ 8c** decreased the bacterial load in lung and spleen tissues with 2.78 and 4.15-log10 protections respectively and was considered to be promising in reducing bacterial count in lung and spleen tissues. When compared to gatifloxacin at the same dose level **NQ 8c** decreased the bacterial load with 0.81 and 2.05-log10 protections in lung and spleen tissues respectively. Compound **NQ 8c** was found to be less active than isoniazid in the *in vivo* study.

The 6-nitroquinolone-3-carboxylic acid derivatives synthesized were evaluated for their ability to inhibit DNA supercoiling activity of DNA gyrase isolated from *M. smegmatis*. Quinolones and fluoroquinolones are synthetic compounds which inhibit bacterial type II DNA topoisomerases. These enzymes facilitate DNA replication, transcription and other DNA transaction processes. They do so by transiently creating a double strand break in the DNA followed by religation of the broken strands after the passage of intact duplex DNA through the cleaved enzyme-DNA complex. This leads to the change in linking number of DNA in an ATP dependent reaction cycle [Levine, C.H., *et al.*, 1998]. DNA gyrase, an essential enzyme in bacteria, is unique in catalyzing the negative supercoiling of DNA and as a result, the enzyme is vital for almost all cellular processes that involve duplex DNA. In all the species of mycobacteria including MTB, DNA gyrase is the sole type II topoisomerase

and topoisomerase IV is not found in these genomes. Earlier studies have revealed that DNA gyrase from MTB and MC^2 are highly similar in antigenic and biochemical properties [Manjunatha, U. H., *et al.*, 2000]. The supercoiling assay results with various compounds using MC^2 DNA gyrase are presented in figures 6.1 (2a and 2b). The IC_{50} values presented in Table 6.5 show that the compounds **NQ 8j**, **NQ 8i**, **NQ 8n, NQ 8b, NQ 8k, NQ 8c, NQ 8d, NQ 9h** and **NQ 10f** inhibit DNA gyrase in the range of 45.31 – 68.11 μM. The compounds **NQ 9e** and **NQ 10b** have IC_{50} of 34.81 μM and 42.69 μM respectively and compound **NQ 10a** inhibits the enzyme activity with an IC_{50} value as low as 8.69 μM and was more active than standard CIP (IC_{50}: 15.09 μM) and MXFX (IC_{50}: 12.46 μM).

Quinolones in general have favorable safety profiles; phototoxicity has become a significant factor in the clinical use of some. Indeed, the first quinolone, nalidixic acid, caused light-induced dermal effects. This type of response has now been demonstrated for almost all fluoroquinolones, although the relative phototoxic potential varies greatly among compounds. Phototoxicity is considered to be an acute, light-induced irritation response characterized by dermal inflammation, with erythema and edema as primary clinical endpoints. Phototoxicity with the quinolones is generally thought to result from the absorption of light by the parent compound or a metabolite in tissue. This photosensitized chromophore may then transfer its absorbed photo energy to oxygen molecules, creating an environment for the production of reactive oxygen species such as singlet oxygen. These reactive species are then thought to attack cellular lipid membranes, initiating the inflammatory process.

Three (**NQ 8c**, **NQ 8d** and **NQ 8i**) compounds were evaluated for potential phototoxicity in a standardized *in vivo* test system that has been used previously to assess quinolone antibiotics [Mayne, T. N., *et al.*, 1997]. The test compounds (140 mg/kg) and the positive control lomefloxacin hydrochloride (140 mg/kg) were evaluated for phototoxicity and both ears of each mouse were evaluated for changes indicative of a positive response: erythema, edema or a measurable increase in ear thickness. Change from baseline was calculated separately for each animal and time point and analyzed for statistical significance and presented in Table 6.6. The results indicated that lomefloxacin showed significant increase in ear thickness from 4 - 96 h and 24 - 96 h when compared within time points and with the control respectively.

The test compounds were found to show a significant difference in ear thickness at various time - points when compared with the pre-drug reading (0 h) but were less or not toxic except **NQ 8c** (72 h) and **NQ 8i** (72 and 96 h) when compared with the negative (vehicle - treated) and positive control (lomefloxacin hydrochloride). No erythema occurred in mice dosed with 140 mg/kg of **NQ 8c** and **NQ 8d** throughout the 96 h study, while compound **NQ 8i** showed a significant erythema after irradiation at the 72 h time point only while lomefloxacin hydrochloride showed erythema after irradiation throughout the period of testing.

In theory, quantum mechanical (QM) methods enable completely accurate prediction of any property; there are some important classes of property (notably reactivity, electronic, magnetic, and optical behavior) that can only be modeled using QM methods, because they are determined by electronic behavior that cannot be approximated well using other methods. In the present study the titled compounds were geometry optimized by semi-empirical PM3 QM method and subjected to single-point energy calculation to determine their HOMO and LUMO surfaces. Electron-rich and electron-poor species tend to reveal the localization or delocalization of the partial or full charge by the shape of the HOMO or LUMO. Molecular orbitals, when viewed in a qualitative graphical representation, can provide insight into the nature of reactivity, and some of the structural and physical properties of molecules.

In the present study the HOMO and LUMO surfaces were visualized for the titled compounds for comparison and the following observations were made. The N_1, oxygen of nitro group at C_6, and the 4-oxo functions were found to play a crucial role in the antitubercular activity of nitroquinolones. This hypothesis was confirmed with the HOMO surface analysis (Figure 6.2), in which the most active compounds with lower MICs showed HOMO surfaces on the N_1, oxygen of nitro group at C_6, and the 4-oxo functions. The compounds with 1,3-benzodioxlyl group at the C_7 end showing electron cloud on the oxygen as in compound **NQ 8c** was beneficial (Figure 6.2). The less active compounds were devoid of electron cloud around either of N_1, oxygen of nitro group at C_6 and the 4-oxo functions as seen with compounds **NQ 9b**, **NQ 9o** and **NQ 10n** in figure 6.2. The least active compounds **NQ 9o** and **NQ 10n** showed electron cloud in the C_7 side chain electronegative groups and were devoid of electron cloud at N_1, oxygen of nitro group at C_6, and the 4-oxo functions. This observation was observed with all the less active compounds. With respect to N_1

substituent cyclopropyl was more preferable over 4-fluorophenyl and *t*-butyl in retaining the electron-rich cloud over the N_1 nitrogen. There was no significant difference observed in the LUMO orbital surfaces.

6.8 STRUCTURE - ACTIVITY RELATIONSHIP

The extensive studies on the activity profile against mycobacterium shows the following relationship between activity and the structure.

1. With respect to the substituents at N_1 position, the order of activity is cyclopropyl > 4-fluorophenyl > *tert*-butyl.
2. With respect to the substituents at C_7 position, the order of activity is substituted piperazines > substituted piperidines > fused piperazines and piperidines ≥ (thio) morpholines.
3. The N_1, oxygen of nitro group at C_6, and the 4 - oxo functions were found to play a crucial role in the antitubercular activity of nitroquinolones.
4. 4 - Fluorophenyl substituted compounds showed increase in cytotoxicity.

MOST POTENT NITROQUINOLONE (NQ) DERIVATIVE

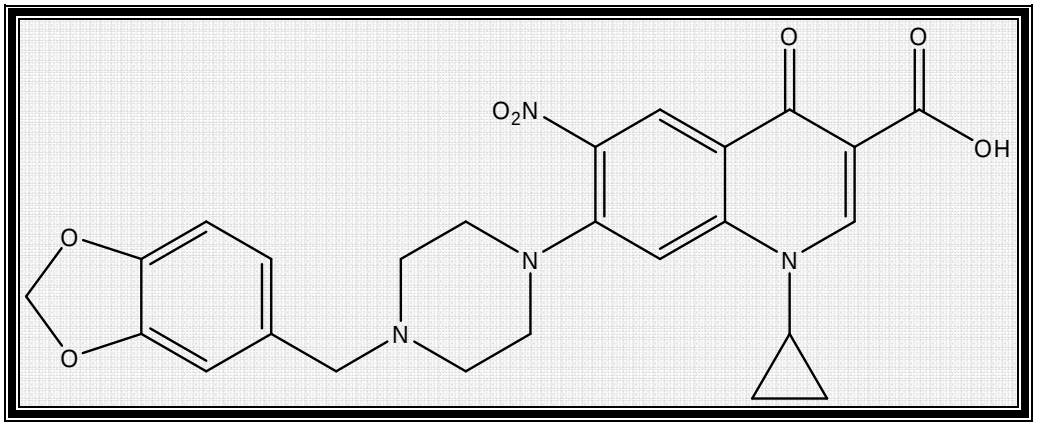

NQ 8c

7-(4-((Benzo[d][1,3]dioxol-5-yl)methyl)piperazin-1-yl)-1-cyclopropyl-1,4-dihydro-6-nitro-4-oxoquinoline-3-carboxylic acid

- ***In vitro***:
  - **Against MTB**: 13 and 4.5 times more potent than GAT and INH respectively.
  - **Against MDR-TB:** 52 and 284 times more potent than GAT and INH respectively.
  - **Against MC^2:** 3.54 and 57.68 times more active than GAT and INH respectively.
- ***Cytotoxicity***: Non-toxic up to 126.90 µM and showed selectivity index (CC_{50}/MIC) of more than 1586.
- ***In vivo***: Compared to GAT at the same dose level **NQ 8c** decreased the bacterial load with 0.81 and 2.05-log10 protections in lung and spleen tissues respectively.

CHAPTER 7

8-METHOXYQUINOLONE (MQ) DERIVATIVES

7.1 SYNTHESIS

Various 1-cyclopropyl-1,4-dihydro-6-fluoro-7-(substituted secondary amino)-8-methoxy-5-(sub)-4-oxoquinoline-3-carboxylic acids were synthesized from 1,2,3,4-tetrafluoro benzene by the following steps of reaction:

STEP 1: Synthesis of 1-bromo-2,3,4,5-tetrafluorobenzene (MQ 2)

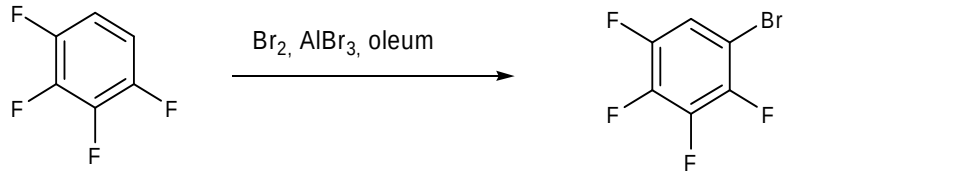

1,2,3,4-Tetrafluorobenzene
MQ 1

1-Bromo-2,3,4,5-tetrafluorobenzene
MQ 2

1,2,3,4-tetrafluorobenzene (10 g) (**MQ 1**) was added dropwise, with stirring, to a cooled (0° C) solution of bromine (20 g) and aluminium bromide (0.1 g) in oleum (20 % SO_3: 30 ml). After 5 h at 0° C, the reaction mixture was poured into ice and the product was isolated by ether extraction; distillation gave 1-bromo-2,3,4,5-tetrafluorobenzene (**MQ 2**)

Yield: 80 %; B.P.: 138 – 140 °C (lit ref. 137 °C); IR (KBr) cm^{-1}: 1599, 1402, 1265, 582; ^1H NMR (DMSO-d_6) δ ppm: 7.80 (s, 1H, ArH); Anal (C_6HBrF_4) C, H, N.

STEP 2: Synthesis of 1-bromo-3-methoxy-2,4,5-trifluoro benzene (MQ 3)

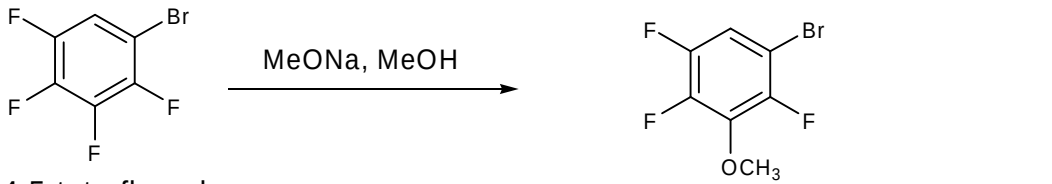

1-Bromo-2,3,4,5-tetrafluorobenzene
MQ 2

1-Bromo-2,4,5-trifluoro-3-methoxybenzene
MQ 3

Compound **MQ 2** (1.5 g) was refluxed with 0.5 N sodium methoxide in methanol (1 mol).

The reaction mixture was poured into water and the crude products isolated by ether extraction and then distilled to give **MQ 3**.

Yield: 95 %; B.P.: 194 – 196 ºC (lit ref. 194 ºC); IR (KBr) cm^{-1}: 1599, 1402, 1265, 582; ^1H NMR (DMSO-d_6) δ ppm: 3.85 (s, 3H, -OCH_3), 7.66 (s, 1H, ArH); Anal ($C_7H_4BrF_3O$) C, H, N.

STEP 3: Synthesis of 3-methoxy-2,4,5-trifluorobenzonitrile (MQ 4)

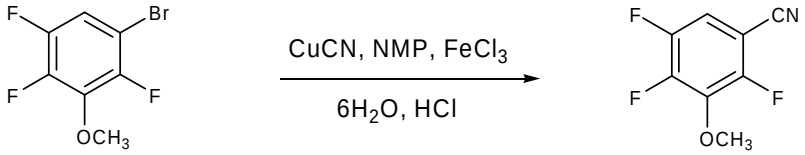

1-Bromo-2,4,5-trifluoro-3-methoxybenzene
MQ 3

2,4,5-Trifluoro-3-methoxybenzonitrile
MQ 4

A mixture of **MQ 3** (22 g), cuprous cyanide (10 g) and N-methyl-2-pyrrolidone (37 ml) in sealed tube was heated for 4.5 h at 140 – 150 °C. After cooling, a solution of ferric chloride hexahydrate (44 g) and concentrated hydrochloric acid (11 ml) in water (60 ml) was added to the reaction mixture and then stirred at 50 - 60 °C for 20 minutes. The reaction mixture was extracted with ether and the organic layer was washed with dilute hydrochloric acid, with water and with saturated saline solution successively, and dried over anhydrous sodium sulphate and then concentrated. The residue was purified by distillation under reduced pressure to give 3-methoxy-2,4,5-trifluorobenzonitrile (**MQ 4**) as colourless oil.

Yield: 63 %; B.P.: 96 – 98 ºC (lit ref. 94 ºC); IR (KBr) cm^{-1}: 2225, 1599, 1402, 1265; ^1H NMR (DMSO - d_6) δ ppm: 3.85 (s, 3H, -OCH_3), 7.66 (s, 1H, ArH); Anal ($C_8H_4F_3NO$) C, H, N.

STEP 4: Synthesis of 3-methoxy-2,4,5-trifluorobenzamide (MQ 5)

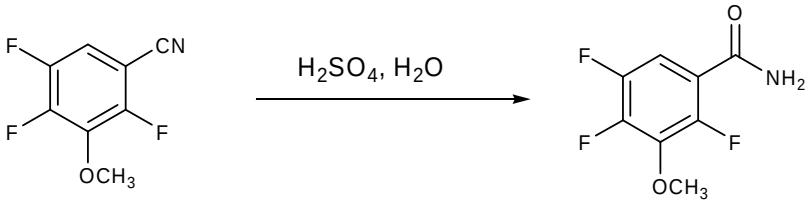

2,4,5-Trifluoro-3-methoxybenzonitrile
MQ 4

2,4,5-Trifluoro-3-methoxybenzamide
MQ 5

To the oily product **MQ 4** (14.2 g) were added concentrated sulphuric acid (8.5 ml) and

water (40 ml) and the mixture was stirred for 1 hour at 110 °C. After cooling the reaction mixture was poured into ice water (50 ml) and the resulting precipitate was collected by filtration, washed with water and recrystallized from a solution of dichloromethane-*n*-hexane to give 3-methoxy-2,4,5-trifluorobenzamide (**MQ 5**) as white needles.

Yield: 71 %; M.P.: 133 – 135 ºC (lit ref. 130-133 ºC); IR (KBr) cm^{-1}: 3350, 1710, 1599, 1402, 1265; ^1H NMR (DMSO - d_6) δ ppm: 3.85 (s, 3H, -OCH_3), 7.66 (s, 1H, ArH), 9.86 (s, 2H, NH_2); Anal ($C_8H_6F_3NO_2$) C, H, N.

STEP 5: Synthesis of 3-methoxy-2,4,5-trifluorobenzoic acid (MQ 6)

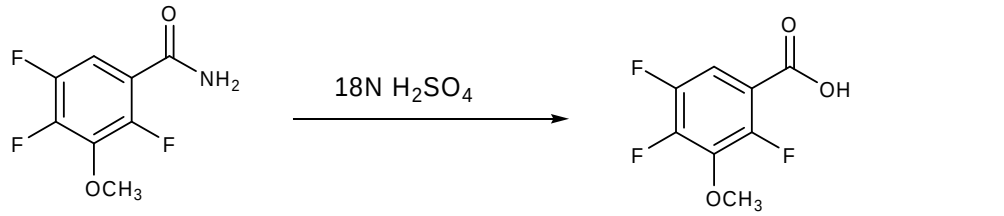

2,4,5-Trifluoro-3-methoxybenzamide **MQ 5**

2,4,5-Trifluoro-3-methoxybenzoic acid **MQ 6**

To the crystals of **MQ 5**, were added 18 N sulphuric acid (150 ml) and the mixture was heated for 3.5 h at 100 °C. After cooling water (400 ml) was added to the mixture and the resulting crystals were recrystallized from n-hexane to give 3-methoxy-2,4,5-trifluorobenzoic acid (**MQ 6**) as colorless needles.

Yield: 68 %; M.P.: 100 – 102 ºC (lit ref. 98-101 ºC); IR (KBr) cm^{-1}: 3550, 2650, 1710, 1599, 1402, 1265; ^1H NMR (DMSO - d_6) δ ppm: 3.81 (s, 3H, -OCH_3), 7.54 (s, 1H, ArH), 13.9 (s, 1H, COOH); Anal ($C_8H_5F_3O_3$) C, H, N.

STEP 6: Synthesis of ethyl 3-(2,4,5-trifluoro-3-methoxyphenyl)-3-oxopropanoate (MQ 7)

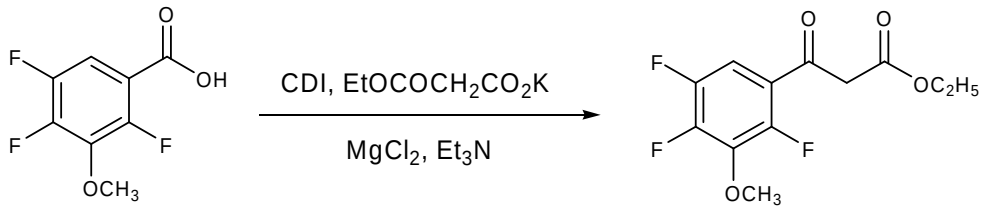

2,4,5-Trifluoro-3-methoxybenzoic acid **MQ 6**

Ethyl 3-(2,4,5-trifluoro-3-methoxyphenyl)-3-oxopropanoate **MQ 7**

To a solution of **MQ 6** (1.0 equiv.) in tetrahydrofuran, CDI (1.2 equiv.) was added for 30 minutes at a temperature of 70 ºC. The resulting crude imidazolide was used without further purification in the next step. To a solution of potassium salt of ethyl malonate (1.3 equiv.) in acetonitrile was added drop wise magnesium chloride (2.0 equiv.) and triethyl amine (4.0 equiv.) at 0 ºC and stirred at room temperature for 2.5 h. To this solution, the imidazolide prepared above was added and the reaction mixture was refluxed at 70 ºC for 2.5 h. After completion of reaction, the solvent was distilled off and poured into ice water and acidified to pH 5 - 6 with 20 % HCl, then extracted with ethyl acetate (3 x 25 ml) and dried over magnesium sulphate and distilled the solvent to give **MQ 7.**

Yield: 82 %; M.P.: 162 – 164 ºC; IR (KBr) cm^{-1}: 2900, 1726, 1710, 1705, 1599; ^1H NMR (DMSO - d_6) δ ppm:1.45 (t, 3H, $-CH_2CH_3$), 3.40 (s, 2H, CH_2), 3.84 (s, 3H, $-OCH_3$), 4.2 (m, 2H, $-CH_2CH_3$), 7.66 (s, 1H, ArH); Anal ($C_{12}H_{11}F_3O_4$) C, H, N.

STEP 7: Synthesis of ethyl 1-cyclopropyl-6,7-difluoro-1,4-dihydro-8-methoxy-4-oxoquinoline-3-carboxylate (MQ 10)

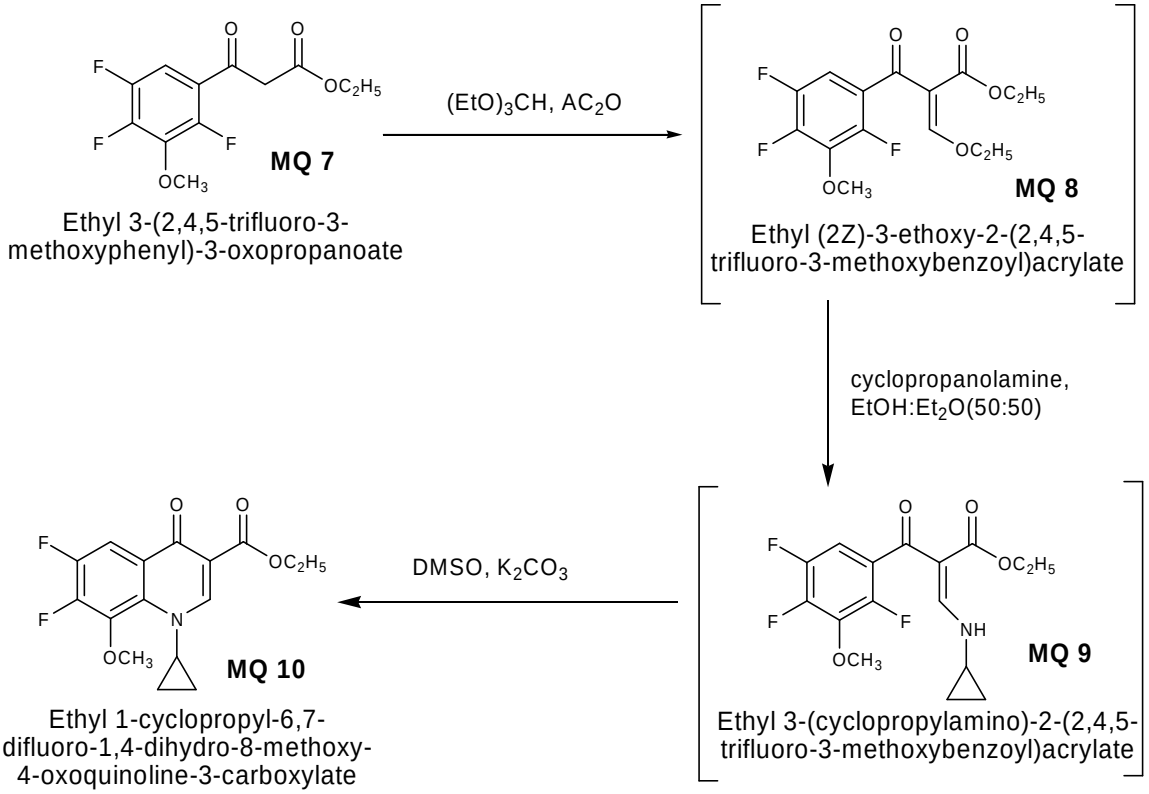

A mixture of **MQ 7** (1.00 equiv.), triethylorthoformate (1.5 equiv.) and acetic anhydride (2.5 equiv.) were refluxed at 140 ºC for 1 h. The ethyl acetate produced as a by product was distilled simultaneously under atmospheric pressure. After completion of reaction the reaction mixture was concentrated under reduced pressure to yield intermediate ethyl (2Z)-3-ethoxy-2-(2,4,5-trifluoro-3-methoxybenzoyl)acrylate (**MQ 8**) as an oil. The above residue was dissolved in a mixture of ether (20 ml) and ethanol (20 ml). Added cyclopropylamine (1.1 equiv.) at 0 ºC and stirred for 30 minutes under nitrogen atmosphere, followed by distillation yielded 67 % of **MQ 9** as an oily residue. The above oily residue (**MQ 9**) (1.0 equiv.) was dissolved in DMSO (30 ml) and added anhydrous potassium carbonate (1.6 equiv.) and refluxed at 60 ºC for 3 h. After completion of reaction, the mixture was diluted with ice cold water and neutralized with 20 % HCl to a pH of 5-6. The precipitate thus formed was filtered and washed with water followed by isopropanol to yield ethyl 1-cyclopropyl-6,7-difluoro-1,4-dihydro-8-methoxy-4-oxoquinoline-3-carboxylate (**MQ 10**).

Yield: 62 %; M.P.: > 250 ºC; IR (KBr) cm^{-1}: 2900, 1726, 1705, 1616; ^1H NMR (DMSO - d_6) δ ppm: 0.28-0.44 (m, 4H, cyclopropyl), 1.36 (m, 1H, cyclopropyl), 1.45 (t, 3H, $-CH_2CH_3$), 3.86 (s, 3H, $-OCH_3$), 4.2 (m, 2H, $-CH_2CH_3$), 9.34 (s, 1H, C_5-H), 9.52 (s, 1H, C_2-H); Anal ($C_{16}H_{16}F_3NO_4$) C, H, N.

STEP 8: Synthesis of 1-cyclopropyl-6,7-difluoro-1,4-dihydro-8-methoxy-4-oxoquinoline-3-carboxylic acid (MQ 11 a)

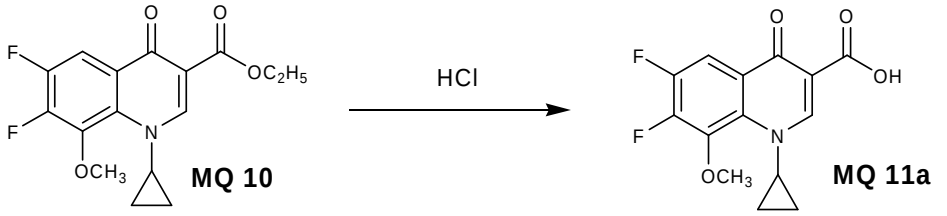

MQ 10

Ethyl 1-cyclopropyl-6,7-difluoro-1,4-dihydro-8-methoxy-4-oxoquinoline-3-carboxylate

MQ 11a

1-Cyclopropyl-6,7-difluoro-1,4-dihydro-8-methoxy-4-oxoquinoline-3-carboxylic acid

The product **MQ 10** (3 g) was suspended in 6N HCl (50 ml) and refluxed for 3 h and then cooled to 0 ºC. The precipitate obtained was filtered, washed with water and dried.

Yield: 90 %; M.P.: > 250 ºC; IR (KBr) cm^{-1}: 2900, 1726, 1705, 1616; ^1H NMR (DMSO - d_6) δ ppm: 0.28-0.44 (m, 4H, cyclopropyl), 1.36 (m, 1H, cyclopropyl), 3.86 (s, 3H, $-OCH_3$), 9.34 (s, 1H, C_5-H), 9.52 (s, 1H, C_2-H), 14.60 (s, 1H, COOH); Anal ($C_{14}H_{11}F_2NO_4$) C, H, N.

STEP 9: Synthesis of 1-cyclopropyl-6,7-difluoro-1,4-dihydro-8-methoxy-5-nitro-4-oxoquinoline-3-carboxylic acid (MQ 11 b)

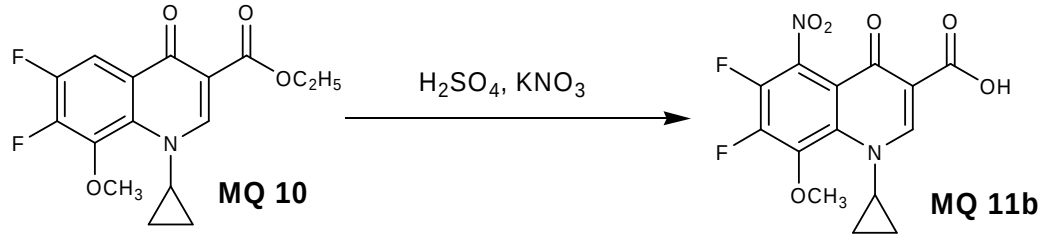

MQ 10

Ethyl 1-cyclopropyl-6,7-difluoro-1,4-dihydro-8-methoxy-4-oxoquinoline-3-carboxylate

MQ 11b

1-Cyclopropyl-6,7-difluoro-1,4-dihydro-8-methoxy-5-nitro-4-oxoquinoline-3-carboxylic acid

A solution of **MQ 10** (3 g, 1.00 equiv.) in concentrated sulfuric acid (30 ml) was treated portion wise with potassium nitrite (1.5 equiv.) over 30 minutes. The reaction was stirred at room temperature for 6 h. Then poured into ice cold water and the solid obtained was filtered and washed with water and dissolved in dichloromethane. The DCM layer was washed successively with water and 5 % sodium bicarbonate. Dried over sodium sulfate and distilled and recrystallized from methanol.

Yield: 88 %; M.P.: > 250 ºC; IR (KBr) cm^{-1}: 2900, 1726, 1705, 1616; ^1H NMR (DMSO-d_6) δ ppm: 0.28 - 0.44 (m, 4H, cyclopropyl), 1.36 (m, 1H, cyclopropyl), 3.86 (s, 3H, -OCH_3), 9.52 (s, 1H, C_2-H), 14.60 (s, 1H, COOH); Anal ($C_{14}H_{10}F_2N_2O_6$) C, H, N.

STEP 10: Synthesis of 1-cyclopropyl-1,4-dihydro-6-fluoro-7-(substituted secondary amino)-8-methoxy-5-(sub)-4-oxoquinoline-3-carboxylic acid (MQ 12-13 a-p)

MQ 11 a,b
a: R=H
b: R=NO_2

1-Cyclopropyl-6,7-difluoro-1,4-dihydro-8-methoxy-5-(sub)-4-oxoquinoline-3-carboxylic acid

MQ 12a-q: R=H
MQ 13a-q: R=NO_2

1-Cyclopropyl-1,4-dihydro-6-fluoro-7-(substituted secondary amino)-8-methoxy-5-(sub)-4-oxoquinoline-3-carboxylic acid

To a solution of **MQ 11 a, b** (1.0 equiv.) in dimethyl sulphoxide and substituted secondary amines (1.1 equiv.), add potassium carbonate (1.2 equiv.) and was placed in microwave and

allowed to react at 320 watts for a period of 2 minutes. After completion of the reaction, the mixture was poured into ice cold water and kept overnight. Filtered and washed with water to yield **MQ 12-13 a-p**.

Physical constants of the synthesized compounds are presented in table 7.1

Spectral and elemental analysis data of representative 8-methoxyquinolones (**MQ**) are presented in table 7.2.

7.2 *IN VITRO* ANTIMYCOBACTERIAL AND CYTOTOXICITY

The synthesized compounds were tested for antimycobacterial activities against *Mycobacterium tuberculosis*, multi-drug resistant *Mycobacterium tuberculosis* and *Mycobacterium smegmatis* by agar dilution method and the results are tabulated in table 7.3. The compounds were also tested for there cytotoxicity in mammalian vero cell lines and the results are tabulated in table 7.3.

7.3 *IN VIVO* ANTIMYCOBACTERIAL STUDY

Two compounds **MQ 12l** and **13n** were tested in *in vivo* model against *M. tuberculosis* and the results are tabulated in table 7.4

7.4 DNA GYRASE SUPERCOILING ASSAY

Eleven compounds were tested for DNA gyrase enzyme supercoiling assay and the results are tabulated in table 7.5. The gel picture of the enzyme inhibition study is shown in figure 7.1.

Table 7.1: Physical constants of 8-methoxyquinolones (MQ 12-13 a-p)

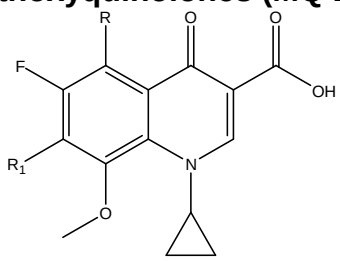

Compd	R	R_1	Yield (%)	M.P. (°C)	Molecular Formula	Molecular Weight	cLog P
MQ 12a	H	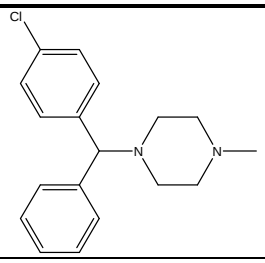	69	115-117	$C_{31}H_{29}ClFN_3O_4$	562.03	3.09
MQ 13a	NO_2	- do -	62	168-170	$C_{31}H_{28}ClFN_4O_6$	607.03	2.74
MQ 12b	H	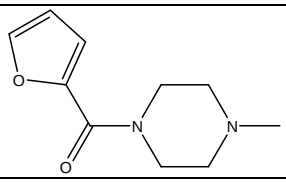	65	215-217	$C_{23}H_{22}FN_3O_6$	455.44	1.11
MQ 13b	NO_2	- do -	66	118-120	$C_{23}H_{21}FN_4O_8$	500.43	0.75
MQ 12c	H	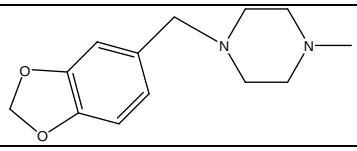	68	95-97	$C_{26}H_{26}FN_3O_6$	495.50	0.99
MQ 13c	NO_2	- do -	80	188-190	$C_{26}H_{25}FN_4O_8$	540.50	0.64
MQ 12d	H	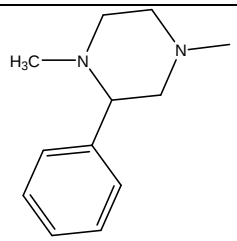	66	115-117	$C_{25}H_{26}FN_3O_4$	451.49	1.02
MQ 13d	NO_2	- do -	80	154-156	$C_{25}H_{25}FN_4O_6$	496.49	0.66
MQ 12e	H	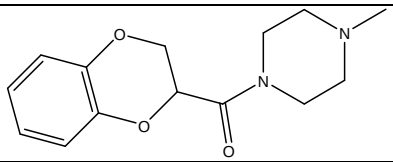	64	171-173	$C_{27}H_{26}FN_3O_7$	523.51	2.38
MQ 13e	NO_2	- do -	83	172-174	$C_{27}H_{25}FN_4O_9$	568.51	2.02
MQ 12f	H	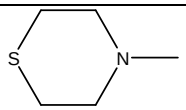	70	170-172	$C_{18}H_{19}FN_2O_4S$	378.42	2.93
MQ 13f	NO_2	- do -	81	163-165	$C_{18}H_{18}FN_3O_6S$	423.42	2.58

Table 7.1: Physical constants of 8-methoxyquinolones (MQ 12-13 a-p) (contd…)

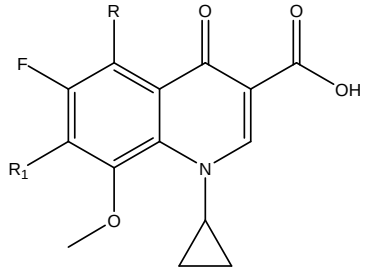

Compd	R	R_1	Yield (%)	M.P. (°C)	Molecular Formula	Molecular Weight	cLog P
MQ 12g	H	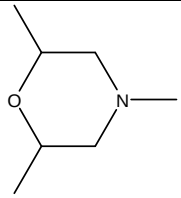	65	229-231	$C_{20}H_{23}FN_2O_5$	390.41	2.98
MQ 13g	NO_2	- do -	84	124-126	$C_{20}H_{22}FN_3O_7$	435.40	2.63
MQ 12h	H	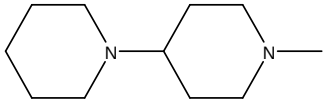	63	163-165	$C_{24}H_{30}FN_3O_4$	443.51	1.18
MQ 13h	NO_2	- do -	69	167-169	$C_{24}H_{29}FN_4O_6$	488.51	0.83
MQ 12i	H	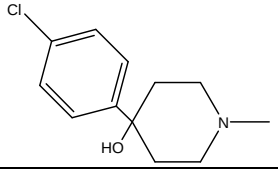	68	112-114	$C_{25}H_{24}ClFN_2O_5$	486.92	3.97
MQ 13i	NO_2	- do -	76	136-138	$C_{25}H_{23}ClFN_3O_7$	531.92	3.61
MQ 12j	H	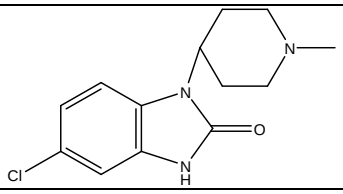	70	259-261	$C_{26}H_{24}ClFN_4O_5$	526.94	4.69
MQ 13j	NO_2	- do -	78	178-180	$C_{26}H_{23}ClFN_5O_7$	571.94	4.34
MQ 12k	H	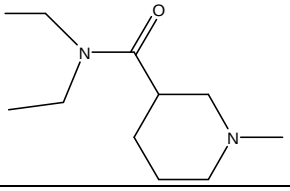	70	85-87	$C_{24}H_{30}FN_3O_5$	459.51	3.41
MQ 13k	NO_2	- do -	75	128-130	$C_{24}H_{29}FN_4O_7$	504.51	3.05
MQ 12l	H	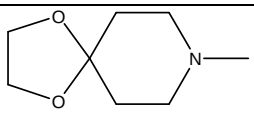	73	256-258	$C_{21}H_{23}FN_2O_6$	418.42	2.02
MQ 13l	NO_2	- do -	69	152-154	$C_{21}H_{22}FN_3O_8$	463.41	1.67

Table 7.1: Physical constants of 8-methoxyquinolones (MQ 12-13 a-p) (contd…)

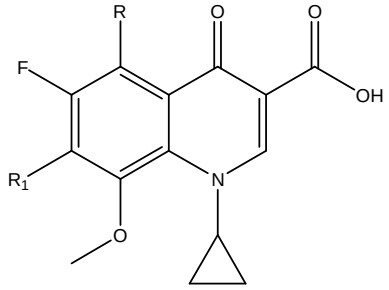

Compd	R	R_1	Yield (%)	M.P. (°C)	Molecular Formula	Molecular Weight	cLog P
MQ 12m	H	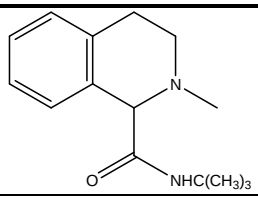	63	70-72	$C_{28}H_{30}FN_3O_5$	507.55	4.48
MQ 13m	NO_2	- do -	82	172-174	$C_{28}H_{29}FN_4O_7$	552.55	3.81
MQ 12n	H	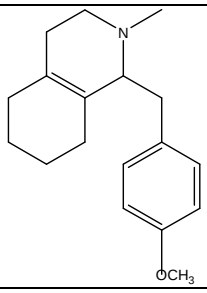	62	176-178	$C_{31}H_{33}FN_2O_5$	532.60	6.64
MQ 13n	NO_2	- do -	60	108-110	$C_{31}H_{32}FN_3O_7$	577.60	6.28
MQ 12o	H	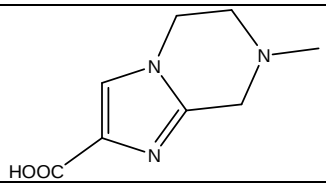	79	169-171	$C_{21}H_{19}FN_4O_6$	442.40	2.48
MQ 13o	NO_2	- do -	84	208-210	$C_{21}H_{18}FN_5O_8$	487.39	2.12
MQ 12p	H	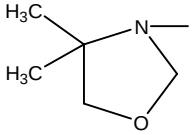	62	180-182	$C_{19}H_{21}FN_2O_5$	376.38	3.04
MQ 13p	NO_2	- do -	77	160-162	$C_{19}H_{20}FN_3O_7$	421.38	2.69

Table 7.2: Spectral data and elemental analysis data of representative 8-methoxyquinolone (MQ) derivatives

Compd	IR Spectroscopy (cm^{-1}; KBr)	^1H NMR (δ ppm, DMSO - d_6)	Elemental Analyses (Calculated/Found)		
			C	H	N
MQ 12a	2900, 1724, 1708, 1620	0.28 - 0.48 (m, 4H, cyclopropyl), 1.35 (m, 1H, cyclopropyl), 2.59 (t, 4H, 2 CH_2 of piperazine), 3.32 (t, 4H, 2 CH_2 of piperazine), 3.77 (s, 3H, OCH_3), 5.2 (s, 1H, CH of diphenylmethyl), 7.0 - 7.18 (m, 9H, Ar-H), 7.9 (s, 1H, C_5-H), 8.79 (s, 1H, C_2-H), 14.6 (s, 1H, COOH)	66.25 66.22	5.20 5.19	7.48 7.48
MQ 13b	2890, 1724, 1710, 1624, 1460 - 1360	0.28 - 0.48 (m, 4H, cyclopropyl), 1.35 (m, 1H, cyclopropyl), 3.16 (t, 4H, 2 CH_2 of piperazine), 3.26 (t, 4H, 2 CH_2 of piperazine), 3.52 (s, 3H, OCH_3), 6.5 - 7.28 (m, 3H, Ar-H), 8.81 (s, 1H, C_2-H), 14.6 (s, 1H, COOH)	55.20 55.19	4.23 4.23	11.20 11.21
MQ 12c	3250, 2890, 1724, 1710, 1624	0.28 - 0.48 (m, 4H, cyclopropyl), 1.35 (m, 1H, cyclopropyl), 2.82 (t, 4H, 2 CH_2 of piperazine), 3.1 (t, 4H, 2 CH_2 of piperazine), 3.55 (s, 3H, OCH_3), 3.6 (s, 2H, CH_2 of piperanoyl), 5.86 (s, 2H, -OCH_2O-), 6.42 - 6.62 (m, 3H, Ar-H), 7.8 (s, 1H, C_5-H), 8.8 (s, 1H, C_2-H), 14.6 (s, 1H, COOH)	63.02 63.00	5.29 5.29	8.48 8.46
MQ 13d	2890, 1724, 1710, 1620, 1460 - 1368	0.28 - 0.52 (m, 4H, cyclopropyl), 1.38 (m, 1H, cyclopropyl), 2.2 (s, 3H, CH_3), 2.6 (t, 2H, 5-CH_2 of piperazine), 3.15 (t, 2H, 6-CH_2 of piperazine), 3.4 (d, 2H, 2-CH_2 of piperazine), 3.53 (s, 3H, OCH_3), 4.12 (t, 1H, 3-CH of piperazine), 7.0 - 7.2 (m, 5H, Ar-H), 8.5 (s, 1H, C_2-H), 14.4 (s, 1H, COOH)	60.48 60.46	5.08 5.05	11.28 11.30
MQ 12e	2890, 1724, 1710, 1624	0.28 - 0.48 (m, 4H, cyclopropyl), 1.35 (m, 1H, cyclopropyl), 3.26 (t, 4H, 2,6-CH_2 of piperazine), 3.4 (t, 4H, 3,5-CH_2 of piperazine), 3.51 (s, 3H, OCH_3), 4.6 (d, 2H, 3-CH_2 of dihydrobenzodioxinyl), 5.14 (t, 1H, 2-CH of dihydrobenzodioxinyl), 6.5 - 6.71 (m, 4H, Ar-H), 7.75 (s, 1H, C_5-H), 8.79 (s, 1H, C_2-H), 14.6 (s, 1H, COOH)	61.95 61.95	5.01 5.00	8.03 8.02
MQ 13f	2890, 1724, 1710, 1624, 1464 - 1360	0.28 - 0.54 (m, 4H, cyclopropyl), 1.36 (m, 1H, cyclopropyl), 2.64 (t, 4H, 2 CH_2 of thiomorpholine), 3.38 (t, 4H, 2 CH_2 of thiomorpholine), 3.51 (s, 3H, OCH_3), 8.9 (s, 1H, C_2-H), 14.4 (s, 1H, COOH)	51.06 51.02	4.28 4.25	9.92 9.91
MQ 12g	2890, 1724, 1710, 1620	0.28 - 0.48 (m, 4H, cyclopropyl), 1.35 (m, 1H, cyclopropyl), 1.2 (d, 6H, 2 CH_3 of morpholino), 3.0 (d, 4H, 2 CH_2 of morpholine), 3.56 (s, 3H, OCH_3), 3.9 (m, 2H, 2 CH of morpholine), 7.1 (s, 1H, C_5-H), 7.9 (s, 1H, C_2-H), 14.6 (s, 1H, COOH)	61.53 61.53	5.94 5.96	7.18 7.19
MQ 13h	2892, 1724, 1710, 1628, 1460 - 1360	0.28 - 0.48 (m, 4H, cyclopropyl), 1.35 (m, 1H, cyclopropyl), 1.5 - 1.6 (m, 10H, 5 CH_2), 2.2 (t, 4H, 2 CH_2), 2.7 (m, 1H, CH), 2.8 (t, 4H, 2 CH_2), 3.57 (s, 3H, OCH_3), 8.2 (s, 1H, C_2-H), 14.6 (s, 1H, COOH)	59.01 59.01	5.98 5.97	11.47 11.49

Table 7.2: Spectral data and elemental analysis data of representative 8-methoxyquinolone (MQ) derivatives (contd…)

Compd	IR Spectroscopy (cm^{-1}; KBr)	^1H NMR (δ ppm, DMSO-d_6)	Elemental Analyses (Calculated/Found)		
			C	H	N
MQ 12i	2890, 1724, 1710, 1624	0.28 - 0.46 (m, 4H, cyclopropyl), 1.33 (m, 1H, cyclopropyl), 2.0 (t, 4H, 2 CH_2 of piperidine), 2.7 (t, 4H, 2 CH_2 of piperidine), 3.51 (s, 3H, OCH_3), 7.1-7.18 (m, 4H, Ar-H), 7.82 (s, 1H, C_5-H), 8.88 (s, 1H, C_2-H), 10.0 (bs, 1H, OH), 14.6 (s, 1H, COOH)	61.67 61.69	4.97 4.99	5.75 5.74
MQ 13j	2900, 1724, 1708, 1620, 1460 - 1370	0.28 - 0.48 (m, 4H, cyclopropyl), 1.35 (m, 1H, cyclopropyl), 1.6 - 2.4 (m, 8H, 4 CH_2 of piperidine), 3.52 (s, 3H, OCH_3), 4.1 (bm, 1H, CH of piperidine), 6.8 - 7.7 (m, 3H, Ar-H), 8.3 (s, 1H, C_2-H), 10.8 (s, 1H, NH), 14.6 (s, 1H, COOH)	54.60 54.61	4.05 4.06	12.24 12.23
MQ 12k	3110, 2896, 1728, 1712, 1710, 1624	0.28 - 0.48 (m, 4H, cyclopropyl), 1.35 (m, 1H, cyclopropyl), 1.2 (t, 6H, 2 CH_3 of ethyl), 1.78-2.7 (m, 9H, H of piperidine), 3.24 (q, 4H, 2 CH_2 of ethyl), 3.53 (s, 3H, OCH_3), 7.8 (s, 1H, C_5-H), 8.94 (s, 1H, C_2-H), 14.6 (s, 1H, COOH)	62.73 62.72	6.58 6.60	9.14 9.14
MQ 13l	2890, 1724, 1710, 1624, 1464 - 1360	0.28 - 0.52 (m, 4H, cyclopropyl), 1.38 (m, 1H, cyclopropyl), 1.78 - 2.4 (m, 8H, 4 CH_2 of azaspirodecane), 3.51 (s, 3H, OCH_3), 3.96 (m, 4H, 2 CH_2 of azaspirodecane), 8.9 (s, 1H, C_2-H), 14.4 (s, 1H, COOH)	54.43 54.43	4.79 4.78	9.07 9.05
MQ 12m	2890, 1724, 1712, 1618	0.28 - 0.48 (m, 4H, cyclopropyl), 1.35 (m, 1H, cyclopropyl), 1.3 (s, 9H, 3 CH_3), 2.66 - 2.9 (m, 4H, 2 CH_2 of isoquinoline), 3.53 (s, 3H, OCH_3), 4.85 (s, 1H, CH of isoquinoline), 6.7 - 7.1 (m, 4H, Ar-H), 7.8 (s, 1H, C_5-H), 8.8 (s, 1H, C_2-H), 10.2 (s, 1H, NH), 14.6 (s, 1H, COOH)	66.26 66.26	5.96 5.95	8.28 8.28
MQ 13n	2890, 1724, 1712, 1626, 1468 - 1360	0.28 - 0.54 (m, 4H, cyclopropyl), 1.36 (m, 1H, cyclopropyl), 1.6 - 1.95 (m, 8H, 4 CH_2 of isoquinolinyl), 2.2 - 3.4 (m, 7H, 2 CH_2 and 1 CH of isoquinolinyl, and CH_2), 3.52 (s, 3H, OCH_3), 3.73 (s, 3H, -OCH_3), 6.8 - 7.1 (m, 4H, Ar-H), 8.56 (s, 1H, C_2-H), 14.4 (s, 1H, COOH)	64.46 64.44	5.58 5.55	7.27 7.27
MQ 12o	3200, 2890, 1724, 1710, 1624	0.28 - 0.48 (m, 4H, cyclopropyl), 1.35 (m, 1H, cyclopropyl), 3.1 - 3.8 (m, 6H, 3 CH_2), 3.55 (s, 3H, OCH_3), 7.6 (s, 1H, CH), 7.63 (s, 1H, C_5-H), 8.78 (s, 1H, C_2-H), 12.12 (s, 1H, 2-COOH), 14.6 (s, 1H, 3-COOH)	57.01 57.01	4.33 4.33	12.66 12.66
MQ 13p	3210, 2890, 1724, 1710, 1620, 1460 - 1368	0.28 - 0.48 (m, 4H, cyclopropyl), 1.35 (m, 1H, cyclopropyl), 1.16 (s, 6H, 2 CH_3), 3.41 (s, 2H, 5-CH_2 of oxazolidinyl), 3.57 (s, 3H, OCH_3), 4.6 (s, 2H, 2-CH of oxazolidinyl), 8.85 (s, 1H, C_2-H), 14.6 (s, 1H, COOH)	54.16 54.14	4.78 4.77	9.97 9.99

Table 7.3: *In vitro* antimycobacterial and cytotoxicity data of 8-methoxyquinolones (MQ 12-13 a-p)

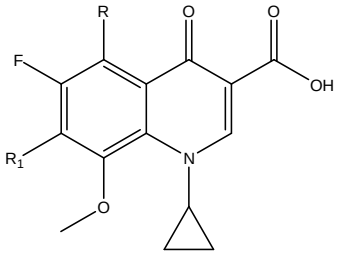

Compd	R	R_1	CC_{50} (μM)	MIC (μM)		
				MTB	MDR-TB	MC^2
MQ 12a	H	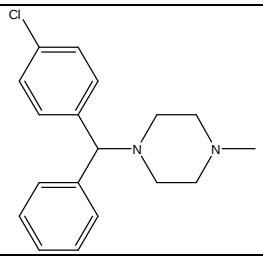	NT	11.12	NT	44.48
MQ 13a	NO_2	- do -	102.96	1.28	1.28	10.29
MQ 12b	H	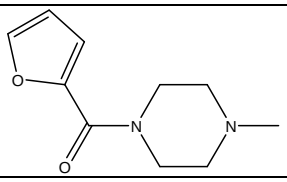	NT	13.72	NT	13.72
MQ 13b	NO_2	- do -	NT	6.25	NT	12.49
MQ 12c	H	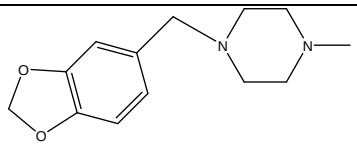	126.14	1.57	1.57	3.15
MQ 13c	NO_2	- do -	115.63	0.35	0.35	1.44
MQ 12d	H	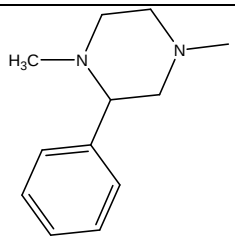	NT	3.06	NT	6.13
MQ 13d	NO_2	- do -	NT	13.84	NT	27.69
MQ 12e	H	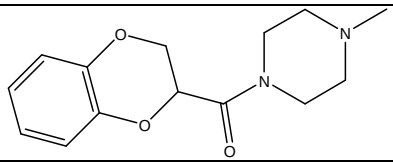	125.88	3.14	3.14	6.30
MQ 13e	NO_2	- do -	119.39	1.49	0.74	1.49
MQ 12f	H	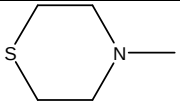	109.94	1.37	2.74	2.74
MQ 13f	NO_2	- do -	165.16	2.06	2.06	4.12

Table 7.3: *In vitro* antimycobacterial and cytotoxicity data of 8-methoxyquinolones (MQ 12-13 a-p) (contd…)

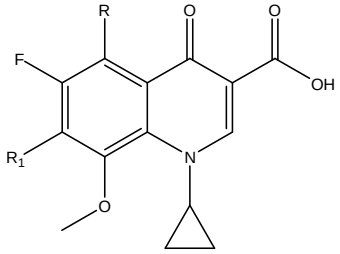

Compd	R	R_1	CC_{50} (μM)	MIC (μM)		
				MTB	MDR-TB	MC^2
MQ 12g	H	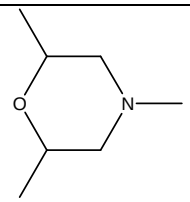	160.09	3.99	3.99	16.01
MQ 13g	NO_2	- do -	143.55	0.89	1.79	1.79
MQ 12h	H	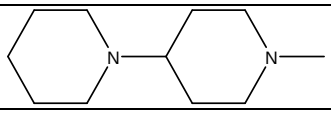	NT	7.06	NT	14.09
MQ 13h	NO_2	- do -	NT	6.41	NT	12.79
MQ 12i	H	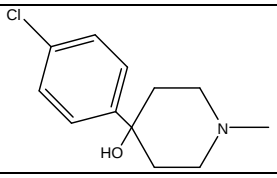	NT	6.43	NT	12.84
MQ 13i	NO_2	- do -	NT	5.88	NT	11.75
MQ 12j	H	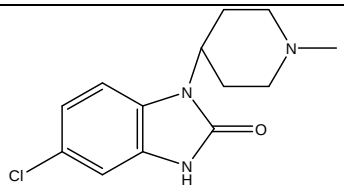	NT	5.94	NT	5.94
MQ 13j	NO_2	- do -	NT	5.47	NT	10.93
MQ 12k	H	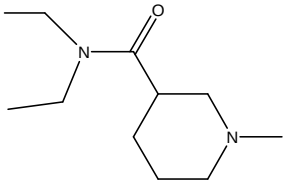	136.01	1.69	3.39	0.85
MQ 13k	NO_2	- do -	123.88	1.55	1.55	12.39
MQ 12l	H	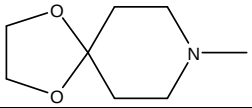	149.37	0.93	1.86	1.86
MQ 13l	NO_2	- do -	134.87	0.84	0.41	6.75

Table 7.3: *In vitro* antimycobacterial and cytotoxicity data of 8-methoxyquinolones (MQ 12-13 a-p) (contd…)

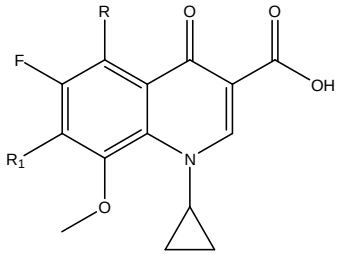

Compd	R	R_1	CC_{50} (μM)	MIC (μM)		
				MTB	MDR-TB	MC^2
MQ 12m	H	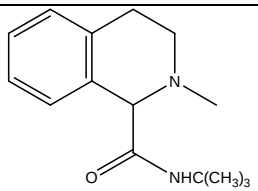	NT	12.31	NT	49.26
MQ 13m	NO_2	- do -	113.11	1.41	2.82	2.82
MQ 12n	H	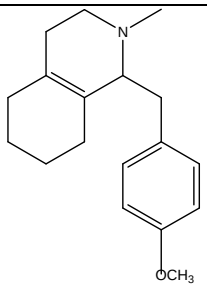	117.35	1.46	1.46	2.93
MQ 13n	NO_2	- do -	108.21	0.16	0.33	0.68
MQ 12o	H	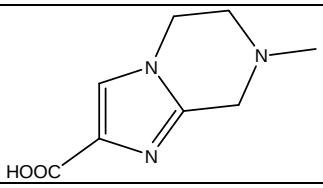	114.13	2.85	2.85	5.72
MQ 13o	NO_2	- do -	141.27	3.53	1.76	7.08
MQ 12p	H	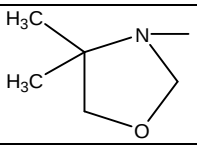	128.23	3.20	1.60	6.42
MQ 13p	NO_2	- do -	166.06	4.14	2.07	16.61
Gatifloxacin	-	-	>155.3	1.04	8.34	2.08
INH	-	-	>455.8	0.36	45.57	45.57

Table 7.4: *In vivo* activity data of MQ 12l, MQ 13n, gatifloxacin and isoniazid against *M. tuberculosis* ATCC 35801 in mice.

Compound	Lungs (log CFU ± SEM)	Spleen (log CFU ± SEM)
Control	7.99 ± 0.16	9.02 ± 0.21
Gatifloxacin (50 mg/kg)	6.02 ± 0.23	6.92 ± 0.07
Isoniazid (25 mg/kg)	5.86 ± 0.23	4.71 ± 0.10
MQ 12l (50 mg/kg)	6.12 ± 0.11	6.41 ± 0.12
MQ 13n (50 mg/kg)	5.41 ± 0.21	6.10 ± 0.18

Table 7.5: IC_{50} values for DNA gyrase inhibition of 8-methoxyquinolones (MQ)

Compounds	IC_{50} (μM)
MQ 12c	>100
MQ 12e	57.31
MQ 12k	>108.81
MQ 12l	>119.49
MQ 12n	75.10
MQ 13e	>87.95
MQ 13f	>118.09
MQ 13g	114.84
MQ 13m	>90.49
MQ 13n	51.94
MQ 13p	>118.66
Ciprofloxacin	15.09
Moxifloxacin	12.46

7.5 PHOTOTOXICITY EVALUATION

Five compounds were evaluated for potential phototoxicity in a standardized *in vivo* test system and the results are tabulated in table 7.6.

7.6 QUANTUM MECHANICAL MODELING

In the present study the HOMO and LUMO surfaces were visualized for the titled compounds for comparison (Figure 7.2)

Table 7.6: Phototoxicity evaluation of 8-methoxyquinolones (MQ)

Group	Ear thickness (mm)[a]						Erythema[b]					
	Time (approximately) after start of irradiation (h)[c]											
	0	4	24	48	72	96	0	4	24	48	72	96
Control[d]	0.37 ± 0.03	0.36 ± 0.02	0.38 ± 0.03	0.37 ± 0.03	0.37 ± 0.03	0.38 ± 0.03	0	0	0	0	0	0
MQ 13c	0.26 ± 0.01	0.27 ± 0.02	0.28 ± 0.01	0.30 ± 0.01$^{\#}$	0.33 ± 0.01$^{\#}$	0.31 ± 0.02$^{\#}$	0	0	0	2	3	4
MQ 12e	0.33 ± 0.01	0.31 ± 0.01	0.32 ± 0.01	0.33 ± 0.01	0.33 ± 0.01	0.32 ± 0.02	0	0	0	0	0	0
MQ 13g	0.28 ± 0.02	0.29 ± 0.01	0.35 ± 0.02$^{\#}$	0.36 ± 0.01$^{\#}$	0.34 ± 0.01$^{\#}$	0.33 ± 0.01$^{\#}$	0	2	0	0	0	0
MQ 12k	0.39 ± 0.04	0.38 ± 0.04	0.36 ± 0.05	0.37 ± 0.06	0.39 ± 0.07	0.39 ± 0.07	0	2	0	0	0	0
MQ 13n	0.32 ± 0.01	0.33 ± 0.01	0.32 ± 0.02	0.33 ± 0.01	0.33 ± 0.01	0.32 ± 0.02	0	0	0	0	0	0
Lomefloxacin	0.31 ± 0.01	0.40 ± 0.02$^{*\#}$	0.48 ± 0.02$^{*\#}$	0.53 ± 0.02$^{*\#}$	0.64 ± 0.04$^{*\#}$	0.60 ± 0.06$^{*,\#}$	0	6	6	6	6	6

[a] Mean Ear Thickness ± SEM; left and right ears were averaged
[b] Number of mice with erythema
[c] Time zero = pre-dose (mice exposed to UVA light immediately after dosing); 4 h = end of irradiation period.
[d] Control = 0.5 % aqueous solution of sodium carboxymethylcellulose (4 Ns/m^2) dosed at 10 mL/kg.
[*] Mean Ear Thickness ± SEM; significant difference from control at $P < 0.05$.
[#] Mean Ear Thickness ± SEM; significant difference from 0 h at $P < 0.05$.

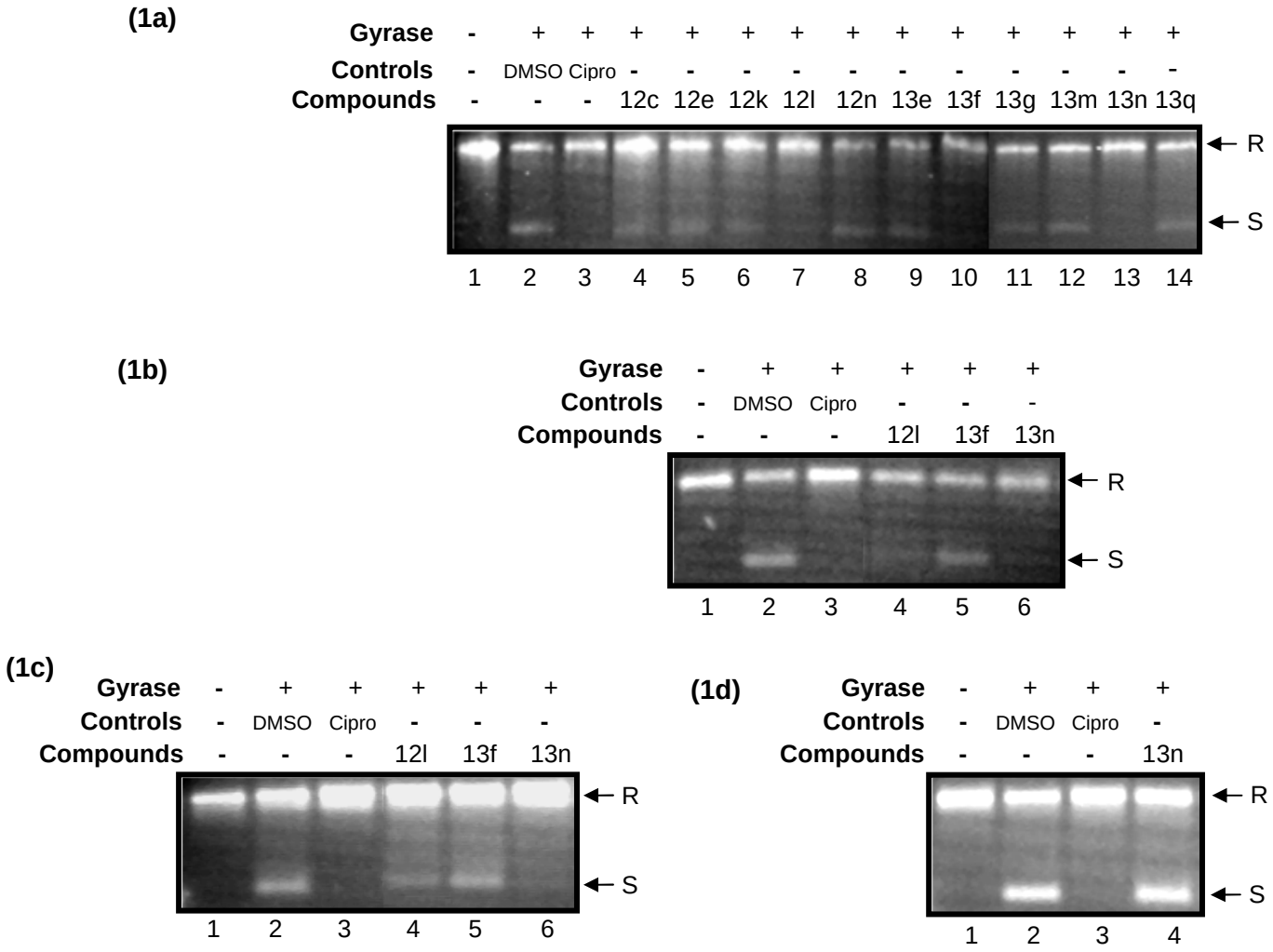

Figure 7.1: Gel picture for DNA gyrase supercoiling assay of 8-methoxyquinolones (**MQ**).
DNA gyrase was pre-incubated with the indicated concentrations of the compounds and then rest of the components of the reaction including relaxed circular DNA was added.
(a) Lane 1: relaxed circular DNA, lane 2: supercoiling reaction in presence of solvent control, 5% DMSO. Lane 3: ciprofloxacin at 10 μg/ml concentration, used as a positive control of gyrase inhibition. Lanes 4 to 14: reactions in presence of 50 μg/ml of compounds **MQ 12c, MQ 12e, MQ 12k, MQ 12l, MQ 12n, MQ 13e, MQ 13f, MQ 13g, MQ 13m, MQ 13n** & **MQ 13q** respectively.
(b) Lane 1: relaxed circular DNA, lane 2: supercoiling reaction in presence of 5% DMSO, Lane 3: ciprofloxacin at 10 μg/ml concentration. Lanes 4 to 6: reactions in presence of 40 μg/ml of compounds **MQ 12l, MQ 13f** & **MQ 13n** respectively.
(c) Lane 1: relaxed circular DNA, lane 2: supercoiling reaction in presence of 5 % DMSO, Lane 3: ciprofloxacin at 10 μg/ml concentration. Lanes 4 to 6: reactions in presence of 30 μg/ml of compounds **MQ 12l, MQ 13f** & **MQ 13n** respectively.
(d) Lane 1: relaxed circular DNA, lane 2: supercoiling reaction in presence of 5 % DMSO, Lane 3: ciprofloxacin at 10 μg/ml concentration. Lanes 4: reaction in presence of 20 μg/ml of compound **MQ 13n**. R and S indicate relaxed and supercoiled DNA respectively.

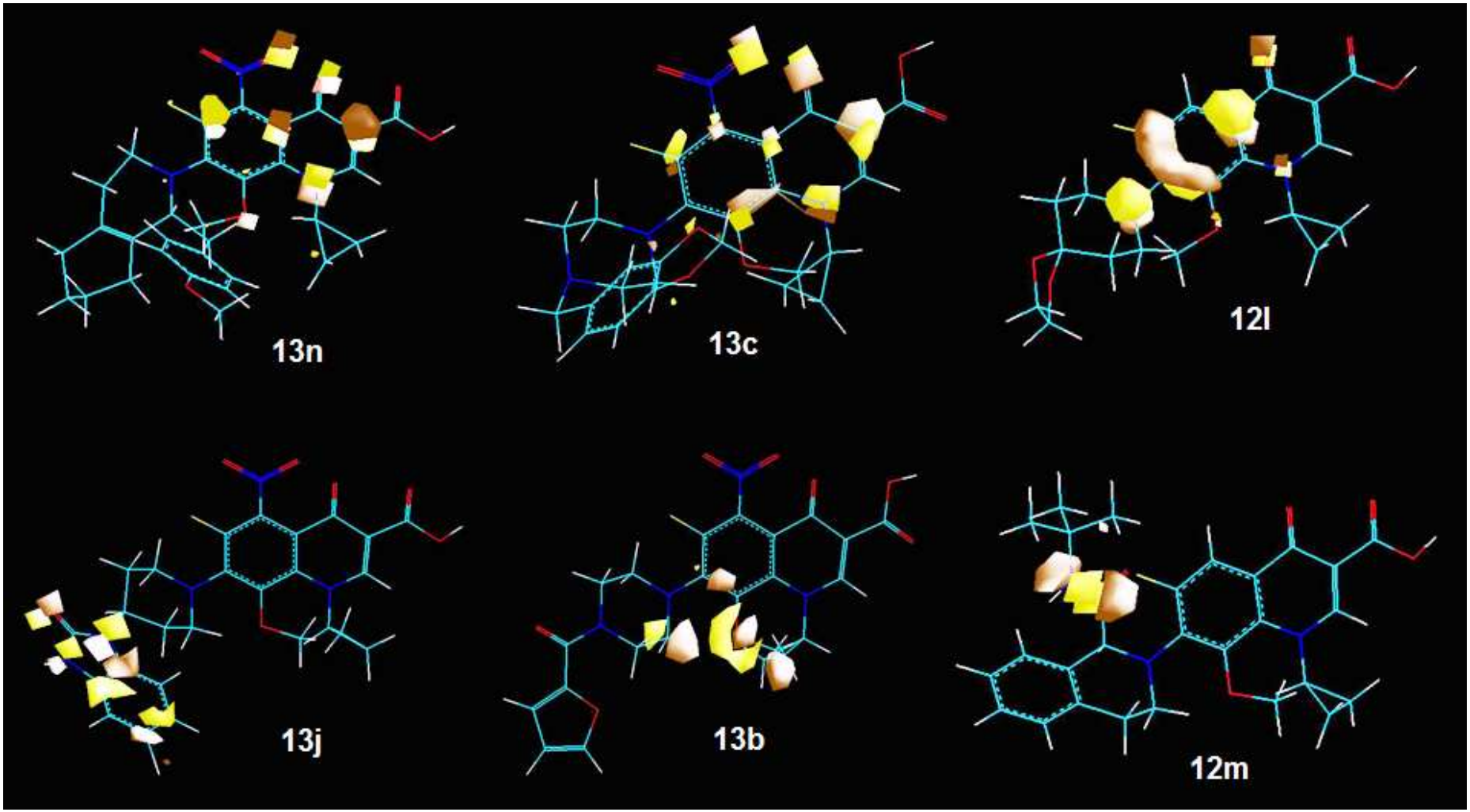

Figure 7.2: HOMO surface visualization (Contour value = 0.05) of some representative 8-methoxyquinolones (**MQ**) in opaque mode. The colors indicate the phase of the orbital in space (orange for positive and yellow for negative).

7.7 DISCUSSION

Thirty four new 8-methoxyquinolone carboxylic acids with variation at C_5 and C_7 positions were synthesized from 1,2,3,4-tetrafluoro benzene (**MQ 1**) according to the literature method [Burdon, J., *et al.*, 1966; Kuniyoshi, M., *et al.*, 1987; Mitscher, L. A., *et al.*, 1987] with modification in some steps (Figure 4.3). Compound **MQ 1** was converted to 1-bromo-2,3,4,5-tetrafluorobenzene (**MQ 2**) using bromine and aluminium bromide in presence of oleum, which was further methoxylated using sodium methoxide in methanol to yield 1-bromo-3-methoxy-2,4,5-trifluoro benzene (**MQ 3**). Compound **MQ 3** on treatment with cuprous cyanide and N-methyl-2-pyrrollidone gave the corresponding cyano derivative, 3-methoxy-2,4,5-trifluorobenzonitrile (**MQ 4**). Compound **MQ 4** was reduced to give the corresponding amide (**MQ 5**) which was further treated with sulphuric acid to form 3-methoxy-2,4,5-trifluoro benzoic acid (**MQ 6**). Compound **MQ 6** on reaction with 1, 1'-carbonyldiimidazole in tetrahydrofuran afforded the corresponding imidazolide, which, *in situ* was treated with neutral magnesium salt of ethyl potassium malonate in presence of triethyl amine to yield ethyl 3-(2,4,5-trifluoro-3-methoxyphenyl)-3-oxopropanoate (**MQ 7**). Ethyl 3-(cyclopropylamino)-2-(2,4,5-trifluoro-3-methoxybenzoyl)acrylate (**MQ 9**) were prepared by a two-step one-pot reaction. First treatment of the keto ester **MQ 7** with triethyl orthoformate in acetic anhydride gave the one-carbon homologue enol ether intermediate, ethyl 3-ethoxy-2-(2,4,5-trifluoro-3-methoxybenzoyl)acrylate (**MQ 8**) as an oil, which on reaction with cyclopropylamine at 0 °C affords 67 % of **MQ 9** as an oily residue. Compound **MQ 9** on cyclization with the base potassium carbonate in dimethyl sulphoxide yielded ethyl 1-cyclopropyl-6,7-difluoro-1,4-dihydro-8-methoxy-4-oxoquinoline-3-carboxylate (**MQ 10**), when compared to earlier report [Mitscher, L. A., *et al.*, 1987], this step proceeds smoothly with out using violently reactive sodium hydride. Ethyl ester was finally hydrolyzed in acidic condition to yield 1-cyclopropyl-6,7-difluoro-1,4-dihydro-8-methoxy-4-oxoquinoline-3-carboxylic acid (**MQ 11a**), which on nitration at C_5 position with sulphuric acid and potassium nitrate yielded 1-cyclopropyl-6,7-difluoro-1,4-dihydro-8-methoxy-5-nitro-4-oxoquinoline-3-carboxylic acid (**MQ 11b**). The titled compounds **MQ 12-13a-p** were prepared by treating **MQ 11a** and **MQ 11b** with appropriate secondary amines in presence of potassium carbonate under microwave irradiation in DMSO. When compared to

conventional method [Mitscher, L. A., *et al.,* 1987] of 12 hours process, microwave assisted synthesis was performed with short reaction times (3 - 6 minutes), with ease and was environment friendly. The over all yield of the synthesized compounds were in the range of 60 – 85 %. The purity of the synthesized compounds was monitored by TLC and elemental analyses and the structures were identified by spectral data.

In general, IR spectra showed C=O stretching peak of carboxylic acid at 1720 - 1730 cm^{-1}; C=O stretching peak of pyridine carbonyl at 1620 - 1630 cm^{-1} and absorption of aryl nitro group at 1470 - 1370 cm^{-1}. In the ^{1}H NMR spectra the signals of the respective protons of the prepared derivatives were verified on the basis of their chemical shifts, multiplicities and coupling constants. The spectra showed a broad singlet at δ 14.6 ppm corresponding to COOH proton; singlet at δ 9.52 ppm corresponding to C_2 proton; singlet at 9.34 ppm corresponding to C_5 proton; singlet at δ 3.51-3.57 ppm corresponding to C_8 methoxy protons; N_1 cyclopropyl protons showed multiplets at δ 1.42 (1H) and 0.28-0.48 (4H) ppm. The elemental analysis results were within ± 0.4% of the theoretical values.

Most of the compounds were found to be more lipophilic indicated by their calculated log of partition coefficient value greater than 2 [log P > 2]. No correlation has been established between the calculated log P and antimycobacterial activity of the compounds, as compounds with low log P were found to be more active than compounds with high log P.

In the first phase of screening against MTB, all the compounds showed excellent *in vitro* activity against MTB with MIC less than 15 μM. Five compounds (**MQ 13c, MQ 13g, MQ 12l, MQ 13l** and **MQ 13n**) inhibited MTB with MIC of less than 1 μM and were more potent than standard GAT (MIC: 1.04 μM). When compared to INH (MIC: 0.36 μM), one compound (**MQ 13n**) was found to be more active against MTB and one compound (**MQ 13c**) was found to be equally active to that of INH.

Compound 7-(1-(4-methoxybenzyl)-3,4,5,6,7,8-hexahydroisoquinolin-2(1*H*)-yl)-1-cyclopropyl-6-fluoro-1,4-dihydro-8-methoxy-5-nitro-4-oxoquinoline-3-carboxylic acid (**MQ 13n**) was found to be the most active compound *in vitro* with MIC of 0.16 μM against MTB and was 2.25 and 6.5 times more potent than INH and GAT respectively.

With respect to structure-MTB activity relationship, the results demonstrated that the antimycobacterial activity enhanced to varying degree (upto 9 fold) by the introduction nitro group at C_5 position. The *in vitro* antimycobacterial activity suggests that the favorable substitution C_5 at were NO_2 > H. At C_7 position we have studied with various substituted piperazines (**MQ 12-13a-e**), (thio) morpholines (**MQ 12-13f-g**), substituted piperidines (**MQ 12-13h-k**), fused piperazines & piperidines (**MQ 12-13l-o**) and oxazolidine (**MQ 12-13p**). Overall, a comparison of the substitution pattern at C_7 demonstrated that the order of activity was fused piperazines & piperidines ≥ (thio) morpholines and oxazolidine > substituted piperazines > substituted piperidines. By introducing bulky lipophilic secondary amines at C_7, enhanced the antimycobacterial activity which might be due to more penetration of these compounds into mycobacterial cells.

Subsequently some of the compounds were evaluated against MDR-TB, and among the twenty two compounds screened, all the compounds inhibited MDR-TB with MIC ranging from 0.33 - 3.99 μM and were found to be more active than INH (MIC: 45.57 μM), and GAT (MIC: 8.34 μM). Five compounds (**MQ 13c**, **MQ 12e, MQ 13l, MQ 13n** and **MQ 13p**) inhibited MDR - TB with MIC of less than 1 μM.

Compound **MQ 13n** was found to be most active *in vitro* with MIC of 0.33 μM against MDR - TB and was 25 and 138 times more potent than GAT and INH respectively.

In MDR-TB, the results demonstrated that the antimycobacterial activity imparted by C_5 substituents was in the order NO_2 > H. By introducing bulky lipophilic secondary amines at C_7, enhanced the antimycobacterial activity which might be due to more penetration of these compounds into mycobacterial cells.

The compounds were also evaluated against MC^2 in which all the compounds inhibited MC^2 with MIC ranging from 0.68 - 49.26 μM; thirty three compounds were found to be more active than INH (MIC: 45.57 μM) and six compounds were more active than GAT (MIC: 2.08 μM).

In MC^2, the results demonstrated that the antimycobacterial activity imparted by N_1 substituents was in the order NO_2 > H.

Twenty one compounds when tested for cytotoxicity showed CC_{50} values ranging from 102.96 - >166.06 μM. A comparison of the substitution pattern at C_5 demonstrated that nitro group was more cytotoxic than the unsubstituted derivatives. These results are important as the C_5 nitro substituted compounds with their increased cytoliability, are much less attractive in the development of a quinolone for the treatment of TB. This is primarily due to the fact that the eradication of TB requires a lengthy course of treatment, and the need for an agent with a high margin of safety becomes a primary concern. The CC_{50} values of compound **MQ 13n** was found to be 108.21 μM and showed selectivity index (CC_{50}/ MIC) of 676.31.

Compounds **MQ 12l** and **MQ 13n** were tested for *in vivo* efficacy against MTB at a dose of 50 mg/kg (Table 7.4) in CD - 1 mice [Sriram, D., *et al.,* 2005]. Compound **MQ 12l** decreased the bacterial load in lung and spleen tissues with 1.87 and 2.61-log10 protections respectively and was considered to be promising in reducing bacterial count in lung and spleen tissues. Compound **MQ 13n** decreased the bacterial load in lung and spleen tissues with 2.54 and 2.92-log10 protections respectively and was considered to be promising in reducing bacterial count in lung and spleen tissues. When compared to gatifloxacin at the same dose level **MQ 12l** decreased the bacterial load with 0.51-log10 protections and **MQ 13n** with 0.61 and 0.82-log10 protections in lung and spleen tissues respectively.

The 1-cyclopropyl-1,4-dihydro-6-fluoro-7-(substituted secondary amino)-8-methoxy-5-(sub)-4-oxoquinoline-3-carboxylic acid derivatives synthesized were tested for their ability to inhibit supercoiling activity of DNA gyrase. Earlier studies have revealed that DNA gyrase from MTB and MC^2 share many of the properties [Manjunatha, U. H., *et al.,* 2002]. The supercoiling assay results with various compounds using MC^2 DNA gyrase is presented in Figure 7.1 (1a, 1b, 1c and 1d). The IC_{50} values are presented in Table 7.5. Of all the newly synthesized compounds, compound **MQ 13n** inhibited supercoiling reaction with an IC_{50} value of 51.94 μM. Compound **MQ 12e** inhibited supercoiling reaction with an IC_{50} value of 57.31 μM. The other compounds that showed significant supercoiling inhibition include compound **MQ 12n** with IC_{50} values of 75.10 μM. Rest of the compounds tested did not show comparable inhibition of the enzyme (IC_{50} values > 87.95 μM).

Quinolones in general have favorable safety profiles; phototoxicity has become a significant factor in the clinical use of some. Indeed, the first quinolone, nalidixic acid, caused light-induced dermal effects. This type of response has now been demonstrated for almost all fluoroquinolones, although the relative phototoxic potential varies greatly among compounds. Phototoxicity is considered to be an acute, light-induced irritation response characterized by dermal inflammation, with erythema and edema as primary clinical endpoints. Phototoxicity with the quinolones is generally thought to result from the absorption of light by the parent compound or a metabolite in tissue. This photosensitized chromophore may then transfer its absorbed photo energy to oxygen molecules, creating an environment for the production of reactive oxygen species such as singlet oxygen. These reactive species are then thought to attack cellular lipid membranes, initiating the inflammatory process.

Five (**MQ 13c, MQ 12e, MQ 13g, MQ 12k** and **MQ 13n**) compounds were evaluated for potential phototoxicity in a standardized *in vivo* test system that has been used previously to assess quinolone antibiotics [Mayne, T. N., *et al.,* 1997]. The test compounds (140 mg/kg) and the positive control lomefloxacin hydrochloride (140 mg/kg) were evaluated for phototoxicity and both ears of each mouse were evaluated for changes indicative of a positive response: erythema, edema or a measurable increase in ear thickness. Change from baseline was calculated separately for each animal and time point and analyzed for statistical significance and presented in Table 7.6. The results indicated that lomefloxacin showed significant increase in ear thickness from 4 - 96 h and 24 - 96 h when compared within time points and with the control respectively. The test compounds were found to show a significant difference in ear thickness at various time - points when compared with the pre - drug reading (0 h) but were less toxic when compared with the negative (vehicle - treated) and positive control (lomefloxacin). Compounds **MQ 13c** and **MQ 13g** showed a slight increase in ear thickness from 48 - 96 h and 24 - 96 h respectively but were less toxic than the positive control (lomefloxacin). No erythema occurred in mice dosed with 140 mg/kg of **MQ 12e** and **MQ 13n** throughout the 96 h study, while compounds **MQ 13g** and **MQ 12k** showed a significant erythema after irradiation till 4 h only and compound **MQ 13c** developed erythema from 48 h.

In theory, quantum mechanical (QM) methods enable completely accurate prediction of any property; there are some important classes of property (notably reactivity, electronic, magnetic, and optical behavior) that can only be modeled using QM methods, because they are determined by electronic behavior that cannot be approximated well using other methods. In the present study the titled compounds were geometry optimized by semi-empirical PM3 QM method and subjected to single-point energy calculation to determine their HOMO and LUMO surfaces. Electron-rich and electron-poor species tend to reveal the localization or delocalization of the partial or full charge by the shape of the HOMO or LUMO. Molecular orbitals, when viewed in a qualitative graphical representation, can provide insight into the nature of reactivity, and some of the structural and physical properties of molecules.

In the present study the HOMO and LUMO surfaces were visualized for the synthesized compounds for comparison and the following observations were made. The N_1, NO_2 and the 4-oxo functions were found to play a crucial role in the antitubercular activity of 8-methoxyquinolones containing nitro group at 5^{th} position (**MQ 13n**) but in non nitro compounds (**MQ 12l**) N_1, N_7 and the 4-oxo functions were found to play a crucial role. This hypothesis was confirmed with the HOMO surface analysis (Figure 7.2), in which the most of the active compounds with lower MICs possessed the above pattern on HOMO surfaces. The absence of nitro group alters the electron distribution in compounds like **MQ 12l**, but the electrons provided by the oxygen of the nitro group is replaced by the electrons of N_7 and partly by the oxygen of methoxy group. With nitro substitution at C_5 position, the less active compounds were devoid of electron cloud around N_1, NO_2 and the oxo function at C_4. This observation was observed with all the less active compounds as seen with compounds **MQ 13j and MQ 13b** in figure 7.2. Similarly, with compounds with hydrogen at C_5 position, the less active compounds were devoid of electron cloud around N_1, N_7, and the oxo function at C_4. This observation was observed with all the less active compounds as seen with compound **MQ 12m** in figure 7.2. With respect to C_5 substituent, nitro was more preferable over unsubstituted compounds in retaining the electron-rich cloud as seen in the Figure 7.2 with compounds **FQ 13c and FQ 13n**. There was no significant difference observed in the LUMO orbital surfaces.

7.8 STRUCTURE - ACTIVITY RELATIONSHIP

The extensive studies on the activity profile against mycobacterium shows the following relationship between activity and the structure.

1. With respect to the substituents at C_5 position, the order of activity is NO_2 > H
2. With respect to the substituents at C_7 position, the order of activity is fused piperazines and piperidines ≥ (thio) morpholines & oxazolidines > substituted piperazines > substituted piperidines.
3. The N_1, NO_2 and the 4-oxo functions were found to play a crucial role in the antitubercular activity of 8-methoxyquinolones containing nitro group at 5^{th} position but in non-nitro compounds N_1, N_7 and the 4-oxo functions were found to play a crucial role.
4. NO_2 substituted compounds were found to be cytotoxic when compared with unsubstituted compounds.

MOST POTENT 8-METHOXYQUINOLONE (MQ) DERIVATIVE

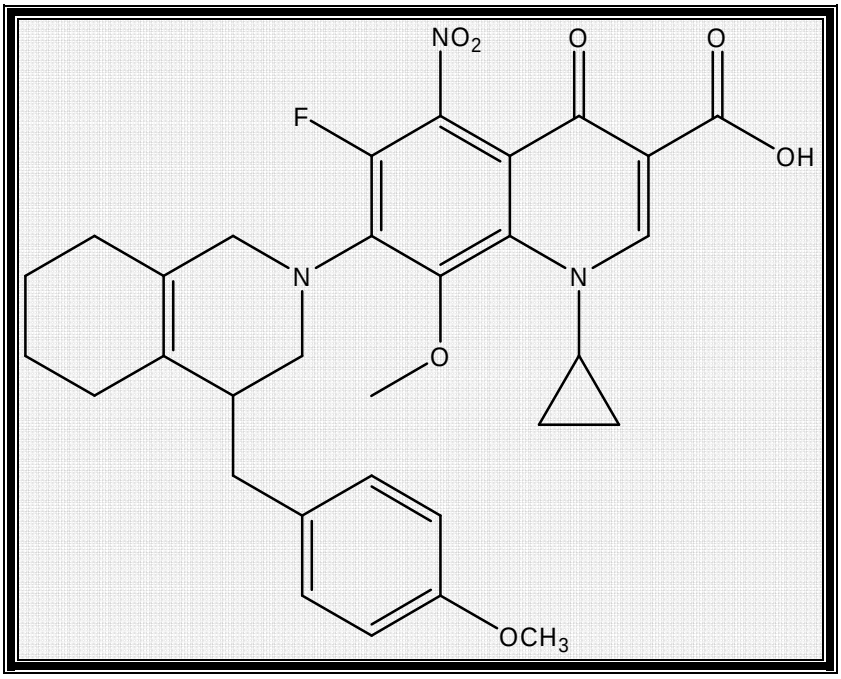

MQ 13n

1-Cyclopropyl-7-(8-(4-methoxybenzyl)-3,4,5,6,7,8-hexahydroisoquinolin-2(1H)-yl)-1,4-dihydro-6-fluoro-8-methoxy-5-nitro-4-oxoquinoline-3-carboxylic acid

- ***In vitro***:
  - **Against MTB**: 6.5 and 2.25 times more potent than GAT and INH respectively.
  - **Against MDRTB:** 25 and 138 times more potent than GAT and INH respectively.
  - **Against MC^2:** 3.06 and 67.01 times more active than GAT and INH respectively.
- ***Cytotoxicity***: Non-toxic up to 108.21 µM and showed selectivity index (CC_{50}/ MIC) of 676.31.
- ***In vivo***: Compared to GAT at the same dose level **MQ 13n** decreased the bacterial load with 0.61 and 0.82-log10 protections in lung and spleen tissues respectively.

CHAPTER 8

NITRO NAPHTHYRIDONE (NN) DERIVATIVES

8.1 SYNTHESIS

Various 1-(cyclopropyl/4-fluorophenyl/*t*-butyl)-1,4-dihydro-7-(sub secondary amino)-6-nitro-4-oxo-1,8-naphthyridone-3-carboxylic acids were prepared from 2,6-dimethoxynicotinic acid by the following steps of reaction:

STEP 1: Synthesis of 2,6-dimethoxy-5-nitropyridine-3-carboxylic acid (NN 2)

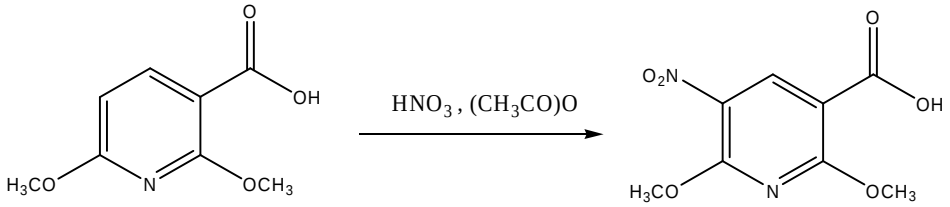

2,6-Dimethoxypyridine-3-carboxylic acid

NN 1

2,6-Dimethoxy-5-nitropyridine-3-carboxylic acid

NN 2

To a mixture of concentrated nitric acid (4 ml) and acetic anhydride (12 ml) was added drop wise 2,6-dimethoxynicotinic acid (**NN 1**) (16.3 mM) at 0 - 5 °C and stirred for 3 h. The temperature was brought upto room temperature and continued stirring for 4 h. The resulting precipitate was poured into ice-cold water and filtered. The precipitate was dissolved in ether and extracted with saturated sodium bicarbonate solution, and the aqueous layer on acidification with 2N HCl yielded **NN 2**.

Yield: 80 %; M.P.: 236 - 238 °C (lit ref. 230 °C); IR (KBr) cm^{-1}: 2900, 1726, 1470 - 1370; ^1H NMR (DMSO - d_6) δ ppm: 3.74 (s, 3H, 2 -OCH_3), 9.26 (s, 1H, C_4 - H), 14.0 (s, 1H, COOH); Anal ($C_8H_8N_2O_6$) C, H, N.

STEP 2: Synthesis of ethyl-3-(2,6-dimethoxy-5-nitropyridin-3-yl)-3-oxopropanoate (NN 3)

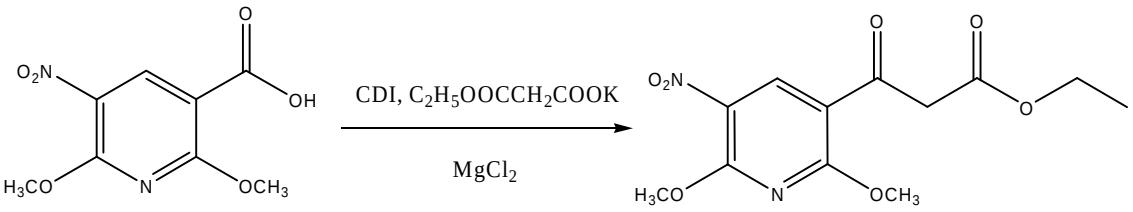

2,6-Dimethoxy-5-nitropyridine-3-carboxylic acid
NN 2

Ethyl 3-(2,6-dimethoxy-5-nitropyridin-3-yl)-3-oxopropanoate
NN 3

To a solution of **NN 2** (1.00 equiv.) in tetrahydrofuran, CDI (1.20 equiv.) was added for 30 minutes at a temperature of 70 ºC. The resulting crude imidazolide was used without further purification in the next step. To a solution of potassium salt of ethyl malonate (1.30 equiv.) in acetonitrile, was added drop wise magnesium chloride (2.00 equiv.) and triethyl amine (4.0 equiv.) at 0 ºC and stirred at room temperature for 2.5 h. To this solution, the imidazolide prepared above was added and the reaction mixture was refluxed at 70 ºC for 2.5 h. After completion of reaction, the solvent was distilled off and poured into ice water and acidified to pH 5-6 with 20 % HCl, then extracted with ethyl acetate (3 x 25ml) and dried over magnesium sulphate and distilled the solvent to give **NN 3**.

Yield: 80 %; M. P.: 235 – 237 °C; IR (KBr) cm^{-1}: 2900, 1726, 1705, 1470 - 1370; ^1H NMR (DMSO - d_6) δ ppm: 1.32 (t, 3H, CH_3 of $-OCH_2CH_3$), 3.42 (s, 2H, $COCH_2CO$), 3.74 (s, 3H, 2 $-OCH_3$), 4.22 (m, 2H, $-OCH_2$), 9.26 (s, 1H, C_4 - H), 14.0 (s, 1H, COOH); Anal ($C_{12}H_{14}N_2O_7$) C, H, N.

STEP 3: Synthesis of ethyl 1-(cyclopropyl/4-fluorophenyl/*t*-butyl)-7-methoxy-6-nitro-4-oxo-1,4-dihydro-1,8-naphthyridone-3-carboxylate (NN 6a-c)

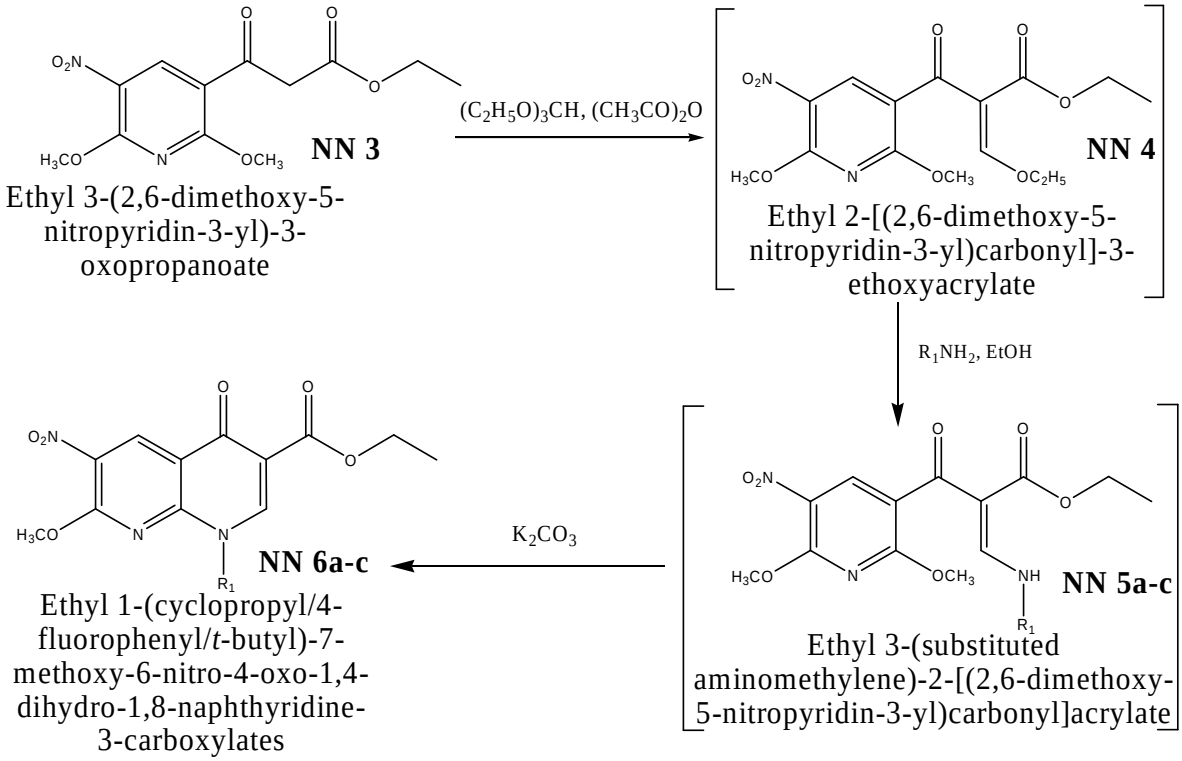

A mixture of **NN 3** (1.00 equiv.), triethylorthoformate (1.5 equiv.) and acetic anhydride (2.5 equiv.) were refluxed at 140 °C for 1 h. The ethyl acetate produced as a by product was distilled simultaneously under atmospheric pressure. After completion of reaction the reaction mixture was concentrated under reduced pressure to yield ethyl 2-[(2,6-dimethoxy-5-nitropyridin-3-yl)carbonyl]-3-ethoxyacrylate (**NN 4**). The above residue was dissolved in a mixture of ether (20 ml) and ethanol (20 ml). Added corresponding primary amine (1.1 equiv.) at 0 ºC and stirred for 30 minutes under nitrogen atmosphere, followed by distillation yielded ethyl 3-(substituted aminomethylene)-2-[(2,6-dimethoxy-5-nitropyridin-3-yl)carbonyl]acrylate (**NN 5a-c**). The above crude solid (1.0 equiv.) was dissolved in DMSO (30 ml) and added anhydrous potassium carbonate (1.6 equiv.) and refluxed at 60 °C for 3 h. After completion of reaction, the mixture was diluted with ice cold water and neutralized with 20 % HCl to a pH of 5-6. The precipitate thus formed was filtered and washed with

water followed by isopropanol to yield Ethyl 1-(cyclopropyl/*t*-butyl/4-fluorophenyl)-7-methoxy-6-nitro-4-oxo-1,4-dihydro-1,8-naphthyridone-3-carboxylates **NN 6a-c**.

Ethyl 1-cyclopropyl-7-methoxy-6-nitro-4-oxo-1,4-dihydro-1,8-naphthyridone-3-carboxylate (NN 6a): Yield: 92 %; M.P.: 210 – 212 ºC; IR (KBr) cm^{-1}: 2900, 1726, 1705, 1616, 1470 - 1370; ^{1}H NMR (DMSO - d_6) δ ppm: 0.28 - 0.53 (m, 4H, cyclopropyl), 1.32 (t, 3H, CH_3 of -OCH_2CH_3), 1.35 (m, 1H, cyclopropyl), 3.74 (s, 3H, -OCH_3), 4.22 (m, 2H, -OCH_2), 9.26 (s, 1H, C_5-H), 9.56 (s, 1H, C_2-H); Anal ($C_{15}H_{15}N_3O_6$) C, H, N.

Ethyl 1-(4-fluorophenyl)-7-methoxy-6-nitro-4-oxo-1,4-dihydro-1,8-naphthyridone-3-carboxylate (NN 6b): Yield: 92 %; M.P.: 204 – 206 ºC; IR (KBr)cm^{-1}: 2900, 1726, 1705, 1616, 1470 - 1370; ^{1}H NMR (DMSO - d_6) δ ppm: 1.32 (t, 3H, CH_3 of -OCH_2CH_3), 3.74 (s, 3H, -OCH_3), 4.22 (m, 2H, -OCH_2), 6.45-6.74 (m, 4H, Ar - H), 9.26 (s, 1H, C_5 - H), 9.56 (s, 1H, C_2 - H); Anal ($C_{18}H_{14}N_3O_6$) C, H, N.

Ethyl 1-*t*-butyl-7-methoxy-6-nitro-4-oxo-1,4-dihydro-1,8-naphthyridone-3-carboxylate (NN 6c): Yield: 92 %; M.P.: > 250 ºC; IR (KBr) cm^{-1}: 2900, 1726, 1705, 1616, 1470 - 1370; ^{1}H NMR (DMSO - d_6) δ ppm: 1.32 (t, 3H, CH_3 of -OCH_2CH_3), 1.76 (s, 9H, *t*-butyl), 3.74 (s, 3H, -OCH_3), 4.22 (m, 2H, -OCH_2), 9.26 (s, 1H, C_5 - H), 9.56 (s, 1H, C_2 - H); Anal ($C_{16}H_{19}N_3O_6$) C, H, N.

STEP 4: Synthesis of 1-(cyclopropyl/4-fluorophenyl/*t*-butyl)-1,4-dihydro-7-methoxy-6-nitro-4-oxo-1,8-naphthyridone-3-carboxylic acid (NN 7a-c)

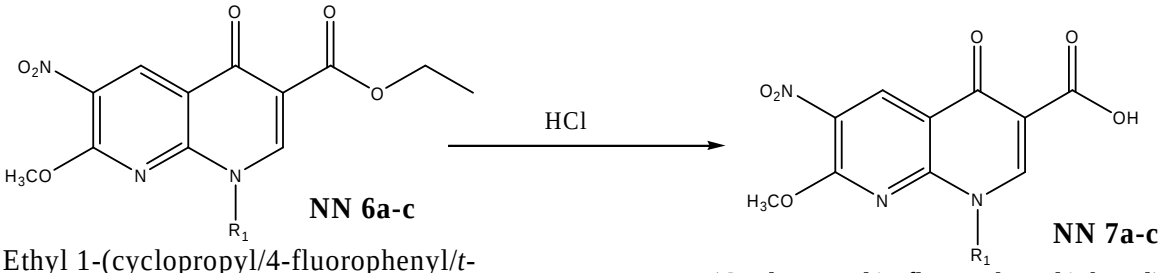

NN 6a-c

Ethyl 1-(cyclopropyl/4-fluorophenyl/*t*-butyl)-7-methoxy-6-nitro-4-oxo-1,4-dihydro-1,8-naphthyridine-3-carboxylates

NN 7a-c

1-(Cyclopropyl/4-fluorophenyl/*t*-butyl)-1,4-dihydro-7-methoxy-6-nitro-4-oxo-1,8-naphthyridine-3-carboxylic acid

Compound **NN 6a-c** (1.0 equiv.) was suspended in 6N HCl (5 ml) and refluxed for 6 h and

then cooled to 0 °C. The precipitate obtained was filtered, washed with water followed by 20% ethyl acetate yielded **NN 7a-c**.

1-Cyclopropyl-1,4-dihydro-7-methoxy-6-nitro-4-oxo-1,8-naphthyridone-3-carboxylic acid (NN 7a): Yield: 92 %; M.P.: 232 – 234 ºC; IR (KBr) cm^{-1}: 2900, 1726, 1705, 1616, 1470 - 1370; ^1H NMR (DMSO - d_6) δ ppm: 0.28 - 0.46 (m, 4H, cyclopropyl), 1.38 (m, 1H, cyclopropyl), 4.28 (s, 3H, methoxy), 9.26 (s, 1H, C_5 - H), 9.56 (s, 1H, C_2 - H), 14.6 (s, 1H, COOH); Anal ($C_{13}H_{11}N_3O_6$) C, H, N.

1-(4-Fluorophenyl)-1,4-dihydro-7-methoxy-6-nitro-4-oxo-1,8-naphthyridone-3-carboxylic acid (NN 7b): Yield: 92 %; M.P.: 196 – 198 ºC; IR (KBr) cm^{-1}: 2900, 1728, 1710, 1620, 1460 - 1370; ^1H NMR (DMSO - d_6) δ ppm: 4.34 (s, 3H, methoxy), 6.48 - 6.68 (m, 4H, Ar - H), 9.24 (s, 1H, C_5 - H), 9.56 (s, 1H, C_2 - H), 14.6 (s, 1H, COOH); Anal ($C_{16}H_{10}FN_3O_6$) C, H, N.

1-*t*-Butyl-1,4-dihydro-7-methoxy-6-nitro-4-oxo-1,8-naphthyridone-3-carboxylic acid (NN 7c): Yield: 92 %; M.P.: 239 – 241 ºC; IR (KBr) cm^{-1}: 2900, 1726, 1705, 1620, 1470 - 1370; ^1H NMR (DMSO - d_6) δ ppm: 1.6 (S, 9H, *t*-butyl), 4.32 (s, 3H, methoxy), 9.26 (s, 1H, C_5 - H), 9.54 (s, 1H, C_2 - H), 14.68 (s, 1H, COOH); Anal ($C_{14}H_{15}N_3O_6$) C, H, N.

STEP 5: Synthesis of 1-(cyclopropyl/4-fluorophenyl/*t*-butyl)-1,4-dihydro-6-nitro-4-oxo-7-(substituted secondary amines)-1,8-naphthyridone-3-carboxylic acid (NN 8-10a-q)

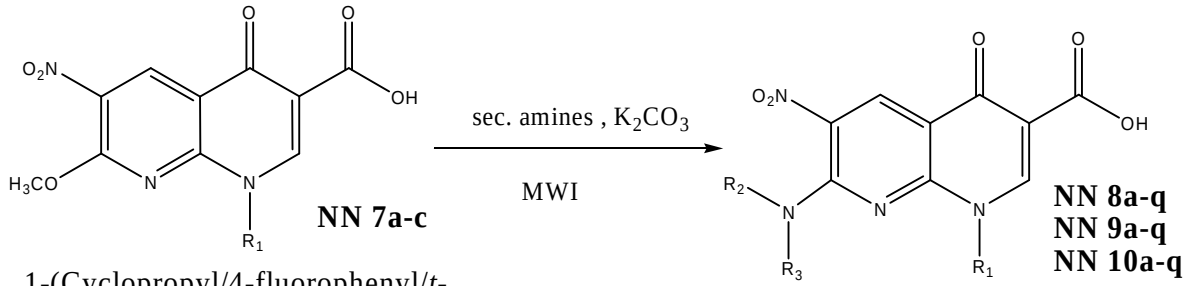

1-(Cyclopropyl/4-fluorophenyl/*t*-butyl)-1,4-dihydro-7-methoxy-6-nitro-4-oxo-1,8-naphthyridine-3-carboxylic acid

1-(Cyclopropyl/4-fluorophenyl/*t*-butyl)-1,4-dihydro-6-nitro-4-oxo-7-(substituted secondary amines)-1,8-naphthyridine-3-carboxylic acid

Compound **NN 7a-c** (1.0 equiv.) in dimethyl sulphoxide (2.5 ml) and appropriate secondary amines (1.1 equiv.) were irradiated in a microwave oven at an intensity of 560 W with 30 sec/cycle. The number of cycle in turn depended on the completion of the reaction, which was checked by TLC. The reaction timing varied from 1.5 - 3 min. After completion of the reaction, the mixture was poured into ice cold water and washed with water and isopropanol to give titled products.

Physical constants of the synthesized compounds are presented in table 8.1.

Spectral and elemental analysis data of representative nitro naphthyridone (**NN**) derivatives are presented in table 8.2.

Table 8.1: Physical constants of 1,8-naphthyridone-3-carboxylic acids (NN 8-10 a-q)

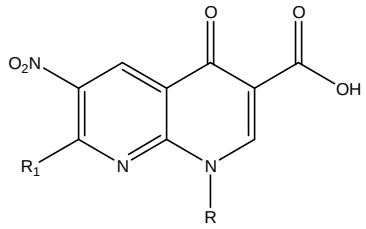

Compd	R	R_1	Yield (%)	M.P. (°C)	Molecular Formula	Molecular Weight	cLog P
NN 8a	Cyclopropyl	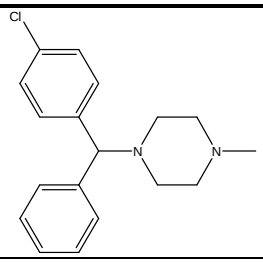	70	146 - 148	$C_{29}H_{26}ClN_5O_5$	560.00	2.03
NN 9a	4-F-Phenyl	- do -	75	110 - 112	$C_{32}H_{25}ClFN_5O_5$	614.02	3.55
NN 10a	*t*-Butyl	- do -	71	157 - 159	$C_{30}H_{30}ClN_5O_5$	576.04	2.91
NN 8b	Cyclopropyl	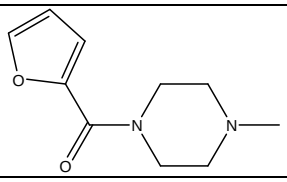	77	116 - 118	$C_{21}H_{19}N_5O_7$	453.40	0.04
NN 9b	4-F-Phenyl	- do -	76	174 - 176	$C_{24}H_{18}FN_5O_7$	507.43	1.56
NN 10b	*t*-Butyl	- do -	70	> 250	$C_{22}H_{23}N_5O_7$	469.45	0.92
NN 8c	Cyclopropyl	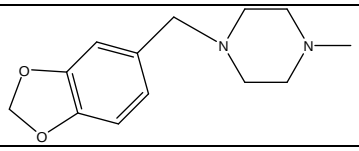	73	127 - 129	$C_{24}H_{23}N_5O_7$	493.47	-0.07
NN 9c	4-F-Phenyl	- do -	82	172 - 174	$C_{27}H_{22}FN_5O_7$	547.49	1.45
NN 10c	*t*-Butyl	- do -	75	180 - 182	$C_{25}H_{27}N_5O_7$	509.51	0.81
NN 8d	Cyclopropyl	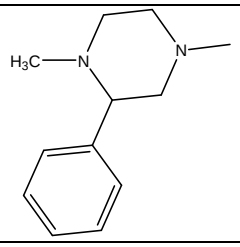	75	245 - 247	$C_{23}H_{23}N_5O_5$	449.46	-0.27
NN 9d	4-F-Phenyl	- do -	83	86 - 88	$C_{26}H_{22}FN_5O_5$	503.48	1.26
NN 10d	*t*-Butyl	- do -	74	232 - 234	$C_{24}H_{27}N_5O_5$	465.5	0.62
NN 8e	Cyclopropyl	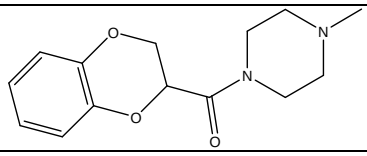	77	144 - 146	$C_{25}H_{23}N_5O_8$	521.48	1.31
NN 9e	4-F-Phenyl	- do -	85	176 - 178	$C_{28}H_{22}FN_5O_8$	575.50	2.83
NN 10e	*t*-Butyl	- do -	73	196 - 198	$C_{26}H_{27}N_5O_8$	537.52	2.19

Table 8.1: Physical constants of 1,8-naphthyridone-3-carboxylic acids (NN 8-10 a-q) (contd...)

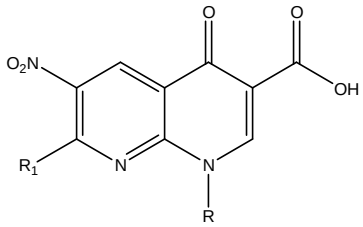

Compd	R	R_1	Yield (%)	M.P. (°C)	Molecular Formula	Molecular Weight	cLog P
NN 8f	Cyclopropyl	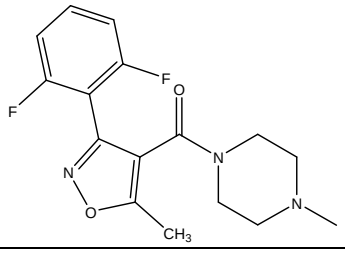	75	239 - 241	$C_{27}H_{22}F_2N_6O_7$	580.50	2.02
NN 9f	4-F-Phenyl	- do -	84	> 250	$C_{30}H_{21}F_3N_6O_7$	634.52	3.54
NN 10f	*t*-Butyl	- do -	70	> 250	$C_{28}H_{26}F_2N_6O_7$	596.54	2.90
NN 8g	Cyclopropyl	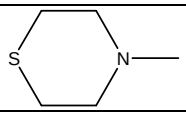	76	200 - 202	$C_{16}H_{16}N_4O_5S$	376.39	1.87
NN 9g	4-F-Phenyl	- do -	83	173 - 175	$C_{19}H_{15}FN_4O_5S$	430.41	3.39
NN 10g	*t*-Butyl	- do -	71	> 250	$C_{17}H_{20}N_4O_5S$	392.43	2.75
NN 8h	Cyclopropyl	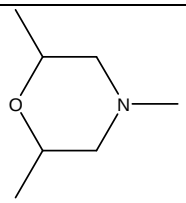	70	99 - 101	$C_{18}H_{20}N_4O_6$	388.37	1.92
NN 9h	4-F-Phenyl	- do -	81	105 - 107	$C_{21}H_{19}FN_4O_6$	442.40	3.44
NN 10h	*t*-Butyl	- do -	74	> 250	$C_{19}H_{24}N_4O_6$	404.42	2.80
NN 8i	Cyclopropyl	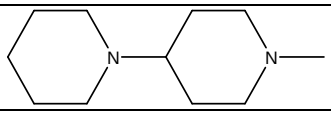	77	112 - 114	$C_{22}H_{27}N_5O_5$	441.48	0.12
NN 9i	4-F-Phenyl	- do -	80	> 250	$C_{25}H_{26}FN_5O_5$	495.50	1.64
NN 10i	*t*-Butyl	- do -	76	154 - 156	$C_{23}H_{31}N_5O_5$	457.52	1.00
NN 8j	Cyclopropyl	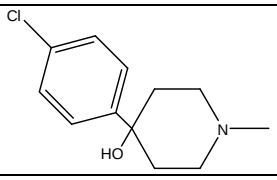	79	162 - 164	$C_{23}H_{21}ClN_4O_6$	484.89	2.90
NN 9j	4-F-Phenyl	- do -	79	225 - 227	$C_{26}H_{20}ClFN_4O_6$	538.91	4.42
NN 10j	*t*-Butyl	- do -	75	239 - 241	$C_{24}H_{25}ClN_4O_6$	500.93	3.79
NN 8k	Cyclopropyl	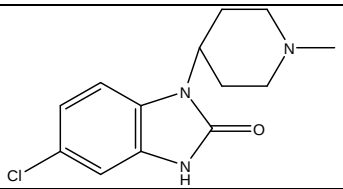	76	> 250	$C_{24}H_{21}ClN_6O_6$	524.91	3.63
NN 9k	4-F-Phenyl	- do -	78	> 250	$C_{27}H_{20}ClFN_6O_6$	578.94	5.14
NN 10k	*t*-Butyl	- do -	72	232 - 234	$C_{24}H_{24}ClN_7O_6$	541.94	3.68

Table 8.1: Physical constants of 1,8-naphthyridone-3-carboxylic acids (NN 8-10 a-q) (contd...)

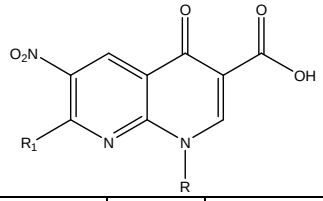

Compd	R	R_1	Yield (%)	M.P. (°C)	Molecular Formula	Molecular Weight	cLog P
NN 8l	Cyclopropyl	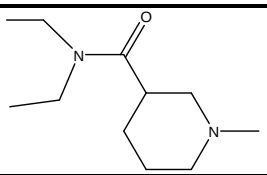	72	> 250	$C_{22}H_{27}N_5O_6$	457.48	3.14
NN 9l	4-F-Phenyl	- do -	75	217 - 219	$C_{25}H_{26}FN_5O_6$	511.50	3.87
NN 10l	*t*-Butyl	- do -	70	> 250	$C_{23}H_{31}N_5O_6$	473.52	3.23
NN 8m	Cyclopropyl	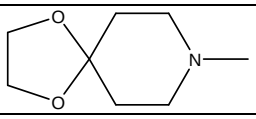	78	124 - 126	$C_{19}H_{20}N_4O_7$	416.38	0.96
NN 9m	4-F-Phenyl	- do -	85	145 - 147	$C_{22}H_{19}FN_4O_7$	470.41	2.48
NN 10m	*t*-Butyl	- do -	71	166 - 168	$C_{20}H_{24}N_4O_7$	432.43	1.84
NN 8n	Cyclopropyl	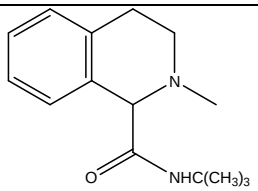	75	200 - 202	$C_{26}H_{27}N_5O_6$	505.52	3.10
NN 9n	4-F-Phenyl	- do -	82	128 - 130	$C_{29}H_{26}FN_5O_6$	559.55	4.63
NN 10n	*t*-Butyl	- do -	72	210 - 212	$C_{27}H_{31}N_5O_6$	521.56	3.99
NN 8o	Cyclopropyl	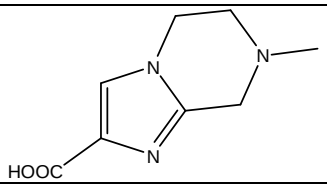	72	106 - 108	$C_{19}H_{16}N_6O_7$	440.37	1.41
NN 9o	4-F-Phenyl	- do -	84	216 - 218	$C_{22}H_{15}FN_6O_7$	494.39	2.93
NN 10o	*t*-Butyl	- do -	72	212 - 214	$C_{20}H_{20}N_6O_7$	456.41	2.29
NN 8p	Cyclopropyl	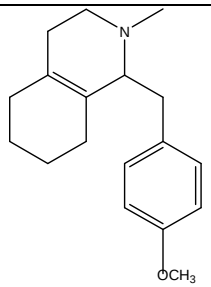	77	101 - 103	$C_{29}H_{30}N_4O_6$	530.57	5.57
NN 9p	4-F-Phenyl	- do -	76	82 - 84	$C_{32}H_{29}FN_4O_6$	584.59	7.09
NN 10p	*t*-Butyl	- do -	73	153 - 155	$C_{30}H_{34}N_4O_6$	546.61	6.46
NN 8q	Cyclopropyl	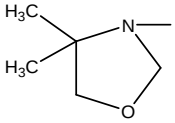	74	> 250	$C_{17}H_{18}N_4O_6$	374.35	2.02
NN 9q	4-F-Phenyl	- do -	81	192 - 194	$C_{20}H_{17}FN_4O_6$	428.37	3.50
NN 10q	*t*-Butyl	- do -	74	235 - 237	$C_{18}H_{22}N_4O_6$	390.39	2.86

Table 8.2: Spectral data and elemental analysis data of representative nitro naphthyridone (NN) derivatives

Compd	IR Spectroscopy (cm^{-1}; KBr)	^1H NMR (δ ppm, DMSO-d_6)	Elemental Analyses (Calculated/Found)		
			C	H	N
NN 8a	2900, 1708, 1724, 1620, 1460 - 1370	0.28 - 0.48 (m, 4H, cyclopropyl), 1.35 (m, 1H, cyclopropyl), 2.59 (t, 4H, 2 CH_2 of piperazine), 3.12 (t, 4H, 2 CH_2 of piperazine), 4.2 (s, 1H, CH of diphenylmethyl), 7.0 - 7.18 (m, 9H, Ar - H), 9.26 (s, 1H, C_5 - H), 9.56 (s, 1H, C_2 - H), 14.6 (s, 1H, COOH)	62.20 62.19	4.68 4.65	12.51 12.46
NN 9b	2890, 1710, 1724, 1624, 1460 - 1360	3.16 (t, 4H, 2 CH_2 of piperazine), 3.26 (t, 4H, 2 CH_2 of piperazine), 6.5 - 7.68 (m, 7H, Ar - H), 9.26 (s, 1H, C_5 - H), 9.56 (s, 1H, C_2 - H), 14.6 (s, 1H, COOH)	56.81 57.00	3.58 3.59	13.80 13.80
NN 10c	3250, 2890, 1710, 1724, 1624, 1464 - 1360	1.76 (s, 9H, *t*-butyl), 2.82 (t, 4H, 2 CH_2 of piperazine), 3.1 (t, 4H, 2 CH_2 of piperazine), 3.6 (s, 2H, CH_2 of piperanoyl), 5.86 (s, 2H, -OCH_2O-), 6.42 - 6.62 (m, 3H, Ar - H), 9.26 (s, 1H, C_5 - H), 9.56 (s, 1H, C_2 - H), 14.6 (s, 1H, COOH)	58.93 59.01	5.34 5.36	13.75 13.76
NN 8d	2890, 1710, 1724, 1620, 1460 - 1368	0.28 - 0.52 (m, 4H, cyclopropyl), 1.38 (m, 1H, cyclopropyl), 2.2 (s, 3H, CH_3), 2.6 (t, 2H, 5-CH_2 of piperazine), 3.15 (t, 2H, 6-CH_2 of piperazine), 3.4 (d, 2H, 2-CH_2 of piperazine), 4.12 (t, 1H, 3-CH of piperazine), 7.0 - 7.2 (m, 5H, Ar - H), 9.28 (s, 1H, C_5 - H), 9.56 (s, 1H, C_2 - H), 14.4 (s, 1H, COOH)	61.46 61.55	5.16 5.16	15.58 15.60
NN 9e	2890, 1710, 1724, 1624, 1460 - 1360	3.26 (t, 4H, 2 CH_2 of piperazine), 3.4 (t, 4H, 2 CH_2 of piperazine), 4.6 (d, 2H, 3-CH_2 of dihydrobenzodioxinyl), 5.14 (t, 1H, 2-CH of dihydrobenzodioxinyl), 6.5 - 6.98 (m, 8H, Ar - H), 9.26 (s, 1H, C_5 - H), 9.56 (s, 1H, C_2 - H), 14.6 (s, 1H, COOH)	58.44 58.44	3.85 3.84	12.17 12.20
NN 10f	2890, 1710, 1724, 1624, 1464 - 1360, 1208	1.74 (s, 9H, *t*-butyl), 2.3 (s, 3H, 5-CH_3 of isoxazolyl), 3.12 (t, 4H, 2 CH_2 of piperazine), 3.28 (t, 4H, 2 CH_2 of piperazine), 6.82 - 7.08 (m, 3H, Ar - H), 9.28 (s, 1H, C_5 - H), 9.54 (s, 1H, C_2 - H), 14.6 (s, 1H, COOH)	56.38 56.36	4.39 4.40	14.09 14.13
NN 8g	2890, 1710, 1724, 1620, 1460 - 1368	0.28 - 0.54 (m, 4H, cyclopropyl), 1.36 (m, 1H, cyclopropyl), 2.64 (t, 4H, 2 CH_2 of thiomorpholine), 3.38 (t, 4H, 2 CH_2 of thiomorpholine), 9.28 (s, 1H, C_5 - H), 9.56 (s, 1H, C_2 - H), 14.4 (s, 1H, COOH)	51.06 51.06	4.28 4.28	14.89 14.93
NN 9h	2892, 1710, 1724, 1628, 1460 - 1360	1.2 (d, 6H, 2 CH_3 of morpholino), 3.0 (d, 4H, 2 CH_2 of morpholine), 3.9 (m, 2H, 2 CH of morpholine), 6.4-6.7 (m, 4H, Ar - H), 9.26 (s, 1H, C_5-H), 9.56 (s, 1H, C_2-H), 14.6 (s, 1H, COOH)	57.01 56.99	4.33 4.31	12.66 12.72

Table 8.2: Spectral data and elemental analysis data of few representative nitro naphthyridone (NN) derivatives (contd…)

Compd	IR Spectroscopy (cm^{-1}; KBr)	^1H NMR (δ ppm, DMSO-d_6)	Elemental Analyses (Calculated/Found)		
			C	H	N
NN 10i	2890, 1710, 1724, 1624, 1464 - 1360	1.5 - 1.6 (m, 10H, 5 CH_2), 1.78 (s, 9H, *t*-butyl), 2.2 (t, 4H, 2 CH_2), 2.7 (m, 1H, CH), 2.8 (t, 4H, 2 CH_2), 9.28 (s, 1H, C_5 - H), 9.54 (s, 1H, C_2 - H), 14.6 (s, 1H, COOH)	60.30 60.22	6.83 6.85	15.31 15.28
NN 8j	2900, 1708, 1724, 1620, 1460 - 1370	0.28 - 0.46 (m, 4H, cyclopropyl), 1.32 (m, 1H, cyclopropyl), 2.0 (t, 4H, 2 CH_2 of piperidine), 2.7 (t, 4H, 2 CH_2 of piperidine), 7.1 - 7.18 (m, 4H, Ar-H), 9.26 (s, 1H, C_5 - H), 9.56 (s, 1H, C_2 - H), 10.0 (bs, 1H, OH), 14.6 (s, 1H, COOH)	56.97 57.01	4.37 4.37	11.55 11.59
NN 9k	3110, 2896, 1712, 1728, 1710, 1624, 1460 - 1360	1.6 - 2.4 (m, 8H, 4 CH_2 of piperidine), 4.1 (bm, 1H, CH of piperidine), 6.4 - 6.9 (m, 7H, Ar - H), 9.26 (s, 1H, C_5 - H), 9.56 (s, 1H, C_2 - H), 10.8 (s, 1H, NH), 14.6 (s, 1H, COOH)	56.01 56.10	3.48 3.46	14.52 14.54
NN 10l	2890, 1710, 1724, 1624, 1464 - 1360, 1208	1.2 (t, 6H, 2 CH_3 of ethyl), 1.7 (s, 9H, *t*-butyl), 1.78-2.7 (m, 9H, H of piperidine), 3.24 (q, 4H, 2 CH_2 of ethyl), 9.28 (s, 1H, C_5 - H), 9.54 (s, 1H, C_2 - H), 14.6 (s, 1H, COOH)	58.34 58.30	6.60 6.59	14.79 14.80
NN 8m	2890, 1712, 1724, 1618, 1466 - 1368	0.28 - 0.52 (m, 4H, cyclopropyl), 1.38 (m, 1H, cyclopropyl), 1.78 - 2.4 (m, 8H, 4 CH_2 of azaspirodecane), 3.96 (m, 4H, 2 CH_2 of azaspirodecane), 9.28 (s, 1H, C_5 - H), 9.56 (s, 1H, C_2 - H), 14.4 (s, 1H, COOH)	54.81 55.00	4.84 4.84	13.4 13.46
NN 9n	2890, 1712, 1724, 1626, 1468 - 1360	1.3 (s, 9H, 3 CH_3), 2.66 - 2.9 (m, 4H, 2 CH_2 of isoquinoline), 4.85 (s, 1H, CH of isoquinoline), 6.7 - 7.1 (m, 8H, Ar - H), 9.26 (s, 1H, C_5 - H), 9.56 (s, 1H, C_2 - H), 10.2 (s, 1H, NH), 14.6 (s, 1H, COOH)	62.25 62.20	4.68 4.69	12.52 12.57
NN 10o	3200, 2890, 1710, 1724, 1624, 1464 - 1360, 1208	1.74 (s, 9H, *t*-butyl), 3.1 - 3.8 (m, 6H, 3 CH_2), 7.6 (s, 1H, CH), 9.28 (s, 1H, C_5 - H), 9.54 (s, 1H, C_2 - H), 12.12 (s, 1H, 2-COOH), 14.6 (s, 1H, 3-COOH)	52.63 52.60	4.42 4.43	18.41 18.46
NN 8p	3210, 2890, 1710, 1724, 1620, 1460 - 1368	0.28 - 0.54 (m, 4H, cyclopropyl), 1.36 (m, 1H, cyclopropyl), 1.6 - 1.95 (m, 8H, 4 CH_2 of isoquinolinyl), 2.2 - 3.4 (m, 7H, 2 CH_2 and 1 CH of isoquinolinyl, and CH_2), 3.73 (s, 3H, -OCH_3), 6.8 - 7.1 (m, 4H, Ar - H), 9.28 (s, 1H, C_5 - H), 9.56 (s, 1H, C_2 - H), 14.4 (s, 1H, COOH)	65.65 65.65	5.70 5.68	10.56 10.60
NN 9q	2892, 1710, 1724, 1628, 1460 - 1360	1.16 (s, 6H, 2-CH_3), 3.41 (s, 2H, 5-CH_2 of oxazolidinyl), 4.6 (s, 2H, 2 CH of oxazolidinyl), 6.4 - 6.7 (m, 4H, Ar - H), 9.26 (s, 1H, C_5 - H), 9.56 (s, 1H, C_2 - H), 14.6 (s, 1H, COOH)	56.08 56.00	4.00 3.98	13.08 13.10

8.2 *IN VITRO* ANTIMYCOBACTERIAL AND CYTOTOXICITY

The synthesized compounds were tested for antimycobacterial activities against *Mycobacterium tuberculosis*, multi-drug resistant *Mycobacterium tuberculosis* and *Mycobacterium smegmatis* by agar dilution method and the results are tabulated in table 8.3. The compounds were also tested for there cytotoxicity in mammalian vero cell lines and the results are tabulated in table 8.3.

8.3 *IN VIVO* ANTIMYCOBACTERIAL STUDY

One compound **NN 10q** was tested *in vivo* model against *M. tuberculosis* and the results are tabulated in table 8.4

8.4 DNA GYRASE SUPERCOILING ASSAY

Nine compounds were tested for DNA gyrase enzyme supercoiling assay and the results are tabulated in table 8.5. The gel picture of the enzyme inhibition study is shown in figure 8.1.

8.5 PHOTOTOXICITY EVALUATION

Six compounds were evaluated for potential phototoxicity in a standardized *in vivo* test system and the results are tabulated in table 8.6.

8.6 QUANTUM MECHANICAL MODELING

In the present study the HOMO and LUMO surfaces were visualized for the titled compounds for comparison (Figure 8.2)

Table 8.3: *In vitro* antimycobacterial and cytotoxicity data of 1,8-naphthyridone-3-carboxylic acids (NN 8-10 a-q)

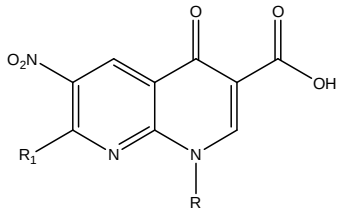

Compd	R	R_1	CC_{50} (μM)	MIC (μM)		
				MTB	MDR-TB	MC[2]
NN 8a	Cyclopropyl	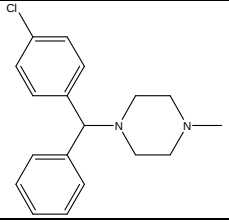	111.6	5.59	NT	22.32
NN 9a	4-F-Phenyl	- do -	101.8	1.27	0.31	5.09
NN 10a	*t*-Butyl	- do -	> 108.5	1.35	NT	173.59
NN 8b	Cyclopropyl	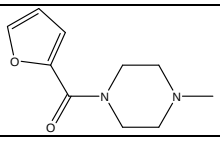	68.9	6.90	3.44	27.57
NN 9b	4-F-Phenyl	- do -	123.2	3.07	1.54	24.63
NN 10b	*t*-Butyl	- do -	133.1	3.32	3.32	6.67
NN 8c	Cyclopropyl	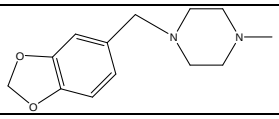	126.7	3.16	1.58	25.33
NN 9c	4-F-Phenyl	- do -	57.1	11.42	NT	45.66
NN 10c	*t*-Butyl	- do -	> 122.7	1.53	3.06	6.14
NN 8d	Cyclopropyl	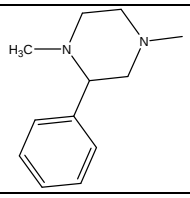	139.1	6.96	NT	27.81
NN 9d	4-F-Phenyl	- do -	124.1	0.77	0.18	3.09
NN 10d	*t*-Butyl	- do -	> 134.3	0.84	0.84	13.43
NN 8e	Cyclopropyl	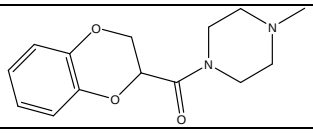	59.9	11.98	1.49	6.00
NN 9e	4-F-Phenyl	- do -	> 54.3	10.86	NT	21.72
NN 10e	*t*-Butyl	- do -	116.3	1.45	2.90	5.82
NN 8f	Cyclopropyl	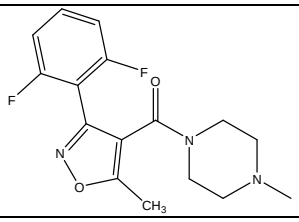	107.7	21.53	NT	86.13
NN 9f	4-F-Phenyl	- do -	98.5	9.85	NT	39.39
NN 10f	*t*-Butyl	- do -	104.8	2.62	1.31	10.48

Table 8.3: *In vitro* antimycobacterial and cytotoxicity data of 1,8-naphthyridone-3-carboxylic acids (NN 8-10 a-q) (contd…)

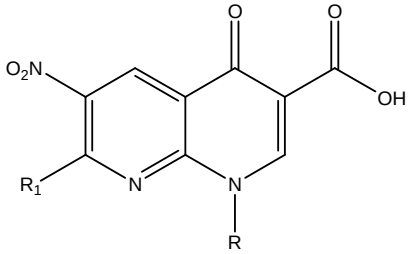

Compd	R	R_1	CC_{50} (μM)	MIC (μM)		
				MTB	MDR-TB	MC^2
NN 8g	Cyclopropyl	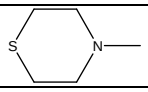	166.1	8.32	NT	33.21
NN 9g	4-F-Phenyl	- do -	72.6	0.44	0.91	1.81
NN 10g	*t*-Butyl	- do -	79.6	0.99	0.48	1.99
NN 8h	Cyclopropyl	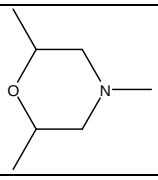	> 160.9	4.02	4.02	32.19
NN 9h	4-F-Phenyl	- do -	141.3	0.43	0.43	1.79
NN 10h	*t*-Butyl	- do -	159.3	7.74	NT	15.45
NN 8i	Cyclopropyl	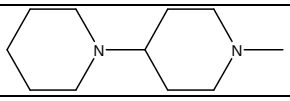	> 141.6	7.09	NT	28.31
NN 9i	4-F-Phenyl	- do -	> 126.1	3.15	1.57	25.23
NN 10i	*t*-Butyl	- do -	> 136.6	1.70	1.70	6.84
NN 8j	Cyclopropyl	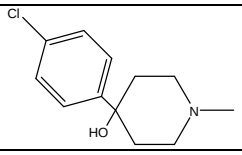	64.4	6.46	NT	25.78
NN 9j	4-F-Phenyl	- do -	59.6	2.89	0.72	11.59
NN 10j	*t*-Butyl	- do -	124.8	3.11	1.56	24.95
NN 8k	Cyclopropyl	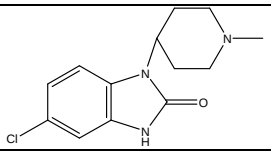	55.5	2.97	0.74	23.81
NN 9k	4-F-Phenyl	- do -	53.9	2.69	0.62	10.79
NN 10k	*t*-Butyl	- do -	57.7	2.88	2.88	11.53
NN 8l	Cyclopropyl	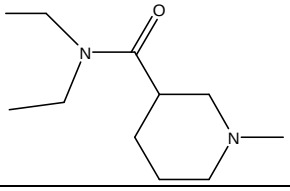	> 136.7	3.41	NT	109.29
NN 9l	4-F-Phenyl	- do -	> 122.2	3.05	1.52	12.22
NN 10l	*t*-Butyl	- do -	> 131.9	3.29	NT	105.59

Table 8.3: *In vitro* antimycobacterial and cytotoxicity data of 1,8-naphthyridone-3-carboxylic acids (NN 8-10 a-q) (contd…)

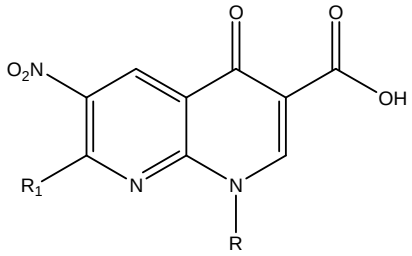

Compd	R	R_1	CC_{50} (μM)	MIC (μM)		
				MTB	MDR-TB	MC^2
NN 8m	Cyclopropyl	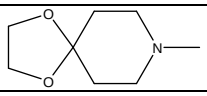	150.1	7.52	NT	30.02
NN 9m	4-F-Phenyl	- do -	132.9	6.65	NT	26.57
NN 10m	*t*-Butyl	- do -	144.5	0.90	0.44	3.61
NN 8n	Cyclopropyl	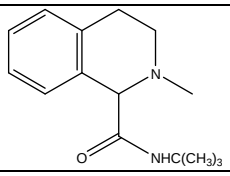	123.6	3.09	6.19	24.73
NN 9n	4-F-Phenyl	- do -	111.7	2.79	1.39	11.17
NN 10n	*t*-Butyl	- do -	119.8	2.99	1.49	6.00
NN 8o	Cyclopropyl	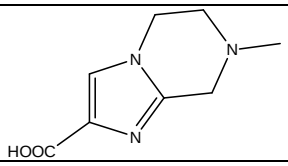	141.9	3.54	1.77	28.39
NN 9o	4-F-Phenyl	- do -	> 126.4	0.38	0.08	1.58
NN 10o	*t*-Butyl	- do -	> 136.9	0.42	0.42	6.86
NN 8p	Cyclopropyl	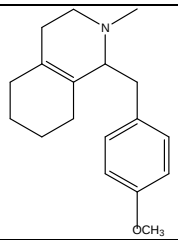	117.8	5.89	0.74	1.47
NN 9p	4-F-Phenyl	- do -	< 53.5	10.69	NT	85.53
NN 10p	*t*-Butyl	- do -	> 114.3	5.73	NT	11.43
NN 8q	Cyclopropyl	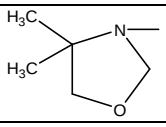	167.1	0.51	NT	4.17
NN 9q	4-F-Phenyl	- do -	> 145.9	0.21	<0.10	1.82
NN 10q	*t*-Butyl	- do -	> 160.1	0.10	0.10	3.99
Gatifloxacin	-	-	> 155.3	1.04	8.34	2.08
INH	-	-	> 455.8	0.36	45.57	45.57

Table 8.4: *In vivo* activity data of NN 10q, gatifloxacin and isoniazid against *M. tuberculosis* ATCC 35801 in mice.

Compound	Lungs (log CFU ± SEM)	Spleen (log CFU ± SEM)
Control	7.99 ± 0.16	9.02 ± 0.21
Gatifloxacin (50 mg/kg)	6.02 ± 0.23	6.92 ± 0.07
Isoniazid (25 mg/kg)	5.86 ± 0.23	4.71 ± 0.10
NN 10q (50 mg/kg)	5.60 ± 0.08	5.13 ± 0.16

Table 8.5: IC_{50} values for DNA gyrase inhibition of 1,8-naphthyridone-3-carboxylic acids (NN)

Compounds	IC_{50} (μM)
NN 8p	56.54
NN 9d	99.31
NN 9g	> 232.34
NN 9h	226.04
NN 9o	> 202.27
NN 9q	116.72
NN 10g	101.93
NN 10m	92.50
NN 10q	256.15
Ciprofloxacin	15.09
Moxifloxacin	12.46

Table 8.6: Phototoxicity evaluation of 1,8-naphthyridone-3-carboxylic acid (NN)

Group	Ear thickness (mm)[a]						Erythema[b]					
	Time (approximately) after start of irradiation (h)[c]											
	0	4	24	48	72	96	0	4	24	48	72	96
Control[d]	0.37 ± 0.03	0.36 ± 0.02	0.38 ± 0.03	0.37 ± 0.03	0.37 ± 0.03	0.38 ± 0.03	0	0	0	0	0	0
NN 9g	0.25 ± 0.01	0.27 ± 0.01	0.26 ± 0.01	0.26 ± 0.01	0.29 ± 0.01$^{\#}$	0.29 ± 0.02$^{\#}$	0	0	0	0	0	0
NN 10g	0.27 ± 0.01	0.28 ± 0.02	0.28 ± 0.02	0.29 ± 0.02	0.30 ± 0.02	0.32 ± 0.02	0	0	0	0	0	0
NN 9h	0.26 ± 0.01	0.25 ± 0.01	0.28 ± 0.01	0.27 ± 0.01	0.30 ± 0.01$^{\#}$	0.30 ± 0.01$^{\#}$	0	0	0	0	0	0
NN 9o	0.27 ± 0.01	0.32 ± 0.01$^{\#}$	0.33 ± 0.03$^{\#}$	0.32 ± 0.02$^{\#}$	0.33 ± 0.01$^{\#}$	0.33 ± 0.02$^{\#}$	0	4	4	0	0	0
NN 8p	0.33 ± 0.01	0.34 ± 0.02	0.34 ± 0.01	0.38 ± 0.02$^{\#}$	0.36 ± 0.01	0.33 ± 0.02	0	0	0	1[e]	0	0
NN 10q	0.24 ± 0.01	0.28 ± 0.02	0.26 ± 0.01	0.29 ± 0.02$^{\#}$	0.30 ± 0.02$^{\#}$	0.30 ± 0.02$^{\#}$	0	0	0	4	4	4
Lomefloxacin	0.31 ± 0.01	0.40 ± 0.02$^{*\#}$	0.48 ± 0.02$^{*\#}$	0.53 ± 0.02$^{*\#}$	0.64 ± 0.04$^{*\#}$	0.60 ± 0.06$^{*\#}$	0	6	6	6	6	6

[a] Mean Ear Thickness ± SEM; left and right ears were averaged
[b] Number of mice with erythema
[c] Time zero = pre-dose (mice exposed to UVA light immediately after dosing); 4 h = end of irradiation period.
[d] Control = 0.5 % aqueous solution of sodium carboxymethylcellulose (4 Ns/m^2) dosed at 10 mL/kg.
[e] Very slight erythema, not considered to be drug-related.
[*] Mean Ear Thickness ± SEM; significant difference from control at $P < 0.05$.
[#] Mean Ear Thickness ± SEM; significant difference from 0 h at $P < 0.05$.

Gyrase	-	+	+	+	+	+	+	+	+	+	+	+	+
Compounds	-	-	-	-	**8p**	**9o**	**9d**	**9h**	**9g**	**9q**	**10m**	**10g**	**10q**
Concentration	-	-	-	-	30	100	50	100	100	50	40	40	100
Controls	-	**DMSO**	**Cipro**	**Moxi**	-	-	-	-	-	-	-	-	-

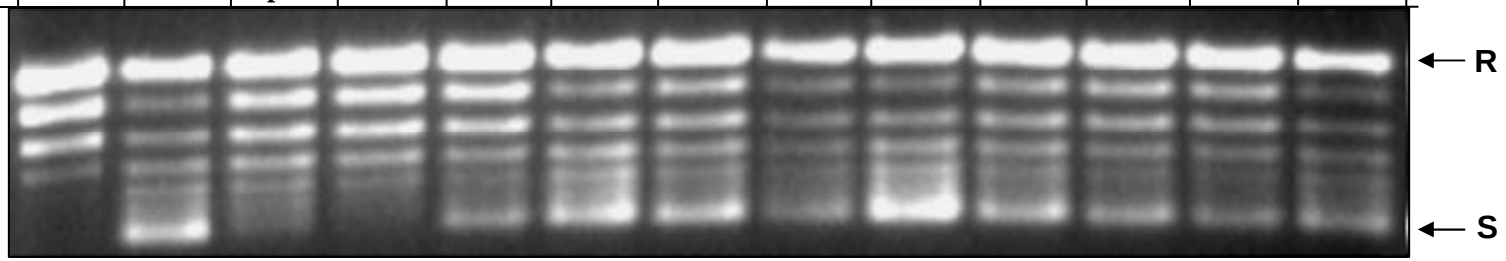

Figure 8.1: Gel picture for DNA gyrase supercoiling assay of 1,8-naphthyridone-3-carboxylic acid (**NN**).
The assays were performed as described in experimental section. DNA gyrase was incubated with indicated concentrations of the compounds before the addition of rest of the components.
Lane 1: relaxed DNA, lane 2: supercoiling reaction in presence of 5 % DMSO, Ciprofloxacin (lane 3) and moxifloxacin at concentration of 5 µg/ml (lane 4) were used as the positive controls for inhibition of enzyme. Lane 5 30 µg/ml **NN 8p**, lane 6: 100 µg/ml of **NN 9o,** lane 78: 50 µg/ml of **NN 9d**, lane 8: 100 µg/ml **NN 9h,** lane 9: 100 µg/ml **NN 9g**, lane 10: 50 µg/ml **NN 9q**, lane 11: 40 µg/ml **NN 10m**, lane 12: 40 µg/ml **NN 10g**, lane 13: 100 µg/ml **NN 10q**. R and S indicate relaxed and super coiled pUC18 DNA respectively.

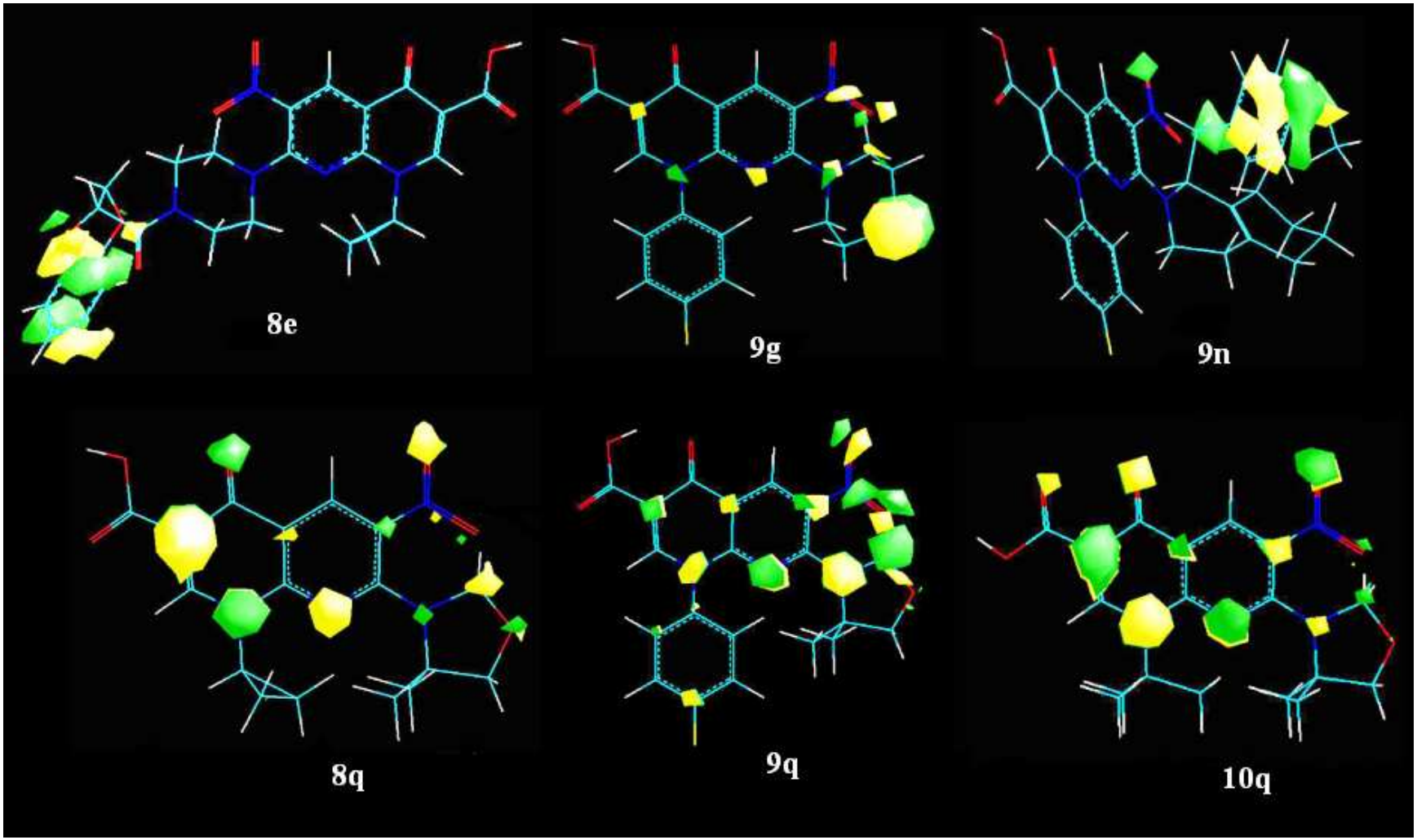

Figure 8.2: HOMO surface visualization (Contour value = 0.05) of some representative 1,8-naphthyridone-3-carboxylic acid (**NN**) in opaque mode. The colors indicate the phase of the orbital in space (green for positive and yellow for negative).

8.7 DISCUSSION

The synthesis of the fifty one compounds **NN 8-10a-q** was accomplished as outlined in figure 4.4. The 2,6-dimethoxynicotinic acid (**NN 1**) was converted to 2,6-dimethoxy-5-nitronicotinic acid (**NN 2**) by treatment with nitric acid in presence of acetic anhydride. Compound **NN 2** on reaction with 1, 1'-carbonyldiimidazole in tetrahydrofuran afforded the corresponding imidazolide, which, in-situ was treated with neutral magnesium salt of ethyl potassium malonate in presence of triethylamine to yield ethyl-3-(2,6-dimethoxy-5-nitropyridin-3-yl)-3-oxopropanoate (**NN 3**). Ethyl 1-(cyclopropyl/4-fluorophenyl/*t*-butyl)-7-methoxy-6-nitro-4-oxo-1,4-dihydro-1,8-naphthyridine-3-carboxylate (**NN 6a-c**) were prepared by a three-step one-pot reaction. First treatment of the keto ester **NN 3** with triethyl orthoformate in acetic anhydride gave the one-carbon homologue enol ether intermediate ethyl 2-[(2,6-dimethoxy-5-nitropyridin-3-yl)carbonyl]-3-ethoxyacrylate (**NN 4**), which upon evaporation to dryness was allowed to react with slight excess of appropriate amines under nitrogen atmosphere in a mixture of ether and ethanol at 0 °C gave the enamino ester ethyl 3-(substituted aminomethylene)-2-[(2,6-dimethoxy-5-nitropyridin-3-yl)carbonyl]acrylate (**NN 5**), and base catalyzed cyclization of **NN 5a-c** with potassium carbonate in DMSO yielded naphthyridone **NN 6a-c**. Ethyl esters were finally hydrolyzed in acidic condition to yield 1-(cyclopropyl/4-fluorophenyl/*t*-butyl)-1,4-dihydro-7-methoxy-6-nitro-4-oxo-1,8-naphthyridine-3-carboxylic acid (**NN 7a-c**). The titled compounds **NN 8-10a-q** was prepared by treating **NN 7a-c** with appropriate secondary amines in presence of potassium carbonate under microwave irradiation in DMSO. When compared to conventional method [Tsuzuki, Y., *et al.,* 2004] of 2 - 3 h process, microwave assisted synthesis was performed with short reaction times (2 - 3 minutes), with ease and was environment friendly. The over all yield of the synthesized compounds were in the range of 70 - 85 %. The purity of the synthesized compounds was monitored by thin layer chromatography (TLC) and elemental analyses and the structures were identified by spectral data.

In general, IR spectra showed C=O stretching peak of carboxylic acid at 1720 - 1730 cm^{-1}; C=O stretching peak of pyridine carbonyl at 1620 - 1630 cm^{-1} and absorption of aryl nitro group at 1470 - 1370 cm^{-1}. In the ^{1}H NMR spectra the signals of the respective protons of the

prepared derivatives were verified on the basis of their chemical shifts, multiplicities and coupling constants. The spectra showed a broad singlet at δ 14.6 ppm corresponding to COOH proton; singlet at δ 9.52 ppm corresponding to C_2 proton; singlet at δ 9.34 ppm corresponding to C_5 proton; N_1 cyclopropyl protons showed multiplets at δ 1.42 (1H) and 0.28-0.48 (4H) ppm; N_1 *t*-butyl protons showed singlet at δ 1.62 (9H) ppm; and N_1 4-fluorophenyl protons showed multiplet at δ 6.50 - 6.72 (4H) ppm. The elemental analysis results were within ± 0.4% of the theoretical values.

Most of the compounds were found to be more lipophilic indicated by their calculated log of partition coefficient value greater than 2 [log P > 2]. No correlation has been established between the calculated log P and antimycobacterial activity of the compounds, as compounds with low log P were found to be more active than compounds with high log P.

In the first phase of screening against MTB, all the compounds showed excellent *in vitro* activity against MTB with MIC of less than 12 μM. Eleven compounds (**NN 9d**, **NN 10d, NN 9g, NN 10g, NN 9h, NN 10m, NN 9o, NN 10o, NN 8q, NN 9q** and **NN 10q**) inhibited MTB with MIC of less than 1 μM and were more potent than standard fluoroquinolone GAT (MIC: 1.04 μM). When compared to INH (MIC: 0.36 μM), two compounds (**NN 9q** and **NN 10q**) were found to be more active against MTB.

Compound 1-*tert*-butyl-1,4-dihydro-7-(4,4-dimethyloxazolidin-3-yl)-6-nitro-4-oxo-1,8-naphthyridine-3-carboxylic acid (**NN 10q**) was found to be the most active compound *in vitro* with MIC of 0.1 μM against MTB and was 3.6 and 10.4 times more potent than INH and GAT respectively.

With respect to structure-MTB activity relationship, we have studied with various substituted piperazines (**NN 8-10a-f**), (thio) morpholines (**NN 8-10g-h**), substituted piperidines (**NN 8-10i-n**), fused piperazines and piperidines (**NN 8-10o-p**) and oxazolidine (**NN 8-10q**) at C_7 position. The results demonstrated that the contribution of the C_7 position to antimycobacterial activity was dependent on the substituent at N_1 and was in the order of oxazolidine > fused piperazines & piperidines > (thio) morpholines > substituted piperidines > substituted piperazines when N_1 was cyclopropyl; oxazolidine > (thio) morpholines > substituted piperazines > substituted piperidines > fused piperazines & piperidines when N_1

was 4-fluorophenyl; oxazolidine > substituted piperazines > substituted piperidines > (thio) morpholines > fused piperazines & piperidines when N_1 was *tert*-butyl. Overall, a comparison of the substitution pattern at C_7 demonstrated that the order of activity was oxazolidine > fused piperazines & piperidines > (thio) morpholines > substituted piperazines ≥ substituted piperidines.

The results demonstrated that the antimycobacterial activity imparted by N_1 substituent was in the order of *tert*-butyl > 4-flurophenyl > cyclopropyl. This result was in contrast to the other antibacterial fluoroquinolones, where cyclopropyl group was the favorable substituent. This result correlate well with the previous report on the importance of *tert*-butyl group as antimycobacterial pharmacophore [Artico, M., *et al.,* 1999]. The enhanced activity of the *tert*-butyl group could be supported by its better electron-donating property and its higher hydrophobicity than the cyclopropyl group which provide support for the cooperative-binding model for the inhibition of DNA gyrase proposed by Shen, in which two quinolone molecules self associate by π-π ring stacking and tail-to-tail hydrophobic interaction between the N_1 substituents [Shen, L. L., 1994].

Subsequently some of the compounds were evaluated against MDR-TB, and among the thirty three compounds screened; all the compounds inhibited MDR-TB with MIC ranging from 0.08 - 6.19 μM and were found to be more active than INH (MIC: 45.57 μM) and GAT (MIC: 8.34 μM). Fifteen compounds (**NN 9a**, **NN 9d, NN 10d, NN 9g, NN 10g, NN 9h, NN 9j, NN 8k, NN 9k, NN 10m, NN 9o, NN 10o, NN 8p, NN 9q** and **NN 10q**) inhibited MDR-TB with MIC of less than 1 μM.

Compound 7-(2-carboxy-5,6-dihydroimidazo[1,2-a]pyrazin-7(8H)-yl)-1-(4-fluorophenyl)-1,4-dihydro-6-nitro-4-oxo-1,8-naphthyridine-3-carboxylic acid (**NN 9o**) was found to be the most active compound *in vitro* with MIC of 0.08 μM against MDR-TB and was 104 and 570 times more potent than GAT and INH respectively.

In MDR-TB, the results demonstrated that the antimycobacterial activity imparted by N_1 substituents was in the order 4-fluorophenyl > *tert*-butyl > cyclopropyl. By introducing bulky lipophilic secondary amines at C_7, enhanced the antimycobacterial activity which might be due to more penetration of these compounds into mycobacterial cells.

The compounds were also evaluated against MC^2 in which all the compounds inhibited MC^2 with MIC ranging from 1.47 - 173.59 μM and forty five compounds were found to be more active than INH (MIC: 45.57 μM).
In MC^2, the results demonstrated that the antimycobacterial activity imparted by N_1 substituents was in the order *tert*-butyl > 4-flurophenyl > cyclopropyl.

Fifteen compounds when tested for cytotoxicity showed CC_{50} values ranging from 55.5 - >160.1 μM. A comparison of the substitution pattern at C_7 demonstrated that piperidine-substituted analogs were more cytotoxic than the substituted piperazines. These results are important as the piperidine substituted compounds with their increased cytoliability, are much less attractive in the development of a quinolone for the treatment of TB. This is primarily due to the fact that the eradication of TB requires a lengthy course of treatment, and the need for an agent with a high margin of safety becomes a primary concern. The most active compound **NN 10q** was found to be non-toxic up to 160.1 μM and showed selectivity index (CC_{50}/ MIC) of more than 1600.

Compound **NN 10q** showed no effect or adverse reactions/toxicity at the maximum dose tested (300 mg/kg). Subsequently, compound **NN 10q** was tested for efficacy against MTB at a dose of 50 mg/kg (Table 8.4) in CD-1 mice. Compound **NN 10q** decreased the bacterial load in lung and spleen tissues with 2.39 and 3.89-log10 protections respectively and was considered to be promising in reducing bacterial count in lung and spleen tissues. When compared to gatifloxacin at the same dose level **NN 10q** decreased the bacterial load with 0.42 and 1.79-log10 protections in lung and spleen tissues respectively. Compound **NN 10q** was found to be less active than isoniazid in the *in vivo* study. The reason for this less *in vivo* activity might be due to the low bioavailability of the compound.

The naphthyridone derivatives synthesized and studied were tested for their ability to inhibit supercoiling activity of DNA gyrase. The bacterial targets for quinolones and fluoroquinolones are the type II DNA topoisomerases, DNA gyrase and topoisomerase IV. These ATP - dependent enzymes act by a transient double - stranded DNA break, followed by strand passage and religation reactions to facilitate DNA transactions processes [Levine,

C. H., *et al.,* 1998]. DNA gyrase is unique in catalyzing the negative supercoiling of DNA and is essential for DNA replication, transcription and recombination. In all the species of mycobacteria including MTB, DNA gyrase is the sole type II topoisomerase carrying out the reactions of both the type II topoisomerases. Further, our earlier studies have revealed that DNA gyrase from MTB and MC^2 are highly similar at protein level, antigenic properties and catalytic activities [Manjunatha, U. H., *et al.,* 2000]. The supercoiling assay results with various compounds using MC^2 DNA gyrase is presented in Figure 8.1. The IC_{50} values presented in Table 8.5 shows that the compounds **NN 8p**, **NN 9d**, **NN 9q**, **NN 10m** and **NN 10g** inhibit DNA gyrase in a range of 56.54 - 116.72 μM. The other compounds viz. **NN 9o**, **NN 9h**, **NN 9g** and **NN 10q** have MIC values greater than 200 μM and yet show comparable antimicrobial activity to those which inhibit DNA gyrase at lower concentrations (Table 8.1). All the molecules tested do not show inhibition of supercoiling activity at very low concentrations. The IC_{50} values were higher compared to that of moxifloxacin and ciprofloxacin, two well characterized fluoroquinolones, used as positive controls. However, in cell based assays, most of the compounds exhibited higher potency. Thus, there is an inverse correlation between IC_{50} values and enzyme inhibition data. Generally the inhibitory molecules which show very good inhibition with enzyme assays has lower degree of efficacy in cell based *in vitro* assays. The reasons attributed for this is poor permeability, intracellular instability and modification of the molecules [Balganesh, T. S., *et al.,* 2004]. The difference in the extent of inhibition found in enzyme assays versus *in vivo* susceptibility tests may be due to the following reasons. (1) The molecules may act as prodrugs and upon entering the cell undergo enzymatic modifications to become a much more potent drug [Speirs, R. J., *et al.,* 1995]. (2) Other proteins and/or ionic environment *in vivo* may influence binding characteristics to better accommodate the compounds to the binding site in the enzyme. The selected compounds showed only weak inhibition activity against target enzyme. Thus the mode of action of these compounds might be different from inhibition of DNA gyrase and probably via through nitro reductase enzyme system [Ferguson, J., *et al.,* 1989].

Quinolones in general have favorable safety profiles; phototoxicity has become a significant factor in the clinical use of some [Domagala, J. M., 1994] quinolones. Indeed, the first quinolone, nalidixic acid, caused light-induced dermal effects. This type of response has now

been demonstrated for almost all fluoroquinolones [Takayama, S., *et al.,* 1995], although the relative phototoxic potential varies greatly among compounds. Phototoxicity is considered to be an acute, light-induced irritation response characterized by dermal inflammation, with erythema and edema as primary clinical endpoints. Phototoxicity with the quinolones is generally thought to result from the absorption of light by the parent compound or a metabolite in tissue [Mayne, T. N., *et al.,* 1997]. This photosensitized chromophore may then transfer its absorbed photo energy to oxygen molecules, creating an environment for the production of reactive oxygen species such as singlet oxygen. These reactive species are then thought to attack cellular lipid membranes, initiating the inflammatory process.

Six (**NN 9g**, **NN 10g**, **NN 9h**, **NN 9o**, **NN 8p**, and **NN 10q**) compounds were evaluated for potential phototoxicity in a standardized *in vivo* test system that has been used previously to assess quinolone antibiotics [Manjunatha, U. H., *et al.*, 2002]. The test compounds (140 mg/kg) and the positive control lomefloxacin hydrochloride (140 mg/kg) were evaluated for phototoxicity and both ears of each mouse were evaluated for changes indicative of a positive response: erythema, edema or a measurable increase in ear thickness. Change from baseline was calculated separately for each animal and time point and analyzed for statistical significance and presented in Table 8.6. The results indicated that lomefloxacin showed significant increase in ear thickness from 4 - 96 h and 24 - 96 h when compared within time points and with the control respectively. The test compounds were found to show a significant difference in ear thickness at various time-points when compared with the pre-drug reading (0 h) but were less or not toxic when compared with the negative (vehicle - treated) and positive controls (lomefloxacin). No erythema occurred in mice dosed with 140 mg/kg of **NN 9g**, **NN 10g**, **NN 9h** and **NN 8p** throughout the 96 h study, while compound **NN 9o** showed a significant erythema after irradiation till 24 h only and compound **NN 10q** developed erythema from 48 h.

In theory, quantum mechanical (QM) methods enable completely accurate prediction of any property; there are some important classes of property (notably reactivity, electronic, magnetic, and optical behavior) that can only be modeled using QM methods, because they are determined by electronic behavior that cannot be approximated well using other methods. Electron-rich and electron-poor species tend to reveal the localization or delocalization of the

partial or full charge by the shape of the HOMO or LUMO. Molecular orbitals, when viewed in a qualitative graphical representation, can provide insight into the nature of reactivity, and some of the structural and physical properties of molecules.

In the present study the HOMO and LUMO surfaces were visualized for the synthesized compounds for comparison and the following observations were made. The N_1, N_7 and N_8 nitrogen's were found to play a crucial role in the antitubercular activity of naphthyridines. This hypothesis was confirmed with the HOMO surface analysis (Figure 8.2), in which the most active compounds with lower MICs showed HOMO surfaces on the N_1, N_7 and N_8 nitrogen. The compounds with bulkier substituents (phenyl, fused aryl system) at the N_7 end showed electron cloud over the aryl function and hence the N_7 becomes electron deficient. The less active compounds were devoid of electron cloud around N_1, N_7, and N_8. This observation was observed with all the less active compounds. This observation reveals that the N_7 substituent should not be bulky and introduction of polar groups as in morpholine (O), thiomorpholine (S) as in **NN 8g**, **NN 9g**, **NN 10g**, **NN 8h**, **NN 9h** and **NN 10h** provide extra electron rich cloud due to lone pair of electrons and has been found to be beneficial for activity. With respect to N_1 substituent *t*-butyl was more preferable over cyclopropyl and 4-fluorophenyl in retaining the electron-rich cloud over nitrogen as seen in the Figure 8.2 with compounds **NN 8q**, **NN 9q** and **NN 10q**. There was no significant difference observed in the LUMO orbital surfaces.

8.8 STRUCTURE - ACTIVITY RELATIONSHIP

The extensive studies on the activity profile against mycobacterium shows the following relationship between activity and the structure.

1. With respect to the substituents at N_1 position, the order of activity is *t*-butyl > 4-fluorophenyl > cyclopropyl.
2. With respect to the substituents at C_7 position, the order of activity is oxazolidine > fused piperazines and piperidines > (thio) morpholines > substituted piperazines ≥ substituted piperidines.
3. N_1, N_7 and N_8 nitrogens play a crucial role in the antitubercular activity of naphthyridones.
4. The N_7 substituent should not be bulky and introduction of polar groups is beneficial for activity.
5. Piperidine substituted compounds increased the cytotoxicity.

MOST POTENT NITRO NAPHTHYRIDYL (NN) DERIVATIVE

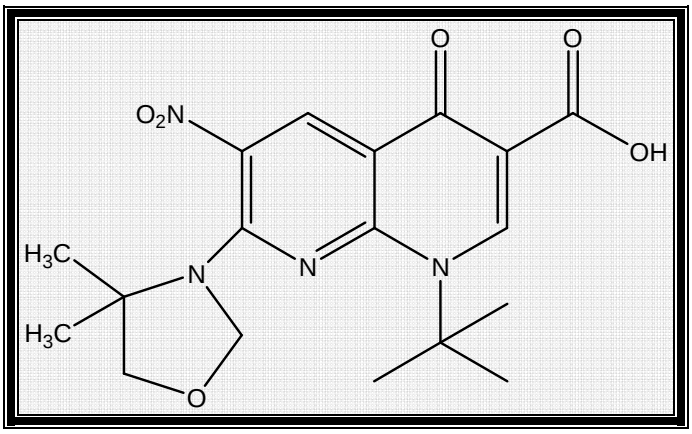

NN 10q

1-*tert*-Butyl-1,4-dihydro-7-(4,4-dimethyloxazolidin-3-yl)-6-nitro-4-oxo-1,8-naphthyridine-3-carboxylic acid

- ***In vitro***:
  - **Against MTB**: 3.6 times more active than INH & 10.4 times more active than GAT.
  - **Against MDRTB:** 455 times more active than INH & 83 times more active than GAT.
  - **Against MC^2:** 11.4 times more active than INH.
- ***Cytotoxicity***: Non-toxic up to 160.10 µM and showed selectivity index (CC_{50}/ MIC) of more than 1600.
- ***In vivo***: Compared to GAT at the same dose level **NN 10q** decreased the bacterial load with 0.42 and 1.79-log10 protections in lung and spleen tissues respectively.

CHAPTER 9

PHARMACOPHORE MODELING

9.1 PHARMACOPHORES AS VIRTUAL SCREENING TOOLS

The pharmacophore concept has been widely used over the past decades for rational drug design approaches and has now been routinely incorporated into virtual screening strategy. A pharmacophore model has often been considered as the ensemble of steric and electrostatic features of different compounds which are necessary to ensure optimal supramolecular interactions with a specific biological target structure and to trigger or to block its biological response [Li, H., *et al.*, 2000].

When the 3D structure of the protein target has not been characterized, and/or when a certain number of ligands (with or without associated binding affinity) are available, pharmacophore models can be developed and used as search queries for virtual screening of databases. Pharmacophore models may range from sub-structural type pharmacophores [Sprague, P., 1999] to feature - based pharmacophores, in the latter the pharmacophoric points are represented by chemical features like hydrogen - bond acceptors/donors, hydrophobic points, acidic or basic features etc. Moreover when the necessity occurs to move to the 3D level, virtual screening has to deal with enhanced complexity with regard to functionality and flexibility of molecules, which requires more sophisticated tools for analyzing this type of data. For implementation of this concept into virtual screening, the chemical function based approach is the most generic one. The originality of this type of pharmacophores mostly resides in the fact that their definition is general and represents different types of interactions between organic molecules and proteins. The utility of such models as queries for 3D database search has been recently reviewed [Sprague, P. W., 1995]. Such pharmacophores can be generated indifferently from ligand sets or from an active site structure. At the end of virtual screening filtering procedure a reliable method for ranking the hits obtained according to their expected bioactivity is required.

9.2 OBJECTIVE OF THE PRESENT STUDY

In the absence of a 3D structure for a particular receptor protein of therapeutic interest, drug discovery and design efforts are often based on a model inferred from the different ligands that bind to it. Ligand - based drug design approach depends on a principle, which states that structurally similar compounds are more likely to exhibit similar properties. Thus, ligand based drug design appears to be the best choice, based on which several molecules can be designed. It can aid the identification of the common 3D features present in diverse molecules that act at the same biological target. The aim of the work was to derive feature - based 3D model from a large set of molecules and evaluate the model using certain synthesized compounds using HipHop module of **Catalyst 4.11**. This hypothesis would serve as a potentially valuable tool in the design of novel antitubercular drugs.

9.3 METHODS FOR PHARMACOPHORE GENERATION

There are two ways to deduce a pharmacophore: direct- and indirect- methods. The former uses both the ligand and the receptor information, while the latter employs only a collection of ligands that have been experimentally observed to interact with a given receptor. Indirect methods can be used even in the absence of structure of the receptor and hence are more advantageous in the present scenario where the crystal structures of less than 10 % of drug targets are available. However, direct methods are becoming extremely important with the rapidly increasing number of known protein structures, which is the outcome of the Structural Genomics project. Once identified, a pharmacophore model is a versatile tool for the discovery and development of new lead compounds.

9.4 STEPS IN IDENTIFYING A PHARMACOPHORE

In general, all the algorithms for pharmacophore identification utilize the following six steps:

1) Input
2) Conformational Search

3) Feature extraction
4) Structure Representation
5) Pattern Identification
6) Scoring

9.4.1 Inputs required for pharmacophore identification

Selecting the ligands that will be used in the pharmacophore analysis will have a huge impact on the resulting pharmacophore model. In this context, there are three issues that should be considered: the type of the ligand molecules, the size of the data set and its diversity.

9.4.1.1 Ligand Type

A major application of a pharmacophore is in its use as a query (in the preliminary screening layer) for the elimination of inactives, which also implies prioritization of actives. Hence the development of such models often referred to as common feature pharmacophores, requires the input of set of molecules that share the same activity. However in the recent years it is increasingly clear that models that are trained using just the data of actives are incapable of discriminating between actives and inactives. Hence the subsequent attempts to improvise this methodology focused on including the data from inactives as well into the training set. Finally a third type of model, the predictive pharmacophoric model can be developed in cases where a range of activity data exists for the training set molecules.

9.4.1.2 Data Set Size

Most of the currently available methods are designed to handle small data sets, which are composed of less than 100 ligands. This is usually a reasonable limitation especially at the early stages of the project when a large data set of ligands is unavailable.

9.4.1.3 Data Set Diversity

In order to get an accurate pharmacophore model, the data set should be as diverse as possible. This will allow identifying features that are most critical for the binding. However, it is important that the outliers will not have a high influence on the obtained model. In addition, one should remember that very different ligands may bind at different binding sites and this may lead to a wrong pharmacophore model [Smellie, A., *et al.*, 1995a].

9.4.2 Conformational Search

The pharmacophore identification problem is complicated substantially by the fact that ligands are very flexible molecules. That is, they possess many internal degrees of freedom. The most common one is the rotation of molecular parts around a connecting single bond [Sprague, P. W., 1995; Smellie, A., *et al.*, 1995a]. As a result, a ligand may have many possible conformations. Each conformation may bind in the active site of the considered receptor. Thus, all the conformations of each input ligand have to be considered during a search for a pharmacophore.

9.4.3 Feature Extraction

In order to perform pharmacophore analyses relevant features in a molecule need to be identified. This can be achieved through the use of predefined atom types with optionally additional centroid "dummy" atoms [Smellie, A., *et al.*, 1995a; Smellie, A., *et al.*, 1995b] or topological substructural definitions at search time or function based pharmacophoric features.

There are three main levels of resolution for defining the features:

- **Atom-Based:** One of the simplest ways to define a feature is by the 3D position of an atom, associated with the atom type.
- **Topology-Based:** In some methods the atoms are grouped into topological features like phenyl ring and carbonyl group.

- **Function-Based:** In other methods the atoms are grouped into chemical functional features that describe the kind of interactions important for ligand-receptor binding. The most common functional groups are:

    1. Hydrogen bond acceptor, for example carbonyl, aliphatic ether and hydroxyl
    2. Hydrogen bond donor, such as primary/secondary amide, aniline nitrogens and hydroxyl
    3. Base (positively charged at physiological pH 7), for example sp^3 N aliphatic amines, hydrazines, guanidines and 2/4 amino pyridines
    4. Acid (negatively charged at physiological pH 7), such as carboxylic acid, acyl sulfonamide, unsubstituted tetrazole and on occasion phenols
    5. Aromatic ring, generally (but not always) in the form of ring centroid
    6. Hydrophobic group, for example certain 5/6 membered aromatic rings, isopropyl, butyl and cyclopentyl

The difference between the topological representations to the functional representation is that the resolution of the functional features is lower. For example, a phenyl ring is only one specific type of aromatic ring. Several topological features may have the same chemical function and thus can be classified as the same functional feature. Note that the functional features are not mutually exclusive. For example, hydroxyl oxygen can be classified as both a hydrogen-bond acceptor and donor. In addition, hydrogen-bond acceptor can also be negatively charged.

9.4.4 Structure Representation

For each ligand structure the selected features are combined to form a representation of the whole structure.

9.4.5 Pattern Identification

The various stages involved in identification of common features of pharmacophore are:

a. The constructive stage identifies pharmacophore candidates that are common among the most active set of ligands. This is done in the following way: First the set of maximum eight most active compounds is determined. Then, all pharmacophore candidates consisting of up to five features between the two most active ligands are identified by a pruned exhaustive search on all their conformations. Finally, only pharmacophore candidates which fit a minimum subset of features of the remaining most active compounds are retained. The resulting pharmacophore candidates are influenced by the diversity of the data set. For example, the diversity of the two most active ligands influences the number of enumerated pharmacophore candidates.

b. The subtractive stage removes those pharmacophore candidates constructed in the previous stage that are also present in more than half of the least active ligands.

c. The optimization stage attempts to improve the score of the pharmacophore candidates that pass the subtractive stage by simulated annealing.

9.4.6 Scoring

In this stage, the pharmacophore candidates were scored and ranked, which are obtained by the previous stages. The basic requirement from a scoring scheme is that the higher the scoring, the less likely it is that the ligands satisfy the pharmacophore model by a chance correlation. The size of the pharmacophore candidates can sometimes be misleading as a score. For instance, a charged center is rarer than a hydrophobic one.

In HipHop the scoring scheme can account for partial fits. Specifically, pharmacophore candidates are ranked based on the portion of input ligands that fit the proposed pharmacophore model. Furthermore, the scoring function takes into account the infrequent and exceptional of the features. For example, a negative charge center is an infrequent and exceptional feature and, therefore, has the largest weight. [Smellie, A., *et al.*, 1995b]

9.5 MATERIALS AND METHODS

9.5.1 Rational selection of test and training sets

Pharmacophore is a set of structural features including 3D (hydrophobic groups, charged/ionizable groups, hydrogen bond donor/acceptors, etc), 2D (substructures), and 1D (physical and biological properties) aspects that are considered to be responsible for the molecule's biological activity. The most critical aspect in the generation of the pharmacophore hypothesis using Catalyst 4.11 [**Catalyst**, version **4.11**; Accelrys, 9685 Scranton Road, San Diego, CA 92121, 2006] is selection of the training set. Some basic guidelines have been followed for selection of training set e.g. a minimum of 12 - 14 diverse compounds have been selected to avoid any chance correlation; the compounds are selected to provide clear, concise information to avoid redundancy or bias in terms of both structural features and activity range and the most of the highly active compounds are included so that they provide information on the most critical features required for a reliable/rational pharmacophore model. The derivatives of quinolones (**FQ**, **NQ**, **MQ** and **NN**) consisting of over 182 molecules was chosen as training and test sets for the present study. The training set consisting of 18 compounds was selected considering the above guidelines while the other remaining molecules were taken for test set for further validation of the pharmacophore model (Table 9.1).

Table 9.1: Antimycobacterial Activity data of molecules used as training sets

No.	Name	MIC (μM)
1	**NQ 8c**	0.08
2	**FQ 8l**	1.56
3	**FQ 9a**	1.42
4	**MQ 13f**	2.06
5	**NN 8q**	0.51
6	**NN 9d**	0.77
7	**NN 10e**	1.45
8	**FQ 8n**	11.37
9	**FQ 9h**	16.60
10	**MQ 12m**	12.31
11	**NN 8f**	21.53
12	**NQ 10n**	12.01
13	**NQ 8k**	1.49
14	**FQ 8j**	5.92
15	**MQ 12o**	2.85
16	**NQ 9i**	6.33
17	**NN 10p**	5.73
18	**NQ 10b**	6.68

1-18 molecules were used as training set and the other molecules were taken as test set.

9.5.2 Computational Methods

All molecular modeling studies were performed using Catalyst 4.11. All the structures were built and geometry optimized using CHARMm force field implemented in the program. The conformations were generated using the maximum limit of 255 conformations within a 20 K_{cal} cutoff for the common feature pharmacophore generation using the HipHop module. [Smellie, A., *et al.,* 1995a; Brooks, B. R., *et al.,* 1983]

Considering the prospects of quinolones as potential agents for the treatment of tuberculosis, we have generated a pharmacophore model of anti-tubercular agents. HipHop, 3D pharmacophore generation, is a common feature based alignment. Here quantitative activity of the molecules is not taken into consideration for hypothesis generation, rather hypotheses are produced by comparing a set of conformational models and a number of 3D configurations of chemical features of training set molecules. [Kurogi, Y., *et al.,* 2001]

Catalyst automatically generated conformational models for each compound. Conformation generating algorithms were adjusted to produce a diverse set of conformations, avoiding repetitious groups of conformations all representing local minima. The conformations generated were used to align common molecular features and generate pharmacophore hypotheses. HipHop used the generated conformations to align chemically important functional groups common to the molecules in the test set and generate a pharmacophore hypothesis from these aligned structures. The models showed a conformational diversity under the constraint of 20 kcal/mol energy threshold above the estimated global minimum based on the CHARMm force field. Catalyst provides two types of conformational analysis: fast and best quality. Best option was used, specifying 255 as the maximum number of conformers [Smellie, A., *et al.,* 1995a; Smellie, A., *et al.,* 1995b]. The molecules associated with the conformational model were submitted to Catalyst hypothesis generation. Hypotheses approximating the pharmacophore were described as a set of features distributed within a 3D space. This process only considered surface accessible functions such as hydrogen-bond acceptor (HBA), hydrogen-bond acceptor lipid (HBAl), hydrogen-bond donor (HBD), hydrophobic (HY), ring aromatic (RA), and positive ionizable (PI).

The pharmacophore model was generated for the synthesized quinolone molecules (**FQ**, **NQ**, **MQ** and **NN**) from the training set of eighteen molecules using HipHop method. HipHop provides feature-based alignment of a group of molecules without considering activity. It matches the chemical features of a molecule, against drug candidate molecules. HipHop utilizes a collection of conformational models of molecules and a selection of chemical features, and produces a series of molecular alignments. HipHop also maps partial features of molecules in the alignment set. This provision gives the option to use partial mapping during the alignment. Partial mapping allows to identify larger, more diverse, more significant hypotheses and alignment models without the risk of missing compounds that do not map to all of the pharmacophore features. [Kurogi, Y., *et al.*, 2001; Purushottamachara, P., *et al.*, 2007; Hirashima, A., *et al.*, 2002]

In the model generation methodology, the highest weight was assigned to the most active compounds for eg., First molecule, **NQ 8c,** in the training set. This was achieved by assigning a value of ***2*** (which ensures that all of the chemical features in the compound will be considered in building hypothesis) and ***0*** (which forces mapping of all features of the compound) in the ***Principal*** and ***Maximum Omitting Features*** columns, respectively. A value of ***1*** for the principal column ensures that at least one mapping for each of generated hypotheses will be found, and a value of ***1*** for the maximum omitting features column ensures that all but one feature must map for all other molecules in the training set. All other parameters were kept at the default settings. In the absence of the activity data, all the features of the training set of molecules were taken as reference molecule data in such a way that it would satisfy features of all the compounds. [Purushottamachara, P., *et al.*, 2007; Hirashima, A., *et al.*, 2002]

Table 9.2: Characteristics for the common feature hypothesis run.

Compound	Principal[a]	MaxOmitFeat[b]
NQ 8c	2	0
FQ 8l	2	0
FQ 9a	2	0
MQ 13f	2	0
NN 8q	2	0
NN 9d	2	0
NN 10e	2	0
FQ 8n	2	1
FQ 9h	2	1
MQ 12m	2	1
NN 8f	2	1
NQ 10n	1	1
NQ 8k	1	1
FQ 8j	1	1
MQ 12o	1	1
NQ 9i	1	1
NN 10p	1	1
NQ 10b	1	1

[a] Principal = 1 means that the molecule must map onto the hypotheses generated by the search procedure. Partial mapping is allowed. Principal = 2 means that this is a reference compound. The chemical feature space of the conformers of such a compound is used to define the initial set of potential hypotheses.

[b] MaxOmitFeat = 1 means a feature of a compound may not be mapped to a hypothesis model. MaxOmitFeat = 0 means all features of a compound are mapped to a hypothesis model.

9.6 RESULTS AND DISCUSSION

9.6.1 Common feature-based pharmacophore model

From HipHop method, 10 hypotheses were generated based on the test set of molecules and had scores ranging from 298.067 to 281.050 (Table 9.3). This diverse range of ranking score in the hypotheses suggests that the features are spatially arranged in a distinct manner in the hypotheses. Also the molecules of the training set were mapped on to each of the hypotheses and checked for fit values. As all the hypotheses had the same features, selection of best hypothesis was done based on the rank, relative energies of training set and fit value of test set. Based on the above criteria, Hypothesis 1 (*Hypo 1*) of rank 298.067 is taken as the best hypothesis. Hypothesis model has eight features, and hence, the maximum fit value of any ligand alignment with this model would be atmost 8.0. All the molecules (both test and training sets) were in energy - minimized conformations.

Table 9.3: Results of the common feature hypothesis run.

Hypothesis	Feature[a]	Rank
1	RZZZZHHH	298.067
2	RZZZZHHH	297.112
3	RZZZZHHH	295.881
4	RZZZZHHH	292.126
5	RZZZHHH	289.589
6	RZZZHHH	286.994
7	RZZZHHH	285.023
8	RZZZHHH	283.722
9	RZZZHHH	281.677
10	RZZZHHH	281.050

[a] Feature **H**: Hydrophobic (HY); **Z**: Hydrogen Bond Acceptor-Lipid (HBAl); **R**: Ring Aromatic (RA)

The selected pharmacophore model ***Hypo 1*** totally contained eight chemical features namely three hydrophobic (**HY-1**, **HY-2** and **HY-3**), four hydrogen bond acceptors-lipid (**HBAl-1**, **HBAl-2**, **HBAl-3** and **HBAl-4**) and one aromatic ring (**RA**) (Fig. 10.1).

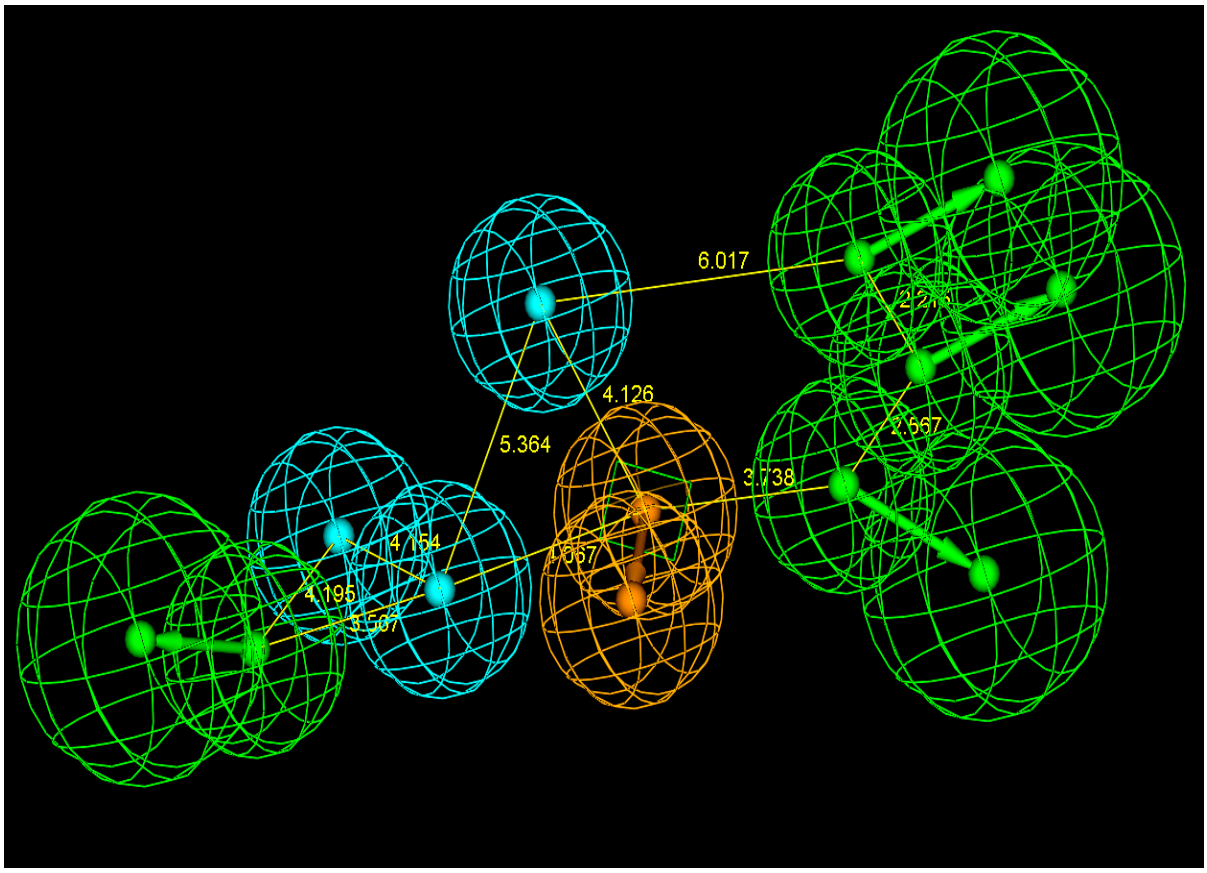

Figure 9.1: Common feature-based (HipHop) pharmacophore model *Hypo1* for the synthesized quinolone molecules (**FQ**, **NQ**, **MQ** and **NN**) against *Mycobacterium tuberculosis*. The Model (*Hypo 1*) contains eight features: three hydrophobic (cyan), four hydrogen bond acceptor-lipid (green), and one aromatic ring (orange) & Distance between chemical features in Å unit. For clarity, distances between certain features are not shown

9.6.2 Validation of Pharmacophore model *Hypo 1*

Alignment of ***Hypo 1*** with test set of compounds was performed (Tables 9.4, 9.5, 9.6 and Figures 9.2, 9.3, 9.4, 9.5, 9.6, 9.7, 9.8, 9.9, 9.10, 9.11). Molecules **FQ 7f**, **FQ 9f**, **FQ 9k**, **NN 10f**, **NQ 8f**, **NQ 9f** and **NQ 10f** showed mapping to all the features of the model generated by HipHop. Other molecules didn't show mapping to at least one of the features. Most of the active molecules didn't show mapping to one of the hydrophobic features which lead to fit value less than 7.0. From this, we can deduce that the particular hydrophobic feature is not a essential chemical feature or Pharmacophore. Molecule **FQ 7f** had the highest fit value among the set of selected molecules. The model could not differentiate between most active and moderately active molecules but is successful in differentiating between active and inactive molecules. Diverse fit values for molecules in active and inactive series indicates that a certain chemical feature is probably essentially involved in the activity.

Table 9.4: Fit values of the most active molecules of the test set with the model *Hypo 1*

Mol	Fit value	Mol	Fit value	Mol	Fit value	Mol	Fit value
NN 9a	1.81	**FQ 7a**	5.77	**NQ 8b**	6.14	**MQ 13a**	4.11
NN 10a	4.60	**FQ 7c**	3.53	**NQ 8d**	5.68	**MQ 12c**	2.48
NN 10c	1.72	**FQ 9c**	6.39	**NQ 8i**	5.98	**MQ 13c**	1.18
NN 10d	6.04	**FQ 7d**	5.67	**NQ 8j**	6.77	**MQ 12e**	5.63
NN 10e	6.02	**FQ 9d**	5.59	**NQ 8n**	5.40	**MQ 13e**	5.17
NN 9g	5.59	**FQ 7h**	6.59	**NQ 8o**	5.36	**MQ 12f**	4.07
NN 10g	5.74	**FQ 7i**	5.48			**MQ 13g**	3.01
NN 9h	6.72	**FQ 9i**	4.59			**MQ 12k**	3.63
NN 10i	4.74	**FQ 7j**	4.49			**MQ 13k**	3.55
NN 10m	6.41	**FQ 9k**	6.45			**MQ 12l**	1.58
NN 9o	4.72	**FQ 7l**	5.84			**MQ 13l**	5.67
NN 10o	5.44	**FQ 9l**	6.98			**MQ 13m**	2.20
NN 9q	2.96	**FQ 7m**	6.20			**MQ 12n**	2.96
NN 10q	3.26	**FQ 9o**	4.86			**MQ 13n**	2.04
		FQ 7q	5.00			**MQ 13p**	2.54
		FQ 9q	3.79				

In Table 9.4, molecules belonging to the **FQ** series and **NQ** series produced good fit values (> 4.0). Though fit values do not indicate direct correlation with activity, similar fit values between a series of active molecules gives valuable information of pharmacophore probably involved. All the Molecules belonging to **MQ** series and **NN** series did not fit to the model properly which indicates the failure of the model to depict active molecules of these series.

Table 9.5: Fit values of inactive or least active molecules of the test set with the model *Hypo1*

Mol	Fit value	Mol	Fit value	Mol	Fit value	Mol	Fit value
NN 9c	5.32	**FQ 8a**	5.41	**NQ 9a**	0.27	**MQ 12a**	4.82
NN 8e	5.67	**FQ 8f**	3.44	**NQ 10d**	3.97	**MQ 12b**	3.95
NN 9e	4.13	**FQ 8g**	5.69	**NQ 9o**	4.77	**MQ 12d**	1.05
NN 9f	3.30	**FQ 9h**	3.15			**MQ 12m**	2.20
NN 9p	6.26	**FQ 8o**	5.19				

Table 9.6: Fit values of moderately active molecules of the test set with the model *Hypo 1*

Compd	Fit value	Compd	Fit value	Compd	Fit value	Compd	Fit value
NN 8a	3.74	**FQ 7b**	5.26	**NQ 8a**	1.98	**MQ 13b**	4.71
NN 8b	6.50	**FQ 8b**	6.07	**NQ 10a**	5.71	**MQ 13d**	6.02
NN 9b	6.39	**FQ 9b**	5.44	**NQ 9b**	5.29	**MQ 12g**	3.46
NN 10b	6.51	**FQ 8c**	3.68	**NQ 9c**	1.93	**MQ 12h**	4.38
NN 8c	3.76	**FQ 8d**	5.23	**NQ 10c**	2.41	**MQ 13h**	4.23
NN 8d	6.17	**FQ 7e**	4.87	**NQ 9d**	5.98	**MQ 12i**	2.96
NN 10f	7.68	**FQ 8e**	6.11	**NQ 8e**	4.22	**MQ 13i**	1.59
NN 8g	5.86	**FQ 9e**	3.43	**NQ 9e**	4.10	**MQ 12j**	5.05
NN 8h	2.48	**FQ 7f**	7.73	**NQ 10e**	6.02	**MQ 13j**	3.58
NN 10h	4.60	**FQ 9f**	7.52	**NQ 8f**	7.28	**MQ 13o**	0.50
NN 8i	4.62	**FQ 7g**	5.69	**NQ 9f**	7.25	**MQ 12p**	2.55
NN 9j	0.99	**FQ 9g**	5.82	**NQ 10f**	7.63		
NN 10j	0.81	**FQ 8h**	5.14	**NQ 8g**	5.73		
NN 9k	5.08	**FQ 8i**	4.73	**NQ 10g**	5.85		
NN 10k	6.34	**FQ 9j**	1.87	**NQ 8h**	3.85		
NN 8l	5.60	**FQ 7k**	5.18	**NQ 9h**	3.98		
NN 9l	4.47	**FQ 8k**	5.59	**NQ 10h**	2.90		
NN 10l	4.21	**FQ 8m**	6.09	**NQ 10i**	4.86		
NN 8m	6.41	**FQ 9m**	6.25	**NQ 9j**	0.71		
NN 9m	6.21	**FQ 7n**	3.24	**NQ 10j**	2.96		
NN 8n	2.66	**FQ 9n**	5.04	**NQ 9k**	4.84		
NN 9n	4.90	**FQ 7o**	5.33	**NQ 10k**	5.83		
NN 10n	4.44	**FQ 7p**	0.05	**NQ 8l**	4.35		
NN 8o	5.33	**FQ 8p**	0.03	**NQ 9l**	4.02		
NN 8p	3.26	**FQ 9p**	1.56	**NQ 10l**	4.32		
		FQ 8q	4.73	**NQ 8m**	6.19		
				NQ 9m	6.23		
				NQ 10m	6.19		
				NQ 9n	5.11		
				NQ 10o	4.86		
				NQ 8p	0.59		
				NQ 9p	2.62		
				NQ 10p	0.03		

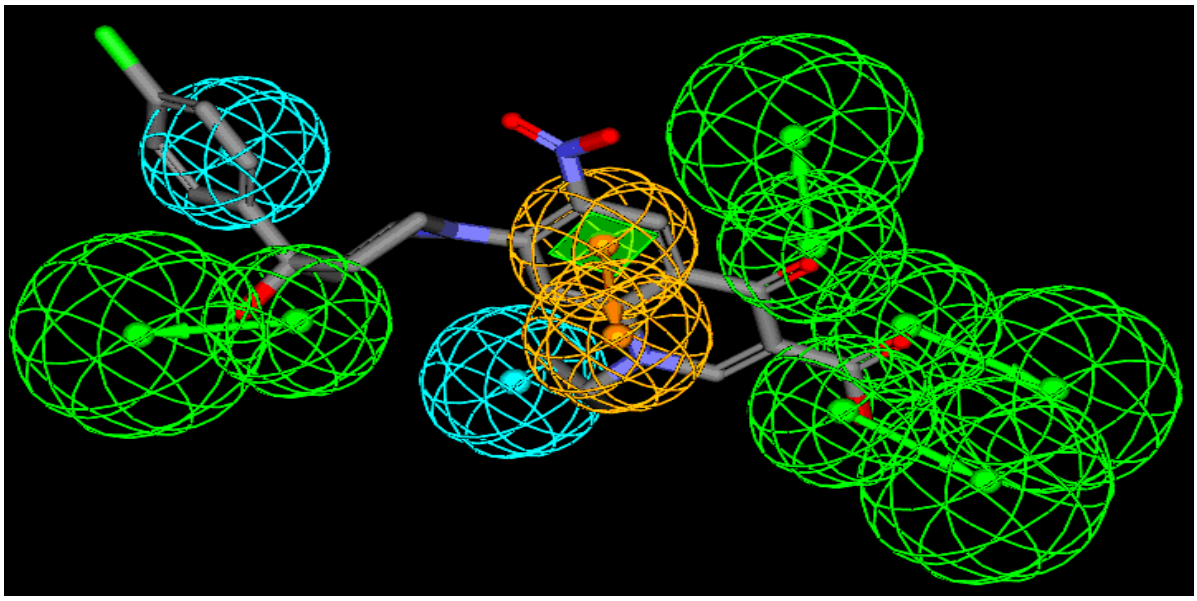

Figure 9.2: Mapping of the molecule **NQ 8j** to the model ***Hypo 1***.
The HBAl-1 (right-top) maps the oxygen attached to C_4, HBAl-2 (below HBA-1) maps the oxygen of acid group attached to C_3, HBAl-3 (below HBA-2) maps the oxygen of OH of acid group attached to C_3, HBAl-4 (left side) maps the oxygen of side chain, the HY-1 feature (right side ones) maps the cyclopropyl group N_1, the HY-2 (left side ones) feature maps the phenyl group and aromatic ring (RA) feature maps the phenyl ring of quinolone nucleus.

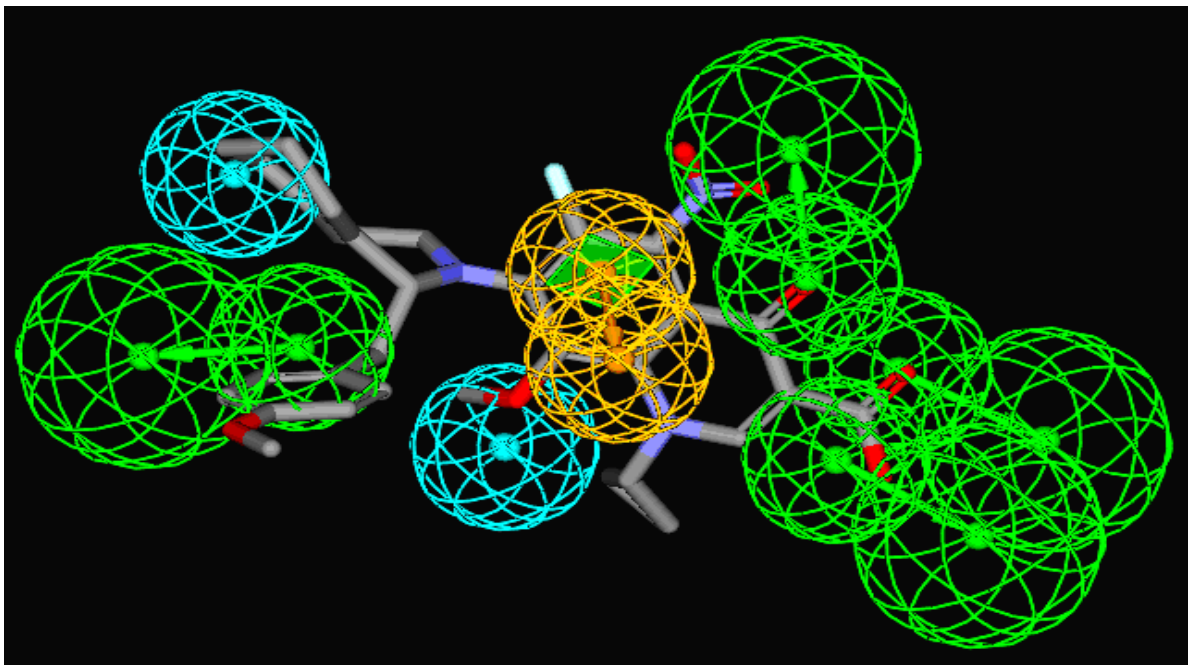

Figure 9.3: Mapping of the molecule **NN 9h** to the model ***Hypo 1.***

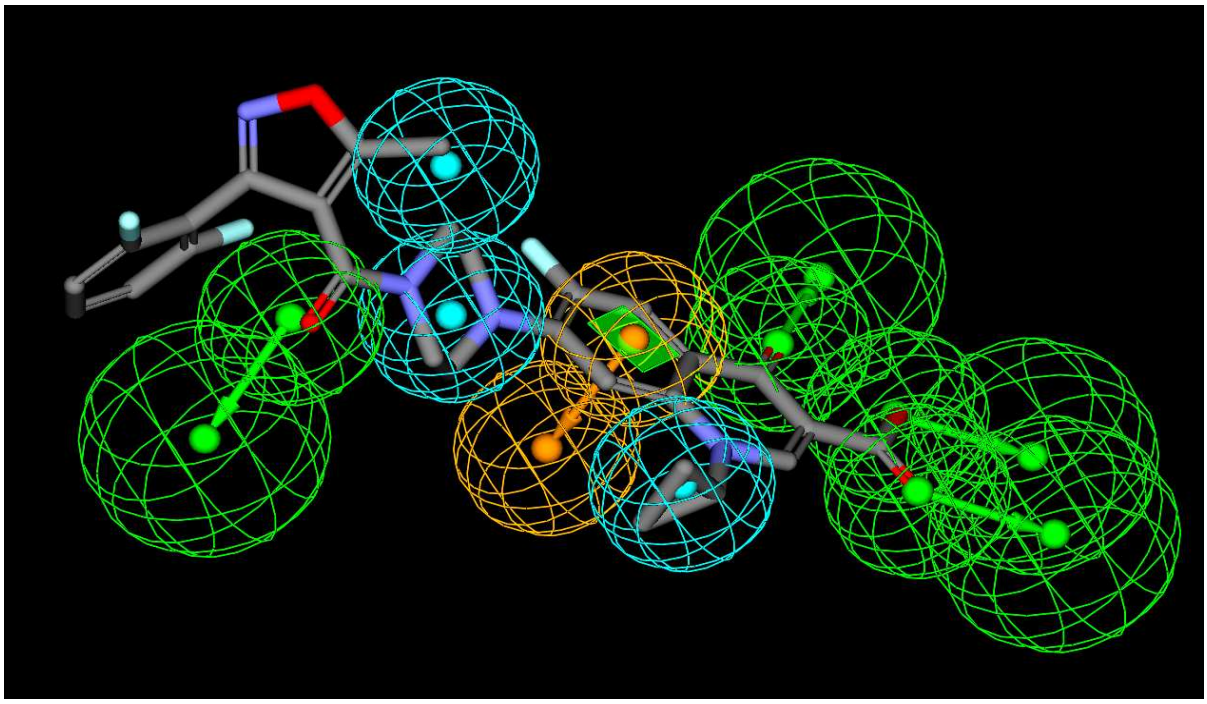

Figure 9.4: Mapping of the molecule **FQ 7f** to the model ***Hypo 1*.**

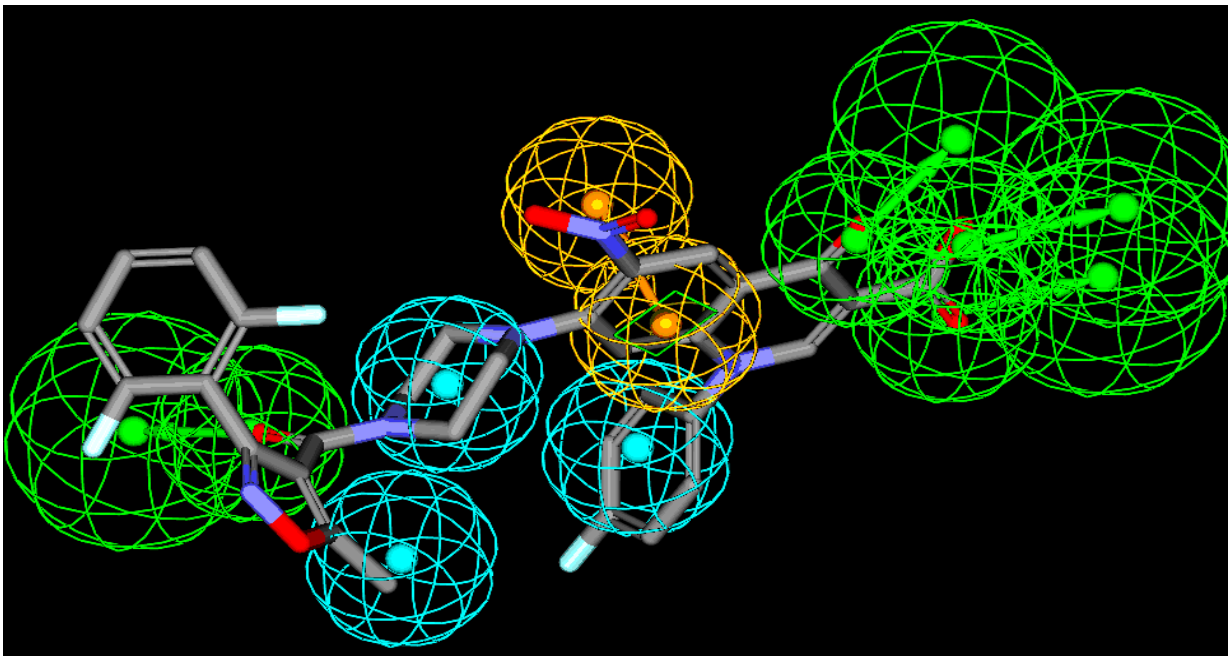

Figure 9.5: Mapping of the molecule **FQ 9f** to the model ***Hypo 1*.**

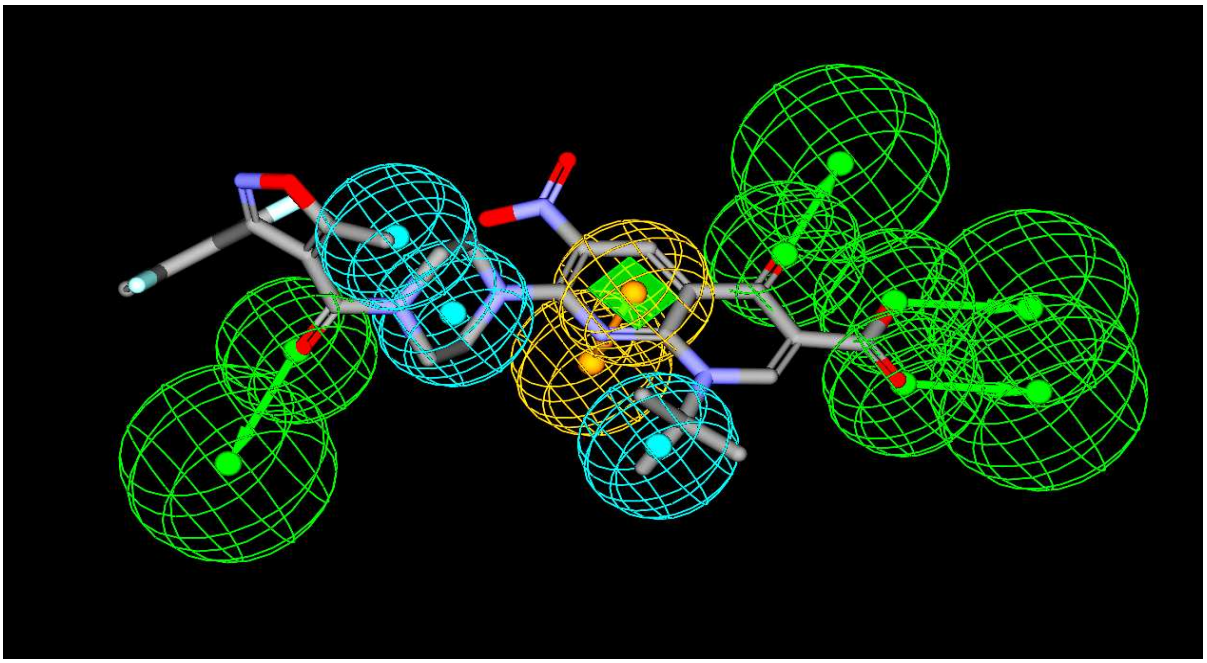

Figure 9.6: Mapping of the molecule **NN 10f** to the model ***Hypo 1*.**

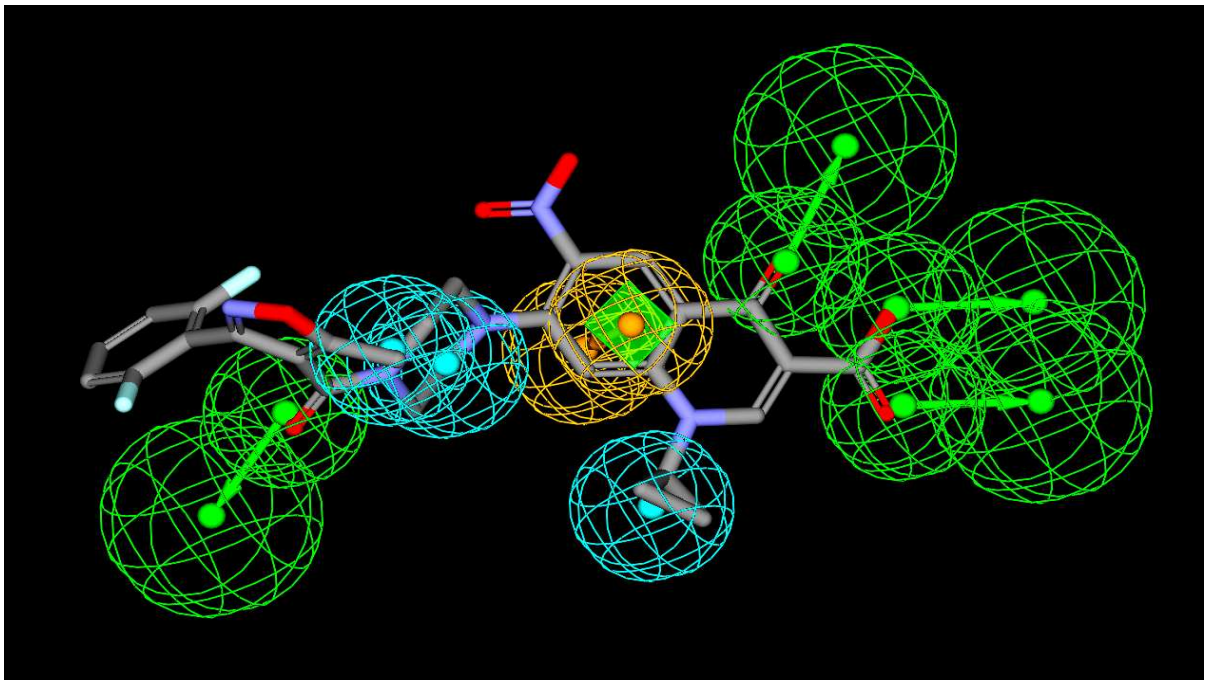

Figure 9.7: Mapping of the molecule **NQ 8f** to the model ***Hypo 1*.**

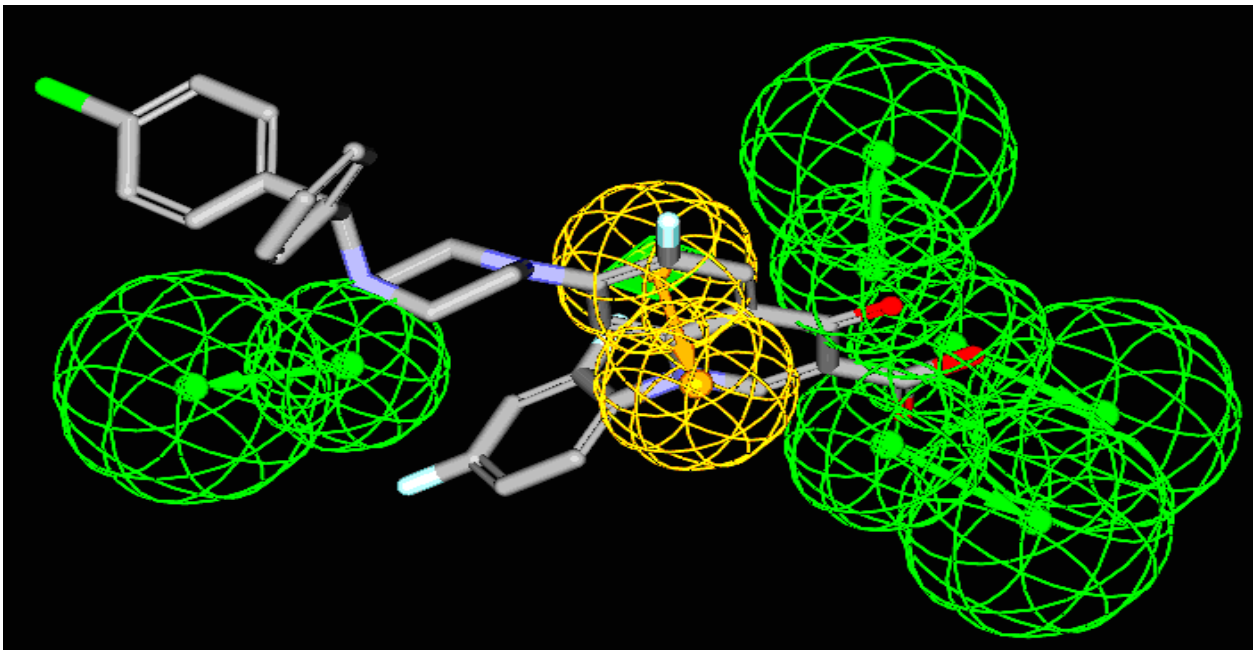

Figure 9.8: Mapping of the molecule **FQ 8a** to the model ***Hypo 1*.**

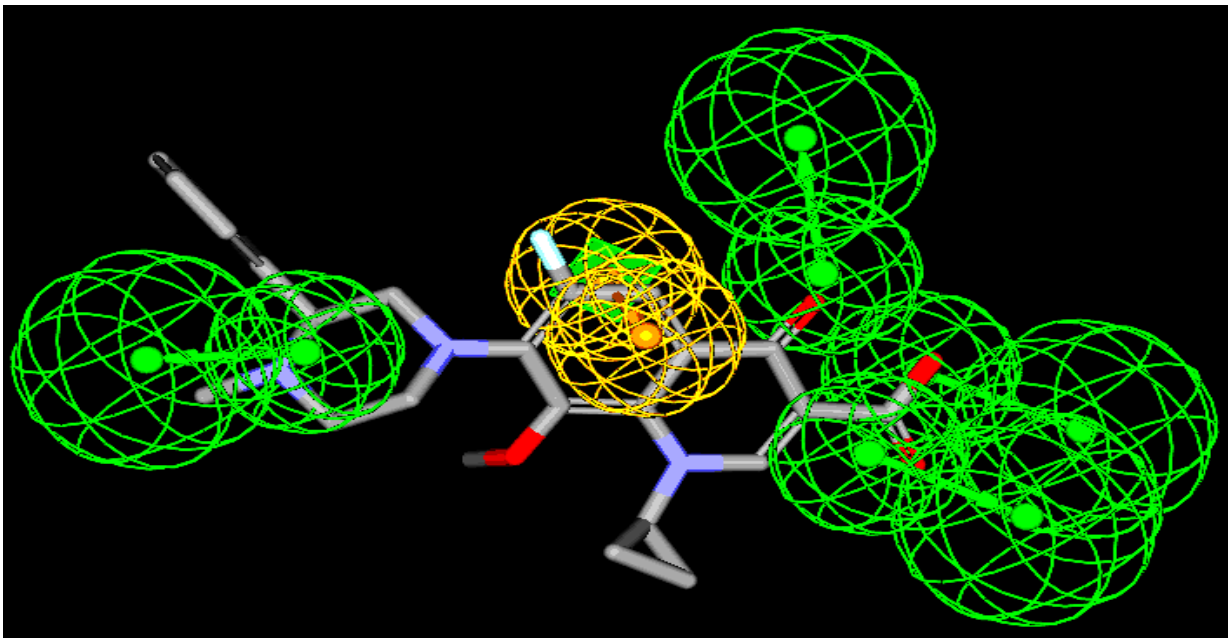

Figure 9.9: Mapping of the molecule **MQ 12d** to the model ***Hypo 1*.**

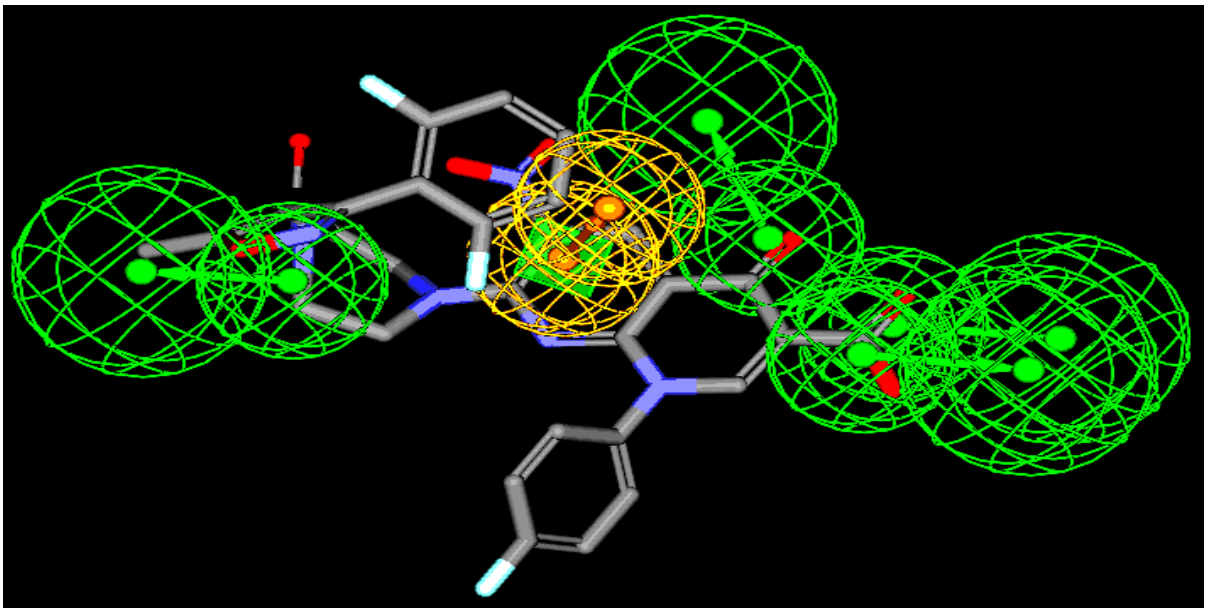

Figure 9.10: Mapping of the molecule **NN 9f** to the model ***Hypo 1*.**

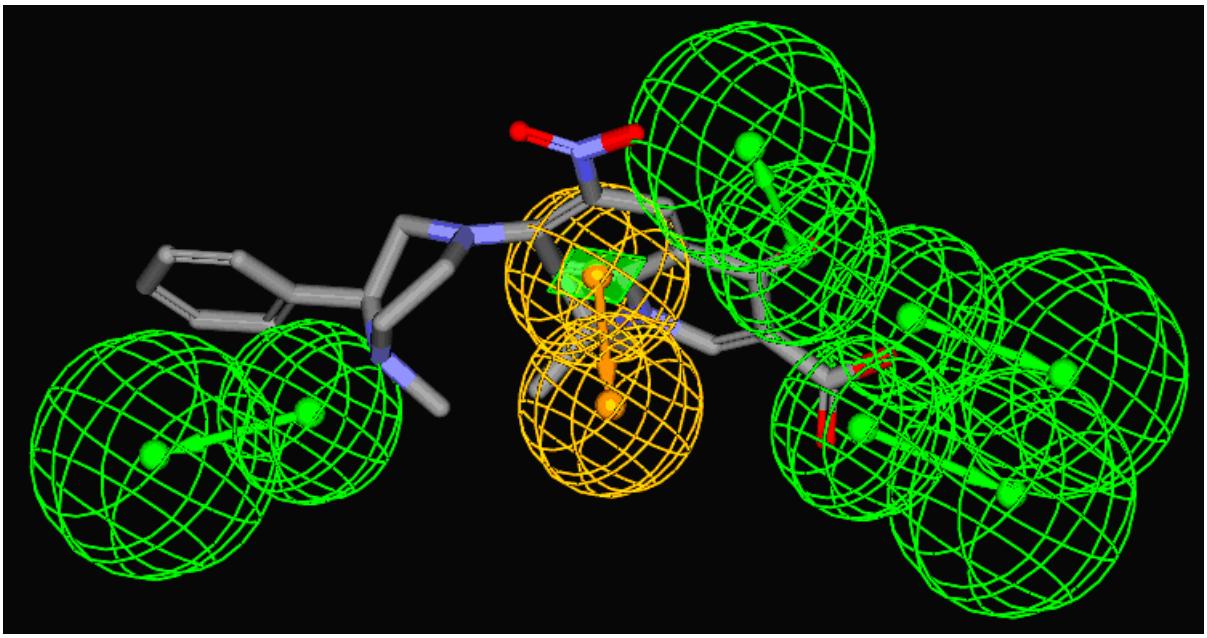

Figure 9.11: Mapping of the molecule **NQ 10d** to the model ***Hypo 1*.**

9.7 CONCLUSIONS

In rational drug design process, it is common that the biological activity data of a set of compounds acting on a particular protein is known while information of the three-dimensional structure of the protein active site is absent. A three-dimensional pharmacophore hypothesis that is consistent with existing molecules should be useful and predictive in evaluating new compounds and directing further synthesis. The pharmacophore modeling of the synthesized molecules shows how a set of active molecules can uncover the molecular characteristics or features essential for activity.

The pharmacophore mapping figures are shown in fig. 9.2 to 9.11. From fig. 9.8 to 9.11, it can be noted that the hydrophobic feature is absent or the molecules didn't show mapping to it. This can be the reason for the absence of activity of the molecules. The results of the pharmacophore model revealed that four hydrogen bond acceptors (lipid), three hydrophobic features and an aromatic ring are significant for effective antitubercular activity. The model generated hypotheses (1 - 10) with rank scores ranging from 298 - 281 and results with training set and test set led to the selection of ***Hypo 1*** as the best hypothesis. The mapping of compounds of test set to ***Hypo 1*** yielded considerable fit values with a maximum fit value of 7.73 for **FQ 7f**. Active molecules **NN 9h** and **NQ 8j** can be modified by introducing hydrophobic groups like halogen, phenyl or other bulky groups in a specific 3D orientation, which satisfies the distance - criteria. Further, inactive molecules can be modified by introducing bulkier groups in order to increase the fit values with the model. This study can be utilized in the design of new molecules, keeping in view the 3D orientation of the aforementioned eight chemical features.

CHAPTER 10

SUMMARY AND CONCLUSIONS

Totally four series of compounds (**182 compounds**) viz., fluoroquinolone (**FQ**); nitroquinolone (**NQ**); 8-methoxyquinolone (**MQ**); and nitro naphthyridone (**NN**), were synthesized.

Purity of the compounds was ascertained by TLC and their structures were elucidated by IR spectroscopy, ^{1}H NMR spectroscopy, and elemental analysis. Melting points and clog P values were determined for the synthesized compounds.

The synthesized compounds were evaluated for *in vitro* antimycobacterial activity against MTB; MDR-TB; and MC^{2}.

Against MTB, all the synthesized compounds (182 compounds) showed good activity profile. Thirty two compounds showed more potent activity than gatifloxacin (MIC: 1.04 µM) and nine compounds were more potent that isoniazid (MIC: 0.36 µM). Of all the compounds screened against MTB, compound **NQ 8c** (MIC: 0.08 µM) was found to be the most active and is 13 & 4.5 times active than gatifloxacin & isoniazid respectively.

Against MDR-TB, a total of ninety six compounds were screened and all the compounds were found to be more active than gatifloxacin (MIC: 8.34 µM) and isoniazid (MIC: 45.57 µM). Amongst the screened compounds, compound **NN 9o** (MIC: 0.08 µM) was found to be the most active and is 104.25 & 569.63 times active than gatifloxacin & isoniazid respectively.

All of the synthesized compounds were screened against MC^{2}. Twenty one compounds showed potent activity than gatifloxacin (MIC: 2.08 µM) and one hundred sixty one compounds were potent than isoniazid (MIC: 45.55 µM). Of all the compounds screened

against MC^2, compound **MQ 13n** (MIC: 0.68 µM) was found to be the most active and is 3.06 & 66.99 times more active than gatifloxacin & isoniazid respectively.

Further ninety one compounds were tested for cytotoxicity in mammalian Vero cell lines. Most of the compounds were not found to be cytotoxic upto 62.5 µg/ml.

Five compounds (**FQ 7l**, **NQ 8c**, **MQ 12l**, **MQ 13n**, and **NN 10q**) were tested in *in vivo* model against MTB. The compounds were more or equipotent as compared to gatifloxacin (lung: log 6.02 ± 0.23; spleen: log 6.92 ± 0.07) or isoniazid (lung: log 5.86 ± 0.23; spleen: log 4.71 ± 0.10). Amongst all the compounds tested, compound **NQ 8c** (lung: log 5.21± 0.17; spleen: log 4.87± 0.13), was found to be the most active.

Thirty eight molecules were further tested for their ability to inhibit DNA gyrase enzyme *in vitro*. Amongst the compounds tested, compound **NQ 10a** was found to be the most active compound inhibiting the enzyme at a concentration (IC_{50}) as low as 8.69 µM, which is much lower than the standard ciprofloxacin (IC_{50}: 15.09 µM).

Sixteen molecules were selected among the synthesized compounds to evaluate the phototoxicity in standard *in vivo* model. All the compounds were found to be non-phototoxic or less phototoxic at a dose of 140 mg/kg when compared with vehicle and lomefloxacin hydrochloride at the same dose level.

Quantum mechanical modeling was performed for all the synthesized compounds. The HOMO and LUMO surfaces were observed. The HOMO surface analysis shows the importance of **N_1**, **N_7**, **N_8**, **4-oxo functions** and **nitrogen of the nitro group** for the antitubercular activity of quinolones. There was no significant difference observed in the LUMO orbital surfaces.

A pharmacophore for antitubercular drugs was modeled using the synthesized compounds, which stated that a molecule to be active as antitubercular, it should have eight features: **three hydrophobic**, **four hydrogen bond acceptor-lipid**, and **one aromatic ring**. The three

hydrophobic centers in the quinolones are the N_1 substituent, and two in the side chain attached to C_7; the four hydrogen bond acceptor-lipid in the quinolones are C_4 oxo function, carbonyl group of acid group at C_3, hydroxyl group of acid group at C_3 and one oxygen present in the substituent at C_7; the aromatic ring feature in quinolone is the aryl ring of quinolone nucleus.

The **Structure-Activity Relationship** (SAR) which can be derived overall is as follows:

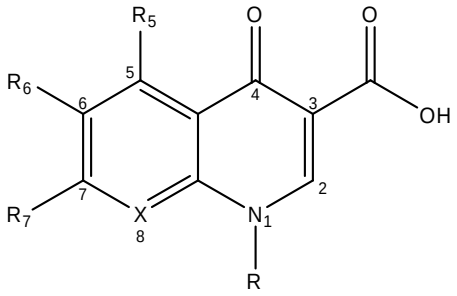

- With respect to the substituents at N_1 position, the order of activity is **cyclopropyl > *tert*-butyl > 4-fluorophenyl.**

  The N_1 substituents should be electron donating, which increase the acidity of carboxyl group at C_3 position which in turn increases the amount of un-ionized drug that is able to penetrate the cell membranes.

- The pharmacophore model states the importance of C_3 carboxylic acid group. So the carboxylic acid group at C_3 is an important requirement for antitubercular activity.

- The pharmacophore model and quantum mechanical modeling shows that the presence of C_4 oxo group is a must for antitubercular activity.

- The presence of nitro group at C_5 position favours the activity as seen with **MQ** derivatives.

- Nitro or Fluoro groups at C_6 favour the antitubercular activity.
  The C_6 should also be substituted with an electronegative or an electron withdrawing substituent.
- The order of activity at C_7 position was dependent on the substituent at N_1 position and C_6 position.
  In general, the C_7 substituent should be bulky in nature and should increase the lipophilicity of the molecule, to facilitate penetration into the cell wall of mycobacteria.

- Fluorophenyl at N_1 and nitro substitution at C_6 or C_5 in the compounds increased the toxicity.

Among the 182 compounds, compound **NQ 8c** was found to be the most active

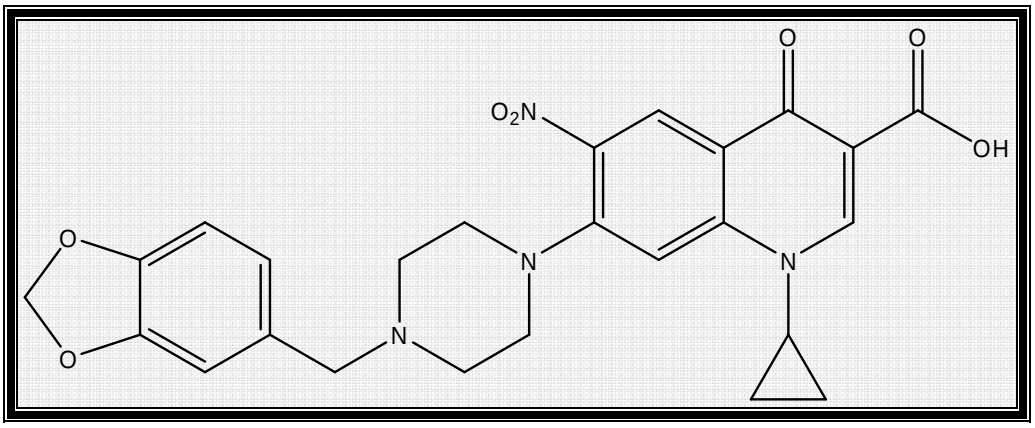

NQ 8c

7-(4-((Benzo[d][1,3]dioxol-5-yl)methyl)piperazin-1-yl)-1-cyclopropyl-1,4-dihydro-6-nitro-4-oxoquinoline-3-carboxylic acid